Invariance and Sliding Modes.

Application to coordination of multi-agent systems, bioprocesses estimation, and control in living cells

ALEJANDRO VIGNONI

EDITORIAL
UNIVERSITAT POLITÈCNICA DE VALÈNCIA

Collection doctoral thesis

© 2014, of the present edition: Editorial Universitat Politècnica de València
Telf.: 963 877 012 / www.lalibreria.upv.es

ISBN: 978-84-9048-256-8 (printed version)

Invariance and Sliding Modes

Application to coordination of multi-agent systems, bioprocesses estimation, and control in living cells

UNIVERSITAT POLITÈCNICA DE VALÈNCIA

Ph.D. Dissertation

AUTHOR: Alejandro Vignoni

SUPERVISOR: Jesús Picó

Instituto Univ. de Automática e Informática Industrial (AI2)
Departamento de Ingeniería de Sistemas y Automática (ISA)
Universitat Politècnica de València, Spain

May 8, 2014

Invariance and Sliding Modes

Application to coordination of multi-agent systems, bioprocesses estimation, and control in living cells

PH.D. IN CONTROL, ROBOTICS AND INDUSTRIAL COMPUTING

PROGRAMA DE DOCTORADO EN AUTOMÁTICA, ROBÓTICA E INFORMÁTICA INDUSTRIAL

Supervised by Dr. Jesús Picó, Catedrático de Universidad

Instituto Univ. de Automática e Informática Industrial (AI2)
Departamento de Ingeniería de Sistemas y Automática (ISA)
Universitat Politècnica de València, Spain

May 8, 2014

This work has been partially supported by the Spanish Government (Program CICYT FEDER DPI2008-06880-C03-01 and DPI2011-28112-C04-01). The author was recipient of the fellowship *Formación de Personal Investigador* by the Universitat Politècnica de València (FPI/2009-21).

He was also recipient of the competitive grants for pre-doctoral stays PAID-00-11/2714 and PAID-00-12/0082 of Universitat Politècnica de Valéncia.

Support from the Centre for Synthetic Biology and Innovation and Bioengineering Department from Imperial College London, and Tabor Lab and Department of Bioengineering from Rice University Houston are also acknowledged, both for accepting the author in its facilities as predoctoral stay and for its valuable collaboration sharing knowledge.

In the following site the reader will find an updated version of this thesis. This includes erratas, corrections and clarifications.

http://goo.gl/P3914x

A mis abuelos JRV y VMA.

Agradecimientos

Ojalá que todo el mundo tenga tantos problemas para escribir palabras de agradecimientos por tener tanto que agradecer y tener tan poca elocuencia para plasmarlo en una hoja. Por suerte yo tengo estos problemas. Sobre todo tener tanto y tanta gente a la que agradecer. En primer lugar quiero agradecer a Jesús por haberme permitido aprender de su ejemplo, ya sea en el ámbito académico como en el personal. Por haberme brindado infinitas oportunidades, sin las cuales, por ejemplo, no hubiera conocido el fascinante mundo de la biología sintética. Por haberme enseñado a no desperdiciarlas. Por ser un guía más que un director. Por recibirme desde otro continente sin más que una referencia. Por los cafés y las cervessetas. A Hernán y Fabricio por haberse acordado de mi cuando Jesús estaba buscando alguien. Por haberme acompañado cuando estaba solo, haciendo de padre y amigo; trabajando o disfrutando, en Valencia o en La Plata, o en algún otro lugar del mundo. A Vale y a Lau por prestarme a sus maridos. To Guy-Bart and Jeff for allowing me to learn from their work, to know their awesome institutions, to explore two beautiful countries and to know many friends. A Diego, colega, amigo y compadre. To the Imperial's RSM 4.35, especially to Ani, Olga, Eugene, Lucas, Jason, Chema and Sietse. To Florian and the rest of the Imperial Outdoor club, for letting me know new stuff about life and about me. To Evan (especially), Lucas, Karl and Kevin (and the rest of the Tabor Lab) for the warm welcome into the lab and into their lives, and for Valhalla's. A Fer, Fede y el Pitu, que desde la distancia siempre estuvieron cerca; cada vez que volvía era como si nunca me hubiera ido. A José Luis porque durante estos cinco años siempre estuvo cerca, amistades como estas duran toda la vida, espero que nuestros caminos se vuelvan a cruzar en algún momento, aunque sea una paella o un asado. A Pancho, por ser un muy buen compañero de piso y

de la vida.

A los chicos de la sala, Kiko, David, Fátima, Gil, Ana, Laguna, Diego, Gaby, Vane, Jesús compañeros de este viaje, de cafés y cervezas, y de La Vella, el conservatorio o la Tarongeria. No tengo palabras para agradecer. En especial a Gil, por ser el primero, el primero que me recibió, el primero en llegar y el ultimo en irse, por los intentos de solucionar los problemas del mundo cerveza mediante, junto a Jopipe; por invitarme a embarcarme con él en las aventuras en la roca, perdón por no haber podido seguirte. A Santiaga, Racera y Nacha por dejarme enseñarles y por dejarme aprender de ustedes. A Sergio por el apoyo en esta última parte en la que tratamos de implementar lo inimplementable. A Natalia, por haberme hecho volver al yoga. A Entertainment, por estar para hablar cosas totalmente ajenas al trabajo.

A Yadira, por mostrarme la vida más allá de la investigación y junto a ella. Por soportarme, por entenderme y por no entenderme. Por permitirme compartir tantas cosas en tan poco tiempo, por ayudarme a crecer como persona. Gracias, sin vos no habría llegado donde llegué, nena!. Quiero seguir este camino con vos.

A mis padres por haberme permitido llegar a donde he llegado y por incentivarme a seguir. Por haberme apoyado siempre, e incluso en la decisión tan difícil de irme tan lejos para continuar mi educación académica y en la vida. A mis hermanas, por ser un ejemplo a seguir, las dos cada una con su estilo pero siempre presentes. Los quiero. Los quiero mucho.

A muchos más que no entran en esta página, pero que también agradezco.

Gracias a todos y a todas!

Abstract

The present Thesis employs ideas of set invariance and sliding modes in order to deal with different relevant problems in control of nonlinear systems. Initially, it reviews the techniques of set invariance as well as the more relevant results about sliding modes control. Then the main methodologies used are presented: sliding mode reference conditioning, second order sliding modes and continuous approximation of sliding modes. Finally, the methodologies are applied to different problems in control theory and to a variety of biologically inspired applications.

The contributions of the thesis are:

- The development of a method to coordinate dynamical systems with different dynamic properties by means of a sliding mode auxiliary loop shaping the references given to the systems as function of the local and global goals, the achievable performance of each system and the available information of each system.

- The design of tuning methods for second order sliding mode algorithms. The methods decouple the problem of stability analysis from that of finite-time convergence of the super-twisting sliding mode algorithm. A nonlinear change of coordinates and a time-scaling are used to provide simple, yet flexible design methods and stability proofs. Application of the method to the design of finite-time convergence estimators of bioprocess kinetic rates and specific biomass growth rate, from biomass measurements. Also the estimators are validated with experimental data.

- The proposal of a strategy to reduce the variability of a cell-to-cell communication signal in synthetic genetic circuits. The method uses set invariance and sliding mode ideas applied to gene expression networks to obtain a reduction in the variance of the commu-

nication signal. Experimental approaches available to modify the characteristics of the gene regulation function are described.

Resumen

La presente Tesis emplea técnicas de invarianza geométrica de conjuntos y modos deslizantes para tratar diferentes problemas en control de sistemas. Inicialmente revisa las técnicas existentes de invarianza de conjuntos, así como los resultados más relevantes del control por modos deslizantes. Luego se presentan las principales metodologías utilizadas: acondicionamiento de referencia, modos deslizantes de segundo orden, y aproximación continua de modos deslizantes. Finalmente las metodologías presentadas son utilizadas para tratar diferentes problemas en teoría de control y biología sintética, y utilizadas en una variedad de aplicaciones.

Las aportaciones de la tesis son:

- **Coordinación de sistemas dinámicos con dinámicas distintas.** Se presenta una metodología para coordinar sistemas dinámicos con diferentes características y propiedades. Esta nueva metodología se basa en principios de invarianza y control por modos deslizantes para modificar las referencias que se envían a los sistemas involucrados, teniendo en cuenta las características propias de cada sistema junto con sus restricciones.

- **Diseño de algoritmos de control por modo deslizante de segundo orden.** Se proponen métodos para diseñar algoritmos de modos deslizantes de segundo orden desacoplando el problema de estabilidad del problema de la convergencia en tiempo finito. Se utilizan un cambio de coordenadas no lineales y un escalado temporal, con lo que se obtiene una prueba de estabilidad simple junto con un método de diseño flexible para el algoritmo super twisting. Se aplica el método propuesto al diseño de observadores de convergencia finita de tasas cinéticas de bioprocesos y se valida con datos experimentales.

- **Reducción de la variabilidad celular en circuitos genéticos de biología sintética.** La metodología propuesta reduce la varianza de la señal de comunicación entre células utilizando ideas de geometría invariante y modos deslizantes aplicadas a redes de expresión genética. También se describen los enfoques experimentales con los que se debería modificar las redes genéticas para obtener los resultados deseados.

Resum

La present Tesi empra tècniques de invariància geomètrica de conjunts i modes lliscants per tractar differentes problemes en control de sistemes. Inicialment revisa les tècniques existents invariància de conjunts, així com els resultats més rellevants del control per modes lliscants. Després es presenten les principals metodologies utilitzades: condicionament de referència, modes lliscants de segon ordre, i aproximació contínua de maneres lliscants. Finalment les metodologies presentades són utilitzades per tractar diferents problemes en teoria de control i biologia sintètica, i utilitzades en una varietat d'aplicacions.

Les aportacions de la tesi són:

- **Coordinació de sistemes dinàmics amb dinàmiques diferents.** Es presenta una metodologia per coordinar sistemes dinàmics amb diferents característiques i propietats. Aquesta nova metodologia es basa en principis de invariància i control per modes lliscants per modificar les referències que s'envien als sistemes involucrats tenint en compte les característiques pròpies de cada sistema juntament amb les seves restriccions.

- **Disseny d'algoritmes de control per mode lliscant de segon ordre.** Es proposen mètodes per dissenyar algoritmes de modos lliscants de segon ordre desacoblant el problema d'estabilitat del problema de la convergència en temps finit. S'utilitzen un canvi de coordenades no lineals i un escalat temporal amb el que s'obté una prova d'estabilitat simple juntament amb un mètode de disseny flexible per l'algorisme super Twisting. S'aplica el mètode proposat al disseny d'observadors de convergència finita de taxes cinètiques de bioprocessos. Tambe es valida els estimadors amb data experimental.

- **Reducció de la variabilitat cel·lular en circuits genètics de biologia sintètica.** La metodologia proposada redueix la variància del senyal de comunicació entre cèl·lules utilitzant idees de geometria invariant i maneres lliscants aplicades a xarxes d'expressió genètica. També, es descriuen els enfocaments experimentals amb què s'hauria de modificar les xarxes genètiques per obtenir els resultats desitjats.

Contents

Chapter 1

Introduction

Cominciate col fare ciò che è necessario,
poi ciò che è possibile.
E all'improvviso vi sorprenderete
a fare l'impossibile.

Francesco d'Asisi

Control theory can be dated back to the beginning of last century when the Wright brothers made their first flight in 1903. Since then, control theory has received more and more attention, especially during the World War II when control theory has been developed and applied to fire-control systems, missile navigation and control, and various electronic devices. Over the past several decades, modern control theory has been developed due to the booming of spacecraft technology and large-scale systems.

During the development of the control theory, control of a single system has relatively matured and many control methodologies have been developed, such as proportional-integral-derivative (PID) control, adaptive control, intelligent control, and robust control.

Invariance and Sliding Modes, as a part of robust control techniques, have been around for several decades. In one hand, invariance in differential equations dates back to Nagumo (1942) with the Nagumo condition. More recently Blanchini (1999) made a survey recognising the importance of set invariance conditions in control theory. After that in Mareczek et al. (2002) an invariance control was presented achieving semiglobal asymptotic stabilization for a class of cascade nonlinear systems. In Astolfi and Ortega (2003) a method to design asymptotically stabilizing and adaptive control laws for nonlinear systems was introduced using invariance together with immersion techniques. Also, in Blanchini and Miani (2008) invariance methods are used in combination with Lyapunov stability analysis methods to cope with fundamental problems in control theory from a set-theoretic perspective.

On the other hand, the interest in variable structure systems (VSS) ans sliding modes (SM) started to grow in the end of the 70's . And then there have been great theoretical advances in the field. There are several general revisions of VSS (Utkin, 1977; Hung et al., 1993; Edwards and Spurgeon, 1998; Utkin et al., 1999; Young et al., 1999; Barbot et al., 2002; Edwards et al., 2006). The interesting properties of the SM and the last technological development increased the possibilities of practical implementations of SM algorithms (Herrmann et al., 2003; Chen and Peng, 2005; Lai et al., 2006; Hung et al., 2007).

In this work, a different approach is taken and an attempt to combine this two techniques is investigated.

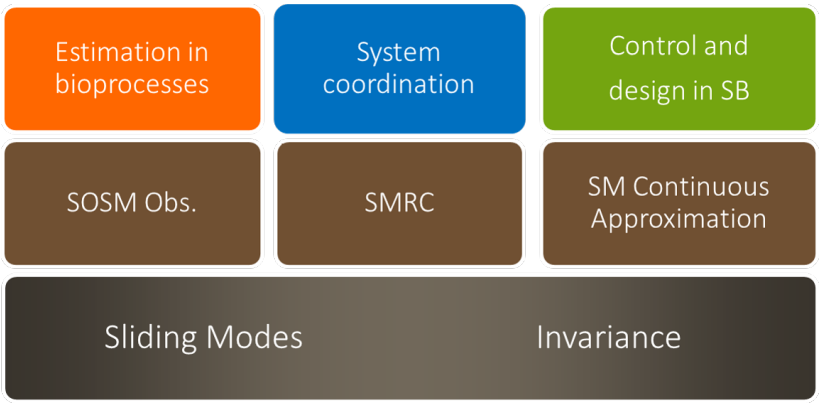

Figure 1.1: Thesis Road map. From Theory (bottom) to methodology to application(top).

Road map. Introduction to the introduction.

In a research project like a Thesis, is common to follow a linear path. Although, truth to be told is more interesting to follow the path lead by research itself (Alon, 2009) which is a convoluted path, and is far away of being a linear path. In this Thesis (Fig. 1.1) the path followed goes more in agreement with the second one explained. In order to help understand this path a brief raconteur will be performed.

Mainly all the work presented in this Thesis has a common underlying framework: Invariance and Sliding modes, as in the bottom of the Fig. 1.1 and this two are the fundamental building bricks of the subsequent work.

The first part uses both Invariance and Sliding Modes together with a methodology called Sliding Mode Reference Conditioning (SMRC, middle of Fig. 1.1), recently developed by collaborators, which combines those two building blocks to deal with constrained systems. Moreover, the work done here goes beyond and applies the SMRC methodology in order to deal with the problem of interconnected systems coordination in Part I (top of Fig. 1.1). In the next sections, the basics of Invariance (Section 1.1) and Sliding modes (Section 1.2) are introduced first and then SMRC methodology is presented in Section 1.3. This background is necessary in order to understand the application work which is integrated in Part I.

Continuing with the roadmap but in parallel, and motivated by the chattering problem (Section 1.2.5), second order sliding modes (SOSM, middle of Fig. 1.1) are exploited to design observers in order to robustly estimate kinetic rates in bioprocesses (top of Fig. 1.1), using different approaches to the design of the observers in Part II. In Section 1.4 a brief introduction of higher order sliding modes, with emphasis in second order sliding mode is performed. This is a key background for the design of second order sliding modes algorithms in Part II.

As a final stop in this journey, and motivated by the appearance of sigmoidal functions when modeling biological systems, continuous approximation of sliding mode control (CA and RD2, middle of Fig. 1.1, see section 1.5) is explored as an analytical framework for new understanding of biological systems. Using also invariance techniques, the invariance of a set (the boundary layer set) is proven for a system with a sigmoidal nonlinearity and a relative degree of two between the controlled output and the sigmoidal function. This framework is applied to the design and control of genetic circuits in synthetic biology approaches in Part III (top of Fig. 1.1).

1.1 Invariance

Invariant is something that never changes. An invariance property is a mathematical property of an object or space which remains unchanged after a number of transformations applied to it.

The concept of invariance in Control Theory naturally arises when dealing with stability and Lyapunov functions, since any cut of a Lyapunov function defines an invariant set. However, the invariance concept does not require the introduction of the notion of Lyapunov functions. More precisely, the idea of invariance for a set can be easily understood using a simple system in state space form:

$$\frac{dx(t)}{dt} = f(x(t)) \tag{1.1}$$

where $x \in \mathcal{O} \subseteq \mathbb{R}^{\mathrm{n}}$ and that there exist a globally defined solution, for all $t \geq 0$ for every initial condition $x(0) \in \mathcal{O}$.

Then a set $\mathcal{S} \subseteq \mathcal{O}$ is said to be invariant with respect to (1.1) if every trajectory of the system (1.1) with initial condition inside $\mathcal{S}$ remains inside $\mathcal{S}$ for $t > 0$.

Geometric set invariance

Consider the following dynamical system

$$\Sigma : \begin{cases} \dot{\boldsymbol{x}} = \boldsymbol{f}(\boldsymbol{x}) + \boldsymbol{g}(\boldsymbol{x})\boldsymbol{u}, \\ \boldsymbol{y} = \boldsymbol{h}(\boldsymbol{x}) \end{cases} \tag{1.2}$$

where $\boldsymbol{x} \in \mathbf{X} \subset \mathbb{R}^n$ is the state vector, $\boldsymbol{u} \in \mathbf{U} \subset \mathbb{R}^m$ is a control input (possibly discontinuous), $\boldsymbol{f} : \mathbb{R}^n \longrightarrow \mathbb{R}^n$ and $\boldsymbol{g} : \mathbb{R}^n \longrightarrow \mathbb{R}^n$ are vector fields, and $\boldsymbol{h} : \mathbb{R}^n \longrightarrow \mathbb{R}^b$, scalar fields; all of them defined in $\mathbf{X}$.

The variable $\boldsymbol{y}$ denotes the system output vector, which has to be bounded so as to fulfill $j = 1, \ldots, \mathrm{N}$ user-specified system constraints ϕ_i. The corresponding bounds on $\boldsymbol{y}$ are given by the set:

$$\Phi = \{\boldsymbol{x} \in \mathbf{X} \mid \phi_i(\boldsymbol{y}) \leq 0\}, \ i = 1, \ldots, \mathrm{N}. \tag{1.3}$$

From a geometrical point of view, the goal is to find a control input $\boldsymbol{u}$ such that the region Φ becomes a robust controlled invariant set (Blanchini and Miani, 2008) (*i.e.* trajectories originating in Φ remain in Φ for all times t).

To ensure the invariance of Φ Nagumo's *sub-tangenciality condition* must hold(Blanchini and Miani, 2008):

$$f(\boldsymbol{x}) + g(\boldsymbol{x})w \in \mathcal{T}_\Phi(\boldsymbol{x}), \ \forall \ \boldsymbol{x} \in \partial\Phi. \tag{1.4}$$

For instance, the control input $\boldsymbol{u}$ must guarantee that the right hand side of the first equation in (1.2) belongs to the tangent cone $\mathcal{T}_\Phi(\boldsymbol{x})$ at all points on the boundary of Φ, denoted by $\partial\Phi$, defined as:

$$\partial\Phi = \bigcup_{i=1}^{\mathrm{N}} \partial\Phi_i, \quad \partial\Phi_i = \{\boldsymbol{x} \in \Phi \mid \phi_i(\boldsymbol{y}) = 0\}. \tag{1.5}$$

The following assumption will be needed for later development, and will allow us to compute the gradient vector $\nabla\phi_j$ of the functions ϕ_i.

Assumption 1.1. All the ϕ_i functions are assumed to be differentiable in the boundary $\partial\Phi_i$

Mathematically, the invariance of Φ may be ensured by an input $\boldsymbol{u}$, such that, $\forall i$, $\dot{\phi}_i \leq 0$, when $\phi_i(\boldsymbol{y}) = 0$. In the context of convex sets, this

condition can be expressed as:

$$\begin{aligned}\dot{\phi}_i(\boldsymbol{x},\boldsymbol{d},\boldsymbol{u}) &= \nabla\phi_i^\top\dot{\boldsymbol{x}} = \|\nabla\phi_i\|\|\boldsymbol{f}+\boldsymbol{g}\boldsymbol{u}\|\cos\theta \\ &= \nabla\phi^\top\boldsymbol{f}+\nabla\phi^\top\boldsymbol{g}\boldsymbol{u} \\ &= L_f\phi_i+\boldsymbol{L_g}\phi_i\boldsymbol{u},\ \forall\boldsymbol{x}\in\partial\Phi_i,\ j=1,\ldots,\mathrm{N}, \quad (1.6)\end{aligned}$$

which constitute in standard form the *implicit invariance condition* (Amann, 1990; Mareczek et al., 2002):

$$\inf_{\boldsymbol{u}}\left\{\dot{\phi}_i(\boldsymbol{x},\boldsymbol{d},\boldsymbol{u})\leq 0,\ \forall\boldsymbol{x}\in\partial\Phi_i\right\},\quad j=1,\ldots,\mathrm{N}. \qquad (1.7)$$

Solving equation (1.7) for $\boldsymbol{u}$, results in the *explicit invariance condition* for system (1.2) and a particular constraint ϕ_i. The set $\mathcal{U}_i$ of feasible solutions is obtained:

$$\mathcal{U}_i(\boldsymbol{x},\boldsymbol{d})=\begin{cases}\boldsymbol{u}\in\{\mathbf{U}|L_f\phi_i+\boldsymbol{L_g}\phi_i\boldsymbol{u}\leq 0\}:\boldsymbol{x}\in\partial\Phi_i\wedge\boldsymbol{L_g}\phi_i\neq\mathbf{0}_{\mathrm{m}'}^\top \\ \text{empty}:\boldsymbol{x}\in\partial\Phi_i\wedge\boldsymbol{L_g}\phi_i=\mathbf{0}_{\mathrm{m}'}^\top\wedge L_f\phi_i>0 \\ \boldsymbol{u}=\text{free}:\boldsymbol{x}\in\partial\Phi_i\wedge\boldsymbol{L_g}\phi_i=\mathbf{0}_{\mathrm{m}'}^\top\wedge L_f\phi_i\leq 0 \\ \boldsymbol{u}=\text{free}\ :x\in\Phi\setminus\partial\Phi,\end{cases} \qquad (1.8)$$

where $\mathbf{0}_{\mathrm{m}}^\top$ denotes the $m-$dimensional null column vector, and the first set corresponding to $\boldsymbol{L_g}\phi_i\neq\mathbf{0}_{\mathrm{m}}^\top$ is always non empty.

Note that the control $\boldsymbol{u}$ in the interior of Φ can be freely assigned. Particularly, $\boldsymbol{u}=\mathbf{0}_{\mathrm{m}}^\top$, could be taken so that the system evolves autonomously throughout the interior of Φ. Then, the control action becomes active only when some constraint becomes active, i.e. when the state trajectory reaches the boundary $\partial\Phi$ trying to leave the set Φ. The invariance condition will hold if the intersection $\bigcap_i\mathcal{U}_i(\boldsymbol{x})$ for all constraints of the solution sets $\mathcal{U}_i(\boldsymbol{x})$ is not empty.

1.2 Sliding modes

A variable structure system (VSS) is composed by two or more subsystems and a logic which decides when the switching between those systems will take place. The resulting control law is a discontinuous function of the states of the system. When the switching frequency is elevated, a very interesting operation mode is obtained: the states of

the system are constrained to a manifold in the state space. This particular operation mode is named sliding mode (SM), and it presents very attractive features. Robustness to external disturbances and parametric uncertainties, the closed loop systems is order reduced and its dynamic is defined by the switching function.

The SM control principles will be explained in this section, following the general lines of (Sira-Ramírez, 1988, 1989).

1.2.1 Description of the sliding mode

Consider the following non-linear dynamical system:

$$\begin{cases} \dfrac{dx}{dt} = f(x) + g(x)u, \\ y(t) = h(x), \end{cases} \tag{1.9}$$

where $x \in \mathbf{X} \subset \mathbb{R}^n$ is the system state, $u \in \mathbb{R}$ the control signal (possibly discontinuous), $f : \mathbb{R}^n \longrightarrow \mathbb{R}^n$ and $g : \mathbb{R}^n \longrightarrow \mathbb{R}^n$ two vectorial fields in $\mathcal{C}^n$ (many times differentiable) and $h(x) : \mathbb{R}^n \longrightarrow \mathbb{R}$ a scalar field also in $\mathcal{C}^n$, all defined in $\mathbf{X}$, with $g(x) \neq 0$, $\forall x \in \mathbf{X}$. This kind of systems are named affine in control systems.

Define $s(x)$ as a smooth function on $\mathbf{X}$ like $s : \mathbf{X} \longrightarrow \mathbb{R}$, with $\nabla s \neq 0, \forall x \in \mathbf{X}$. Then the set

$$\mathcal{S} = \{x \in \mathbf{X} : s(x) = 0\}, \tag{1.10}$$

defines a locally regular manifold of $(n-1)$ dimension on $\mathbf{X}$, named *sliding manifold* or *switching surface*.

A variable structure control law can be defined to enforce the control action u to take one of two different values according to the sign of the switching function $s(x)$ (often addressed as an auxiliary output),

$$u = \begin{cases} u^+(x) & \textit{if} \quad s(x) > 0 \\ u^-(x) & \textit{if} \quad s(x) < 0 \end{cases} \qquad u^-(x) \neq u^+(x) \tag{1.11}$$

where the upper and lower values of u are smooth functions of x and, without loss of generality, they are assumed to satisfy $u^-(x) < u^+(x)$ and $u^-(x) \neq u^+(x)$ locally in $\mathbf{X}$.

Then a sliding mode will exist on $\mathcal{S}$, as a result of the switching law (1.11), when the system reaches the manifold $\mathcal{S}$ and stays locally in its

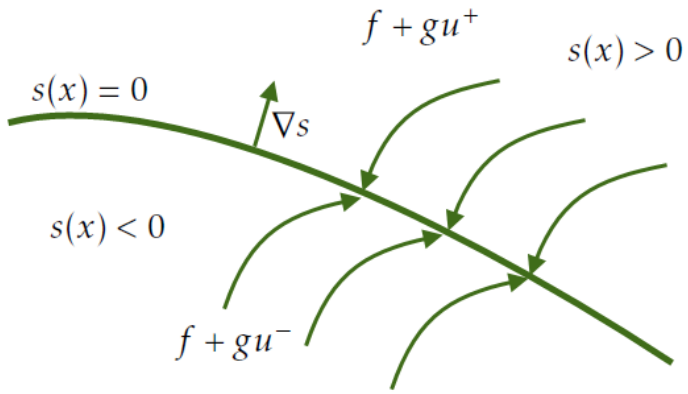

Figure 1.2: Sliding regime on the switching manifold $s(x) = 0$

neighborhood. For a sliding regime to exist on $\mathcal{S}$, both controlled vector fields of each continuous subsystem, $(f + gu^+)$ and $(f + gu^-)$, should point locally towards the manifold $\mathcal{S}$.

The geometrical representation of the previous situation is depicted in figure 1.2. The necessary conditions that must hold will be shown in the next section.

1.2.2 Sliding mode existence necessary condition

The objective of this section is to determine which conditions must hold to ensure that a sliding mode sets up in the surface $s(x) = 0$. It has been mentioned before that both controlled vector fields switched by 1.11 should point towards the manifold $\mathcal{S}$. This implies mathematically that:

If the next inequalities hold for the switching function, locally on $\mathcal{S}$ as a result of the control action (1.11):

$$\begin{cases} \dot{s}(x) < 0 & \textit{if} \quad s(x) > 0 \\ \dot{s}(x) > 0 & \textit{if} \quad s(x) < 0 \end{cases} \tag{1.12}$$

then the state trajectories of the system (1.9) locally reach the sliding manifold $\mathcal{S}$ and, from there on, their motion is constrained to immediate

vicinity of $\mathcal{S}$.

Before continuing, it will be useful to know some notions of differential geometry, to take advantage of the natural geometric interpretation of some sliding mode related concepts.

Consider a scalar field $h(x) : \mathbb{R}^n \longrightarrow \mathbb{R}$ and a vectorial field $f(x) : \mathbb{R}^n \longrightarrow \mathbb{R}^n$, then the *Lie derivative* of the scalar field h in the direction of the field f denoted by

$$L_f h(x) : \mathbb{R}^n \longrightarrow \mathbb{R}$$

is defined as:

$$L_f h(x) = \frac{dh}{dx} f$$

Lets note that $L_f h(x)$ is a scalar operator and it can be applied in a recursive way:

$$L_f^k h(x) = \frac{\partial}{\partial x}\Big(L_f^{k-1} h(x)\Big) f(x)$$

In this way, a compact notation of scalar function derivatives in the direction of vectorial fields, either in the direction of a single vector field or various vector fields. For example in the case of two fields $f(x)$ and $g(x)$:

$$L_g L_f h(x) = \frac{\partial}{\partial x}(L_f h(x)) g(x)$$

Like every derivative, the *Lie derivative* is a linear operator. Then taking derivative of the switching function $s(x)$ one gets

$$\dot{s}(x) = L_{f+gu} s(x) = L_f s(x) + L_g s(x) u \tag{1.13}$$

The using the last differential geometry tools, equation (1.12) can be rewritten using the first equality of (1.13),

$$\begin{cases} \lim\limits_{s(x)\to 0^+} L_{f+gu^+} s(x) < 0 \\ \lim\limits_{s(x)\to 0^-} L_{f+gu^-} s(x) > 0 \end{cases} \tag{1.14}$$

This last equation implies the rate of change of the scalar surface coordinate function $s(x)$, measured in the direction of the controlled field, is such that a crossing of the surface is guaranteed, from each side of the

surface, by use of the switching policy (1.11). The same can be written in a more compact form:

$$\lim_{s(x)\to 0} s(x)\cdot \dot{s}(x) < 0. \tag{1.15}$$

Then thanks of the linearity properties of the *Lie derivative*, equation (1.13) can be expressed in a equivalent way:

$$\begin{cases} L_f s + L_g s u^+ < 0 \quad if \quad s > 0 \\ L_f s + L_g s u^- > 0 \quad if \quad s < 0 \end{cases} \tag{1.16}$$

Note: From now on, we will drop parenThesis unless we want to expressly show some function dependance from a particular variable.

So in order to establish the sliding mode on $s(x) = 0$ the following should be satisfied

$$L_g s = \frac{\partial s}{\partial x} g \neq 0 \tag{1.17}$$

locally in $\mathcal{S}$. The previous condition is a necessary reaching condition for sliding mode, and is known as *transversality condition*.

Remark 1.1. Supposing, without loss of generality, that $u^-(x) < u^+(x)$ is satisfied, then the necessary existence condition of a sliding regime over $\mathcal{S}$ is given by

$$L_g s = \frac{\partial s}{\partial x} g < 0 \tag{1.18}$$

locally in a vicinity of $\mathcal{S}$.

The demonstration is immediate from (1.16): subtracting both expressions for $\dot{s}$ it must hold

$$\left(u^+(x) - u^-(x)\right) L_g s < 0$$

And as it was $u^+(x) - u^-(x) > 0$, the condition becomes $L_g s < 0$.

Anyway, the transversality condition is only a necessary condition, but not a sufficient one to guarantee the existence of the sliding mode. In the Section 1.2.4 we will see a necessary and sufficient condition.

1.2.3 Equivalent control method

The system in a sliding regime, ideally implies infinite frequency switching, *i.e.*, is discontinuous at every time instant. This precludes obtaining

an analytical solution of the state equation. One way to obtain the sliding mode dynamics consist in finding a continuous system equivalent to the sliding mode. To this end, the *ideal sliding mode* is the regime of ideal operation in which the manifold $\mathcal{S}$ is an invariant manifold of the system. In this conditions, once the system trajectories reach the manifold, they slide exactly on the manifold and never leave it. The invariance condition of the manifold $\mathcal{S}$ is given by:

$$\begin{cases} s(x) = 0 \\ \dot{s}(x) = L_f s(x) + L_g s(x) u_{eq} = 0 \end{cases} \tag{1.19}$$

The second equation of (1.19) indicates the trajectories will remain on the surface, meanwhile $u_{eq}(x)$ represents a smooth control law for which $\mathcal{S}$ is an invariant manifold of the system. Then the control $u_{eq}(x)$ is known as *equivalent control* and it can be cleared from (1.19), resulting:

$$u_{eq}(x) = -\frac{L_f s(x)}{L_g s(x)} \tag{1.20}$$

In equation (1.20) it is possible to see the transversality condition (1.17) is a necessary and sufficient condition for the well definition of the equivalent control.

1.2.4 A necessary and sufficient condition for existence of Sliding Mode

By definition, the equivalent control action, is the necessary continuous control to make the trajectories of the system remain in the invariant manifold. As a consequence, the derivative of the switching function, should also be zero along that trajectory:

$$\dot{s}(x) = L_f s + L_g s u_{eq} = 0 \tag{1.21}$$

which was established in the invariance condition (1.19) of the manifold $\mathcal{S}$.

The next theorem, demonstrated in (Sira-Ramírez, 1988), defines a necessary and sufficient condition for the existence of a sliding mode, in terms of the equivalent control u_{eq}.

Theorem 1.1. *Let $u^-(x) < u^+(x)$ and $L_g s < 0$, a necessary and sufficient condition for the local existence of a sliding regime on $\mathcal{S}$, that is locally in $\mathbf{X}$ for $x \in \mathcal{S}$,*

$$u^-(x) < u_{eq}(x) < u^+(x) \tag{1.22}$$

In other words, the equivalent control $u_{eq}(x)$ is a kind of average between the lower and upper bounds of the control action. The discontinuous control action can be interpreted as the sum of a low frequency component ($u_{eq}(x)$) and a high frequency one which is filtered out by the system.

1.2.5 Discontinuous Control Action in Sliding Mode Control. Chattering Problem

One of the main drawbacks of the first-order sliding-mode control in certain applications is the direct use of discontinuous control actions. In actual implementations, the discontinuous control law, together with unmodelled dynamics and finite switching frequency, may produce fast oscillations in the outputs of the system. This effect is known as *chattering* phenomenon. During the mid-1980s, the following three main approaches to reduce chattering in sliding-mode controlled systems were proposed (Bondarev et al., 1985):

- The use of a saturation control instead of the discontinuous action (Slotine and Li, 1991). This well-established approach allows the control to be continuous, restraining the system dynamics not strictly onto the sliding manifold, but within a thin boundary layer of the manifold. This method ensures the convergence to the boundary layer, whose size is defined by the slope of the saturation linear region.

- The observer-based approach (Bondarev et al., 1985; Utkin et al., 1999). This method allows bypassing the plant dynamics by the chattering loop. This approach successfully reduces the problem of robust control to the problem of exact robust estimation. However, in some applications it can be sensitive to the plant uncertainties, due to the mismatch between the observer and plant dynamics (Young et al., 1999).

- The Higher-Order Sliding-Mode approach (HOSM) (Levant, 2003). This method allows the finite-time convergence of the sliding variable and its derivatives. This approach was actively developed

since the 1990s (Bartolini et al., 1998, 2003; Levant, 2003), not only providing chattering attenuation, but also robust control of plants of relative degree one and higher. Theoretically, an r-order sliding mode would totally suppress the chattering phenomenon in the model of the system (but not in the actual system) when the relative degree of the model of the plant (including actuators and sensors) is r. Yet, no model can fully account for parasitic dynamics, and, consequently, the chattering effect cannot be totally avoided. Nevertheless, theoretical results in HOSM, especially Second-Order Sliding-Mode algorithms, have been successfully proven in practice, encouraging the progress of the research activities.

1.3 Sliding Mode Reference Conditioning

The concept of reference conditioning to achieve a realizable reference, arises in the context of control with restrictions. Specifically, Hanus and Walgama (Hanus et al., 1987; Walgama et al., 1992) applied this kind of solutions to solve the problem of saturation in the actuators (windup). Based on these approaches and getting advance of the possibilities of sliding modes, Mantz and De Battista (2002); Mantz et al. (2004); Garelli et al. (2006b) have applied sliding mode reference conditioning (SMRC) to obtain realizable references under restrictions both in the actuators, in the outputs or in any state or combination of states.

The sliding control loop appears here as an additional loop that makes the reference realizable under certain constraints instead of representing the main control loop. In that way, in contrast with conventional variable structure controllers and sliding modes, the sliding regime is intended as a transitional operation mode.

The conditioning loop is inactive until the system state reaches by itself the sliding surface. It becomes inactive again, when the closed loop system is able to operate again in the non-constrained zone.

It is important to note that, due to the special characteristic of this application, the typical drawbacks of variable structure control and sliding modes (*i.e.* chattering and reaching modes) are avoided.

Now, in order to find the necessary $\boldsymbol{u}$ to achieve the invariance of some set $\Phi(y)$ (1.3), with the system Σ (1.2), consider the following implementation (Fig. 1.3).

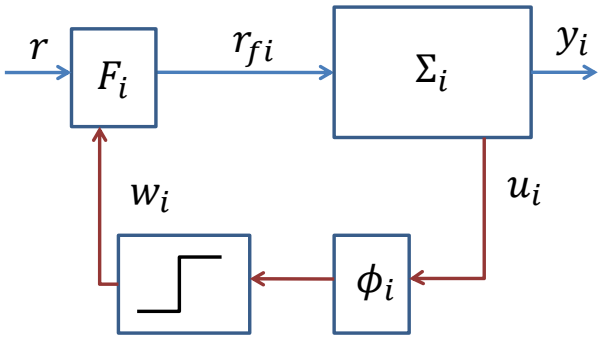

Figure 1.3: SM Reference conditioning general scheme.

A discontinuous decision block, will drive the search to find $\boldsymbol{u} \in \mathcal{U}_i(\boldsymbol{x})$ so as to fulfill the constraint $\Phi(y)$ and make $\boldsymbol{r}_f$ remain as close as possible to the external signal $\boldsymbol{r}$. Also, a filter F is incorporated. Its purpose is to filter out the conditioned signal r_f, in order to feed the system Σ with a smooth signal.

The filter F is implemented as the first-order filter

$$\dot{\boldsymbol{r}}_f = -\Lambda\left(\boldsymbol{r}_f + \boldsymbol{u} - \boldsymbol{r}\right), \tag{1.23}$$

where $\boldsymbol{u} \in \mathbf{U} \subset \mathbb{R}m'$ is the discontinuous control action, $\boldsymbol{r}$, $\boldsymbol{r}_f \in \mathbb{R}^{m'}$ are the input and the conditioned input signal, and $\Lambda \in \mathbb{R}^{m'}$ is a diagonal matrix, a design parameter of the filter.

The discontinuous decision block is implemented by means of the variable structure control law:

$$u = \begin{cases} 0 & \text{if} \quad \max_i\{\phi_i(\boldsymbol{y})\} \leq 0 \\ \boldsymbol{u}_{SM} & \text{otherwise,} \end{cases} \tag{1.24}$$

where $\phi_i(\boldsymbol{y})$ are the constraints defined previously, *i.e.* the boundaries of the set Φ, and $\boldsymbol{u}_{SM}$ is such that $u \in \bigcap_i \mathcal{U}_i(\boldsymbol{x})$.

Notice that the block Σ in Fig. 1.3 represents the entire dynamics from the constrained variables $(\boldsymbol{y})$ to the input signal $\boldsymbol{u}$. Then the sys-

tem (1.2) becomes:

$$\begin{cases} \dot{\boldsymbol{x}} = \boldsymbol{f}(\boldsymbol{x}, \boldsymbol{d}) + \boldsymbol{g}(\boldsymbol{x})\boldsymbol{r}_f, \\ \dot{\boldsymbol{r}}_f = -\Lambda\left(\boldsymbol{r}_f + \boldsymbol{u} - \boldsymbol{r}\right), \\ \boldsymbol{y} = \boldsymbol{h}(\boldsymbol{x}) \end{cases} \tag{1.25}$$

In the case of a control system, (1.2) is the plant dynamic together with a control loop, in which case $\boldsymbol{r}_f$ is the reference, and $\boldsymbol{x}$ in (1.2) is the extended state comprising the plant and controller.

The choice of $\boldsymbol{u}_{SM}$ depends on whether there is only one active constraint or more than one. For a single active constraint, the analysis is very similar to that of a SMRC in a SISO system (Vignoni et al., 2011, 2012b; Garelli et al., 2011), and is the approach we will use hereafter. The case of several active constraints (see Gracia et al. (2012)), is not analyzed in this work since we are defining only one constraint per system in the formation control problem.

1.4 Higher Order Sliding Mode

As discussed in Section 1.2, first-order sliding-mode control has certain properties that make it particularly attractive to apply to uncertain nonlinear systems. Among them, it can be highlighted finite convergence to the surface, system order reduction and robustness against certain disturbances. In this context, Higher-Order Sliding-Mode control will inherit some of these properties. This control approach generalizes the idea of first-order sliding mode, by acting on the higher-order derivatives of the constraint function $s(x)$, instead of influencing the first derivative (as in (1.13)).

Keeping the main advantages of the original approach, the HOSM control works with continuous action over $\dot{s}(x)$, relegating the discontinuous control to operate on the higher derivatives of $s(x)$. This weakens the effect of chattering in the output, providing greater accuracy in realization. Additionally, in some applications (namely, plants with relative degree 1 with respect to s), the resultant physical control input to the plant is continuous, contributing to the longer service life of certain actuators. A significant number of these controller proposals can be found in (Bartolini et al., 1998, 2003; Levant, 2003)

1.4.1 Sliding Mode order

An important concept in HOSM is the notion of sliding order. If the goal is to maintain a constraint given by $s(x) = 0$, the sliding order is defined as the number of continuous time derivatives of $s(x)$ (including the zero-order one) in the vicinity of a sliding point.With these considerations, a sliding mode of order r is determined by the following equalities:

$$s = \dot{s} = \ddot{s} = \ldots = s^{(r-1)} = 0 \tag{1.26}$$

Expression (1.26) represents an r-dimensional condition in the dynamic system, which implies an order reduction of r (that is, (1.26) specifies r algebraic equations that bond the state variables).

1.4.2 Regularity conditions

Reconsider the constraint given by $s(x) = 0$, where $s : \mathbb{R}^n \to \mathbb{R}$ is a function smooth enough. Assume also that the time derivatives of $s(x)$, i.e. $\dot{s}, \ddot{s}, \ldots, s^{(r-1)}$ exist and are single-valued functions of x (which is not trivial in discontinuous dynamical systems). Recall that the discontinuity does not appear in the first $r-1$ derivatives of the constraint function s, or analogously, s is an output of relative degree r with respect to the discontinuous input. When these assumptions hold, the sliding set of order r will be unequivocally determined by (1.26), implying that the reduced system dynamics has order $n - r$. Now consider a manifold S given by the equation s(x) = 0. Suppose that $s, \dot{s}, \ddot{s}, \ldots, s^{(r-1)}$ are smooth functions of x and

$$\operatorname{rank}\{\nabla s, \nabla \dot{s}, \nabla \ddot{s}, \ldots, \nabla s^{(r-1)}\} = r \tag{1.27}$$

holds locally. Then, since all $S_i, i = 1, ..., r-1$, are smooth manifolds, S_r is a differentiable manifold determined by (1.26). Recall that the rank of a set of vectors indicates the dimension of the subspace they define. Equation 1.27, together with the requirement that the corresponding time derivatives of s are smooth functions of x, is referred to as the *sliding regularity condition* (Levant, 2001; Fridman and Levant, 2002).

1.4.3 Convergence time

Convergence in HOSM can be either asymptotic or in finite time. Examples of asymptotically stable sliding-mode algorithms of arbitrary order

are well known in the literature (Fridman and Levant, 2002). On the other hand, fewer examples can be cited for r-sliding controllers that converge in finite time. For instance, these can be found for $r = 1$ (which is trivial), for $r = 2$ (Bartolini et al., 1998, 2003; Levant, 2003) and for $r = 3$ (Levant, 2001; Fridman and Levant, 2002). Despite the fact that some arbitrary-order sliding-mode controllers of finite-time convergence have already been presented (Levant, 2005), its implementation is not yet widespread.

1.4.4 Second Order Sliding Mode

Consider the uncertain nonlinear system (initially, not necessarily affine in the control), explicitly defined as

$$\begin{cases} \dot{x} = F(x, u, t) \\ s = s(x, t) \in \mathbb{R} \\ u = U(x, t) \in \mathbb{R} \end{cases} \tag{1.28}$$

with $x \in \mathbb{R}$, u the single control input, and F and s smooth functions. Note that in this section the possible direct dependence on t has been explicitly manifested in system (1.28), in order to better explain the subsequent SOSM design procedure.

As always, the ultimate control objective would be steering the sliding output s to zero. However, the SOSM approach enables not only that $s = 0$ and its time derivative $\dot{s} = 0$, but also finite time stabilisation of both, as long as s is of relative degree 1 or 2 with respect to the control input u. Moreover, in the former case the physical control action synthesised by the SOSM algorithm is continuous.

The SOSM design procedure depends on the bounds of certain functions that constitute the second time derivative of the sliding output s. Hence, as a first step, s is differentiated twice, and the following general expressions are derived:

$$\dot{s} = \frac{\partial}{\partial t} s(x, t) + \frac{\partial}{\partial x} s(x, t) F(x, u, t) \tag{1.29}$$

$$\ddot{s} = \frac{\partial}{\partial t} \dot{s}(x, t) + \frac{\partial}{\partial x} \dot{s}(x, t) F(x, u, t) + \frac{\partial}{\partial u} \dot{s}(x, t) \dot{u}(t) \tag{1.30}$$

Then, two different cases will be addressed, depending on the relative degree of s with respect to input u. Systems with relative degree 1 will be considered.

1.4.4.1 Systems with relative degree 1

In relative degree 1 systems, u appears in $\dot{s}$, thus in the expression of $\ddot{s}$ the derivative $\dot{u}$ is explicitly presented in affine form, as in (1.30). Therefore the last expression can be given as follows:

$$\ddot{s} = \varphi(x, u, t) + \gamma(x, u, t)\dot{u}(t) \tag{1.31}$$

with $\varphi(x, u, t)$ and $\gamma(x, u, t)$ uncertain but uniformly bounded functions in a bounded domain. In order to specify the control problem, the following conditions must be assumed (Levant, 1993):

1. There are bounds Γ_m and Γ_M such that within the region $|s(x, t)| < s_0$ the following inequality holds for all $t, x \in \mathcal{X}, u \in \mathcal{U}$:

$$0 < \Gamma_m \leq \gamma(x, u, t) = \frac{\partial}{\partial u}\dot{s}(x, t) \leq \Gamma_M \tag{1.32}$$

   The constant s_0 defines a region of operation around the sliding manifold, where the bounds are valid. Note that, eventually, an appropriate control action has to be included in the controller, in order to attract the system into this validity region.

2. There is also a bound Φ that, within the region $|s(x, t)| < s_0$,

$$|\varphi(x, u, t) = \frac{\partial}{\partial t}\dot{s}(x, t) + \frac{\partial}{\partial x}\dot{s}(x, t)F(x, u, t)| \leq \Phi \tag{1.33}$$

   for all $t, x \in \mathcal{X}, u \in \mathcal{U}$

With these bounds at hand, the following differential inclusion can be proposed to replace (1.31) (Levant, 2005):

$$\ddot{s} \in [-\Phi, \Phi] + [\Gamma_m, \Gamma_M]\dot{u}(t) \tag{1.34}$$

This is a very important relation when considering robustness. As it will be demonstrated in the following subsection, many SOSM controllers ensure finite time stabilisation of both $s(x, t) = 0$ and $\dot{s}(x, t) = 0$, not merely for the nominal original system, but for (1.34). Since the differential inclusion does not remember whether or not the original system (1.28) is perturbed (it will include both cases, as far as perturbations had been computed into the bounds), then such a controller will be obviously robust with respect to any perturbation or uncertainty existing in (1.28) and, consequently, translated to (1.34).

1.5 SM Continuous approximation and Relative degree 2

As discussed in Section 1.2.5, in first-order sliding-mode control a saturation control can be used instead of the discontinuous action (Slotine and Li, 1991). This well-established approach allows the control to be continuous, restraining the system dynamics not strictly onto the sliding manifold, but within a boundary layer neighboring the switching surface:

$$B(t) = \{\boldsymbol{x} \in \mathbf{X} \mid s(\boldsymbol{x}, t) \leq \Upsilon\}, \Upsilon > 0 \tag{1.35}$$

This method ensures the convergence to the boundary layer, whose size is defined by the slope of the saturation linear region.

Ultimately boundedness of the set $B(t)$ was shown in Esfandiari and Khalil (1991) for systems where the relative degree between the output and the control signal is unitary.

In the last part of this work, invariance of a set similar to $B(t)$ is shown for systems where the relative degree between the output and the control signal is two.

1.6 Motivation

In the following lines there is an attempt to motivate the different problems that have been addressed within this Thesis. As the topics are broad and apart to some extent, it will be done in a separate way.

1.6.1 Coordination and interconnected systems

When the designer tries to address a control problem, many questions related to modelling accuracy, controller complexity, kind of design approach, etc, arise in mind and, therefore, many choices have to be made.

Any system is a group of two or more parts (subsystems) which interact functioning as a whole. In fact the word system, cames from late Latin *systema* and from Greek $\sigma\acute{\upsilon}\sigma\tau\eta\mu\alpha$ "organized whole, body," from *syn-* "together" + root of *histanai* "cause to stand". Moreover, when evolving from systems with simple behavior (at least in the beginning) to networks of such systems, emerging from the interaction between

those simple systems, a new *emergent* behavior arises, more rich and complex than just the sum of individual ones.

The topology of the interaction network and also *how* these systems interact will determine the complexity of the collective behavior (Jensen, 1998) in such way that understanding this connections and the coordination of those systems is essential in order to analyze and perhaps design superior kinds of organization.

Moreover, nature has many examples of individual systems getting together and organizing to form a superior kind of organization with its inherent complexity. Fenomena like bird flocking, fish schooling and consensus in general, are inspirational concepts when the time to analyze and design coordination strategies. Wise implementation, is much more easy to go for an electromechanical setup, for instance, of mobile robots or unmanned aerial vehicles, than a population of ant or a group of birds. For this reason, but without forgetting the original inspiration by nature, the systems involved in this work will be referred just as systems in general.

Paraphrasing Richard Feynman's "What I cannot create I do not understand.", creating and designing coordination and control of a collection / group of systems is an essential part for understanding the interaction between systems and the emergence of complexity. In this work, an attempt to design coordination in electromechanical systems is done.

1.6.2 Estimation in Bioprocesses

White biotechnology, this is using enhanced microorganisms as cell factories, to produce enzymes and/or high-added values specialty biopolymers is of paramount importance for the future of process industries. This notion of small-scale, advanced, highly-responsive flexible manufacturing facilities for the production of new, low-tonnage, high-added value products (factories of the future), where competitive advantage is achieved through innovation and highly automated processes.

The better knowledge about the microorganisms involved and its optimization using Synthetic Biology tools, needs to be complemented by knowledge of automatic control methods and estimation allowing the desired culture profiles and specifications to be achieved in an industrial setting.

Bioprocesses are characterized by complex dynamic behavior, non-

linearities, model uncertainty, unpredictable parameter variations, etc.. In addition, most representative variables are typically not accessible for on-line measurement. Consequently, bioprocess control and monitoring is a difficult task in general. In this context, the development of robust and reliable algorithms to estimate key variables and parameters of the process is of prime interest, and extended work has been carried out in this field (Bastin and Dochain, 1986).

1.6.3 Control theory in synthetic biology

In the design, optimization and control of bioprocesses, the population of microorganism has been typically considered as an aggregate quantity, characterized by average properties. Although it is a fact that even isogenetic (i.e. with the same genetic content) microbial populations have certain degree of heterogeneity. Indeed, individual microorganisms, even if part of a "clonal" or isogenetic population, may differ greatly in terms of genetic composition, physiology, biochemistry, or behaviour (Elowitz et al., 2002). This heterogeneity at the population level has been shown to be one of the causes of decrease in productivity when scaling-up to an industrial production fermentation process (Lencastre Fernandes et al., 2011).

Thus, it is evident that the appearance of control theory (Sontag, 2004) in synthetic biology approaches is essential and that protein production control and indeed heterogeneity and variability reduction at the microorganisms level are appealing goals for the biotechnology industry.

1.7 Scope and objectives

The main objective of this work is to explore the possibilities of invariance principles to design new methodologies and to apply them in different fields. With this in mind, this Thesis is focused in contributing to the following problems:

- Systems Coordination: designing methodologies for coordination of sets of constrained systems. The systems involved may have different dynamics and constraints and no need to be identical. Centralized and decentralized strategies have been developed to

deal with the coordination problem using sliding modes reference conditioning and set invariance ideas.

- Unknown input estimation: designing robust observers with second order sliding mode algorithms. Moreover, guaranteeing performance indexes in systems with presence of noise, model mismatches and disturbances. Applications to estimation of kinetic rates in bioprocesses.

- Systems and control design in genetic circuits: reducing the variance in protein production when working with synthetic gene network. Using negative feedback control and quorum sensing strategies to reduce the variance

In the last stages of the work, modelling and experimental data collection from real plants has been undertaken. The estimation methodologies have been validated in practice, and there is ongoing work on testing the theoretical results from this Thesis on these platforms.

1.8 Thesis outline

The manuscript is organized in three blocks:

Part I deals with coordination of dynamical systems using sliding mode reference conditioning and set invariance ideas. Chapters 2 and 3 are more abstract approaches to systems coordination focusing on the methodology design. Chapter 2 corresponds to the following journal paper:

- VIGNONI, A., GARELLI, F. and PICÓ, J. Coordinación de sistemas con diferentes dinámicas utilizando conceptos de invarianza geométrica y modos deslizantes. *Revista Iberoamericana de Automática e Informática Industral (RIAI)*, vol. 10(4), pages 390–401, 2013a

It deals with a unified approach, involving global and local solutions to the coordination problem in SISO systems with no perturbations. As the article is published in Spanish so will be the chapter 2. This chapter is based in turn in the following international conferences papers (refer to them for an English version):

- VIGNONI, A., PICÓ, J., GARELLI, F. and DE BATTISTA, H. Dynamical systems coordination via sliding mode reference conditioning.

In *Proceedings of the 18th IFAC ...*, vol. 18 of *1*, pages 11086–11091. 2011

- VIGNONI, A., PICÓ, J., GARELLI, F. and DE BATTISTA, H. Sliding mode reference conditioning for coordination in swarms of non-identical multi-agent systems. In *Variable Structure Systems, 12th IEEE International Workshop on*, pages 231–236. Mumbai, India, 2012b. ISBN 9781457720673

The Chapter 3 corresponds to the following journal paper:

- VIGNONI, A., GARELLI, F. and PICÓ, J. Sliding Mode Reference Coordination of constrained feedback systems. *Mathematical Problems in Engineering*, vol. 2013(Article ID 764348), page 12 pages, 2013b

Chapter 4, the final chapter of this part, on the contrary deals with a practical problem on formation control for unmanned aerial vehicles (UAVs) and is based in the international conference article:

- VIGNONI, A., GARELLI, F., GARCÍA-NIETO, S. and PICÓ, J. UAV reference conditioning for formation control via set invariance and sliding modes. In *3rd IFAC Workshop on Distributed Estimation and Control in Networked Systems*, pages 317–322. Santa Barbara, CA, USA, 2012a

The second Part, focus on the design of second order sliding mode observers with application to specific growth rate estimation in bioprocesses. Chapters 5, 6 and 7 correspond to the following journal papers:

- DE BATTISTA, H., PICÓ, J., GARELLI, F. and VIGNONI, A. Specific growth rate estimation in (fed-)batch bioreactors using second-order sliding observers. *Journal of Process Control*, vol. 21(7), pages 1049–1055, 2011. ISSN 09591524

- PICÓ, J., PICÓ-MARCO, E., VIGNONI, A. and DE BATTISTA, H. Stability preserving maps for finite-time convergence: Super-twisting sliding-mode algorithm. *Automatica*, vol. 49(2), pages 534–539, 2013. ISSN 00051098

- NUÑEZ, S., DE BATTISTA, H., GARELLI, F., VIGNONI, A. and PICÓ, J. Second-order sliding mode observer for multiple kinetic rates

estimation in bioprocesses. *Control Engineering Practice*, vol. 21(9), pages 1259–1265, 2013

These articles are evidently the result of a coordinated effort of a research group and a fruitful collaboration between the present research group in Spain and the former and alma mater research group in Argentina. Thus, a short description of the authors respective contributions will be assessed in order to clarify the actual contribution of the author of this Thesis in those articles.

In De Battista et al. (2011), H.D.B. had the original transformation idea; all the authors conceived the research project and H.D.B. and J.P. supervised the project. H.D.B and F.G. designed the observer. A.V. designed and developed the stability analysis and solved the GEVP problem. H.D.B. performed the simulations. J.P. provided experimental data to validate the design and J. P. and A.V. analysed the experimental results. H.D.B and A.V. wrote the manuscript.

In Picó et al. (2013), J.P. and H.D.B. had the idea and supervised the project. J.P. and A.V. worked in the constructive design and developed the stability analysis with support of E.P.M. for the stability preserving map theorem. A.V. performed the finite time convergence analysis and the simulations. J. P., A.V. and H.D.B analyzed the results. J.P. and A.V. wrote the manuscript.

In Nuñez et al. (2013), H.D.B. had the idea; all the authors conceived the research project and H.D.B. and F.G. supervised the project. H.D.B and F.G. and S.N. designed the observer. A.V. designed and developed the stability analysis and solved the BMI problem. S.N. performed the simulations. J.P. provided experimental data to validate the design and J. P., H.D.B., F.G, S.N. and A.V analyzed the experimental results. S.N. and H.D.B. wrote the manuscript.

At the end of Part II, in Chapter 8 a proof of concept by simulation is performed in order to test the estimators in a closed loop set up. This chapter corresponds to the following international conference paper:

- VIGNONI, A., NUÑEZ, S., DE BATTISTA, H., PICÓ, J., PICÓ-MARCO, E. and GARELLI, F. Specific Kinetic Rates Regulation in Multi-Substrate Fermentation Processes. In *12th International Symposium on Computer Applications in Biotechnology*, in press. 2013c

Finally, Part III changes subject and approaches the design of genetic networks in synthetic biology with a control systems approach and

set invariance ideas. This chapter corresponds to the following international conference paper:

- VIGNONI, A., OYARZÚN, D. A., PICÓ, J. and STAN, G.-B. Control of protein concentrations in heterogeneous cell populations. In *2013 European Control Conference (ECC)*, pages 3633–3639. 2013d

The Thesis ends with a summary of the main conclusions extracted from the research work and some ideas about interesting problems for future work.

1.9 Publications

The research work done within this Thesis has led to several publications, listed below.

Referred journal papers

VIGNONI, A., OYARZÚN, D. A., PICÓ, J. and STAN, G.-B. Control of protein concentrations in heterogeneous cell populations. (in revision), 2014

VIGNONI, A., GARELLI, F. and PICÓ, J. Coordinación de sistemas con diferentes dinámicas utilizando conceptos de invarianza geométrica y modos deslizantes. *Revista Iberoamericana de Automática e Informática Industral (RIAI)*, vol. 10(4), pages 390–401, 2013a

VIGNONI, A., GARELLI, F. and PICÓ, J. Sliding Mode Reference Coordination of constrained feedback systems. *Mathematical Problems in Engineering*, vol. 2013(Article ID 764348), page 12 pages, 2013b

PICÓ, J., PICÓ-MARCO, E., VIGNONI, A. and DE BATTISTA, H. Stability preserving maps for finite-time convergence: Super-twisting sliding-mode algorithm. *Automatica*, vol. 49(2), pages 534–539, 2013. ISSN 00051098

DE BATTISTA, H., PICÓ, J., GARELLI, F. and VIGNONI, A. Specific growth rate estimation in (fed-)batch bioreactors using second-order sliding observers. *Journal of Process Control*, vol. 21(7), pages 1049–1055, 2011. ISSN 09591524

NUÑEZ, S., DE BATTISTA, H., GARELLI, F., VIGNONI, A. and PICÓ, J. Second-order sliding mode observer for multiple kinetic rates estimation in bioprocesses. *Control Engineering Practice*, vol. 21(9), pages 1259–1265, 2013

Referred Conference papers

VIGNONI, A., NUÑEZ, S., DE BATTISTA, H., PICÓ, J., PICÓ-MARCO, E. and GARELLI, F. Specific Kinetic Rates Regulation in Multi-Substrate Fermentation Processes. In *12th International Symposium on Computer Applications in Biotechnology*, in press. 2013c

VIGNONI, A., OYARZÚN, D. A., PICÓ, J. and STAN, G.-B. Control of protein concentrations in heterogeneous cell populations. In *2013 European Control Conference (ECC)*, pages 3633–3639. 2013d

VIGNONI, A., PICÓ, J., GARELLI, F. and DE BATTISTA, H. Sliding mode reference conditioning for coordination in swarms of non-identical multi-agent systems. In *Variable Structure Systems, 12th IEEE International Workshop on*, pages 231–236. Mumbai, India, 2012b. ISBN 9781457720673

VIGNONI, A., PICÓ, J., GARELLI, F. and DE BATTISTA, H. Dynamical systems coordination via sliding mode reference conditioning. In *Proceedings of the 18th IFAC . . .* , vol. 18 of *1*, pages 11086–11091. 2011

VIGNONI, A., GARELLI, F., GARCÍA-NIETO, S. and PICÓ, J. UAV reference conditioning for formation control via set invariance and sliding modes. In *3rd IFAC Workshop on Distributed Estimation and Control in Networked Systems*, pages 317–322. Santa Barbara, CA, USA, 2012a

DE BATTISTA, H., PICÓ, J., GARELLI, F. and VIGNONI, A. Specific growth rate estimation in bioreactors using second-order sliding observers. In *11th International Symposium on Computer Applications in Biotechnology*, vol. 11, pages 251–256. 2010

And the following oral and poster presentations in international conferences (Referred Conferences Abstracts):

ALEJANDRO VIGNONI, GABRIEL BOSQUE, JEFFREY J. TABOR, JESÚS PICÓ, How to tell bi-stable cells in which state they should be? On modelling of population fraction control using light, *BioBricks Foundation SB6.0: The 6th International Meeting on Synthetic Biology*. Imperial College London, UK, July 9-11, 2013.

ALEJANDRO VIGNONI, EVAN J. OLSON, JEFFREY J. TABOR, Light driven characterization and control of a synthetic bistable gene circuit in Escherichia coli. *Computational and Theoretical Biology Simposium*, BioScience Research Collaborative, Houston, TX. US. November 30 - December 1, 2012.

ALEJANDRO VIGNONI, GUY-BART STAN, DIEGO A. OYARZÚN, JESÚS PICÓ, Population-level control of heterologous protein production in bacteria. *EFB Applied Synthetic Biology in Europe*, Barcelona. February 6-8, 2012.

Guidance of Master Thesis and Final Undergrad Project

RIBELLES FERRÁNDIZ, IGNACIO. Master Thesis: Calibración de observadores de modo deslizante. Universitat Politècnica de València and Biopolis SL. July 2014.

SASTRE CANTÓN, SANTIAGO. Trabajo fin de Carrera: Diseño e implementación de un sistema grafico para el control de formación de vuelo de UAVs. Universitat Politècnica de València. July 2014.

RACERO ROBLES, JOSÉ LUÍS. Trabajo fin de Carrera: Instrumentación con GPS de vehiculos aereos no tripulados (UAV) para control de formación de vuelo. Universitat Politècnica de València. July 2014.

RIBELLES FERRÁNDIZ, IGNACIO. Trabajo fin de Carrera: Diseño e implementación en UAVs de un sistema de control de formación de vuelo. Universitat Politècnica de València. July 2013.

Part I

Coordination of dynamical systems

Chapter 2

Coordinación de sistemas dinámicos

Los hermanos sean unidos
Porque esa es la ley primera
Tengan union verdadera
En cualquier tiempo que sea
Porque si entre ellos pelean
Los devoran los de afuera.

La vuelta de Martin Fierro. José Hernandez.

Note: This chapter is based in the author's first publication on dynamical systems coordination using sliding mode reference conditioning and set invariance ideas. It Is an unified approach, involving global and local solutions to the coordination problem in SISO systems with no perturbations. As the article is published in Spanish so will be this Chapter. Although the content is similar to the Chapter 3, due to regulations it should appear as it is published.

ABSTRACT: Dentro de las posibles acepciones de la palabra, en este trabajo hablaremos de *coordinación* para referirnos a la acción de actuar sobre las referencias de los sistemas para lograr algún comportamiento colectivo deseado pero considerando las restricciones y capacidades de cada sistema. Con este objetivo, se desarrolla una novedosa metodología basada en técnicas de acondicionamiento de referencia utilizando invarianza geométrica de conjuntos y control por modos deslizantes. A partir de un marco general, se proponen dos enfoques: uno global del tipo sistema supervisor, y otro local a través de interacciones entre los distintos sistemas, generando una red de interacciones.

La metodología desarrollada permite abordar el el problema de coordinación de sistemas cuya dinámica no necesariamente es igual para todos los sistemas, pudiendo ser lineal, no lineal, de diferente orden, con restricciones, etc. Para ello, la dinámica propia de cada sub-sistema se mantiene *oculta* al sistema de coordinación. Por otro lado, el sistema de coordinación dispone sólo de la información necesaria sobre las limitaciones y restricciones de cada sistema. La idea principal de enfoque de este trabajo es que para coordinar varios sistemas es necesario modular las referencias locales de cada uno, teniendo en cuenta los objetivos globales, las interacciones locales y las capacidades de cada uno de los sistemas.

2.1 Introducción

La coordinación de sistemas de dinámicos es un tema muy actual (Ren et al., 2007; Cao et al., 2013; Antonelli, 2013). Este problema ha sido, en general. entendido como la acción de lograr consenso entre un grupo de agentes. En este contexto, consenso se refiere a la idea de alcanzar un acuerdo sobre un estado de información entre un conjunto de sistemas individuales con el fin de lograr un objetivo común, en general, dependiendo de las condiciones iniciales.

En la literatura se suele suponer que todos los sistemas implicados son idénticos y que, por lo tanto, tienen la misma dinámica. Por otra parte, generalmente se considera que estos sistemas son integradores de primer orden. Recientemente, el problema del consenso se ha abordado mediante la teoría de grafos algebraica y las propiedades de la

matriz laplaciana de un grafo, para sistemas integradores de primer orden, véase (Olfati-Saber et al., 2007; Ren et al., 2007) y sus referencias. Este enfoque se ha extendido a una cadena de integradores en (He and Cao, 2011).

El uso de técnicas de control por modos deslizantes (MD) se ha propuesto para el control de sistemas multi-agente para lograr consenso. El más popular es el control de formación de vehículos aéreos no tripulados (UAV). En esas situaciones, en general se utiliza una configuración maestro-esclavo o líder-seguidor. En (Galzi and Shtessel, 2006), se utiliza MD de orden superior en configuración líder-seguidor para controlar formaciones.

En (Cao et al., 2010) se utilizan estimadores de modo deslizantes de tiempo finito para lograr un consenso en control de formación descentralizada, con líder virtual. También se ha utilizado una acción de control discontinua en (Corteś, 2006) elegida de forma proporcional al gradiente de una función definida por el Laplaciano del grafo que forman los sistemas, que conduce a un algoritmo de consenso de modo deslizante.

En este trabajo nos alejamos de algunos supuestos habituales en la literatura. Utilizamos técnicas de MD para inducir la coordinación, sin embargo, no asumimos que los sistemas que van a ser coordinadas tienen la misma dinámica. Por el contrario, el enfoque aborda el problema de coordinación de sistemas con dinámicas posiblemente diferentes (por ejemplo, lineales y no lineales, diferentes órdenes y limitaciones, etc).

La idea detrás de nuestro enfoque del problema de coordinación es que a fin de coordinar los sistemas, podemos dar forma a sus referencias locales en función de los objetivos locales, las capacidades de cada sistema y la información disponible que cada sistema tiene sobre sus vecinos, siguiendo las ideas originales de la *regla del vecino más cercano* (Tanner et al., 2007). Esto se ha realizado desde dos enfoques diferentes. Una global, con un sistema jerárquico supervisor que modifica las referencias de los sistemas, y otra local, que se basa en interacciones directas entre los sistemas, y en la que no hay ningún líder.

La estructura del artículo es la siguiente. En la sección 2.2 se presenta el problema de coordinación en forma general. Luego en la sección 2.3 se explican algunos resultados previos conocidos en invarianza de conjuntos y acondicionamiento de referencia por modos deslizantes

que se utilizan para plantear la estrategia propuesta para coordinación de sistemas con dinámicas diferentes. La sección 2.4 propone un método global supervisado para resolver el problema de coordinación, mientras que en la sección 2.5 se reformula el problema de forma descentralizada y se presenta una solución alternativa que no asume distintas jerarquías entre los sistemas, ni necesita la existencia de un líder del grupo. Finalmente la sección 2.6 muestra ejemplos de ambas configuraciones para clarificar las metodologías propuestas y una sección de conclusiones resume las ideas principales del trabajo y presenta algunas líneas futuras.

2.2 Coordinación de sistemas

En esta sección se presenta el planteo general del problema de coordinación, como así también definiciones y suposiciones generales relacionadas con la coordinación de sistemas.

2.2.1 Presentación del problema

Considere un conjunto de N sistemas, no necesariamente con la misma dinámica. Asimismo, considere que cada sistema posee un lazo de control estable. Los sistema intervinientes, como se ha dicho, pueden tener diferentes restricciones y capacidades a la hora de seguir su referencia. En este contexto de control con restricciones aparece el concepto de *referencia realizable* (Hanus et al., 1987): la referencia mas rápida que el sistema es capaz de seguir sin violar sus restricciones, manteniéndose siempre en lazo cerrado. Por ejemplo, en el caso de un sistema con restricciones de actuador, una referencia realizable nunca intentará llevar a los actuadores fuera de su rango de operación, ya que esto dejaría al sistema en lazo abierto (pudiendo dar lugar al fenómeno de *windup*).

La *coordinación* será entendida como la acción de lograr un comportamiento colectivo deseado para un conjunto de sistemas considerados. En este trabajo, se aborda el problema actuando sobre las referencias de los sistemas. De esta manera se tienen dos tipos de referencia sobre las que actuar: la referencia local de cada sistema y la referencia global.

Entre los comportamientos colectivos deseados podrían encontrarse:

- Mantener una función χ de las referencias locales lo mas cerca posible de la referencia global.

- Mantener una distancia entre las referencias locales de los sistemas, una a una o entre centroides de agrupamientos.
- Lograr sincronización generalizada, como un caso límite de los anteriores.

Cabe destacar que la función χ puede ser cualquier tipo de combinación de las referencias locales, por ejemplo el promedio, la moda, el máximo, el mínimo, *etc.*. En consecuencia, esta definición de coordinación es muy general, y depende de qué tipo de función se elija para χ. Asimismo la definición de la distancia utilizada para medir las referencias, también puede ser general, dando lugar a una amplia gama de comportamientos colectivos admisibles.

2.2.2 Intercambio de información entre sistemas

Uno de los elementos necesarios para llevar a cabo la coordinación entre sistemas dinámicos, es el intercambio de información entre ellos. La forma en que se ataca dicho problema en este trabajo es uno de sus principales aportes. La idea principal es que cada sistema envía información de sus restricciones locales a los otros sistemas intervinientes a través de su referencia realizable.

Dependiendo del nivel jerárquico al que se transmite la información (ver Fig. 2.1) resulta:

la topología global cuando la información se transmite a un nivel superior tipo supervisor;

la topología local cuando la información se distribuye en el mismo nivel jerárquico a sistemas vecinos.

En cualquiera de las dos topologías, los sistemas individuales ocultan sus estados y salidas al resto de sistemas, enviando solamente la referencia realizable y minimizando la información transmitida. La referencia realizable refleja en qué situación se encuentra el sistema con respecto a sus restricciones físicas locales.

Aunque la información transmitida se minimice, la comunicación es en general el cuello de botella de las topologías centralizadas, ya que el tiempo para recoger toda la información de los sistemas depende directamente del número de sistemas y no del diámetro de la red, como en el caso descentralizado.

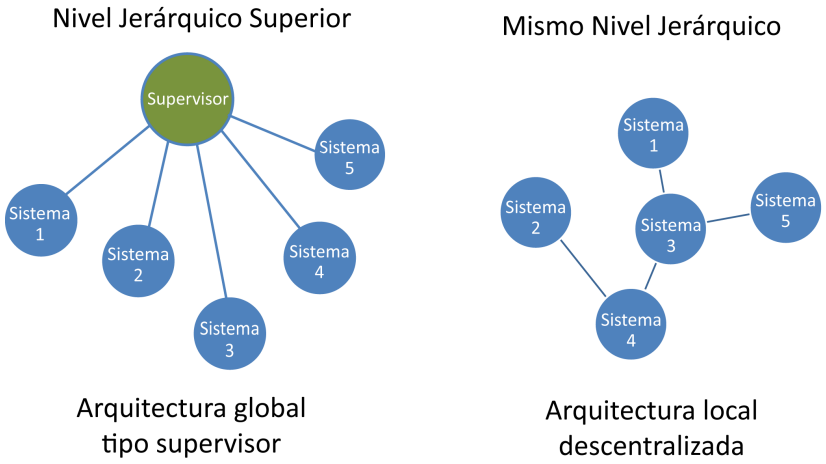

Figure 2.1: Topología de conexión en las distintas configuraciones.

Asimismo, la topología global presenta los problemas normales de vulnerabilidad, puesto que el nodo supervisor centraliza toda la información, y es por lo tanto el punto débil de la red, ya que un fallo en el supervisor acarrea el fallo de todo el conjunto de sistemas.

2.2.3 Suposiciones y definiciones generales

Bajo la siguiente suposición,

Suposición 2.1. Cada sistema interviniente es un lazo cerrado internamente estable y puede seguir una referencia realizable,

se puede definir la coordinación de sistemas de la siguiente manera:

Definición 2.1. El objetivo de coordinación se puede definir en términos de un conjunto al que se desea convertir en un conjunto controlado invariante $\Phi_c(\mathbf{x}, \rho)$, a través de modificar la referencia realizable de cada sistema. El conjunto $\Phi_c(\mathbf{x}, \rho)$ más general se define como:

$$\Phi_c(\mathbf{x}, \rho) = \{\mathbf{x} \in \mathbf{X} : \phi_c(\mathbf{x}, \rho) = \|r(\mathbf{x}) - \rho\| - \delta \leq 0\} \tag{2.1}$$

donde $\mathbf{x} \in X \in \mathbb{R}^n$ son los estados de los sistemas, $r(\mathbf{x})$ es una referencia realizable función de los estados $\mathbf{x}$, ρ es una función que depende de

la información que llega de los otros sistemas y δ es un valor preestablecido. La norma $\|\cdot\|$ puede hacer referencia a cualquier norma definida en $\mathbb{R}^n$, sin embargo de aquí en adelante se referirá a la norma euclídea.

2.3 Invarianza y Acondicionamiento de Referencia por MD

A continuación se describe la metodología utilizada para obtener la referencia realizable, basada en ideas de invariancia y acondicionamiento de referencia por modos deslizantes.

La idea del acondicionamiento de referencia, está basada en el concepto de lograr una referencia realizable, nace originalmente en el contexto del control con restricciones. En concreto, Hanus y Walgama (Hanus et al., 1987; Walgama et al., 1992) han aplicado este tipo de soluciones para resolver el problema de saturación en los actuadores (windup).

Basándose en este enfoque y aprovechando las posibilidades del control por modos deslizantes, como por ejemplo la robustez frente a perturbaciones externas y a incertidumbre en los parámetros (Sira-Ramírez, 1989; Utkin et al., 1999), Mantz y colegas (Mantz et al., 2004) han aplicado acondicionamiento de referencia por modos deslizantes (SMRC) para obtener referencias realizables teniendo en cuenta las restricciones, tanto en los actuadores, como en las salidas. En (Garelli et al., 2006a,b, 2011) se ha utilizado SMRC para acotar interacciones cruzadas en sistemas lineales MIMO. Luego en (Picó et al., 2009b) se ha utilizado SMRC para búsqueda de consigna en sistemas no lineales con restricciones dependientes del estado. En (Gracia et al., 2012) se ha utilizado SMRC para resolver redundancia y acondicionar caminos evitando trampas en algoritmos de robótica móvil.

El el contexto de coordinación de sistemas, en (Vignoni, 2011; Vignoni et al., 2011) se ha realizado un esquema de coordinación, en donde se coordinan las referencias de dichos sistemas involucrados utilizando SMRC y una topología global de modo supervisor. A continuación, en (Vignoni et al., 2012b) se ha abordado la coordinación desde una topología local, teniendo en cuenta las interacciones entre los distintos sistemas, como así también las restricciones de los mismos. En este trabajo se presenta un esquema unificado para coordinar sistemas

dinámicos utilizando ideas de invarianza de conjuntos y acondicionamiento de referencia.

El modo de funcionamiento básico del acondicionamiento de referencia por modo deslizante es el siguiente. El control por modos deslizantes aparece aquí como un lazo adicional que actúa de manera transitoria para generar la referencia realizable. El lazo de acondicionamiento estará *inactivo* hasta que las trayectorias del sistema alcancen por sí mismas la superficie de deslizamiento (intentando violar alguna restricción), pasando el lazo de acondicionamiento al estado *activo*. Una vez que las trayectorias dejen de querer violar dichas restricciones y el lazo principal pueda operar normalmente, entonces el lazo de acondicionamiento pasará nuevamente al estado inactivo.

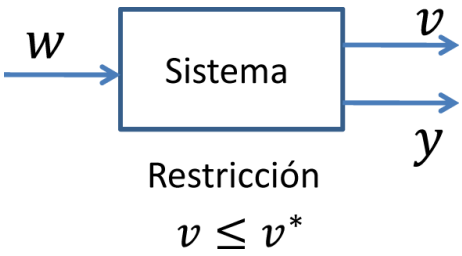

Figure 2.2: Sistema con restricciones.

2.3.1 Invarianza geométrica de conjuntos

Considere el siguiente sistema dinámico (Fig. 2.2):

$$\begin{cases} \dot{\boldsymbol{x}} = f(\boldsymbol{x}) + g(\boldsymbol{x})w, \\ y = h_1(\boldsymbol{x}) \\ v = h_2(\boldsymbol{x}) \end{cases} \tag{2.2}$$

donde $\boldsymbol{x} \in \mathbf{X} \subset \mathbb{R}^n$ es el vector de estados del sistema, $w \in \mathbb{R}$ es la acción de control (posiblemente discontinua), $f : \mathbb{R}^n \longrightarrow \mathbb{R}^n$ es el campo de deriva, $g : \mathbb{R}^n \longrightarrow \mathbb{R}^n$ es el campo de control, y $h_1(\boldsymbol{x})$, $h_2(\boldsymbol{x}) : \mathbb{R}^n \longrightarrow \mathbb{R}$, campos escalares definidos en $\mathbf{X}$, con $g(\boldsymbol{x}) \neq 0$, $\forall \boldsymbol{x} \in \mathbf{X}$.

Las variables y y v son ambas salidas reales del sistema, y es la salida controlada principal mientras que v es una variable que debe ser acotada para cumplir con alguna restricción especificada por el usuario

del sistema (*e.g.* algún estado medible, o una función de los estados o acciones de control).

La cota superior sobre la variable v define el siguiente conjunto acotado superiormente:

$$\Phi\left(\boldsymbol{x}, w, v^*\right) = \{\boldsymbol{x} \in \mathbf{X} \mid \phi(v^*) = v - v^* \leq 0\} \tag{2.3}$$

El conjunto $\Phi\left(\boldsymbol{x}, w, v^*\right)$ especifica una región en el espacio de estados compatible con la restricción $\phi(v^*)$. Cabe destacar que esta región definida por Φ, en general, puede depender de las restricciones, de los mismos estados del sistema o incluso entradas al sistema. En particular v^* podría ser una función variante en el tiempo, y puede depender por ejemplo de información recibida de alguno de los otros sistemas intervinientes.

Remark 2.1. Es importante notar que si se desea definir un conjunto completamente acotado para la variable v, basta con definir dos restricciones y obtener el conjunto final como la intersección de estos dos conjuntos. Por ejemplo, si se desea $v_1^* < v < v_2^*$, es posible definir

- $\Phi_1\left(\boldsymbol{x}, w, v_1^*\right) = \{\boldsymbol{x} \in \mathbf{X} \mid \phi(v_1^*) = -v + v_1^* \leq 0\}$,
- $\Phi_2\left(\boldsymbol{x}, w, v_2^*\right) = \{\boldsymbol{x} \in \mathbf{X} \mid \phi(v_2^*) = v - v_2^* \leq 0\}$

y luego $\Phi = \Phi_1 \cap \Phi_2$.

Desde un punto de vista geométrico, el objetivo es encontrar una acción de control w, de modo que la región Φ se convierta en un conjunto controlado invariante robusto (Blanchini and Miani, 2008), es decir, que queremos encontrar una acción de control w, tal que para todo $\boldsymbol{x}(0) \in \Phi \subseteq \mathbf{X}$ la condición de que $\boldsymbol{x}(t) \in \Phi$ se cumple para todo $t > 0$.

Para asegurar la invarianza del conjunto Φ, se debe cumplir la *condición de sub-tangencialidad* de Nagumo (Blanchini and Miani, 2008):

$$f(\boldsymbol{x}) + g(\boldsymbol{x})w \in \mathcal{T}_\Phi(\boldsymbol{x}),\ \forall\, \boldsymbol{x} \in \partial\Phi. \tag{2.4}$$

Conceptualmente significa que, cuando las trayectorias del sistema se encuentren sobre $\partial\Phi$ (la frontera del conjunto Φ), la acción de control w debe ser tal que el campo controlado $f(\boldsymbol{x})+g(\boldsymbol{x})w$ pertenezca a $\mathcal{T}_\Phi(\boldsymbol{x})$, el cono tangente del conjunto Φ.

Cuando se utilizan conjuntos convexos (con fronteras continuas y diferenciables), la condición anterior se puede reformular (ver Fig. 2.3)

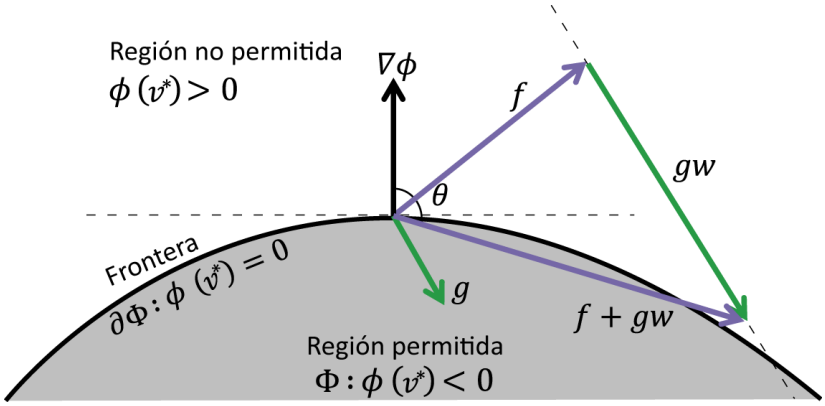

Figure 2.3: Interpretación geométrica de la condición de invarianza.

en términos del gradiente de la restricción ($\nabla\phi$) que acota al conjunto, pidiendo que la proyección del campo $\dot{\boldsymbol{x}} = f(\boldsymbol{x}) + g(\boldsymbol{x})w$ sobre el gradiente $\nabla\phi$ sea menor que cero, es decir, que apunte hacia adentro del conjunto:

$$\nabla\phi^\top \dot{\boldsymbol{x}} = \dot{\phi}(\boldsymbol{x}, w) \leq 0, \forall \boldsymbol{x} \in \partial\Phi \tag{2.5}$$

lo que constituye una forma estándar de *condición implícita de invarianza* para conjuntos convexos (Mareczek et al., 2002):

$$\inf_{w} \ \dot{\phi}(\boldsymbol{x}, w) \leq 0, \ \textit{cuando } \boldsymbol{x} \in \partial\Phi \tag{2.6}$$

Ahora considere la definición de $\dot{\phi}(\boldsymbol{x}, w)$ en notacion de derivadas de Lie, siendo $L_{(\cdot)}\phi$ la *derivada de Lie* en la dirección de un campo vectorial $(\cdot)$ de la función ϕ

$$\dot{\phi}(\boldsymbol{x}, w) = L_f\phi + L_g\phi w. \tag{2.7}$$

Luego resolviendo para w y con $L_g\phi \neq 0$, se obtiene:

$$w = (L_g\phi)^{-1}\left[\dot{\phi} - L_f\phi\right] = w^\phi + (L_g\phi)^{-1}\dot{\phi} \tag{2.8}$$

con $w^\phi = -L_f\phi / L_g\phi$. Luego despejando $\dot{\phi}$ se obtiene

$$\dot{\phi} = \left(w - w^\phi\right) L_g\phi \tag{2.9}$$

De esta manera, utilizando (2.9) para resolver (2.6), se obtiene el conjunto solución $\mathcal{W}(\boldsymbol{x})$ al cual debe pertenecer w, para hacer al conjunto Φ invariante, *condición explícita de invarianza* (Picó et al., 2009b; Vignoni, 2011) para el sistema (2.2):

$$\mathcal{W}(\boldsymbol{x}) = \begin{cases} w \leq w^{\phi} & : \boldsymbol{x} \in \partial\Phi \wedge L_g\phi > 0 \\ w \geq w^{\phi} & : \boldsymbol{x} \in \partial\Phi \wedge L_g\phi < 0 \\ \text{vacio} & : \boldsymbol{x} \in \partial\Phi \wedge L_g\phi = 0 \wedge L_f\phi > 0 \\ w = \text{libre} & : \boldsymbol{x} \in \partial\Phi \wedge L_g\phi = 0 \wedge L_f\phi \leq 0 \\ w = \text{libre} & : \boldsymbol{x} \in \Phi \setminus \partial\Phi, \end{cases} \tag{2.10}$$

en donde se ha tenido en cuenta que si $\boldsymbol{x} \in \partial\Phi$ y al mismo tiempo $L_f\phi < 0$, las trayectorias del sistema no están intentando abandonar el conjunto Φ. Luego para los dos primeros casos de (2.10), se asume $L_f\phi > 0$. Asimismo notese que, cuando $\boldsymbol{x} \in \partial\Phi$, para que exista w^{ϕ} y la invarianza del conjunto sea factible, debe cumplirse

$$L_g\phi = \frac{d\phi}{d\boldsymbol{x}} g(\boldsymbol{x}) \neq 0 \tag{2.11}$$

Luego (2.11) constituye una condición de existencia del control invariante w. En particular, una vez que tanto la frontera del conjunto, $\partial\Phi$, como la campo de control $g(\boldsymbol{x})$ estan definidos, solo uno de los dos primeros casos de (2.10) se cumple, es decir, $L_g\phi$ es positiva o negativa, pero no cambia de signo sobre la frontera. Luego la condición de invarianza del conjunto Φ se cumplirá siempre que el conjunto $\mathcal{W}(\boldsymbol{x})$ no sea vacio. Note que la acción de control w puede ser tomada arbitrariamente del conjunto $\mathcal{W}(\boldsymbol{x})$ (2.10) de modo tal que se cumpla la condición de invarianza. En particular, en el interior de Φ puede ser seleccionada $w = 0$, y permitir al sistema evolucionar libremente en el interior del conjunto.

2.3.2 Acondicionamiento de referencia por MD

A continuación se va a proceder a obtener la w necesaria para lograr en tiempo finito la invarianza del conjunto Φ definido en (2.3), con el sistema Σ presentado en (2.2). En este trabajo se implementa un lazo auxiliar con un bloque de decisión discontinuo, que permite encontrar el valor de referencia que cumple con las restricciones y fuerza al sistema a

permanecer en el conjunto invariante. También se incorpora un filtro de primer orden F, cuyo propósito es suavizar la referencia acondicionada r_f.

En la figura 2.4, se puede ver la implementación del lazo de acondicionamiento de referencia implementado con modos deslizantes.

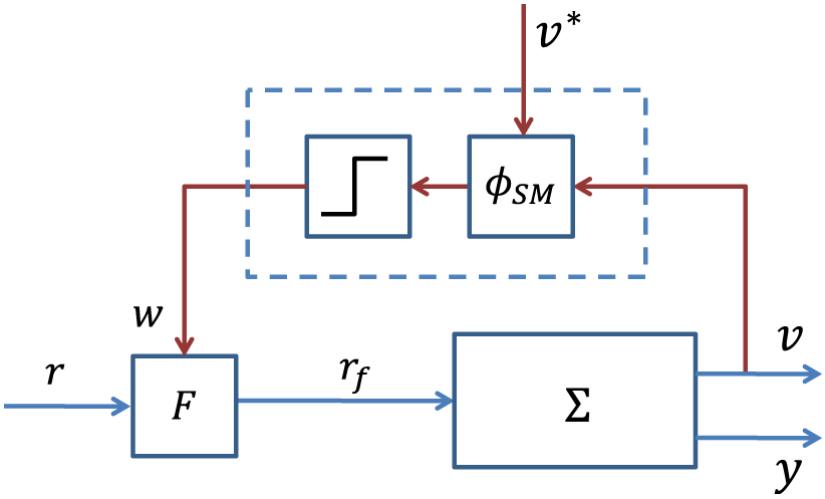

Figure 2.4: Esquema genérico de acondicionamiento de referencia por modos deslizantes.

El bloque discontinuo es implementado con la siguiente ley de control de estructura variable:

$$w = \begin{cases} w_{\mathrm{SM}} & \text{si} \quad \phi(v^*) > 0 \\ 0 & \text{si} \quad \phi(v^*) \leq 0 \end{cases} \tag{2.12}$$

donde ϕ es la superficie de deslizamiento o salida auxiliar, definida de la siguiente forma y de acuerdo con (2.3):

$$\phi(v^*) = v - v^* \tag{2.13}$$

donde v^* es la restricción impuesta a la señal v y w_{SM} es la amplitud de la señal discontinua. El valor de w_{SM} debe ser diseñado de forma tal que cuando las trayectorias del sistema intenten salir del conjunto Φ, se establezca modo deslizante sobre la frontera del conjunto, para lo cual debe cumplirse localmente alrededor de $\partial\Phi$ la condición necesaria

y suficiente de existencia del modo deslizante (Edwards and Spurgeon, 1998; Barbot et al., 2002):

$$\dot{\phi}(\boldsymbol{x}) = \begin{cases} L_f\phi + L_g\phi\, w_{\mathrm{SM}} < 0 & \text{si} \quad \phi(v^*) > 0 \\ L_f\phi > 0 & \text{si} \quad \phi(v^*) < 0 \end{cases} \tag{2.14}$$

La segunda desigualdad de (2.14) se satisface localmente cuando las trayectorias del sistema tratan de salir del Φ. Mientras que la primera desigualdad de (2.14) implica que para que se establezca modo deslizante en $\phi(v^*) = 0$, se debe cumplir localmente alrededor de $\partial\Phi$ la condición de transversalidad (Sira-Ramírez, 1989),

$$L_g\phi = \frac{d\phi}{d\boldsymbol{x}} g(\boldsymbol{x}) \neq 0 \tag{2.15}$$

Cabe destacar también que utilizando el método del control equivalente (Utkin et al., 1999; Edwards and Spurgeon, 1998), una vez que el modo deslizante se establece, el control equivalente continuo se obtiene como:

$$w_{eq} = -L_f\phi / L_g\phi = w^{\phi}, \tag{2.16}$$

el cual de acuerdo con (2.10) es el control requerido para mantener el sistema justo en la frontera $\partial\Phi$. En consecuencia, el modo deslizante realiza el mínimo cambio necesario en la referencia para lograr que el conjunto Φ sea invariante. Además, la condición de necesaria y sufuiciente para el modo deslizante (2.14) garantiza la existencia del control invariante en (2.10).

Remark 2.2. En caso de que las trayectorias se inicien fuera del conjunto Φ, se puede obtener convergencia en tiempo finito a la frontera $\partial\Phi$ tomando w_{SM} tal que $L_f\phi + L_g\phi\, w_{\mathrm{SM}} < -\gamma$, para una determinada constante positiva γ (Barbot et al., 2002). Lo mismo se aplica en caso de una perturbación abrupta que envíe al sistema fuera de la region permitida.

Por otro lado el filtro F es implementado como un filtro de primer orden,

$$\dot{r}_f = -\alpha\,(r_f + w - r)\,, \tag{2.17}$$

con α, parámetro de diseño que representa la frecuencia de corte del filtro, que debe ser tal, que la dinámica del filtro no interfiera con la dinámica del sistema (es decir debe ser más rápido).

En resumen, el acondicionamiento de referencia obtiene la referencia realizable correspondiente que se aplicará al sistema, en determinado instante de tiempo, para evitar que se violen las restricciones. Una característica interesante es que no se requiere ningún modelo del sistema para obtener dicha referencia.

2.4 Topología global tipo supervisor

En esta sección se presenta la coordinación de sistemas utilizando una topología global tipo supervisor y constituye uno de los resultados del presente trabajo, junto con la coordinación de sistemas con topología local que se presentara en la Sección 5.

El problema que se plantea, es el primero de los presentados en la Sección 2.2.1, para lo cual se particulariza la Definición 2.1 de la siguiente manera:

Definición 2.2. El objetivo de coordinación se puede definir en términos de un conjunto Φ_χ al que se desea convertir en un conjunto controlado invariante, modificando la referencia acondicionada r. El conjunto Φ_χ se define como

$$\Phi_\chi(\boldsymbol{x}, r_{fi}) = \left\{\boldsymbol{x} \in \mathbf{X}, r_{fi} \in \mathbb{R}^N : \phi_\chi(r_{fi}) = |r - \chi(r_{fi})| - \Delta \leq 0\right\} \tag{2.18}$$

donde $\boldsymbol{x} \in X \in \mathbb{R}^n$ son los estados de los sistemas, $r \in \mathbb{R}$ es la referencia acondicionada global, y $\chi(r_{fi})$ es una función que depende de las referencias acondicionadas de los sistemas intervinientes, finalmente Δ es un valor preestablecido, para el ancho de la banda permitida.

Luego el objetivo de coordinación es hacer al conjunto Φ_χ un conjunto controlado invariante, para lo cual se propone el siguiente esquema de coordinación global.

2.4.1 Esquema propuesto de coordinación

Considere un conjunto de N sistemas dinámicos, que cumplen con la Suposición 2.1. Se plantea el objetivo de coordinación como en Definición 2.2. Si los sistemas cumplen con la proposición 2.1 entonces es posible lograr coordinación, entendida como en Sección 2.2.1 utilizando un

esquema como el propuesto a continuación, donde se incorpora el objetivo de coordinación (Definición 2.2) en un lazo de acondicionamiento de la referencia global.

Si bien en la práctica cada sistema puede tener restricciones, de entrada, estados o salida, a lo largo de este trabajo y a los efectos de clarificar la exposición del esquema propuesto, se han utilizado sistemas con saturación de actuador y controladores bipropios.

Proposición 2.1. Cada sistema interviniente posee un lazo de acondicionamiento de referencia por modos deslizantes, como el presentado en la sección 2.3.2. Este lazo permite manejar las restricciones locales comandando una referencia realizable al lazo cerrado y aporta información a través de la referencia condicionada, al resto de los sistemas.

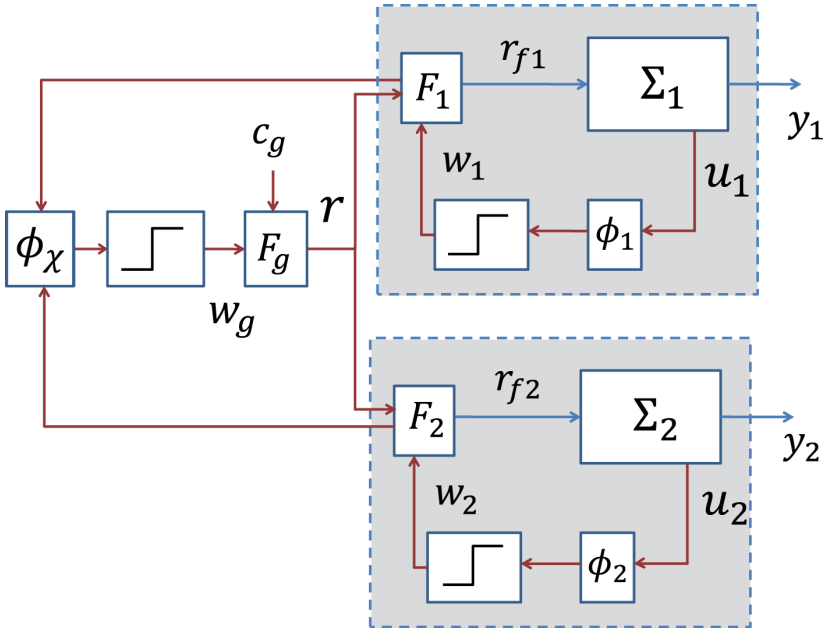

Figure 2.5: Topología del modo supervisado.

En la Fig. 2.5 se muestra el esquema de coordinación global propuesto. Cada sistema Σ_i, donde $i = 1, \ldots, N$ identifica al sistema en cuestión, posee su lazo local de acondicionamiento de referencia (ϕ_i, w_i y F_i), que genera la referencia acondicionada r_{fi} a partir de la referencia

global r.

En un nivel jerárquico superior se encuentra otro lazo de acondicionamiento, esta vez de la referencia global. Dicho lazo está formado por una función de conmutación ϕ_χ en la que interviene la referencia global y la función χ de las referencias locales.

Este lazo, también posee una acción discontinua (w_g), la cual a través del filtro global de coordinación F_g y a partir de la consigna global c_g, genera la referencia global suave r.

Table 2.1: Variables utilizadas en Fig. 2.5

	Variable	Símbolo
	Referencia global	r
	Consigna global	c_g
	Filtro de coordinación	F_g
	Función de conmutación global	ϕ_χ
	Acción discontinua global	w_g
Sistema i	Sistema i	Σ_i
	Referencia acondicionada	r_{fi}
	Salida	y_i
	Variable con restricción	u_i
	Filtro de primer orden	F_i
	Función de conmutación	ϕ_i
	Acción discontinua de la función ϕ_i	w_i

2.4.1.1 Filtro de Coordinación

El filtro de coordinación (F_g) es el encargado de suavizar la acción discontinua global (w_g). Además, es el encargado de integrar las distintas acciones discontinuas que pueden formar parte de la coordinación global, que procedan de las distintas funciones de conmutación. El filtro junto con la función de conmutación global ϕ_χ determinará la política de coordinación y la dinámica global. La dinámica del filtro es la siguiente:

$$\dot{r} = -\lambda \left(r - c_g - \mathbf{k}^T \cdot \mathbf{w}_g \right) \tag{2.19}$$

donde $\mathbf{w}_g$ es el vector de acciones discontinuas globales, y $\mathbf{k}$ es un vector de pesos, que define la política de coordinación, en caso de que exista mas de una restricción global. De aquí en adelante, el vector $\mathbf{w}_g$ pasará a ser un escalar w_g, ya que sin pérdida de generalidad, trabajaremos con una sola función de conmutación global.

2.4.1.2 Definición de la superficie de deslizamiento ϕ_χ

A partir del conjunto que deseamos hacer invariante, debemos definir a sus fronteras como restricciones (que luego se convertirán en superficies de deslizamiento cuando el modo deslizante se encuentre activo). Para eso definimos las fronteras de Φ_χ como

$$\begin{aligned} \phi_\chi^+ &= r - \chi(r_{fi}) - \Delta \\ \phi_\chi^- &= r - \chi(r_{fi}) + \Delta \end{aligned} \tag{2.20}$$

y la acción discontinua, que forzará al sistema a permanecer dentro del conjunto Φ_χ en caso de que la dinámica del mismo sistema trate de salir fuera del conjunto

$$w_g = \begin{cases} w_g^+ & \textit{si} \quad \phi_\chi^+ > 0 \\ w_g^- & \textit{si} \quad \phi_\chi^- < 0 \\ 0 & \textit{caso contrario}. \end{cases} \tag{2.21}$$

Para asegurar la invarianza del conjunto Φ_χ (2.10) se debe elegir $w_g^- \leq -w_g^\star$ y $w_g^+ \geq w_g^\star$, siendo $w_g^\star$ la cota obtenida en el A.1.

2.4.2 Función χ: el mínimo

Un ejemplo interesante de política de coordinación es que la función χ sea la función *mínimo* de las referencias acondicionadas,

$$\chi(r_{fi}) = r_{f\min} = \min\{r_{fi} \ : i \in \{1, \ldots, N\}\}. \tag{2.22}$$

Esta función se utilizará en el ejemplo de la Sección 2.6, para lo cual en el A.3 se demuestra la invarianza de Φ_χ para esta función utilizando análisis de funciones no suaves.

2.5 Topología local distribuida

En esta sección se presenta la coordinación de sistemas utilizando una topología local distribuida. El problema que se plantea, es el segundo de los presentados en la Sección 2.2.1, para lo cual se particulariza la Definición 2.1 de la siguiente manera:

Definición 2.3. El objetivo local entre dos sistemas conectados es mantener entre sus referencias una distancia menor que un valor preestablecido δ_{ij}. Con lo que se puede definir el conjunto Φ_{ij} como

$$\Phi_{ij}(\boldsymbol{x}, r_{fk}) = \{\boldsymbol{x} \in \mathbf{X}, r_{fk} \in \mathbb{R}, k = 1, 2 : \phi_{ij} = |r_{fi} - r_{fj}| - \delta_{ij} \leq 0\} \quad (2.23)$$

donde $\boldsymbol{x} \in X \in \mathbb{R}^n$ son los estados de los sistemas, y $r_{fi} \in \mathbb{R}$ y $r_{fj} \in \mathbb{R}$ son las referencias acondicionadas de los sistemas i y j respectivamente.

Además, los sistemas estarán conectados según la siguiente suposición:

Suposición 2.2. La topología de la red de interconexión de los sistemas es fija, en el sentido de cual sistema puede conectarse con otro. Esta red puede ser representada por un grafo dirigido cuya matriz de adyacencia es $A = [a_{ij}]$, con $a_{ij} = 1$ cuando el sistema i se puede comunicar con el sistema j, y $a_{ij} = 0$ en caso contrario. Se asume que dicho grafo es un grafo simplemente conexo (Olfati-Saber et al., 2007).

Luego se puede definir el conjunto Φ como la unión de los conjuntos anteriores, cuando estén conectados ($a_{ij} = 1$), para todos los sistemas integrantes del grupo.

$$\Phi = \bigcup_{i=1,j=1,i\neq j}^{N} a_{ij}\Phi_{ij} \quad (2.24)$$

Entonces el objetivo de coordinación es hacer al conjunto Φ un conjunto controlado invariante, para lo cual se propone el siguiente esquema de coordinación local.

Esquema propuesto de coordinación

Considere un conjunto de N sistemas dinámicos, con $N \geq 2$, que cumplen con la Suposición 2.1, con una topología de conexión que cumple con la Suposición 4.3, con un lazo de acondicionamiento como en Proposición 2.1 y un objetivo de coordinación como en Definición 2.3, entonces es posible lograr coordinación, entendida como en Sección 2.2.1 utilizando un esquema como el propuesto a continuación, donde se incorporan los objetivos de coordinación (Definición 2.3) en cada lazo de acondicionamiento de la referencia local de los sistemas individuales.

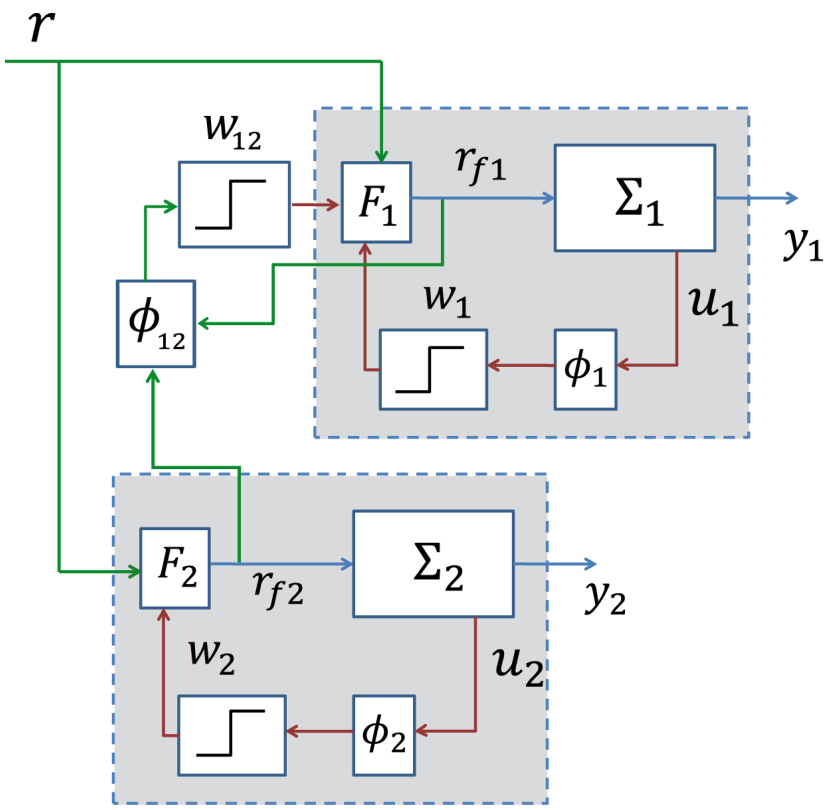

Figure 2.6: Objetivos locales incorporados al esquema de acondicionamiento de referencia.

Table 2.2: Variables utilizadas en Fig. 2.6

	Variable	Símbolo
	Referencia global	r
Sistema i	Sistema i	Σ_i
	Referencia acondicionada	r_{fi}
	Salida	y_i
	Variable restringida	v_i
	Filtro de primer orden	F_i
	Restricción	ϕ_i
	Acción discontinua de ϕ_i	w_i
	Restricción virtual de coordinación entre sistemas i y j	ϕ_{ij}
	Acción discontinua de ϕ_{ij}	w_{ij}

En la Fig. 2.6 se muestra el esquema propuesto, donde aparecen sólo dos sistemas, por simplicidad. La símbolos que aparecen en dicha figura se explican en la Tabla 2.2. El lazo cerrado del sistema i, Σ_i incorpora la planta y un controlador bipropio:

$$\Sigma_i : \begin{cases} \dot{x}_i = f_i(x_i) + g_i(x_i)v_i \\ y_i = h_i(x_i) \\ \dot{x}_{ci} = A_{ci}x_{ci} + b_{ci}e_i \\ v_i = c_{ci}x_{ci} + d_{ci}e_i \end{cases} \tag{2.25}$$

con x_{ci} y e_i los estados del controlador y la señal de error definida como $e_i = r_{fi} - y_i$. A_{ci}, b_{ci}, c_{ci}, d_{ci} son parámetros constantes del controlados.

El objetivo de coordinación local, incorporado en el lazo de acondicionamiento, junto con el filtro de primer orden, dan lugar a la siguiente estructura para el filtro F_i:

$$F_i : \ \dot{r}_{fi} = -\alpha_i(r_{fi} - r + \tilde{w}_i) \tag{2.26}$$

donde $\tilde{w}_i$ es una combinación de las acciones discontinuas provenientes de las restricciones física (w_i), y de la virtual que sintetiza el objetivo de coordinación (w_{ij}); esta definida de la siguiente manera:

$$\tilde{w}_i = w_i + \sum_{j=1, j\neq i}^{N} a_{ij}w_{ij} \tag{2.27}$$

La acción discontinua w_i se define como en Garelli et al. (2006a):

$$w_i = \begin{cases} M_i & \textit{si} \quad \phi_i^+ = v_i - v_{ip}^+ > 0 \\ -M_i & \textit{si} \quad \phi_i^- = v_i - v_{ip}^- < 0 \\ 0 & \textit{caso contrario} \end{cases} \tag{2.28}$$

en donde M_i es la amplitud de la acción discontinua w_i. Asimismo, la acción discontinua w_{ij} se define de acuerdo con las fronteras del conjunto Φ_{ij} que se definen a continuación como restricciones virtuales (ϕ_{ij}).

$$w_{ij} = \begin{cases} M_{ij}\ \text{sign}(r_{fi} - r_{fj}) & \textit{si} \quad \phi_{ij}\left(r_{fi}, r_{fj}\right) \geq 0 \\ 0 & \textit{si} \quad \phi_{ij}\left(r_{fi}, r_{fj}\right) < 0 \end{cases} \tag{2.29}$$

con M_{ij} siendo la amplitud de la acción discontinua. Finalmente las restricciones física y virtual están definidas de la siguiente manera (2.23):

$$\phi_i^{\pm} = v_i - v_{ip}^{\pm} \tag{2.30}$$

$$\phi_{ij} = |r_{fi} - r_{fj}| - \delta_{ij} \tag{2.31}$$

con v_{ip}^+ y v_{ip}^- las cotas superior e inferior de la saturación de actuador y δ_{ij} la cota para la diferencia deseada entre las referencias.

En el A.2 se realiza el análisis correspondiente y se demuestra la invarianza del conjunto Φ_{ij}, de donde se obtienen las siguientes cotas para las acciones discontinuas w_{ij}:

$$M_{ij} > -\frac{\alpha_i r_{fi} - \alpha_j r_{fj}}{\alpha_i + \alpha_j} - \frac{\alpha_i - \alpha_j}{\alpha_i + \alpha_j} r \tag{2.32}$$

y para las acciones discontinuas w_i

$$M_i > \sum_{i \neq j} M_{ij} - \frac{\bar{b}_{ci} v_{ip}^{\pm} + \bar{A}_{ci} x_{ci}}{b_i} - \rho_i. \tag{2.33}$$

2.6 Simulaciones

En esta sección se muestran las características principales de las topología de coordinación propuestas, para un conjunto de 5 sistemas con distinta dinámica, controladores y restricciones (ver C.1); a través de resultados de simulación obtenidos con MATLAB®. Entre los sistemas simulados hay de primero y de segundo orden. Asimismo las saturaciones

de actuador consideradas varían en un amplio rango y los controladores fueron ajustados utilizando diferentes criterios. Por otro lado, cada sistema posee un lazo de acondicionamiento de referencia, con su respectivo filtro ajustado teniendo en cuenta la dinámica del lazo cerrado. Las amplitudes de las acciones discontinuas fueron ajustadas de acuerdo con los resultados obtenidos en cada caso.

2.6.1 Topología Global

Utilizando la topología global tipo supervisor hay varias posibles políticas de coordinación dependiendo de que función se elija para $\chi(r_{fi})$ y del ancho de la región permitida para r alrededor de $\chi(r_{fi})$.

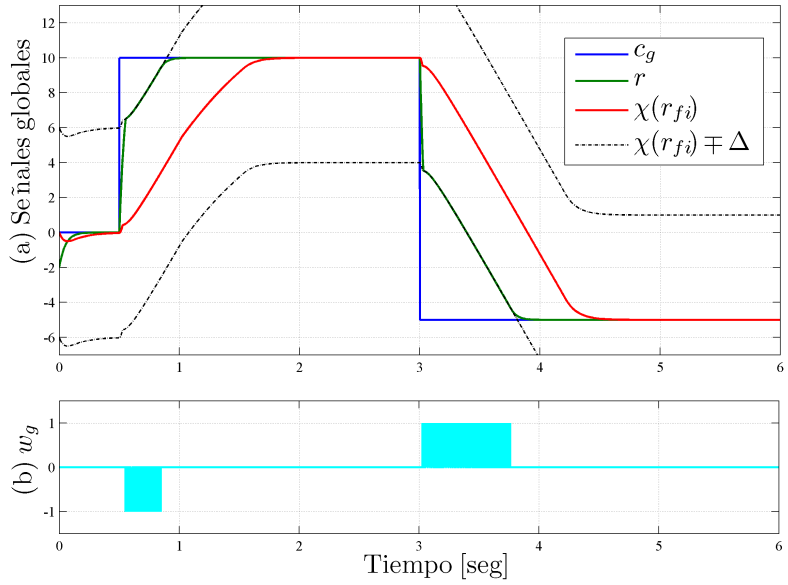

Figure 2.7: Topología global: (a) Consigna global, referencia global y media de las referencias locales, junto con la banda o región permitida. (b) Acción discontinua.

A modo de ejemplo se considera el mínimo de de las referencias acondicionadas como política de coordinación y por ende como función $\chi(r_{fi})$:

$$\chi(r_{fi}) = r_{f\,\min} = \min\{r_{fi} \ : i \in \{1, \ldots, N\}\}\,. \tag{2.34}$$

La invarianza del conjunto Φ_χ para esta función se demuestra en el A.3.

La consigna global c_g es un escalón positivo en $t = 0.5seg$, y uno negativo en $t = 3seg$. El ancho de la región alrededor de $\chi(r_{fi})$ donde se quieren mantener a r fue seleccionado como $\Delta = 6$. Las siguientes figuras muestran los resultados obtenidos mediante simulación. En la Fig. 2.7a se observa la consigna global c_g, la referencia acondicionada global r y la función $\chi(r_{fi})$. Además también se puede ver la región permitida.

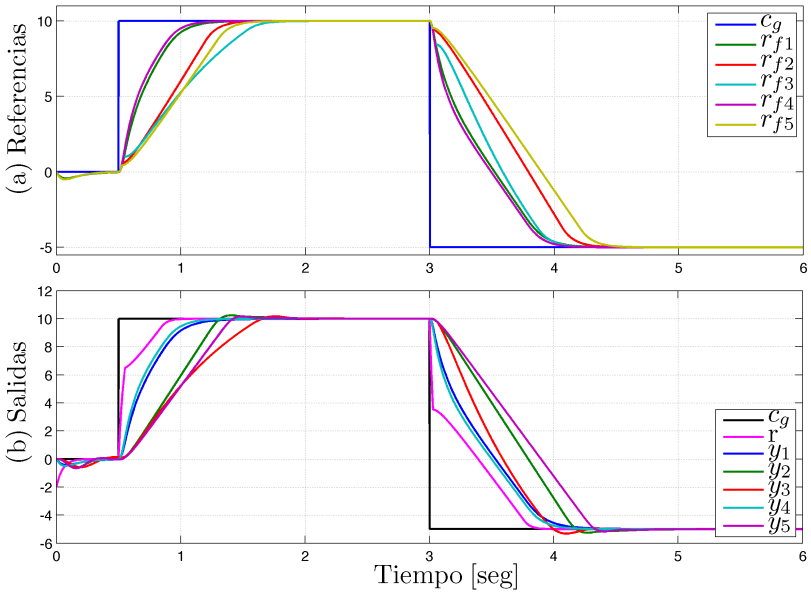

Figure 2.8: Topología global: (a) Consigna global y referencias acondicionadas locales. (b) Salidas de los sistemas individuales.

En la Fig. 2.7b se muestra la acción discontinua global w_g. En interesante observar que cuando la acción discontinua está activa, la referencia global acondicionada r se encuentra en la frontera del conjunto Φ, es decir $r = \chi(r_{fi}) \pm \Delta$. Cuando r vuelve dentro del la región permitida, llevado por la propia dinámica de los sistemas, la acción discontinua se desactiva.

En la Fig. 2.8a se muestran las referencias acondicionadas. Aquí se pueden observar algunas particularidades. En primer lugar, la dinámica

global es más lenta, para poder cumplir con las restricciones, y que todos los sistemas puedan seguir la referencia global. Como consecuencia, ocurre un fenómeno de agrupamiento, dividiendo al grupo en diferentes subgrupos que comparten alguna característica, en principio relacionada con las restricciones de los sistemas. Este agrupamiento es un comportamiento colectivo emergente, que aparece cuando se coordinan sistemas dinámicos.

Finalmente en la Fig. 2.8b se muestran las salidas de los sistemas individuales. Aquí se aprecia que el transitorio de cada sistema depende de sus restricciones y parámetros de controlador. A pesar de dichas diferencias, se obtiene *coordinación* también a la salida, ya que cada sistema es capaz de seguir una referencia, siempre y cuando ésta sea realizable.

2.6.2 Topología local

Utilizando la topología local, un factor muy importante es la red de conexiones. En particular para este ejemplo se ha utilizado la red propuesta en la Fig. 2.1.

En la Fig. 2.9a se muestran las referencias locales de los cinco sistemas. Se puede ver como se logran los objetivos de coordinación, y la diferencia resultante entre cada referencia concuerda con los parámetros δ_{ij} de la tabla 2.3.

En la Fig. 2.9b se observan las salidas de los sistemas individuales, y cómo se obtiene el objetivo de coordinación incluso en las salidas, aunque con pequeñas diferencias debidas a la configuración de los lazos cerrados de cada sistema.

A continuación se muestra una selección de acciones discontinuas, a modo explicativo. Por motivos de espacio, se han seleccionado los sistemas 2 y 5. En la Fig. 2.10 se muestran las acciones discontinuas w_2 y w_{25} junto con las variables restringidas (u_2) y objetivo de coordinación correspondiente ($r_{f2} - r_{f5}$). Se observa que, por un lado, la señal w_2 maneja la variable restringida u_2; por ejemplo w_2 está activa cuando u_2 se encuentra en su límite. Por otro lado, w_{25} se encarga de que la diferencia entre las referencias r_{f2} y r_{f5} sea menor que $\delta_{25} = 1$.

Finalmente en Fig. 2.11, se muestran las trayectorias de las mismas variables restringidas (u_2 y u_5) y de la diferencia de las referencias ($r_{f2} - r_{f5}$) en línea roja continua, y por otro lado, se ha graficado el

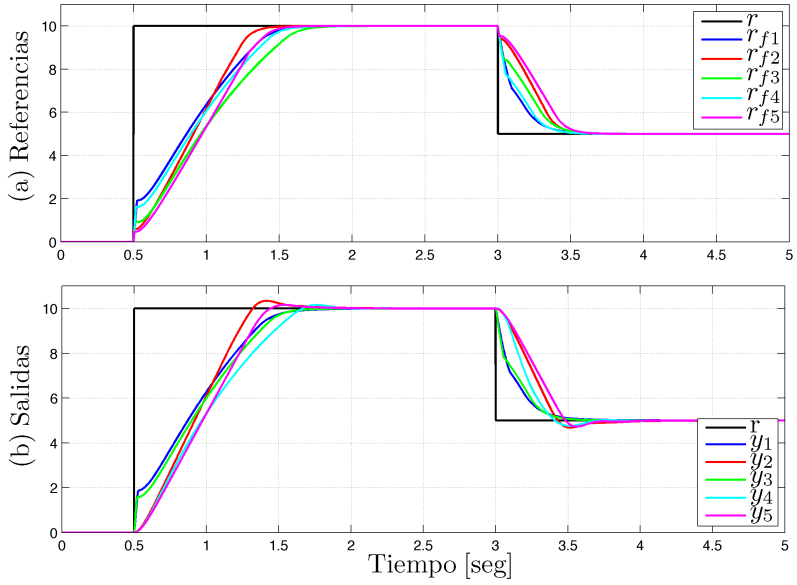

Figure 2.9: Topología local: (a) Consigna y referencias acondicionadas. (b) Salidas de los sistemas individuales.

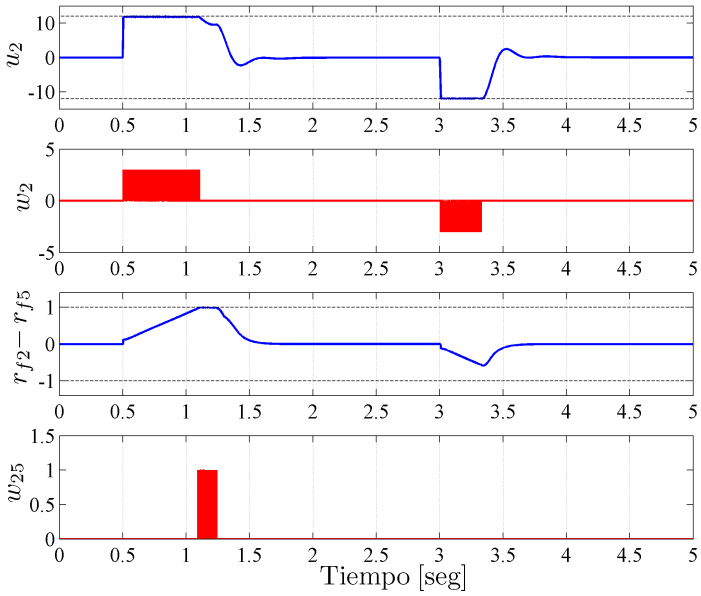

Figure 2.10: Variable restringida u_2, objetivo de coordinación ($r_{f2} - r_{f5}$) y sus respectivas acciones discontinuas (w_2 y w_{25}).

Table 2.3: Parámetros de simulación.

Sistema	δ	Amplitud de la acción discontinua	
1	$\delta_{13} = 1$	$M_{13} = 2$	$M_1 = 5$
2	$\delta_{25} = 1$	$M_{25} = 2$	$M_2 = 3$
3	$\delta_{31} = 1$ $\delta_{34} = 0.7$ $\delta_{35} = 1$	$M_{31} = 2$ $M_{34} = 1.5$ $M_{35} = 2.2$	$M_3 = 8$
4	$\delta_{43} = 0.7$	$M_{43} = 2$	$M_4 = 4$
5	$\delta_{52} = 1$ $\delta_{53} = 1$	$M_{52} = 1$ $M_{53} = 1$	$M_5 = 3$

conjunto invariante deseado, en línea punteada azul. Es evidente que la trayectoria comenzando dentro del conjunto nunca lo abandona, ya que en efecto la metodología propuesta hace al un conjunto invariante.

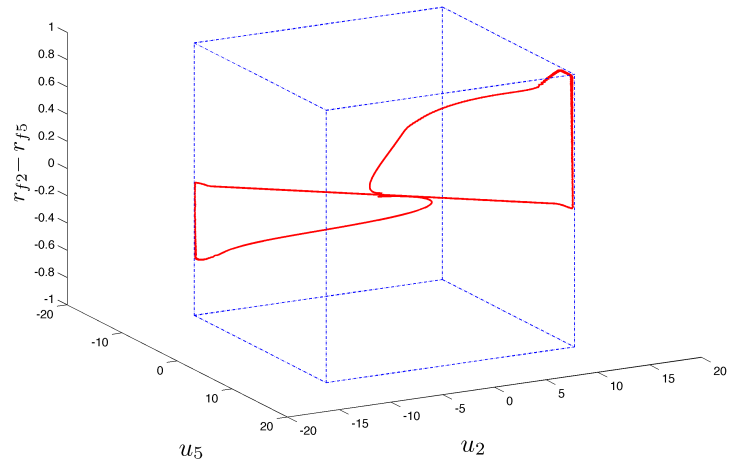

Figure 2.11: Trayectorias de los estados que involucran a los sistemas 2 y 5.

2.7 Conclusión

La coordinación de sistemas es un tema muy actual. En este trabajo se presenta una metodología para coordinar sistemas con distintas dinámicas utilizando invarianza y acondicionamiento de la referencia por modos deslizantes. Esta metodología permite la implementación con diferentes arquitecturas, centralizada o distribuida, y asimismo permite una gran flexibilidad, ya sea desde el punto de vista de aplicaciones (robótica móvil, UAVs, *etc.*), como desde el punto de vista de la robustez, que es inherente al los sistemas de control de estructura variable. El hecho de que cada sistema interviniente incorpore un lazo de acondicionamiento de referencia, para hacer frente a sus limitaciones, es de particular relevancia para que los sistemas siempre estén en lazo cerrado y sean capaces de seguir una referencia (realizable), para luego ser coordinados a través de las mismas. Asimismo, la referencia acondicionada, responsable de la coordinación, es la única información que comparten los sistemas intervinientes ya sea en la topología global tipo supervisor o en la topología local.

Con esta metodología se minimiza el intercambio de información entre sistemas, mejorando la performance del algoritmo de coordinación, teniendo en cuenta que la comunicación suele ser un aspecto limitante en el rendimiento de los mismos. Debido a que el acondicionamiento de referencia es un lazo auxiliar, no representa un problema de implementación, ya que se puede incorporar a cualquier tipo de controlador ya existente en el sistema.

Chapter 3

SMRCoord of constrained feedback systems

El modo de dar una vez en el clavo es
dar cien veces en la herradura.

Miguel de Unamuno

Abstract: This paper addresses the problem of coordinating dynamical systems with possibly different dynamics (e.g. linear and nonlinear, different orders, constraints, etc.) to achieve some desired collective behavior under the constraints and capabilities of each system. To this end, we develop a new methodology based on reference conditioning techniques using geometric sets invariance and sliding mode control: the Sliding Mode Reference Coordination (SMRCoord). The main idea is to coordinate the systems references. Starting from a general framework, we propose two approaches: a local one through direct interactions between the different systems by sharing and conditioning of their own references; and a global centralized one, where a central node makes decisions using information coming from the systems references. In particular, in this work we focus in implementation on multivariable systems like Unmanned Aerial Vehicles (UAVs), and robustness to external perturbations. To show the applicability of the approach, the problem of coordinating UAVs with input constraints is addressed as a particular case of multivariable reference

coordination with both global and local configuration.

3.1 Introduction

Coordination of multi-agents and, in particular, formation control of multiple Unmanned Aerial Vehicles (UAVs) is a very up to-date topic and it supports many practical applications, such as surveillance, weather forecasting, damage assessment, search and rescue, *etc.*. (Ren et al., 2007; Cao et al., 2013; Antonelli, 2013).

Recently, the consensus problem was addressed using algebraic graph theory and properties of the Laplacian Matrix for single integrators (see (Olfati-Saber et al., 2007; Ren et al., 2007) and references therein). He and Cao (2011) extended this approach to a chain of integrators, and Liu (2012) extended to non-linear multi-agent systems.

Sliding mode control is an important topic in nonlinear systems. Research in nonlinear systems goes from stability analysis (for instance with fuzzy polynomial models and sum of squares tools (Pitarch et al., 2013)), to estimation (e.g. with second order sliding mode observers for kinetic rates (Nuñez et al., 2013)) to control (e.g. with bounded L2 gain performance of Markovian jump singular time-delay systems (Wu et al., 2012)).

The use of sliding mode (SM) techniques are generally used for control of swarms and multi-agent systems to achieve consensus. In those situations, a master-slave or leader-follower configuration is implemented, and the discontinuous action is a control signal. In (Galzi and Shtessel, 2006), higher-order sliding mode controllers are used in such configuration to maintain the formation shape. In (Cao et al., 2010) finite-time sliding mode estimators are used to achieve consensus in decentralized formation control with virtual leader. Also in (Corteś, 2006) a discontinuous control input is chosen to be proportional to the gradient of a positive semi-definite disagreement function defined by the graph Laplacian matrix, leading to a sliding mode consensus algorithm. Recently in (Rao and Ghose, 2010) consensus is achieved in connected and also in fully connected swarms of idealized and identical first-order dynamic systems enforced by sliding modes. Also in (Rao and Ghose, 2011) finite-time consensus algorithms for a swarm of self-propelling

agents based on sliding mode control and graph algebraic theories are developed. In (Guo et al., 2013) an LMI approach to multiagent systems control is performed under time-delay and uncertainties. Finally, in (Jafarian and De Persis, 2013) exact formation control is achieved with binary information of the position of the other agents.

In a recent proposal from one of the co-authors, sliding mode control has been used in a non-traditional way: the sliding mode reference conditioning (SMRC) technique (Garelli et al., 2011). This technique combines reference conditioning and sliding mode ideas and has been used in the beginning to bound cross-coupling interactions in multi-variable linear systems (Garelli et al., 2006a, 2007) and for set-point seeking in nonlinear systems with state dependent constraints (Picó et al., 2009b). In (Revert et al., 2013), a SMRC auxiliary loop has been implemented to reduce hypoglycemia in a closed loop glucose control for DM type 1 patients. Also in (Gracia et al., 2012) a geometric invariance and sliding mode ideas have been proposed for redundancy resolution in robotic systems. And in (Gracia et al., 2013) an integrated solution based on the same ideas has been proposed for robotic trajectory tracking, path planning and speed auto-regulation.

In the previous work Vignoni et al. (2011, 2012b,a, 2013a), the authors use Sliding Mode Reference Conditioning to enforce coordination in multi-agent systems. In (Vignoni et al., 2011) sliding mode reference coordination in SISO systems is imposed with a global supervisory approach and two layers of SMRC in a hierarchical structure. In (Vignoni et al., 2012b), the coordination arise from the local interaction between the systems, and the information flows in only one level, as the swarm is assumed to have no leader. In (Vignoni et al., 2012a) the authors make a multivariable reference coordination for ideal unconstrained systems. A preliminary unifying work is done in (Vignoni et al., 2013a) with focus in SISO systems. The present work is a unified approach of the Sliding Mode Reference Coordination (SMRCoord) integrating both local and global approaches with focus on implementation in multivariable systems and robustness to perturbation to the coordination goals.

The rest of the paper is organized as follows. Next section presents the problem of coordination in a general form. Then in Section 3.3 some previous results in set invariance and reference conditioning used thereafter to propose coordination strategy are described. In Section 3.4 a decentralized version is proposed to solve the coordination problem

with only one hierarchical level and no leader. Meanwhile in Section 3.5 the supervised global coordination method is proposed. In Section 3.6 the proposed strategies are used to coordinate UAVs showing the result obtained by simulations. Finally, in Section 3.7 some conclusions are presented and open issues for future study are considered.

3.2 Problem statement

In this section a general form of the coordination problem is presented, together with definitions and assumptions regarding constrained systems and systems coordination.

Consider N stable closed-loop systems with different dynamic behaviour, constraints and performance. In the context of constrained systems, the feasible reference concept arises (Hanus et al., 1987): the fastest reference a system can follow without violating its constraints meanwhile in closed loop. In the case of a system with actuator saturation as a constraint, a feasible reference will never lead the actuators out of their operation range, otherwise it may open the loop, leaving the control system without feedback and leading to a windup effect.

Hereafter, coordination will be understood as the action needed in order to obtain a collective behaviour in a set of considered systems. In this work, the coordination problem, is approached by acting on the systems references.

Among the possible collective behaviours one can count:

- To keep a function of the local references (χ) close to the global reference.
- To maintain a fixed distance between the systems local references, one to one, or between flock centroids.
- To obtain generalized synchronization, as a limit case of the previous cases.

Note the function χ may be some function of the local references, like the mean, mode, max or min. As a consequence of this, the resulting definition of coordination is rather general and broad, depending on the selected χ function.

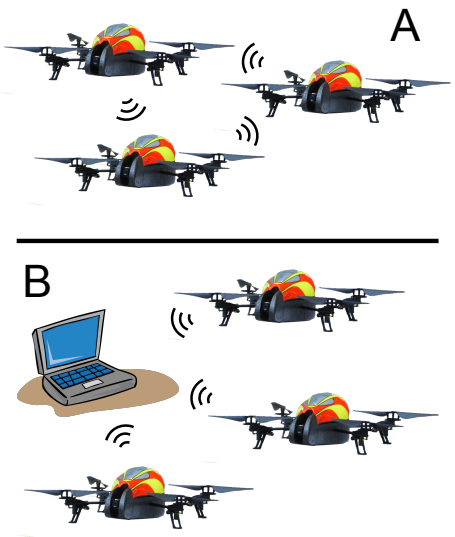

Figure 3.1: Network topology of the different architectures shown implemented in quadrotors. A. Local distributed topology. B. Supervised global topology.

3.2.1 Information exchange

Information exchange is one of the key elements when coordinating a set of systems. Depending in which level this information is exchanged the following architectures may arise Fig. 3.1:

local topology when information flows in the same level among neighbours systems;

global topology when information exchange occurs into a higher hierarchical level, to a supervisory node.

Information exchange still is one of the main bottlenecks of a centralized topology: the data collection time depends on the number of systems involved unlike the decentralized one which depends only on the network radius. Moreover, the global topology presents the common issues of vulnerability and fragility. If the central node has a communication problem or if it is under attack, all the network gets compromised.

3.2.2 Constrained systems

When working with constrained systems, if the constrained variables take different value than the desired ones, inadequate values of the state variables x can destroy control performance. In order to restore the state adequacy, auxiliary inputs $\mathbf{r}_f(\mathbf{x})$, called feasible references are used (Hanus et al., 1987).

Definition 1. The feasible reference $\mathbf{r}_f(\mathbf{x})$ of a closed-loop system is the closest input to the original reference r such that if $\mathbf{r}_f(\mathbf{x})$ had been applied to the controller instead of r, the system constraints would have not been violated; that is, the trajectories of the system and in particular the constrained variables would remain inside (or in the boundary) of a given set Φ, defined by the system constraints.

3.2.3 Assumptions and definitions

Under the following assumption,

Assumption 3.1. Each system has a stabilizing control loop, and can follow a feasible reference;

the coordination is defined as follows:

Definition 2. The systems are said to be coordinated as long as their references belong to the invariant set $\Phi_c(\mathbf{x}, \rho)$, by modifying each systems feasible reference. The set $\Phi_c(\mathbf{x}, \rho)$ is defined as:

$$\Phi_c(\mathbf{x}, \rho) = \{\mathbf{x} \in \mathbf{X} : \phi_c(\mathbf{x}, \rho) = \|\mathbf{r}(\mathbf{x}) - \rho\| - \delta \leq 0\} \tag{3.1}$$

where $\mathbf{x} \in X \in \mathbb{R}^n$ are the system states, $\mathbf{r}(\mathbf{x})$ is a feasible reference function of the states $\mathbf{x}$, ρ a function depending on the information coming from the other systems and δ a predefined value. The norm $\|\cdot\|$ can be any norm defined in $\mathbb{R}^n$. However hereafter we will use the Euclidean norm for simplicity.

3.3 Geometric set invariance and SM reference conditioning

In this section the methodology used in this paper to achieve the coordination of feasible references is described. It is based on concepts of geometric set invariance and sliding mode reference conditioning.

3.3.1 Geometric set invariance

Consider the following dynamical system

$$\Sigma : \begin{cases} \dot{\boldsymbol{x}} = \boldsymbol{f}(\boldsymbol{x}) + \boldsymbol{g}(\boldsymbol{x})\boldsymbol{u}, \\ \boldsymbol{y} = \boldsymbol{h}(\boldsymbol{x}) \end{cases} \tag{3.2}$$

where $\boldsymbol{x} \in \mathbf{X} \subset \mathbb{R}n$ is the state vector, $\boldsymbol{u} \in \mathbf{U} \subset \mathbb{R}m$ is a control input (possibly discontinuous), $\boldsymbol{f} : \mathbb{R}n \longrightarrow \mathbb{R}n$ and $\boldsymbol{g} : \mathbb{R}n \longrightarrow \mathbb{R}n$ are vector fields, and $\boldsymbol{h} : \mathbb{R}n \longrightarrow \mathbb{R}b$, scalar fields; all of them defined in $\mathbf{X}$.

The variable $\boldsymbol{y}$ denotes the system output vector, which has to be bounded so as to fulfill $j = 1, \ldots, \mathrm{N}$ user-specified system constraints ϕ_i. The corresponding bounds on $\boldsymbol{y}$ are given by the set:

$$\Phi = \{\boldsymbol{x} \in \mathbf{X} \mid \phi_i(\boldsymbol{y}) \leq 0\}, \; i = 1, \ldots, \mathrm{N}. \tag{3.3}$$

From a geometrical point of view, the goal is to find a control input $\boldsymbol{u}$ such that the region Φ becomes invariant (*i.e.* trajectories originating in Φ remain in Φ for all times t), while $\boldsymbol{y}$ is driven as close as possible to its desired value $\boldsymbol{r}$.

To ensure the invariance of Φ, the control input $\boldsymbol{u}$ must guarantee that the right hand side of the first equation in (3.2) points to the interior of Φ at all points on the boundary layer of Φ, denoted by $\partial\Phi$, defined as:

$$\partial\Phi = \bigcup_{i=1}^{\mathrm{N}} \partial\Phi_i, \quad \partial\Phi_i = \{\boldsymbol{x} \in \Phi \mid \phi_i(\boldsymbol{y}) = 0\}. \tag{3.4}$$

The following assumption will be needed for later development, and will allow us to compute the gradient vector $\nabla\phi_j$ of the functions ϕ_i.

Assumption 3.2. All the ϕ_i functions are assumed to be differentiable in the boundary $\partial\Phi_i$

Mathematically, the invariance of Φ maybe ensured by an input $\boldsymbol{u}$, such that, $\forall i$, $\dot{\phi}_i \leq 0$, when $\phi_i(\boldsymbol{y}) = 0$. This condition can be expressed as:

$$\begin{aligned} \dot{\phi}_i(\boldsymbol{x}, \boldsymbol{d}, \boldsymbol{u}) &= \nabla\phi_i^\top \dot{\boldsymbol{x}} = \|\nabla\phi_i\| \|\boldsymbol{f} + \boldsymbol{g}\boldsymbol{u}\| \cos\theta \\ &= \nabla\phi^\top \boldsymbol{f} + \nabla\phi^\top \boldsymbol{g}\boldsymbol{u} \\ &= L_f\phi_i + \boldsymbol{L_g}\phi_i\boldsymbol{u}, \; \forall \boldsymbol{x} \in \partial\Phi_i, \; j = 1, \ldots, \mathrm{N}, \end{aligned} \tag{3.5}$$

which constitute in standard form the *implicit invariance condition* (Amann, 1990; Mareczek et al., 2002):

$$\inf_{\boldsymbol{u}} \left\{ \dot{\phi}_i \left(\boldsymbol{x}, \boldsymbol{d}, \boldsymbol{u} \right) \leq 0, \ \forall \boldsymbol{x} \in \partial \Phi_i \right\}, \quad j = 1, \ldots, \mathrm{N}. \tag{3.6}$$

Solving equation (3.6) for $\boldsymbol{u}$, results in the *explicit invariance condition* for system (3.2) and a particular constraint ϕ_i. The set $\mathcal{U}_i$ of feasible solutions is obtained:

$$\mathcal{U}_i \left(\boldsymbol{x}, \boldsymbol{d} \right) = \begin{cases} \boldsymbol{u} \in \{ \mathbf{U} | L_f \phi_i + \boldsymbol{L_g} \phi_i \boldsymbol{u} \leq 0 \} : \boldsymbol{x} \in \partial \Phi_i \wedge \boldsymbol{L_g} \phi_i \neq \mathbf{0}_{\mathrm{m}'}^{\top} \\ \text{empty} : \boldsymbol{x} \in \partial \Phi_i \wedge \boldsymbol{L_g} \phi_i = \mathbf{0}_{\mathrm{m}'}^{\top} \wedge L_f \phi_i > 0 \\ \boldsymbol{u} = \text{free} : \boldsymbol{x} \in \partial \Phi_i \wedge \boldsymbol{L_g} \phi_i = \mathbf{0}_{\mathrm{m}'}^{\top} \wedge L_f \phi_i \leq 0 \\ \boldsymbol{u} = \text{free} \ : x \in \Phi \setminus \partial \Phi, \end{cases} \tag{3.7}$$

where $\mathbf{0}_{\mathrm{m}}^{\top}$ denotes the $m-$dimensional null column vector, and the first set corresponding to $\boldsymbol{L_g} \phi_i \neq \mathbf{0}_{\mathrm{m}}^{\top}$ is always non empty.

Note that the control $\boldsymbol{u}$ in the interior of Φ can be freely assigned. Particularly, $\boldsymbol{u} = \mathbf{0}_{\mathrm{m}}^{\top}$, could be taken so that the system evolves autonomously throughout the interior of Φ. Then, the control action becomes active only when some constraint becomes active, i.e. when the state trajectory reaches the boundary $\partial \Phi$ trying to leave the set Φ. The invariance condition will hold if the intersection $\bigcap_i \mathcal{U}_i(\boldsymbol{x})$ for all constraints of the solution sets $\mathcal{U}_i(\boldsymbol{x})$ is not empty.

3.3.2 Sliding mode reference conditioning

Now, in order to find the necessary $\boldsymbol{u}$ to achieve the invariance of some set $\Phi(y)$ (3.3), with the system Σ (3.2), consider the following implementation (Fig. 3.2).

A discontinuous decision block, will drive the search to find $\boldsymbol{u} \in \mathcal{U}_i(\boldsymbol{x})$ so as to fulfill the constraint $\Phi(y)$ and make $\boldsymbol{r}_f$ remain as close as possible to the external signal $\boldsymbol{r}$. Also, a filter F is incorporated. Its purpose is to filter out the conditioned signal r_f, in order to feed the system Σ with a smooth signal.

The filter F is implemented as the first-order filter

$$\dot{\boldsymbol{r}}_f = -\Lambda \left(\boldsymbol{r}_f + \boldsymbol{u} - \boldsymbol{r} \right), \tag{3.8}$$

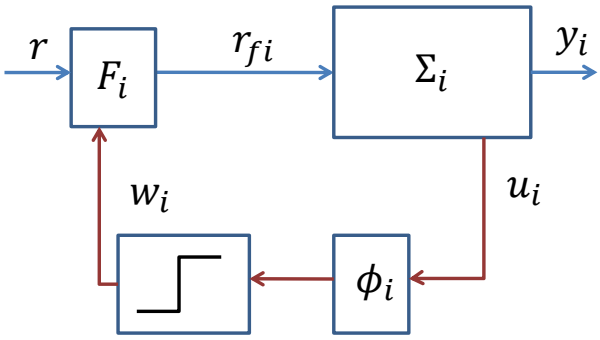

Figure 3.2: SM Reference conditioning general scheme.

with $\boldsymbol{u} \in \mathbf{U} \subset \mathbb{R}m'$ is the discontinuous control action, $\boldsymbol{r}, \boldsymbol{r}_f \in \mathbb{R}m'$ are the input and the conditioned input signal, and $\Lambda \in \mathbb{R}^{\mathrm{m}'\times\mathrm{m}'}$ is a diagonal matrix, a design parameter of the filter.

The discontinuous decision block is implemented by means of the variable structure control law:

$$u = \begin{cases} 0 & \text{if} \quad \max_i\{\phi_i(\boldsymbol{y})\} \leq 0 \\ \boldsymbol{u}_{SM} & \text{otherwise,} \end{cases} \tag{3.9}$$

where $\phi_i(\boldsymbol{y})$ are the constraints defined previously, *i.e.* the boundaries of the set Φ, and $\boldsymbol{u}_{SM}$ is such that $u \in \bigcap_i \mathcal{U}_i(\boldsymbol{x})$.

Notice that the block Σ in Fig. 3.2 represents the entire dynamics from the constrained variables $(\boldsymbol{y})$ to the input signal $\boldsymbol{u}$. Then the system (3.2) becomes:

$$\begin{cases} \dot{\boldsymbol{x}} = \boldsymbol{f}(\boldsymbol{x}, \boldsymbol{d}) + \boldsymbol{g}(\boldsymbol{x})\boldsymbol{r}_f, \\ \dot{\boldsymbol{r}}_f = -\Lambda\left(\boldsymbol{r}_f + \boldsymbol{u} - \boldsymbol{r}\right), \\ \boldsymbol{y} = \boldsymbol{h}(\boldsymbol{x}) \end{cases} \tag{3.10}$$

In the case of a control system, (3.2) is the plant dynamic together with a control loop, in which case $\boldsymbol{r}_f$ is the reference, and $\boldsymbol{x}$ in (3.2) is the extended state comprising the plant and controller.

The choice of $\boldsymbol{u}_{SM}$ depends on whether there is only one active constraint or more than one. For a single active constraint, the analysis is very similar to that of a SMRC in a SISO system (Vignoni et al., 2011, 2012b; Garelli et al., 2011), and is the approach we will use hereafter. The case of several active constraints (see Gracia et al. (2012)), is not analyzed in this work since we are defining only one constraint per system in the formation control problem.

3.4 Reference coordination under local topology

In this section the local topology scheme for systems coordination is presented. The coordination problem approached is the second one described in Section 3.2. To this end, Definition 2 is rewritten in the following way:

Definition 3. The local objective between two connected systems is to bound the distance between their references by a predefined value δ_{ij}. The set Φ_{ij} is defined by:

$$\Phi_{ij}(\boldsymbol{x}, r_{fk}) = \{\boldsymbol{x} \in \mathbf{X}, r_{fk} \in \mathbb{R}, k = 1, 2 : \phi_{ij} = |r_{fi} - r_{fj}| - \delta_{ij} \leq 0\} \quad (3.11)$$

where $\boldsymbol{x} \in X \in \mathbb{R}^n$ are the systems states and $r_{fi} \in \mathbb{R}$, $r_{fj} \in \mathbb{R}$ are the conditioned references of systems i and j respectively.

Moreover, the systems are connected by the assumption:

Assumption 3.3. The topology of the connection network is fixed, in the sense of which system can communicate with each other. This network can be represented by a directed graph with adjacency matrix $A = [a_{ij}]$, with $a_{ij} = 1$ when i-th system can communicate with j-th one. Otherwise $a_{ij} = 0$. This graph is assumed to be connected (Olfati-Saber et al., 2007).

Then, the set Φ is defined as the union of the Φ_{ij}, when they are connected ($a_{ij} = 1$), for all the systems in the group:

$$\Phi = \bigcup_{i=1, j=1, i \neq j}^{N} a_{ij} \Phi_{ij} \quad (3.12)$$

The coordination objective is to make the set Φ a controlled invariant set. To this end the following local coordination scheme is proposed.

Proposed coordination scheme

Consider a swarm of N systems, with $N \geq 2$ satisfying Assumption 3.1, connected in a network topology as in Assumption 3.3, with a sliding mode reference conditioning auxiliary loop, like in Section 3.3.2. This loop allows to handle the local constraints of each system, by commanding a feasible reference to each systems closed loop. Also, the feasible reference provides information to the other systems. The systems will have a goal for every connected neighbor systems as in Definition 3. Then, it is possible to enforce coordination as in Section 3.2 among the system references using the following scheme incorporating the local goal into each system SMRC loop.

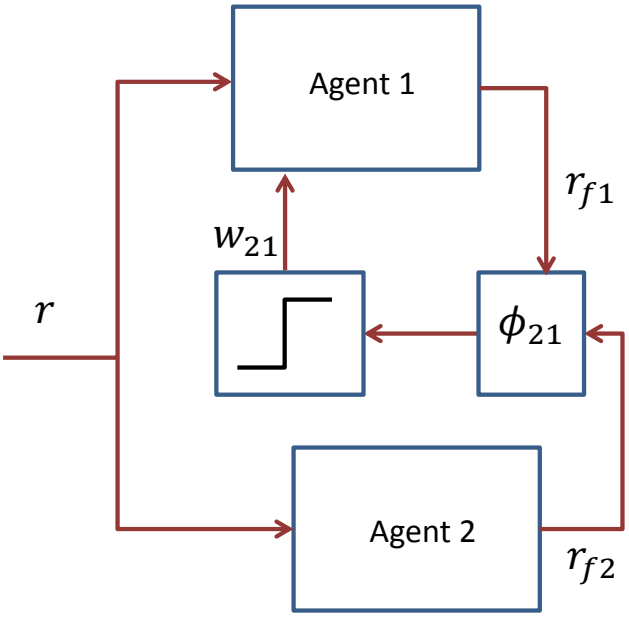

Figure 3.3: Local SMRCoord: Local goal incorporation into the SMRC scheme.

In Fig. 3.3, an implementation of the proposed scheme is depicted, with two systems for the sake of demonstration. The i-th system Σ_i

incorporates the plant and a biproper controller:

$$\Sigma_i : \begin{cases} \dot{x}_i = f_i(x_i) + g_i(x_i)v_i \\ y_i = h_i(x_i) \\ \dot{x}_{ci} = A_{ci}x_{ci} + b_{ci}e_i \\ v_i = c_{ci}x_{ci} + d_{ci}e_i \end{cases} \tag{3.13}$$

with x_{ci} and e_i the the state of the controller and the error signal of the control loop defined as $e_i = r_{fi} - y_i$. A_{ci}, b_{ci}, c_{ci}, d_{ci} are the parameters of the i-th system controller.

The local goal, incorporated in the SMRC, together with the actuator saturation constraint, leads to the following structure for the filter F_i:

$$F_i : \ \dot{r}_{fi} = -\alpha_i(r_{fi} - r + \tilde{w}_i) \tag{3.14}$$

with the combination function $\tilde{w}_i$. This will combine the discontinuous actions from the physical constraints (w_i) and from the virtual coordination constraints (w_{ij}), defined as follows:

$$\tilde{w}_i = w_i + \sum_{j=1, j\neq i}^{N} a_{ij}w_{ij} \tag{3.15}$$

The discontinuous action w_i is defined as in Garelli et al. (2006a):

$$w_i = \begin{cases} M_i & \textit{if} \quad \phi_i^+ = v_i - v_{ip}^+ > 0 \\ -M_i & \textit{if} \quad \phi_i^- = v_i - v_{ip}^- < 0 \\ 0 & \textit{otherwise} \end{cases} \tag{3.16}$$

with M_i being the amplitude of the discontinuous action. And the discontinuous action w_{ij} is defined according to the virtual constraint ϕ_{ij}.

$$w_{ij} = \begin{cases} M_{ij}\ \mathrm{sign}(r_{fi} - r_{fj}) & \textit{if} \quad \phi_{ij}\,(r_{fi}, r_{fj}) \geq 0 \\ 0 & \textit{if} \quad \phi_{ij}\,(r_{fi}, r_{fj}) < 0 \end{cases} \tag{3.17}$$

with M_{ij} being the amplitude of the discontinuous action. Finally the physical constraint and the virtual coordination one which is defined following (3.22) are:

$$\phi_i^{\pm} = v_i - v_{ip}^{\pm} \tag{3.18}$$

$$\phi_{ij} = |r_{fi} - r_{fj}| - \delta_{ij} \tag{3.19}$$

with v_{ip}^{+} and v_{ip}^{-} being the upper and lower limits of the actuator saturation and δ_{ij} a preestablished value for the references difference.

In A.2 the corresponding analysis is done to prove the invariance of the set Φ_{ij}, obtaining the following bound:

$$M_{ij} > -\frac{\alpha_i r_{fi} - \alpha_j r_{fj}}{\alpha_i + \alpha_j} - \frac{\alpha_i - \alpha_j}{\alpha_i + \alpha_j} r \tag{3.20}$$

$$M_i > \sum_{i \neq j} M_{ij} - \frac{\bar{b}_{ci} v_{ip}^{\pm} + \bar{A}_{ci} x_{ci}}{b_i} - \rho_i. \tag{3.21}$$

3.5 Reference coordination under global topology

To address the coordination problem under the global topology, Definition 2 is re-written as follows:

Definition 4. The coordination objective can be defined in terms of a set Φ_χ, which by changing r becomes an invariant set. The set Φ_χ is defined by:

$$\Phi_\chi(\boldsymbol{x}, r_{fi}) = \left\{ \boldsymbol{x} \in \mathbf{X}, r_{fi} \in \mathbb{R}^N : \phi_\chi(r_{fi}) = |r - \chi(r_{fi})| - \Delta \leq 0 \right\} \tag{3.22}$$

where $\boldsymbol{x} \in X \in \mathbb{R}^n$ are the systems states, $r \in \mathbb{R}$ is the global conditioned references, and $\chi(r_{fi})$ is a function of each system's reference. Finally, Δ is a fix predetermined value, the width of the allowed band around r.

Thus, the coordination objective is to make Φ_χ become an invariant set. To this end, the following coordination scheme is proposed:

Proposed coordination scheme

Consider a set of N dynamical systems. Assumption 3.1 holds for each system. Defining the coordination objective as in Definition 4, it follows that coordination understood as in Section 3.2 is enforced using the following scheme and incorporating the coordination objective (Definition 4) in a global reference conditioning loop.

The proposed coordination scheme is shown in Fig. 3.4. Each agent i has a local reference conditioning loop (ϕ_i, w_i and F_i like in Fig. 3.2) to generate the feasible reference r_{fi} from the global reference r.

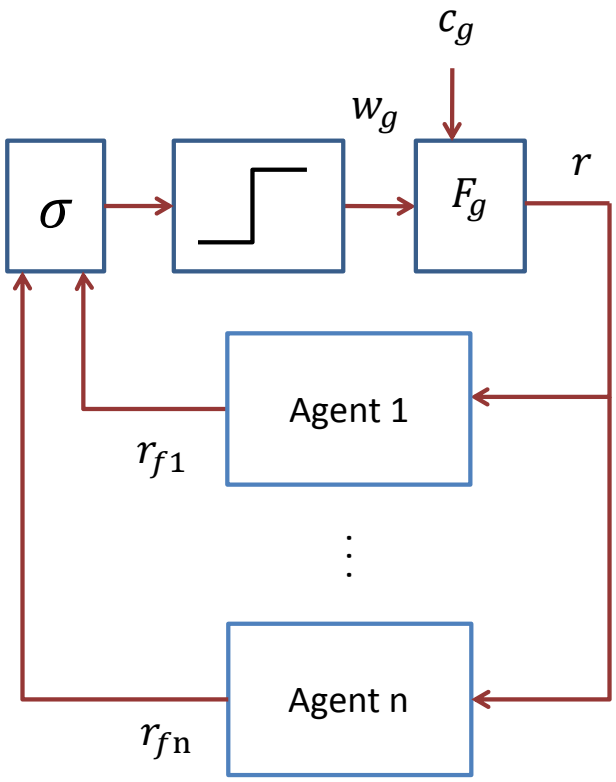

Figure 3.4: Coordination scheme for the global topology.

In a higher hierarchical level, there is another reference conditioning loop, in this case to generate the global reference r. This loop comprises the switching function ϕ_χ, the function χ of the local references, and the discontinuous action (w_g) to create a smooth global reference r from the global target signal c_g.

3.5.0.1 Coordination filter

The coordination filter (F_g) smooths the global discontinuos action (w_g) with the following dynamics:

$$\dot{r} = -\lambda\left(r - c_g - kw_g\right) \tag{3.23}$$

where w_g is the discontinuous action and k is a weight to define the strength of the coordination.

3.5.0.2 Definition of the switching surface ϕ_χ

First we define the boundaries of the set Φ_χ as constraints in the following way

$$\begin{aligned} \phi_\chi^+ &= r - \chi(r_{fi}) - \Delta \\ \phi_\chi^- &= r - \chi(r_{fi}) + \Delta \end{aligned} \tag{3.24}$$

The discontinuous action to force the system remain in the set Φ_χ when the system dynamics make the trajectories go outside of the set is:

$$w_g = \begin{cases} w_g^+ & \textit{if} \quad \phi_\chi^+ > 0 \\ w_g^- & \textit{if} \quad \phi_\chi^- < 0 \\ 0 & \textit{otherwise}. \end{cases} \tag{3.25}$$

To ensure the invariance of the set Φ_χ (3.7) we must choose $w_g^- \leq -w_g^\star$ and $w_g^+ \geq w_g^\star$, where $w_g^\star$ is the bound obtained in A.1.

3.6 Simulation

In this section, the main features of the sliding mode reference coordination (SMRCoord) and formation control developed in Section 3.5 and Section 3.4 are illustrated for quadrotors with cartesian control through simulation results obtained using MATLAB® and using non-linear identified models from (Blasco et al., 2012). A simplified version of the Parrot AR-Drone® Quadrotor models and software for development and implementation of control and navigation strategies can be found in (García-Nieto et al., 2012). Note the strategy is straightforward to implement in MIMO systems, as soon as they are decoupled. This is the case of the quadrotors in cartesian configuration.

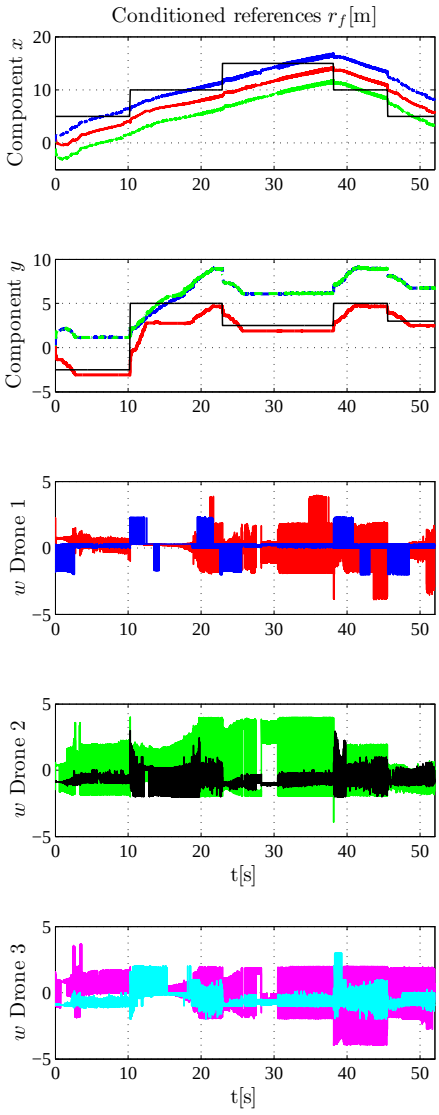

Figure 3.5: Local topology: Conditioned references and discontinuous actions of the individual systems.

3.6.1 Quadrotors and controllers

In this example we considered three quadrotors. The kind of motion considered is cartesian (planar motion). Each one has its own local reference conditioning scheme as in Section 3.3.2. Each agent i sends and receive information from the other agents under the local topology and to the supervisor under the global topology, and incorporates them as constraints (Definition 3) in the SMRC as proposed in Section 3.4.

3.6.2 Information exchange in SMRCoord

The way the information exchange is considered in this work is a key contribution. The main idea is that each system sends key information regarding its local constraints to the other systems by sending its feasible reference. In any of the two topologies, the individual systems hide their states and output to only share the feasible reference with the other systems. Thus minimizing the information exchange. The feasible reference contains information of the system and its state regarding the local constraints.

3.6.3 Simulation results

3.6.3.1 UAV formation with SMRCoord under local topology .

First we implement a triangle-shape formation with three Drones using the SMRCoord under a local topology. The time evolution of the three agents references ($\boldsymbol{r}_{fi}$), together with the resulting discontinuous actions (w) are shown in Fig. 3.5.

It can be seen that the references are coordinated and follow the target trajectory taking into account the saturation in the drones actuators.

In the resulting discontinuous action (plots 3 to 5 in Fig. 3.5) is possible to see that the amplitude in each component is varying with time, as the constraints ϕ also changes, depending on the relative positions of the agent between them. Also the amplitude of the discontinuous action is enough to make (3.21) hold, so as the SM is established in the boundary $\partial\phi$.

In Fig. 3.6 is possible to see how, despite the dynamical difference among the systems and their local controllers parameters, coordination is also achieved in the output of the systems.

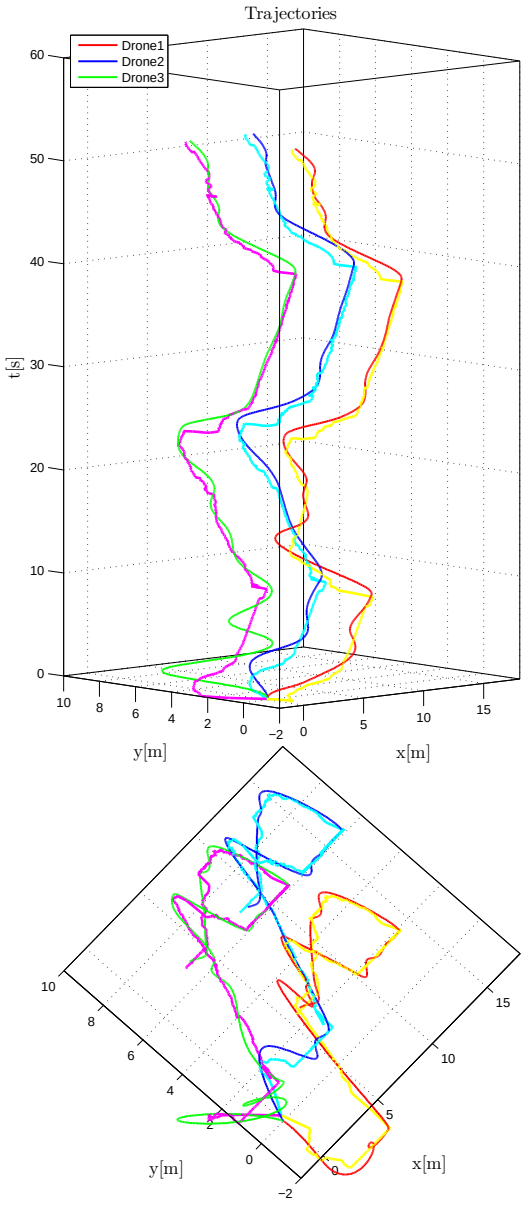

Figure 3.6: Local topology: Drones trajectories in time and cartesian projection. The trajectories are winding along the conditioned references.

3.6.3.2 Formation perturbation rejection with SMRCoord under local topology.

Simulation results in order to test the formation perturbation rejection properties of the SMRCoorc under local topology can be seen in Fig. 3.7. The perturbation consisted of manually stoping the movement of the Drone 1 (red line) in the coordinate x, and has been incorporated after $20sec$ and after $50sec$. It appears as a flattop in the reference (surrounded by a black ellipse in the plot). The strategy rejects the perturbation as the other two Drones *wait*,this is they stop moving as well in order to keep the formation. As a drawback, comparing with the first plot of Fig. 3.5, the time it takes to finish the desired trajectory is longer because the drones had to wait until the perturbation was gone.

3.7 Conclusion

A novel strategy using ideas of set invariance and sliding mode reference conditioning is developed to deal with the coordination of multi-agents and formation control problem. The proposed methodology has an interesting potential to be expanded in order to overcome more general coordination problems. This is inherent to its definition, *i.e.* the coordination goals are reflected in the design of the sliding manifolds.

The fact that the individual systems dynamics are *hidden* to the coordination system, and only the necessary information about the subsystems constraints is communicated to it, makes the proposed methodology transparent and allows dealing with a broad kind of systems to be coordinated, as soon as they can be *reference conditioned*.

Additionally, the features of the SMRC and the SM itself are inherited by the proposal, such as robustness properties of SM control, but not the usual problems of SM like chattering, because the technique is implemented as a part of a numeric algorithm in a digital environment.

Practical applications of the proposed algorithm, for example in AR-Drone® Quadrotors flying in a controlled formation, can be implemented as auxiliary supervisory loops to the trajectory planing algorithm for the virtual leader and stabilizing controllers of the individual agents. The research group is working towards this implementation.

In the theoretical side, an interesting future research line we are working is on the extensions of the proposed methodology to deal with

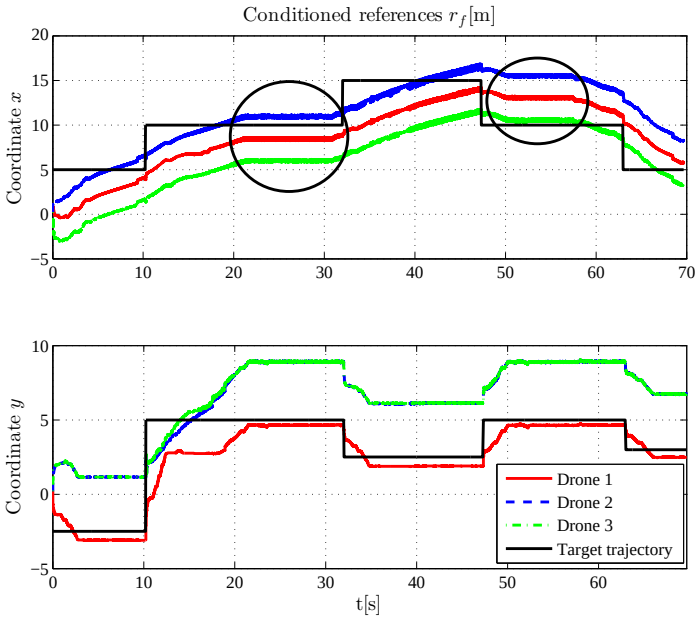

Figure 3.7: Target and conditioned references for x and y components under perturbations in the formation. The black ellipses show the intervals were the perturbation was introduced to Drone 1 (red), and is possible to see how the other two conditioned references *wait* to the reference of Drone 1 until the perturbation vanishes, then the normal course continues.

multiple constraint per system, in which case the problem is how to decide the direction of the control action. Also we are working in the case of constrained systems, and how to incorporate these constraint into the coordination, in order to have a formation control which also takes care of the individual systems constraint, resulting in a robust formation control against disturbances coming from individual limitations in the multi-agent systems.

Chapter 4

UAV reference conditioning for formation control

The airplane stays up because it does not have the time to fall.

Orville Wright

Abstract: A novel methodology is proposed for formation control of UAVs. The scheme is based on the sliding mode reference conditioning technique in a sort of supervisory level. The main idea is to shape the UAVs references in order to keep them coordinated. This implies a virtual leader which has the information of the formation structure, position of the agents in the formation and bounds on the distance between its reference and the ones of the agents. Geometric set invariance techniques together with sliding mode control is used for this purpose in order to make some set, defined from the reference constraints, invariant. To show the applicability of the approach, the problem of coordination and formation a number UAVs in cartesian motion is illustrated through simulation results using non-linear identitled models of the UAVs.

4.1 Introduction

Coordination of multi-agents and, in particular, formation control of multiple Unmanned Aerial Vehicles (UAVs) is a very up to-date topic and it supports many practical applications, such as surveillance, forecasting weather, damage assessment, and search and rescue (Ren et al., 2007).

The use of sliding mode (SM) techniques has been proposed for control of swarms and multi-agent systems to achieve consensus. In those situations, a master-slave or leader-follower configuration is in general used. In (Galzi and Shtessel, 2006), higher-order sliding mode controllers are used in such configuration to maintain the formation shape. In (Cao et al., 2010) finite-time sliding mode estimators are used to achieve consensus in decentralized formation control with virtual leader. Also in (Corteś, 2006) a discontinuous control input is chosen to be proportional to the gradient of a positive semi-definite disagreement function defined by the graph Laplacian matrix, leading to a sliding mode consensus algorithm. Recently in (Rao and Ghose, 2010) consensus is achieved in connected and also in fully connected swarms of idealized and identical first-order dynamic systems enforced by sliding modes. Also in (Rao and Ghose, 2011) a finite-time consensus algorithms for a swarm of self-propelling agents based on sliding mode control and graph algebraic theories are developed.

In the majority of the literature, the sliding mode control acts directly as a control action, but in this contribution we depart from some usual assumptions in the literature, and use invariance ideas and SM techniques to induce coordination. The agents involved are assumed to have a stabilizing controller. This assumption is a common one when dealing with trajectory planning and formation control algorithms (Ren et al., 2007). However, we do not assume that the systems which are going to be coordinated have the same dynamics. On the contrary, the approach addresses the problem of coordinating systems with possibly different dynamics (*e.g.* linear and nonlinear, different orders, constraints, *etc.*).

The idea behind our approach to the coordination problem is that in order to coordinate the systems, we can shape their references as function of the information from the virtual leader. The systems can have different dynamics, but they have to be controlled, in order to follow the multivariable references commanded to them.

The virtual leader reference in fact can be the reference of any system, as the proposed algorithm is easy extendable to different topologies, when the generated graph is connected.

In the future, the achievable performance of each system and information each system has about their neighbors in the group will be considered. Sliding mode reference conditioning (SMRC) is used for this purpose. Each system has an SMRC structure to handle the information coming from the virtual leader. Bounds on the references of each system and the virtual leader are incorporated as constraint in the conditioning loop, running as a supervisory loop and feeding the reference to the already existing stabilizer of each system.

The sliding mode reference conditioning technique (Garelli et al., 2011) is inspired by recent proposals from the co-authors, where they have combined reference conditioning techniques and sliding mode ideas to bound cross-coup-ling interactions in multi-variable linear systems, see (Garelli et al., 2006a, 2007) and for set-point seeking in nonlinear systems with state dependent constraints (Picó et al., 2009b).

In the previous work (Vignoni et al., 2011), coordination in SISO systems is enforced with a global supervisory approach and two layers of SMRC in a hierarchical structure. In (Vignoni et al., 2012b), the coordination arise from the local interaction between the systems and the information will flow in only one level, as the swarm is assumed to have no leader. On the other hand in (Gracia et al., 2012) a geometric invariance and sliding mode ideas are proposed for redundancy resolution in robotic systems. In this work use SMRC to generate multivariable references and command a group of systems, in order to coordinate them.

The rest of the paper is organized as follows. Next section present some previous results in set invariance and reference conditioning. Section 4.2 describes the problem statement and the elements conforming the coordination structure. Section 4.3 describes how the switching surfaces are designed inducing coordination and formation control among the systems. In Section 4.4 the main features of the paper, are illustrated for quadrotors with cartesian control through simulation results. Finally, in section 4.5 some conclusions are presented and open issues for future study are considered.

4.2 Problem Statement

Consider a group of N mobile agents (UAVs) with planar (cartesian) dynamics.

The agents involved may have different dynamics and constraints. A local stabilizing control loop and an SMRC loop are assumed to be present in each individual agent. The information of the virtual leader is incorporated as a constraint in the local reference into the SMRC scheme. The group of agents will follow a virtual leader, according with the information each agent receive from the leader.

The agents are said to be in a coordinated formation when their local references remain inside a predefined set Φ, as long as each systems constraints also hold. This set is defined as the intersection

$$\Phi = \bigcap_{i=1}^{N} \Phi_i \tag{4.1}$$

Then the Φ_i sets are defined as:

Definition 5. The bounds on the references of the agents, relative to the virtual leader reference are given by the sets:

$$\Phi_i = \{\boldsymbol{x} \in \mathbf{X} : \phi_i = \|\boldsymbol{r}_{fi} - (\boldsymbol{r}_{le} + p_i)\| - \delta_i \leq 0\} \tag{4.2}$$

where $x \in X \in \mathbb{R}^n$ is the state vector, $r_{fi} \in \mathbb{R}^n$ is the reference of the i-th agent, r_{le} is the references of virtual leader, $\boldsymbol{p}_i$ is the predefined vector relative to the virtual leader the i-th agent will be formed, and δ_i is the predefined maximum allowed value for the distance between the position of the i-th agent and the desired position $\boldsymbol{p}_i$ in the formation.

Remark 4.1. The so called virtual leader, in fact can be any other agent in the formation. The direction of the information flow is the only restriction. A leader-follower structure is required, but this can be all the agents of the formation as followers of a virtual leader, as shown in this work, or many leader-followers groups, resulting in a connected graph as network topology (Vignoni et al., 2012b). From hereafter the virtual leader case will be used without loose of generality. On the other hand, the bidirectional flow of information, is an interesting challenge and is one of the future lines emerging from this work.

The coordination problem becomes a distributed set invariance problem, where the goal is to maintain the systems reference within some set, and to make that set invariant. It is possible to formulate the whole problem as a set invariance - SMRC one.

4.3 Formation control

In this section the algorithms for coordination and formation control are stated for groups of planar UAVs which may have different dynamics, with virtual leader configuration. The following assumptions are made about the agents:

Assumption 4.1. Each agent has a stabilizing controller.

Assumption 4.2. Each system has an SMRC auxiliary loop (as in Section 3.3.2) to handle the information from the virtual leader.

Assumption 4.3. Each agent can communicate with the virtual leader.

Remark 4.2. The last assumption seems to be a strong one, but taking in to account Remark 4.1, it actually becomes the following: The topology of the connection network is fixed, in the sense of which system can communicate with each other, and in which direction. This network can be represented by a directed graph with adjacency matrix $A = [a_{ij}]$, with $a_{ij} = 1$ when i-th system can communicate with j-th one, otherwise $a_{ij} = 0$. This graph need to be connected (Olfati-Saber et al., 2007).

4.3.1 Proposed coordination scheme.

In the next subsection the main contribution of this work, the coordination and formation control of a group of multi-agents utilizing SMRC, is considered. Consider a group of N multi-agent systems, with $N \geq 2$ satisfying Assumptions 4.1-4.3, with bounds for every agent reference as in Definition 5. Then is possible to enforce coordination among the agents in the group, incorporating the reference bounds (Definition 5) into each system SMRC loops as is shown in the next subsections.

4.3.2 SMRC analysis and design.

In Fig. 4.1, an implementation of the proposed scheme is depicted, with two systems for the sake of demonstration, with the respective variables

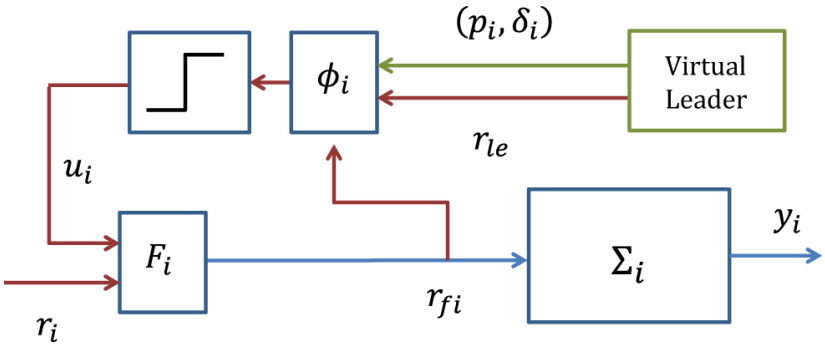

Figure 4.1: Virtual leader and reference bounds incorporation into the SMRC scheme.

explained in Table 4.1.

The reference bounds incorporated in the SMRC, leads to the following structure for the filter F_i:

$$F_i : \dot{\boldsymbol{r}}_{fi} = -\Lambda_i(\boldsymbol{r}_{fi} - \boldsymbol{r}_{le} + \boldsymbol{u}_i) \tag{4.3}$$

which can be rewritten in the following way, because is the only dynamic between the constraints and the discontinuous action.

$$\dot{\boldsymbol{x}} = \boldsymbol{f}_i(\boldsymbol{x}, \boldsymbol{d}) + \boldsymbol{g}_i(\boldsymbol{x})\boldsymbol{u}_i \tag{4.4}$$

where $\boldsymbol{x} = [r_{fix}\ r_{fiy}]^\top$, $\boldsymbol{d} = [r_{lex}\ r_{ley}]^\top$ is the state vector, $\boldsymbol{f}_i(\boldsymbol{x}, \boldsymbol{d}) = -\Lambda_i(\boldsymbol{x} - \boldsymbol{d})$ and $\boldsymbol{g}_i(\boldsymbol{x}) = -\Lambda_i$. Then the constraint ϕ_i can be rewrite as:

$$\phi_i = \|\boldsymbol{x} - (\boldsymbol{d} + p_i)\| - \delta_i \tag{4.5}$$

The variable control law $\boldsymbol{u}_i$ is defined as in Section 3.3.2:

$$\boldsymbol{u}_i = \begin{cases} \mathbf{0}_m & \textit{if} \quad \max_i\{\phi_i(\boldsymbol{y})\} \leq 0 \\ \boldsymbol{u}_{SM} & \textit{otherwise} \end{cases} \tag{4.6}$$

with $\boldsymbol{u}_{SM}$ being the discontinuous action. For only one active constraint it maybe defined with a vector parallel to $\boldsymbol{L_g}\phi_i^\top$, but with negative direction to point inside the set Φ_i, as follows:

$$\boldsymbol{u}_{SM} = -M\boldsymbol{L_g}\phi_i^\top \tag{4.7}$$

where M is a positive constant to be chosen high enough to make the first equation in (3.7) hold, *i.e.* establish a SM on the boundary $\partial\Phi_i$. To fulfill that, the scalar M must be:

$$M > \frac{L_f \phi_i}{\boldsymbol{L_g}\phi_i \boldsymbol{L_g}\phi_i^\top} \tag{4.8}$$

To make the condition (4.8) hold for constraint ϕ_i we have from (4.2)

$$\frac{\partial \phi_i}{\partial x} = [2(r_{fix} - r_{lex} - p_x) \quad 2(r_{fiy} - r_{ley} - p_y)] \tag{4.9}$$

and

$$\boldsymbol{L_g}\phi_i = [-2\lambda_x (r_{fix} - r_{lex} - p_x) \; - 2\lambda_y (r_{fiy} - r_{ley} - p_y)] \tag{4.10}$$

Then

$$\boldsymbol{u}_{SM} = M \begin{bmatrix} -2\lambda_x (r_{fix} - r_{lex} - p_x) \\ -2\lambda_y (r_{fiy} - r_{ley} - p_y) \end{bmatrix} \tag{4.11}$$

Which gives a bound on M in the form of (4.12).

$$M > -\frac{-2\lambda_x (r_{fix} - r_{lex} - p_x)(r_{fix} - r_{lex}) \; - 2\lambda_y (r_{fiy} - r_{ley} - p_y)(r_{fiy} - r_{ley})}{4\lambda_x^2 (r_{fix} - r_{lex} - p_x)^2 + 4\lambda_y^2 (r_{fiy} - r_{ley} - p_y)^2} \tag{4.12}$$

4.3.3 Switching frequency and chattering.

As in all SM controls, the theoretically infinite switching frequency cannot be achieved in practice because all physical systems have finite bandwidth. In computer implementations, the switching frequency is directly the inverse of the sampling period. Finite-frequency commutation makes the system leave the theoretical SM and, instead, its states oscillate with finite frequency and amplitude inside a *band* around $\phi = 0$, which is known as *chattering* (Utkin and Lee, 2006).

For active constraints, the chattering band $\Delta\phi_i = 0$ is given, using the Euler-integration, by:

$$\Delta\phi \leq |\dot{\phi}_i| T_s \leq \|\boldsymbol{L_g}\phi_i \boldsymbol{u}_{SM}\| T_s \leq M \|\Lambda \nabla \phi_i\|^2 T_s \tag{4.13}$$

Therefore, chattering can be reduced if necessary by either decreasing the filters bandwidth (λ_i) or increasing the sampling rate (T_s).

4.4 Simulation

In this section, the main features of the coordination and formation control developed in Section 4.3 are illustrated for quadrotors with cartesian control through simulation results obtained using MATLAB® and using non-linear identified models from (Blasco et al., 2012). A simplified version of the Parrot AR-Drone® Quadrotor models and software for development and implementation of control and navigation strategies can be found in (García-Nieto et al., 2012).

4.4.1 Quadrotors and controllers

In this example we considered five quadrotors. The kind of motion considered is cartesian (planar motion). Each one has its own local reference conditioning scheme as in Assumption 4.2. Each agent j receive information from the virtual leader: the reference ($\boldsymbol{r}_{le}$, the position in the formation ($\boldsymbol{p}_j$) and the size (δ_j) of the allowed region around $\boldsymbol{p}_j$. And incorporate them as constraints (Definition 5) in the SMRC as proposed in Section 4.3.

4.4.2 Virtual leader reference and formation structure

The virtual leader will be considered as a generator of the reference, the formation structure and its parameters at every time, and will be the responsible of sending this information to the agents. The virtual leader reference is given by the following expression:

$$\boldsymbol{r}_{le} = \frac{1}{10}\begin{bmatrix} t \\ (0.1t-5)^2 - 0.5t - 25 \end{bmatrix} \tag{4.14}$$

and is depicted in Fig. 4.2(a) together with the formation structure Fig. 4.2(b) and the values of formation parameter $\boldsymbol{p}$ in Fig. 4.2(c). In Fig. 4.2 red line is the virtual leader, cyan is the first line of the formation, and blue the second. The parameter $\delta = 0.2$ was constant for the entire simulation.

4.4.3 Simulation results

The five agents references ($\boldsymbol{r}_{fi}$), together with the virtual leader reference ($\boldsymbol{r}_{le}$) are shown in the following pictures: In Fig. 4.3 the time

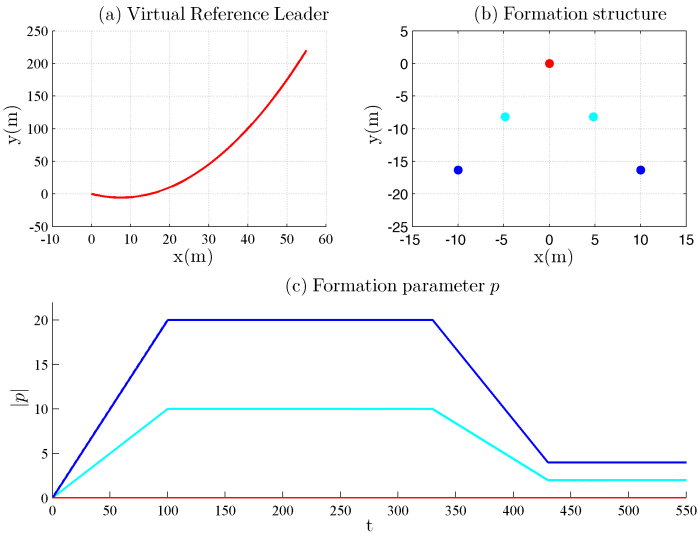

Figure 4.2: Virtual leader. (a) Reference of the virtual leader ($\boldsymbol{r}_{le}$). (b) Formation structure.(c) Formation parameter p.

evolution.

It can be seen that the references are coordinated, *i.e.* they reach a formation around the virtual leader, according to the formation parameters and reference bounds constraint (4.1).

The resulting discontinuous action, depicted for only one of the agents (number 2) for the sake of demonstration, are shown in Fig. 4.4. The original cartesian x and y components are shown in the left. Here is possible to see, the discontinuous action amplitude in each component is varying with time, as the constraint ϕ_2 also changes, depending on the position of agent 2 relative to the virtual leader. On the other hand, in the right side of Fig. 4.4 the discontinuous action of the same agent is shown in polar coordinates ($\rho_2 = \|u_2\|$ and $\theta = \hat{\arctan}(u_2)$) where is easy to see the amplitude of the vector is constant, but the direction (θ) is the one changing, following the (negative)value of the constraint ϕ_2 gradient as defined in (4.7). Also the amplitude of the discontinuous action is enough to make (4.12) hold, so as the SM is established in the boundary $\partial\phi_2$.

Table 4.1: Variables in Fig. 4.1

	Variable	Name
	Virtual leader reference	r_{le}
Agent i	Agent i	Σ_i
	Conditioned reference	r_{fi}
	Position in the formation	p_i
	Allowed region around p_i	δ_i
	Output	y_i
	First order filter	F_i
	Reference bound constraint	ϕ_i
	Discontinuous action of ϕ_i	u_i

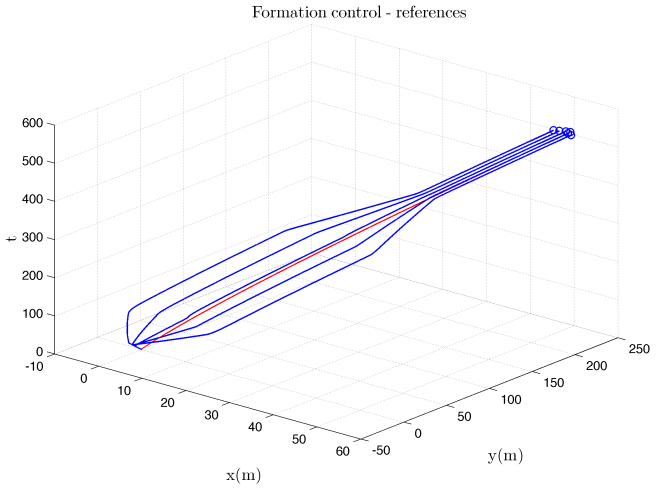

Figure 4.3: Time evolution of the 5 agents (blue) and virtual leader (red) in formation with varying parameter $|p|$.

The system outputs also reach coordination and formation, but depending on their local controllers parameters.

4.5 Conclusion

A novel strategy using ideas of set invariance and sliding mode reference conditioning is developed to deal with the coordination of multi-agents

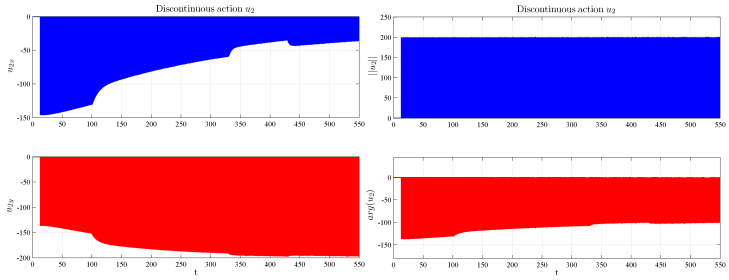

Figure 4.4: Discontinuous action u_2. Cartesian coordinates (x and y) and Polar coordinates (ρ_2 and θ)

and formation control problem. The proposed methodology has an interesting potential to be expanded in order to overcome more general coordination problems. This is inherent to its definition, *i.e.* the coordination goals are reflected in the design of the sliding manifolds.

Additionally, the features of the SMRC and the SM itself are inherited by the proposal, such as robustness properties of SM control.

Practical applications of the proposed algorithm, for example in Parrot AR-Drone® Quadrotors flying in a controlled formation, can be easily implemented as auxiliary supervisory loops to the trajectory planing algorithm for the virtual leader and stabilizing controllers of the individual agents.

In the theoretical side, an interesting future research line we are working is on the extensions of the proposed methodology to deal with multiple constraint per system, in which case the problem is how to decide the direction of the control action. Also we are working in the case of constrained systems, and how to incorporate these constraint into the coordination, in order to have a formation control which also takes care of the individual systems constraint, resulting in a robust formation control against disturbances coming from individual limitations in the multi-agent systems.

Part II

Bioprocesses and sliding modes estimation

Chapter 5

Specific growth rate estimation in (fed-)batch bioreactors using second-order sliding observers

La science d'observation est une science passive;
elle prévoit, se gare, évite, mais ne change rien activement.

Claude Bernard

Abstract: This paper addresses the estimation of specific growth rate of microorganisms in bioreactors using sliding observers. In particular, a second-order sliding observer based on biomass concentration measurement is proposed. Differing from other proposals that only guarantee bounded errors, the proposed observer provides a smooth estimate that converges in finite time to the time-varying parameter. Stability is proved using a Lyapunov approach. The observer exhibits also robustness to process uncertainties since no model of the reaction is used for its design. In addition, the off-surface coordinate of the sliding observer is use-

ful to determine the convergence time as well as to identify sensor faults and unexpected behaviors. Because of the structure of the output error injection, chattering phenomena of conventional sliding mode algorithms are substantially reduced. The features of the proposed observer are assessed by numerical and experimental data.

5.1 Introduction

Bioprocesses are characterized by complex dynamic behavior, nonlinearities, model uncertainty, unpredictable parameter variations, etc.. In addition, most representative variables are typically not accessible for on-line measurement. Consequently, bioprocess control and monitoring is a difficult task in general. In this context, the development of robust and reliable algorithms to estimate key variables and parameters of the process is of prime interest, and extended work has been carried out in this field Dochain (2003).

The existing algorithms differ each other with respect to the measured and estimated variables, the parameters which are assumed to be known, the type of convergence, robustness issues, etc.. A summary of several approaches under different scenarios can be found in Dochain (2003); Venkateswarlu (2004). Asymptotic observers for state and parameter estimations appeared for the first time in Aborhey and Willamson (1978). Adaptive high-gain observers for the same purposes were presented in Bastin and Dochain (1986). Applications of high-gain observers to bioreactors appeared also in Gauthier et al. (1992); Farza et al. (1998). More recently, hybrid observers combining asymptotic with exponential observers to estimate states and identify confidence of the kinetic model were developed Lemesle and Gouzé (2005). Sliding mode observers have been proposed also to deal with model uncertainties González et al. (2001); Picó et al. (2009a). An observer that estimates the substrate consumption rate based on substrate concentration measurement was designed in González et al. (2001). In Picó et al. (2009a), sliding mode techniques were exploited to estimate kinetic rates and concentration variables from biomass measurement.

In this paper we focus on the estimation of reaction rates and, particularly, of specific growth rates. The motivation is that, in many cases,

specifications are related with the growth rate of microorganisms, whether the objective is to maximize biomass production or to maintain a metabolic steady state Zamboni et al. (2009). Besides, growth rate provides a valuable information to monitor the development of microorganisms in the broth.

Substrate concentrations are the key variables in the kinetic models. So, by measuring them, good estimates of the specific growth rate can be obtained by using high-performance observers. However, substrates are usually very difficult to measure on-line and with good precision, particularly when they are in low concentrations.

Alternatively, there currently exist reliable biomass sensors (see for example Navarro et al. (2001a); Kiviharju et al. (2008)). That is why much research has been oriented to develop observers based on biomass sensors, although biomass is a much less informative signal from the point of view of kinetics than substrate. In this approach, the kinetic rate is traditionally treated as an unknown parameter. High-gain observers with some kind of adaptation of the unknown parameter have been extensively used. The observer dynamics are typically enlarged with integral states to adapt the parameter estimates. Advances in the field can be traced back to the work of Bastin and Dochain (1986), where an adaptive Luenberger-like observer is designed so that it achieves bounded error under the assumption that the specific growth rate has bounded time derivative. These results were extended and improved by further work of the authors and contributions of other colleagues.

A different approach is suggested in Picó et al. (2009a) where reaction rates are treated as unknown time-varying signals rather than as unknown parameters. There, a sliding mode observer is designed to estimate the specific growth rate under the same assumptions as in Bastin and Dochain (1986) and related papers. The observer includes a discontinuous term in the estimate that allows achieving finite time convergence to the unknown growth rate. Actually, the estimate converges to the real signal up to a very high frequency component.

In this paper we further exploit the potentialities of the previous approach with the aim of obtaining observers with superior convergence features than the already existing ones. The new observer differs in the structure of the discontinuous output error injection so that discontinuity does not appear in the estimate but in its derivative. Differing from any other approach found in the technical literature, the algorithm

proposed here provides a smooth estimate globally converging to the unknown signal in finite time. This is a particularly attractive property in closed-loop applications. In fact, the separation principle applies, thereby observer and controller can be designed separately. The proposed observer is a variation of the well-known super-twisting sliding algorithm, thereby sharing its excellent performance against noise Levant (1998). Additionally, the information about the process required by the observer is the same as in Bastin and Dochain (1986) and related papers, thereby similar robustness features are expected. Besides, the proposed observer has interesting applications in fault detection and monitoring. Effectively, the switching function is very sensitive to fast variations in biomass concentration. Therefore, observer divergence can be associated to bioreactor malfunctioning or sensor failure.

The work is organized as follows. The next section presents some general assumptions and preliminaries. In section 5.3, the proposed second-order sliding mode observer is developed and its stability is proved using Lyapunov theory and semi-definite programming tools. Section 5.4 shows the observer performance using numerical analysis whereas experimental results are presented in section 5.5. Finally, the main conclusions of the work and future research lines are given.

5.2 Problem formulation and background material

Consider a biomass growth, whose dynamics accept the following description in state-space Bastin and Dochain (1990); Dunn et al. (2003):

$$\mathcal{P}: \begin{cases} \dot{x} = (\mu - D(x,t))x \\ \dot{\mu} = \rho(x,\mu,t)x \end{cases} \tag{5.1}$$

where the state variables are the biomass concentration x and the specific growth rate μ. The dilution rate $D(x,t)$ is function of time and, possibly, of x. The specific growth rate μ is an unknown nonlinear function of biochemical and environmental variables such as substrate, biomass and some product concentration, dissolved oxygen, temperature, pH, etc. In the second line of (5.1), a biomass-proportional representation for the μ-dynamics has been used. This is a sensible choice, particularly for batch processes as well as for fed-batch processes with exponential

growth (in which feeding laws of the form $D(x,t) = \lambda(t)x$, are used). An explicit expression for $\rho(\cdot)$, as function of process parameters, can be derived for some simple –and most commonly found in literature– kinetic models such as Monod and Haldane. However, our purpose is to design robust observers that do not rely on the knowledge of the kinetic structure and process parameters. Therefore, the function $\rho(x,\mu,t)$ is supposed to be unknown.

5.2.1 Main assumptions

The observer to be presented in the following section is designed under the following main assumptions:

Assumption 5.1. Biomass concentration is measured.

Assumption 5.2. Uncertainty ρ is uniformly bounded by $|\rho(\cdot)| < \bar{\rho}$

Assumption 5.3. The dilution rate D is known and uniformly bounded.

Additionally, to show observer convergence, we state the following assumptions which are quite obvious and do not restrict the validity of the proposed observer:

Assumption 5.4. D and ρ are Lebesgue-measurable functions.

Assumption 5.5. Biomass concentration is strictly positive and bounded, that is, for any initial condition $x(0) > 0$ there exist $\underline{x} > 0$ and $\bar{x} < \infty$ such that $\underline{x} < x(t) < \bar{x}\ \forall t > 0$.

5.2.2 Preliminaries

High-gain observers are based on the works of Bastin and Dochain Bastin and Dochain (1986). They have the form

$$\mathcal{O}_{B\&D} : \begin{cases} \dot{\hat{x}} = (\hat{\mu} - D(x,t) + 2\zeta\omega(x-\hat{x}))\, x \\ \dot{\hat{\mu}} = \omega^2(x-\hat{x})x \end{cases} \tag{5.2}$$

This is a Luenberger observer for the measured signal x with an integral state that adapts the unknown parameter μ. That is, the error in the estimation of a measured variable is used in turn to estimate the unknown parameter. The adaptive observer effectively behaves as a low-pass second-order filter of the unknown growth rate μ. Several

tunings, variations and extensions of this observer have been proposed in the literature. In any case, perfect tracking of a time-varying $\mu(t)$ cannot be achieved and only dc errors in $\hat{\mu}$ can be eliminated. This sort of observer is said to be non-exact in the sense that the real signal cannot be recovered even in the absence of noise. In feedback control loops, these observer dynamics add to the controller dynamics, so that the separation principle does not apply. In last sections we will use this traditional observer to make a comparative analysis of the proposed sliding one.

On other side, the first-order sliding mode observer for (5.1) presented in Picó et al. (2009a) is of the form:

$$\mathcal{O}_{1SM}: \begin{cases} \dot{\hat{x}} = \left(z - D(x,t) + \omega(1+a(x))(x-\hat{x}) + \dfrac{M}{\omega}\,\mathrm{sign}(x-\hat{x}) \right) x \\ \dot{z} = \left(\omega^2 a(x)(x-\hat{x}) + M\,\mathrm{sign}(x-\hat{x}) \right) x \\ \hat{\mu} = z + \dfrac{M}{\omega}\,\mathrm{sign}(x-\hat{x}) \end{cases} \tag{5.3}$$

with $\omega > 0$, $M \geq \bar{\rho}$ and $a(x) \geq 0\ \forall x$.

Note that it has the same form as the B&D observer, but discontinuous terms are added to the observer dynamics and output. Thus, the estimated biomass perfectly tracks the measured one after a finite converging time, where the resulting specific growth rate estimate is discontinuous. Further, this estimate coincides with the real growth rate except for a very high (ideally infinite) frequency discontinuous error. Two options have been explored in Picó et al. (2009a) to recover the continuous signal from the discontinuous estimate. The first, and most obvious one, consists in passing the observer output through a low-pass filter of arbitrary order and cut-off frequency. In the second one, the discontinuous $sign(\cdot)$ function is replaced by a continuous function with high gain at the origin. In both cases, the continuous estimate no longer converges in finite time to the real time-varying growth rate but just to a ball centered around. Hence, this observer is not exact either. It is however more flexible and it has been shown to be less noisy in many circumstances than observer (5.2) Picó et al. (2009a).

5.3 Second-order sliding mode observer

The new observer differs from (5.3) in the structure of the discontinuous output error injection so that discontinuity does not appear in the output estimate but only in its derivative. Perfect tracking of biomass concentration and, more importantly, of the specific growth rate is still achieved in the absence of noise, whereas noise effects are substantially reduced. Global finite-time convergence of the observer is proved using concepts of Lyapunov theory and LMIs.

This new observer falls within the category of second-order sliding mode observers because the switching argument must be differentiated twice for discontinuity to appear. Those readers unfamiliar with high-order sliding modes are referred to the comprehensive works Fridman and Levant (2002); Levant (2003) where the main concepts used in this paper can be found.

Consider the biomass dynamic system (5.1), where ρ and D are input signals satisfying Assumptions 5.3 to 5.4. Therefore, a well-defined solution exists for any initial condition. Further, any solution to (5.1) satisfies also the differential inclusion[1]

$$\mathcal{P}_U \begin{cases} \dot{x} = (\mu - D(x,t))x \\ \dot{\mu} \in U\bar{\rho}x \end{cases} \tag{5.4}$$

where U is the set $U = [-1, +1]$. This differential inclusion represents the family of solutions for any unknown specific growth rate satisfying assumption 5.2.

Theorem 5.1. *Let $(x(t), \mu(t))$ be a solution of the differential inclusion (5.4), with $x(t)$ satisfying Assumption 5.5. Then, the observer*

$$\mathcal{O}_{2SM} : \begin{cases} \dot{\hat{x}} = \left(\hat{\mu} - D(x,t) + 2\beta(\bar{\rho}|(x-\hat{x})|)^{\frac{1}{2}}\ \mathrm{sign}(x-\hat{x})\right) x \\ \dot{\hat{\mu}} = (\alpha\bar{\rho}\ \mathrm{sign}(x-\hat{x}))\, x \end{cases} \tag{5.5}$$

converges in finite-time to $(x(t), \mu(t))$ for suitable gains α and β.

Note. Convergence is understood here in the sense that the estimation error vanishes for any solution to (5.4). Note that weaker concepts

[1] In this paper, solutions are understood in the Filippov sense.

of convergence are also used in the literature, meaning that the estimation error reaches a neighborhood of the origin for any solution to (5.4), or that it exponentially or asymptotically approaches the origin for solutions satisfying $\dot{\mu} \to 0$. Finite-time convergence means that there exists $T < \infty$ such that $(\hat{x}(t), \hat{\mu}(t)) \equiv (x(t), \mu(t)) \; \forall \, t > T$.

Observer (5.5) is a variation of the super-twisting sliding mode algorithm, modified here to deal with bioprocess nonlinearity. A conventional super-twisting observer could alternatively be used, but at the cost of using too conservative gains to cope with the large excursions of biomass concentration along batch and fed-batch processes. Convergence of the super-twisting algorithm was originally proved from a geometric approach using majorant curves (see for instance Dávila et al. (2005)). Recently, a Lyapunov-based proof was obtained in Moreno and Osorio (2008). Convergence of the modified super-twisting observer (5.5) is proved here using the more comprehensive Lyapunov approach together with semi-definite programming tools.

Proposition 5.1. *Consider the politopic linear differential inclusion*

$$\dot{z} = A(t)z, \quad A(t) \in \mathcal{A} \tag{5.6}$$

with

$$\begin{aligned} \mathcal{A} &= conv(A_1, A_2) \\ A_1 &= \begin{bmatrix} -\beta & 1/2 \\ -(\alpha - 1) & 0 \end{bmatrix} \\ A_2 &= \begin{bmatrix} -\beta & 1/2 \\ -(\alpha + 1) & 0 \end{bmatrix} \end{aligned} \tag{5.7}$$

Then, for every $\alpha > 1$ there exists suitable values of β such that (5.6) is quadratically stable for all $A(t) \in \mathcal{A}$.

Note. The politopic linear differential inclusion is said quadratically stable if there exists $V(z) = z^T P z, P \succ 0$ that decreases along every nonzero trajectory of (5.6).

Since $\dot{V}(z) = z^T (A(t)^T P + P A(t)) z$, a necessary and sufficient condition for quadratic stability is

$$\begin{aligned} P &\succ 0 \\ A^T(t)P + PA(t) &\prec 0 \quad \forall A(t) \in \mathcal{A} \end{aligned} \tag{5.8}$$

This is equivalent to determine the existence of a common Lyapunov matrix P for all the vertices of the politope $\mathcal{A}$, i.e. that verifies the following constraints

$$\mathcal{F} = \left\{ \begin{array}{l} P \succ 0; \\ Q_1 \stackrel{\triangle}{=} -(A_1^T P + P A_1) \succ 0; \\ Q_2 \stackrel{\triangle}{=} -(A_2^T P + P A_2) \succ 0 \end{array} \right\} \tag{5.9}$$

Now rewriting A_1 and A_2 in a convenient way,

$$\begin{array}{l} A_1 = \beta A_0 + A_1^* \\ A_2 = \beta A_0 + A_2^* \end{array} \tag{5.10}$$

where

$$\begin{array}{l} A_0 = \left[\begin{array}{cc} -1 & 0 \\ 0 & 0 \end{array} \right] \\ A_1^* = \left[\begin{array}{cc} 0 & 1/2 \\ -(\alpha - 1) & 0 \end{array} \right] \\ A_2^* = \left[\begin{array}{cc} 0 & 1/2 \\ -(\alpha + 1) & 0 \end{array} \right] \end{array} \tag{5.11}$$

The problem of determining the existence a Lyapunov P can be computed by solving, i. e. determining the feasibility, of following generalized eigenvalue problem (GEVP) in P and β (5.12) for some fixed $\alpha > 1$ of interest.

$$\begin{array}{lll} \min & & \\ beta & & \\ s.t. & \beta > 0 & \mathcal{F}^* \end{array} \tag{5.12}$$

where

$$\mathcal{F}^* = \left\{ \begin{array}{r} P \succ 0; \\ (A_1^T P + P A_1) + \beta (A_0^T P + P A_0) \prec 0; \\ (A_2^T P + P A_2) + \beta (A_0^T P + P A_0) \prec 0; \end{array} \right\} \tag{5.13}$$

A GEVP is a quasiconvex problem, and can be solved using a bisection algorithm on β and determining the feasibility of the remaining LMI problem.

The problem has been solved using YALMIP Löfberg (2004) and implementing a grid covering the desired values of α.

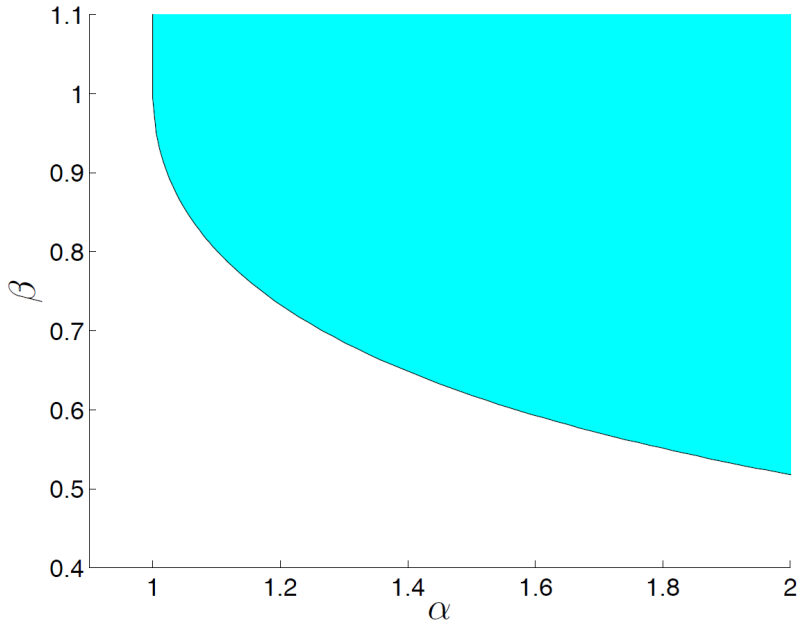

Figure 5.1: Set of pairs (α, β) for which Proposition 7.2 holds.

Proof of Th. 5.1. From process (5.4) and observer (5.5), the observer error dynamics is

$$\begin{cases} \dot{\tilde{x}} = \left(\tilde{\mu} - 2\beta(\bar{\rho}|\tilde{x}|)^{\frac{1}{2}}\ \mathrm{sign}(\tilde{x})\right) x(t) \\ \dot{\tilde{\mu}} \in \left(U - \alpha\ \mathrm{sign}(\tilde{x})\right) \bar{\rho} x(t) \end{cases} \tag{5.14}$$

where $\tilde{x} \stackrel{\triangle}{=} (x - \hat{x})$ and $\tilde{\mu} \stackrel{\triangle}{=} (\mu - \hat{\mu})$. Note that the observer error dynamics are not independent of the process ones.

Apply now to (5.14) the following global homeomorphism Moreno and Osorio (2008)

$$\xi = \begin{bmatrix} (|\bar{\rho}\tilde{x}|)^{\frac{1}{2}}\ \mathrm{sign}\tilde{x} \\ \tilde{\mu} \end{bmatrix} \tag{5.15}$$

Taking into account that $\mathrm{sign}(\xi_1) = \mathrm{sign}(\tilde{x})$ and that $\dot{\xi}_1 = \frac{\bar{\rho}}{2|\xi_1|}\dot{\tilde{x}}$, this coordinate transformation yields

$$\dot{\xi} \in \frac{\bar{\rho}x(t)}{|\xi_1|}\mathcal{A}\xi \tag{5.16}$$

with $\mathcal{A}$ defined in (5.7). Consider now the energy function $V(\xi) = \xi^T P \xi$, where $P \succ 0$ satisfies (5.8). Then,

$$\dot{V}(\xi,t) = \frac{\bar{\rho}x(t)}{|\xi_1|}\xi^T \left(A(t)^T P + PA(t)\right)\xi \tag{5.17}$$

Using (5.8) and recalling assumption 5.5,

$$\dot{V}(\xi,t) \leq -\frac{\bar{\rho}\underline{x}\nu}{|\xi_1|}\|\xi\|^2 < 0 \; \forall \xi \neq 0. \tag{5.18}$$

where $\nu > 0$ is the minimum among all eigenvalues of Q_1 and Q_2. That is, $V(\xi)$ is a Lyapunov function decreasing along all nonzero solutions of (5.16). Note that (5.15) is continuously differentiable everywhere except on the line $\tilde{x} = 0$. Anyway, this line is not an invariant set except the origin. Thus, (5.18) also proves stability of the original observer error dynamics (5.14).

We will prove now that V vanishes in finite time. Let $L > l > 0$ be the maximum and minimum eigenvalues of P. Then $l\|\xi\|^2 \leq V(\xi,t) \leq L\|\xi\|^2 \; \forall t$. It then follows, using $|\xi_1| \leq \|\xi\|$, that

$$\dot{V} \leq -\frac{\bar{\rho}\underline{x}\nu\sqrt{l}}{L}V^{1/2}. \tag{5.19}$$

Then, the comparison lemma establishes that any solution $\xi(t)$ to the differential inclusion (5.16) satisfies

$$\|\xi(t)\| \leq \sqrt{\lambda}\|\xi(0)\| - \frac{\bar{\rho}\underline{x}\nu}{2L}t. \tag{5.20}$$

where $\lambda = \sqrt{L/l}$. This means that the trajectory of the observer error reaches the origin in finite time:

$$\|\tilde{\mu}(t)\| \equiv 0, \; \forall t > T = \frac{2L}{\bar{\rho}\underline{x}\nu}\sqrt{\lambda}\|\tilde{\mu}(0)\| \tag{5.21}$$

where it has been supposed without loss of generality that the observer was initialized with $\hat{x}(0) = x(0)$.

This finishes the proof.

□

□

Remark 5.1. Notice that the proposed observer can be used to estimate the kinetic rate $r(t)$ in any reaction of the form

$$\dot{p} = r(t) \cdot p + f(p,t) \tag{5.22}$$

provided p is measured and analogous assumptions to the ones made here are fulfilled.

5.4 Simulation results

This section presents a pair of numerical examples that illustrate the previous analysis and theoretical results. In the next section, experimental data is provided to assess the observer performance in a realistic scenario.

Let consider the fed-batch process

$$\mathcal{P}_E : \begin{cases} \dot{x} = (\mu(s) - \lambda(t)x)x \\ \dot{s} = (-y_s\mu(s) + \lambda(t)(s_i - s))x \end{cases} \tag{5.23}$$

with haldane kinetics $\mu(s) = \mu_m \frac{s}{k_s+s+s^2/k_i}$ and feeding profile $D(x,t) = \lambda(t)x$. The parameters are $\mu_m = 0.22$, $k_s = 0.14$, $k_i = 0.4$, $y_s = 1.43$ and $s_i = 20$. Note that (5.23) can be rewritten as (5.1) after the change of variable $(x,s) \mapsto (x,\mu(s))$.

For comparative purposes, both the adaptive (5.2) and the proposed sliding observer (5.5) have been implemented to estimate μ.

Open-loop simulation The process input $\lambda(t)$ is a piece-wise constant signal switching every 2.5 hours. Observers (5.2) and (5.5) are tuned with $\omega = 1.5$, $\zeta = \sqrt{2}$, $\bar{\rho} = .4$, $\alpha = 1.1$ and $\beta = 1.8$. Their initial conditions are $(\hat{x}(0), \hat{\mu}(0)) = (x(0), \mu_m)$. The simulation results are shown in Fig. 5.2. The top plot depicts the input $\lambda(t)$ whereas the real and estimated specific growth rates are displayed in the bottom plot. The real $\mu(t)$ is shown in solid line (thick trace), the sliding observer estimate is plotted with solid thin trace and the adaptive observer estimate is plotted in dashed line. It is seen that the sliding observer output converges in less than 2 hours and perfectly tracks $\mu(t)$ thereafter, whereas the adaptive observer (5.2) reaches a neighborhood of $\mu(t)$ but does not converge to it. Naturally, since the measurement is not corrupted with

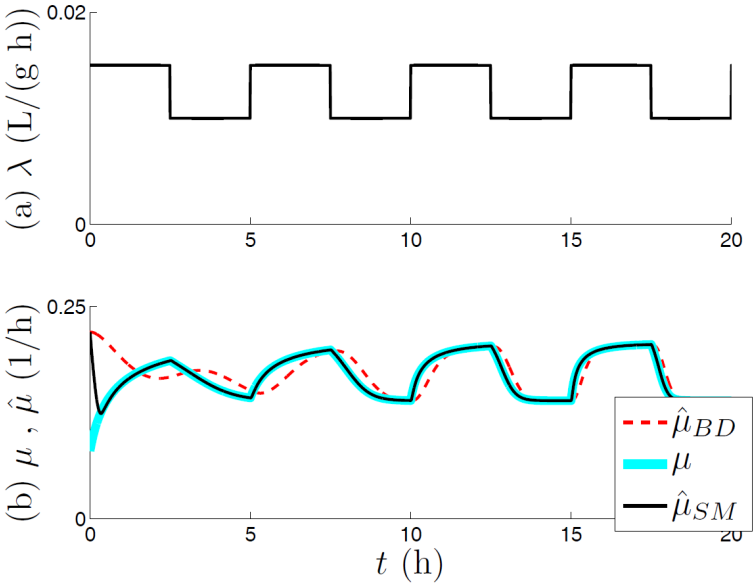

Figure 5.2: Open-loop simulation results. (a) Input signal $\lambda(t)$. (b) Real (μ) and estimated specific growth rate using adaptive ($\hat{\mu}_{BD}$) and sliding ($\hat{\mu}_{SM}$) observers.

noise, the bandwidth of the adaptive observer can be increased to exhibit a faster response. Anyway, the aim of this example is to illustrate qualitatively and comparatively the theoretical convergence features of the proposed sliding observer. Performance under real measurement conditions is evaluated in the next section.

Closed-loop simulation We present here a closed-loop numerical example to illustrate the potential advantages of the sliding mode observer in closed-loop applications. The input signal used in this case is the nonlinear feed-back law:

$$\lambda(\mu) = \frac{y_s \mu_r}{s_i - \mu^{-1}(\mu_r)} \left(1 - k\left(\mu - \mu_r\right)\right). \tag{5.24}$$

It is shown in De Battista et al. (2006) that $\lambda(\mu)$ stabilizes the specific growth rate. Moreover, global stability can be achieved even in the presence of kinetic multiplicity by properly tuning the feed-back gain k. Anyway, the purpose here is not to evaluate the controller performance but

the sliding-mode observer one. Then, $\mu(t)$ in (5.24) is replaced by $\hat{\mu}(t)$. Here, we choose $k = 15$.

The simulation run is planned to show the convergence and tracking properties of the observer. With this purpose, the observer is reset at $t = 0$ h, whereas a set-point step from $\mu_r = .15$ to $\mu_r = .1$ is produced at $t = 10$ h.

The tuning parameters of the sliding observer are $\bar{\rho} = .1$, $\alpha = 1.1$ and $\beta = 1.8$. In this example, its performance is compared with the performance of observer (5.2) for two different tunings ($\omega = 1.5$ and $\omega = 4.5$).

Fig. 5.3 shows the growth rate and its estimates when the real μ -not any of its estimates- is used in the feedback law (5.24). That is, the loop is not closed through an observer. The thick line, labeled with μ_i, is the time evolution of the real growth rate. The estimates provided by observer (5.2) for both tunings and by observer (5.5) are also plotted. After restarting, the adaptive observer estimates exhibit large overshoots that increase with ω. After the set-point step, the adaptive observer estimate lags the real signal, particularly for low ω. On the other hand, the sliding observer perfectly tracks $\mu(t)$ during the transient that follows the set-point step, whereas initial convergence after restarting is significantly better.

Fig. 5.4 shows what happens when the observer estimates are used to construct the feeding law. The first two plots depict responses obtained with the adaptive observer whereas the remaining ones correspond to the sliding observer. Note that the adaptive observer estimates are out of scale during the first hours after restarting. The top plot shows that the closed-loop response becomes highly oscillatory when the slow adaptive observer is used to close the loop. This is because it adds its slow dynamics to the loop. When the fast adaptive observer is used, oscillations are almost eliminated, but an undesirable initial transient still occurs because of the large observer overshoot. In the third plot, the response obtained with the proposed sliding observer is shown. It is seen that the observer converges rapidly, whereas the tracking response is similar to the ideal one. The bottom plot illustrates how the sliding function, which continuously switches after convergence, can be used to improve further the initial transient. In this case, the feed-back loop is closed just after the sliding function switches for the first time.

Fig. 5.5 shows the same responses when gaussian noise is added to

biomass concentration measurement. All comments regarding the initial transient remain valid. Regarding tracking after the set-point step, it is seen that the sliding and fast adaptive observers exhibit similar responses, but the adaptive observer is noisier. Anyway, since both observers smooth out the measured signal in two different ways, noise performance may differ depending on the noise structure. Performance of these observers in a real scenario is presented in the following section.

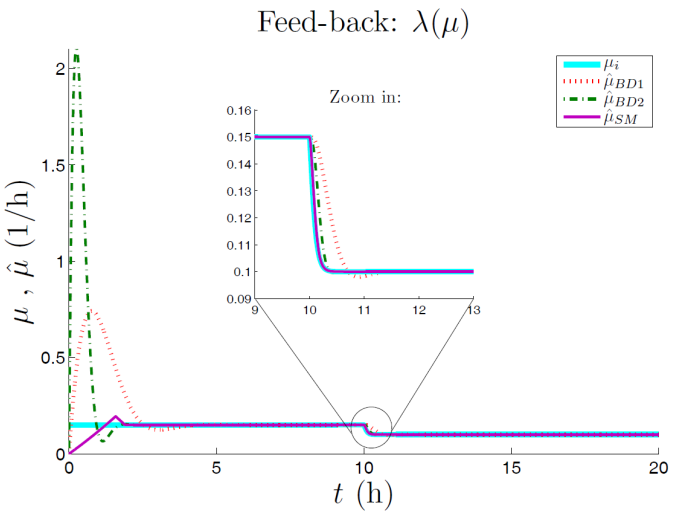

Figure 5.3: Closed-loop simulation results when the real μ is used in the feed-back law (observers are not in loop). μ_i: specific growth rate using ideal feed-back law (5.24); $\hat{\mu}_{BD1}$, $\hat{\mu}_{BD2}$: adaptive observer estimates for $\omega = 1.5$ and $\omega = 4.5$, respectively; $\hat{\mu}_{SM}$: sliding observer estimate.

5.5 Experimental results

Biomass concentration measurements from a batch fermentation of the industrial strain Saccharomyces Cerevisiae T73 (wild type) were injected to the proposed sliding observer as well as to a high-gain one. The measurements were obtained using the sensor described in Navarro et al. (2001a). Sampling was carried out each 12 seconds, and a filtered value over a window of 2 minutes was provided. Figure 5.6a plots the evolution of the measured biomass concentration x_m, whereas Fig-

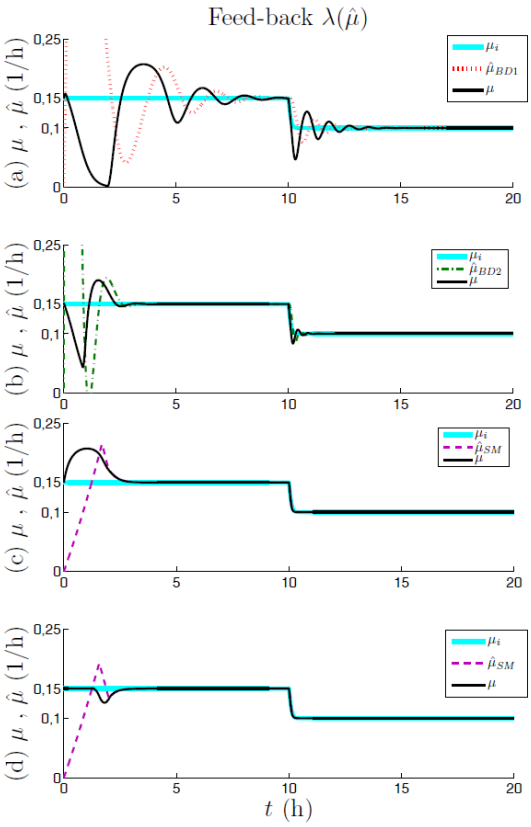

Figure 5.4: Closed-loop simulation results when observers are in the loop. a) Adaptive observer with $\omega = 1.5$, b) adaptive observer with $\omega = 4.5$, c) sliding observer, d) sliding observer in the loop after first switching. μ_i: specific growth rate using ideal feed-back law (5.24); μ: real growth rate; $\hat{\mu}_{BD1}$, $\hat{\mu}_{BD2}$: adaptive observer estimates for $\omega = 1.5$ and $\omega = 4.5$, respectively; $\hat{\mu}_{SM}$: sliding observer estimate.

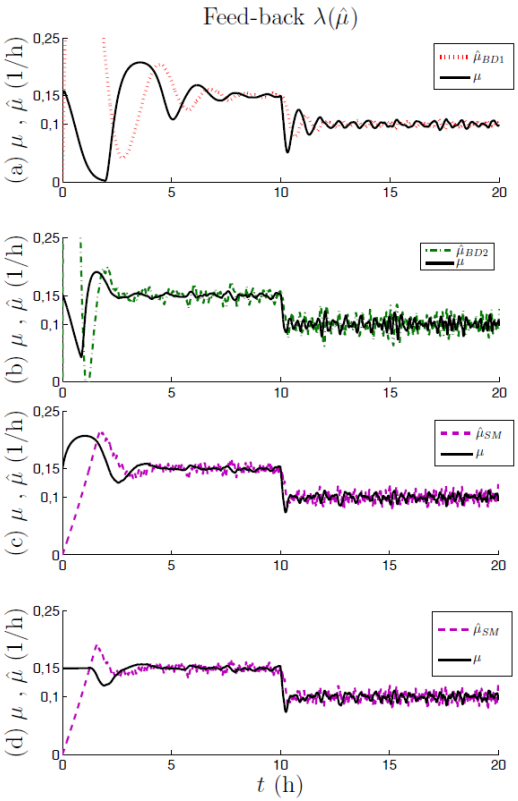

Figure 5.5: Closed-loop simulation results when observers are in the loop, noise added to the measured signal. a) Adaptive observer with $\omega = 1.5$, b) adaptive observer with $\omega = 4.5$, c) sliding observer, d) sliding observer in the loop after first switching. μ_i: specific growth rate using ideal feed-back law (5.24); μ: real growth rate; $\hat{\mu}_{BD1}$, $\hat{\mu}_{BD2}$: adaptive observer estimates for $\omega = 1.5$ and $\omega = 4.5$, respectively; $\hat{\mu}_{SM}$: sliding observer estimate.

ure 5.6b displays some estimates of the specific growth rate obtained from x_m. The noisiest estimate was crudely obtained by differentiating the measured signal: $\hat{\mu}_d(t) = \frac{\dot{x}_m}{x_m}$. The estimate plotted in dashed line was obtained by the high-gain observer (5.2) tuned with $\omega = 1.5$. This estimate coincides with that obtained by smoothing $\hat{\mu}_d(t)$ with a 2nd-order filter with cut-off frequency ωx. The estimate is particularly noisy –as measurement is– around $t = 35$h. This noise is hardly filtered by the observer because their bandwidths overlap. A lower observer bandwidth would help to reduce noise but at the cost of poorer tracking response. Finally, the signal plotted in solid line is the output of the sliding observer (5.5) with $\bar{\rho} = 0.1$, $\alpha = 1.1$ and $\beta = 1.8$ as in the previous example. The estimate is smoother than the previous one, particularly around $t = 35$ hours. This is because the observer is less sensitive to fast, and unfeasible, signal gradients. Fig 5.6c displays the biomass estimation error $\tilde{x}$ smoothed out by a low-pass filter, showing that the observer converges in 11 hours. During this period, the sliding observer is less sensitive to large measurement errors that are typical of the initial phase of batch processes when biomass concentration is too low.

It is of particular interest to analyze the observer outputs around $t = 23$h. As observed in the biomass evolution, the growth almost stops at $t = 18$h, most probably due to the depletion of some essential substrate. After that, a pulse of conjugated linoleic acid vaccine was administered at $t = 23$h, reactivating the microorganism growth. As seen in Figure 5.6b this sudden change in behavior clearly affects both observers. Indeed, from the point of view of the observers, an unpredicted oscillation of the biomass measurement occurred. It is observed that the B&D observer responds with a large undershoot that vanishes just after 1.5 hours. On the contrary, the sliding observer is much less sensitive to this perturbation. In fact, Fig 5.6c shows that the observer diverges and then converges rapidly, putting in evidence the occurrence of an abrupt fault. Note that the surface coordinate is an effective residual to indicate bioreactor malfunctions as well as sensor faults or changes in system behavior (both abrupt and gradual). Thus, on one hand, the observer output is less sensitive to the perturbation while on the other its sliding coordinate is very sensitive to it.

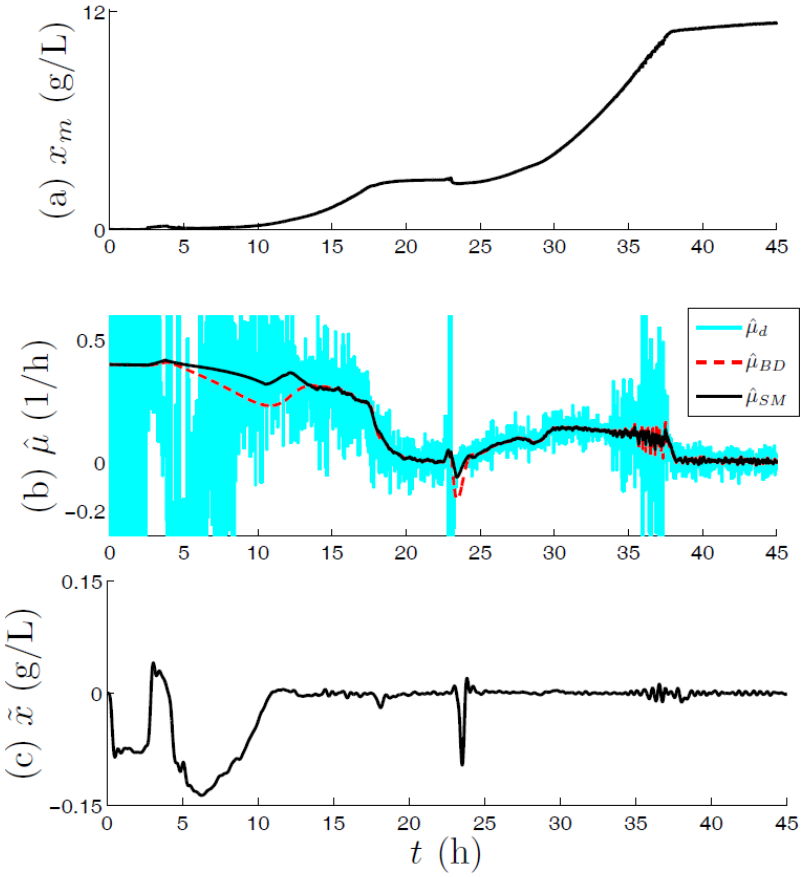

Figure 5.6: Experimental results. (a) Measured biomass concentration (x_m). (b) Estimates of the specific growth rate obtained by sensor output differentiation ($\hat{\mu}_d$) and using B&D ($\hat{\mu}_{BD}$) and sliding ($\hat{\mu}_{SM}$) observers. (c) Biomass estimation error ($\tilde{x}$) of the sliding observer.

5.6 Conclusions

In the article, a second-order sliding mode observer has been developed and analyzed for the estimation of the specific growth rate of microorganisms from measurements of biomass concentration. The resultant observer can be applied to either batch or fed-batch fermentation processes in which the bioreaction exhibits either monotonic or non-monotonic kinetics. Actually, the observer does not use any model of the kinetics of the reaction, just a bound on its time derivative. The proposed observer is based on high-gain observers, to which discontinuous correcting terms have been added in order to cancel the estimation error on the measured variable. The structure of the discontinuous output error injection is modified with respect to previous developments, thus providing a smooth estimate without the need of filtering. In contrast with continuous observers, perfect tracking after finite convergence time can be achieved in the absence of noise. Although convergence to a small ball can only be guaranteed in the presence of noise, this theoretical property has important implications in control. In fact, the separation principle applies, so that observer and controller in the loop can be designed independently. Simulation and experimental results confirm the distinctive convergence properties of the observer, as well as its potential use in fault detection.

Further research is oriented to obtain an estimate of the growth rate with absolute –rather than biomass-proportional– bound on its time derivative. Also, the problem of multiple rates estimation is being addressed. The main problem is that an extra unknown function must be incorporated to the algorithm in order to avoid too conservative bounds. Stability proof of the generalized algorithm is the key issue. The semidefinite programming approach used in this paper provides powerful tools for this purpose.

Chapter 6

Stability preserving maps for finite-time convergence

Make everything as simple as possible,
but not simpler.

Albert Einstein

ABSTRACT: The super-twisting algorithm (STA) has become the prototype of second-order sliding mode algorithm. It achieves finite time convergence by means of a continuous action, without using information about derivatives of the sliding constraint. Thus, chattering associated to traditional sliding-mode observers and controllers is reduced. The stability and finite-time convergence analysis have been jointly addressed from different points of view, most of them based on the use of scaling symmetries (homogeneity), or non-smooth Lyapunov functions. Departing from these approaches, in this contribution we decouple the stability analysis problem from that of finite-time convergence. A nonlinear change of coordinates and a time-scaling are used. In the new coordinates and time space, the transformed system is stabilized using any appropriate standard design method. Conditions under which the combination of the nonlinear coordinates transformation and the time-scaling is a stability preserving map are given. Provided convergence in the transformed space is faster than $\mathcal{O}(1/\tau)$ –where τ is the transformed time– convergence of

the original system takes place in finite-time. The method is illustrated by designing a generalized super-twisting observer able to cope with a broad class of perturbations.

6.1 Introduction

Sliding mode is a powerful technique used both in controller and observer design to reject matched disturbances (Utkin, 1977). The idea is to drive the state trajectory to a prescribed constraint surface where specifications are met and, from then on, to slide on it thanks to an intensive switching action. Because of its robustness and other attractive features, sliding mode has been successfully implemented in a wide variety of real processes (Hung et al., 1993; Šabanovic, 2011; Chiu, 2012). However, its underlying chattering phenomenon may be inadmissible in some control applications and may add severe noise in estimation (Young et al., 1999). Additionally, the prescribed constraint must have unit relative degree. Therefore the control action must explicitly appear in the first time derivative of the constraint function (Sira-Ramírez, 1989). High order sliding mode (HOSM) has been developed to relax the relative degree limitation and, at the same time, to alleviate chattering (Levant, 1993; Bartolini et al., 1998). Among all HOSM algorithms the super-twisting second-order one (SOSM) distinguishes because it achieves finite time convergence by means of a continuous action without using information about derivatives of the sliding function (Levant, 1998; Dávila et al., 2005). This algorithm handles a relative degree equal to one, so it can directly replace standard sliding mode algorithms when the disturbance is smooth and with bounded gradient. The main difference with respect to standard sliding mode is that discontinuity appears in the second derivative of the switching function, whereas a non-Lipschitz term appears in the first derivative to achieve finite-time convergence.

For many years, dissemination and acceptance of HOSM have been resisted due to the lack of powerful design tools and readable stability proofs. Originally, stability conditions were obtained geometrically using worst-case trajectory bounds (Levant, 1998). More recently, homogeneity concepts have been exploited to prove stability of some HOSM

algorithms (Levant, 2005). Homogeneous systems have a scaling symmetry which allows for stability analysis. Despite its advantages, this approach does not provide the convergence time and is a limitation to design new algorithms to deal with broader classes of disturbances since the homogeneity property may be lost during the design process. Lyapunov-based stability analysis appeared for the first time in (Moreno and Osorio, 2008). Since then, very intensive research is being followed in this area (Polyakov and Poznyak, 2009; Shtessel et al., 2010; Utkin, 2010; Santiesteban et al., 2010; Cruz-Zabala et al., 2011). Different Lyapunov functions have been proposed for different sliding algorithms. For instance, in (Moreno and Osorio, 2008), stability of the super-twisting algorithm (STA) is proved by means of a non-smooth Lyapunov function. (Utkin, 2010) uses also non-smooth functions for the twisting and super-twisting algorithms. A strict Lyapunov function to prove stability of the twisting algorithm is presented in (Santiesteban et al., 2010), and a generalization of the method of characteristics is presented in (Polyakov and Poznyak, 2009). In general, the Lyapunov approach allows to obtain less conservative designs, to compute the convergence time and, most importantly, to generalize the original algorithm to deal with more general system dynamics and disturbance structures (Moreno, 2010; De Battista et al., 2011; Pisano et al., 2011; Efimov and Fridman, 2011; Cruz-Zabala et al., 2011). The main drawback of current Lyapunov-based approaches is their dependence on complex tools – e.g. non-smooth analysis, solution of partial differential equations, etc.– to cope with the requirement of finite-time convergence together with the stability analysis. The use of time-scale, already used in other contexts –e.g. achieving feedforward form (Moya et al., 2002), or observer linearization and design of observers with linearizable error dynamics (Guay, 2002; Respondek et al., 2004) – has not been exploited.

The rest of the paper is organized as follows. In Section 6.2 a nonlinear coordinates transformation, and a time-scale one are used so as to transform the original system into a new one amenable for constructively finding a smooth control Lyapunov function. This allows to modify the super-twisting error injection terms so as to cope with a broader class of perturbations. The time-scale is chosen so that convergence faster than asymptotic in the transformed space corresponds to finite-time converge in the original one. In Section 6.3 the technique of stability preserving maps (Michel and Wang, 1995) is used to prove the

original system is also stable. In Section 6.4 a bound on the finite-time convergence is obtained, and simulation results are provided in Section 6.5.

6.2 Constructive design of a generalized super-twisting algorithm.

Consider the system:

$$\begin{aligned} \dot{x}_1 &= \varphi(t)x_2 + u_1(x_1,t) + \rho_1(x,t) \\ \dot{x}_2 &= u_2(x_1,t) + \rho_2(x,t) \end{aligned} \tag{6.1}$$

where $\varphi(t)$ is a known, possibly discontinuous, bounded positive function of time. The functions $\rho_1(x,t)$ and $\rho_2(x,t)$ are perturbation terms for which we assume the structure:

$$\begin{aligned} \rho_1(x,t) &= \varrho_1(t)p_1(x_1)\,|x_1|^{\frac{1}{2}} \ , \ \|p_1(x_1)\| \leq \bar{p}_1(x_1) \\ \rho_2(x,t) &= \varrho_2(t)p_2(x_1,x_2) \ , \ \|p_2(x_1,x_2)\| \leq \bar{p}_2(x_1) \end{aligned} \tag{6.2}$$

where $\bar{p}_1(x_1), \bar{p}_2(x_1)$ are known bounded functions for any bounded x_1 (e.g. class $\mathcal{K}_\infty$ functions), and $\varrho_j(t)$ bounded noises with $\bar{\varrho}_j = \|\varrho_j(\tau)\|_\infty$ for $j = 1, 2$. Notice that $\rho_2(x,t)$ may be not vanishing and discontinuous at $x_1 = 0$, while $\rho_1(x,t)$ vanishes at the origin, and is continuous w.r.t. x_1. System (6.1) may represent a process to be controlled or the error dynamics for some observer design. In this later case, $\rho_1(x,t)$ allows to represent the aproximation error of some dynamics on the first process state to be estimated, and $\rho_2(x,t)$ the unknown derivative of the second process state (De Battista et al., 2011).

The goal is to design the input signals u_1, u_2 so as to robustly stabilize the origin in finite-time. Besides $\varphi(t)$, only the state x_1 is assumed to be measured. To this end, we first apply the coordinates transformation given by the homeomorphism (Moreno, 2010):

$$(z_1, z_2) \longrightarrow \left(|x_1|^{\frac{1}{2}} \ \mathrm{sign}(x_1), x_2 \right) \tag{6.3}$$

transforming system (6.1) into:

$$\begin{aligned} \dot{z}_1 &= \frac{1}{2}\,|z_1|^{-1}\,[\varphi(t)z_2 + u_1(z_1,t) + \rho_1(z,t)] \\ \dot{z}_2 &= u_2(z_1,t) + \rho_2(z,t) \end{aligned} \tag{6.4}$$

Now, apply the time-scaling

$$t = \int |z_1|\, d\tau \tag{6.5}$$

In the new (z, τ)-coordinates:

$$\begin{aligned} z_1' &= \frac{\varphi(\tau)}{2} z_2 + \frac{1}{2} u_1(z_1, \tau) + \frac{1}{2} \varrho_1(\tau) |z_1| p_1(z_1) \\ z_2' &= |z_1|\, u_2(z_1, \tau) + |z_1|\, \varrho_2(\tau) p_2(z_1, z_2) \end{aligned} \tag{6.6}$$

with $z' \stackrel{\triangle}{=} dz/d\tau$. The goal now is to asymptotically stabilize system (6.6). Let us apply, for instance, the Lyapunov redesign methodology. To this end, consider the control signal u_1 is decomposed as:

$$u_1(z_1, \tau) = u_{1b}(z_1, \tau) - \eta_1 \bar{p}_1(z_1) z_1 \tag{6.7}$$

with $\eta_1 \geq \bar{\varrho}_1$ so that $\forall z_1 \in \mathbb{R}$

$$\Psi_1(z_1, \tau) \stackrel{\triangle}{=} \eta_1 \bar{p}_1(z_1) - \varrho_1(\tau) p_1(z_1) \geq 0 \tag{6.8}$$

Now, consider the Lyapunov function $V_1 = \frac{1}{2} z_1^2$. The control signals u_{1b} and u_2 will be designed later to force $z_2 = \eta_2 z_1$ for some constant $\eta_2 > 0$ and achieve $V_1' \leq 0$. Taking τ-time derivative:

$$V_1' = \frac{\varphi(\tau)}{2} \eta_2 z_1^2 + \frac{1}{2} u_{1b}(z_1) z_1 - \frac{1}{2} z_1^2 \Psi_1(z_1, \tau) \tag{6.9}$$

Thus, choosing

$$u_{1b}(z_1, \tau) = -[\eta_2 \varphi(\tau) + k_1(z_1, \tau)] z_1 \tag{6.10}$$

the dynamics of the error signal $\bar{z}_2 = z_2 - \eta_2 z_1$ are:

$$\begin{aligned} \bar{z}_2' = &-\frac{\eta_2 \varphi(\tau)}{2} \bar{z}_2 + |z_1| u_2(z_1) + \\ &+ z_1 \left[\tilde{\varrho}_2(\tau) p_2(z_1, z_2) + \frac{\eta_2}{2} [k_1(z_1, \tau) + \Psi_1(z_1, \tau)] \right] \end{aligned} \tag{6.11}$$

where $\tilde{\varrho}_2(\tau) = \varrho_2(\tau)\ \mathrm{sign}(z_1)$. Consider now the augmented Lyapunov function:

$$V_2 = \frac{1}{2} z_1^2 + \frac{1}{2} \bar{z}_2^2 \tag{6.12}$$

Taking τ-time derivative, choosing

$$u_2(z_1,\tau) = -\frac{1}{2}[\varphi(\tau) + \eta_2[k_1(z_1,\tau) + \eta_1\bar{p}_1(z_1)]]\ \mathrm{sign}(z_1) \tag{6.13}$$

and defining $\mathbf{z} = [z_1, \bar{z}_2]^T$, we have:

$$V_2' \leq -\frac{1}{2}\mathbf{z}^T \begin{bmatrix} k_1(z_1,\tau) & -q_{12}(z,\tau) \\ -q_{12}(z,\tau) & \eta_2\varphi(\tau) \end{bmatrix} \mathbf{z} \stackrel{\triangle}{=} -\frac{1}{2}\mathbf{z}^T\mathbf{Q}\mathbf{z} \tag{6.14}$$

with $q_{12}(z,\tau) \stackrel{\triangle}{=} \bar{\varrho}_2\bar{p}_2(z_1) + \frac{\bar{\varrho}_2\eta_2}{2}\bar{p}_1(z_1)$. At this point, it is interesting to summarize and observe the structure of the injected correction terms in the original x-dynamics:

$$\begin{aligned} u_1(x_1,t) &= -\left[\eta_2\varphi(t) + k_1(x_1,t) + \eta_1\bar{p}_1(x_1)\right]|x_1|^{\frac{1}{2}}\ \mathrm{sign}(x_1) \\ u_2(x_1,t) &= -\frac{1}{2}\left[\varphi(t) + \eta_2[k_1(x_1,t) + \eta_1\bar{p}_1(x_1)]\right]\ \mathrm{sign}(x_1) \end{aligned} \tag{6.15}$$

Notice that for $\mathbf{Q}$ in equation (6.14) to be positive definite, the polynomial $k_1(z_1,\tau)$ will have to dominate the square of the terms in the secondary diagonal. Therefore, for $k_1(z_1,\tau)$ to be bounded –recall this polynomial will form part of the injected correction terms u_1, and u_2– we asked $\bar{p}_j(z_1), j = 1,2$ to be bounded for bounded z_1. Recalling $\bar{\varrho}_1 \leq \eta_1$, and condition (6.8), a sufficient condition for positive definiteness of $\mathbf{Q}$ in equation (6.14) is $k_1(z_1,\tau) = k^2(z_1)/\varphi(\tau) > 0$, and:

$$k(z_1) > \frac{\bar{\varrho}_2}{\sqrt{\eta_2}}\bar{p}_2(z_1) + \frac{\sqrt{\eta_2}\eta_1}{2}\bar{p}_1(z_1) \tag{6.16}$$

Notice that continuity of $u_1(z_1,\tau)$ w.r.t. z_1 at $z_1 = 0$, requires that of $k_1(z_1,\tau)z_1$ and $\bar{p}_1(z_1)z_1$ at that point.

In the simplest case where $p_1(z_1) \equiv 0$, $p_2(z_1) \equiv 1$, and $\varphi(t) \equiv 1$, choosing $\eta_1 = 0$ and $k_1(z_1(x_1)) = k_1$, retrieves the original super-twisting algorithm. The stability region is defined by the bounds $\eta_2 + k_1 > 2\bar{\varrho}_2$, and $\eta_2 k_1 > \bar{\varrho}_2^2$.

As a more complex example, to be used in section 6.5, assume $\varphi(t) \equiv 1$, $p_2(z_1,z_2) = 1$, and $p_1(z_1)$ polynomial so that

$$\rho_1(z,\tau) = \varrho_1(\tau)\left[p_0 + p_1z_1 + \ldots + p_\beta z_1^\beta\right] z_1 \tag{6.17}$$

with $\beta \geq 0$. A bounding function $\bar{p}_1(z_1)$ is needed to fulfill condition (6.8). Assume $p_1(z_1)$ is unknown, but for its order and bounds on the coefficients. Define $\bar{p} = \max(p_0, \ldots, p_\beta)$, $n_\beta = \beta + 1$, and:

$$\bar{p}_1(z_1) \stackrel{\triangle}{=} n_\beta \bar{p} |z_1|^\gamma \quad , \quad \gamma = \begin{cases} \beta \ , \ |z_1| > 1 \\ 0 \ , \ |z_1| \leq 1 \end{cases} \tag{6.18}$$

Condition (6.8) is satisfied, and a sufficient condition for positive definiteness of **Q** is:

$$k(z_1) > \frac{\bar{\varrho}_2}{\sqrt{\eta_2}} + \frac{\sqrt{\eta_2}\eta_1}{2} n_\beta \bar{p} |z_1|^\gamma \tag{6.19}$$

which can be fulfilled choosing $k(z_1) = k_a + k_b |z_1|^\gamma$, with $k_a > \frac{\bar{\varrho}_2}{\sqrt{\eta_2}}$, and $k_b > \frac{\sqrt{\eta_2}\eta_1}{2} n_\beta \bar{p}$. Figure 6.1 shows the stability region for the particular case $p_1(z_1) = 1$.

6.3 Stability analysis

The proof will be split into three parts. First we analyze the homomorphism transforming system (6.1) in the (x, t)-coordinates into (6.4) in the (z, t)-coordinates, given by the change of coordinates (6.3) and the identity transformation for the time parameter. Its is proved this homomorphism is a time-invariant homeomorphism, and consequently preserves asymptotic stability.

Let X_i be the set of current states of system s_i. Any set with subscript i refers to a subset of X_i. The following elementary fact will be used in the proof:

Lemma 6.1. *Given any one-to-one function $f : X_i \to X_j$, if $A_i \subset B_i \subseteq X_i$, then $f(A_i) \subset f(B_i)$.*

Theorem 6.1. *Any homomorphism given by a time-invariant homeomorphic coordinate change and the identity transformation for the time parameter, i.e. with no time-scaling, preserves asymptotic stability.*

Proof Consider a homeomorphism $f : X_1 \to X_2$. By continuity, around any point $x_{1e} \in X_1$, $\forall \epsilon > 0$ there exists a $\delta > 0$ such that whenever $| x_2 - x_{2e} | < \delta$, $| x_1 - x_{1e} | < \epsilon$, with $x_{2e} = f(x_{1e}) \in X_2$.
Now take $\epsilon_1 = \epsilon$, and $\epsilon_2 = \delta$. If the goal system s_2 is stable, and assuming

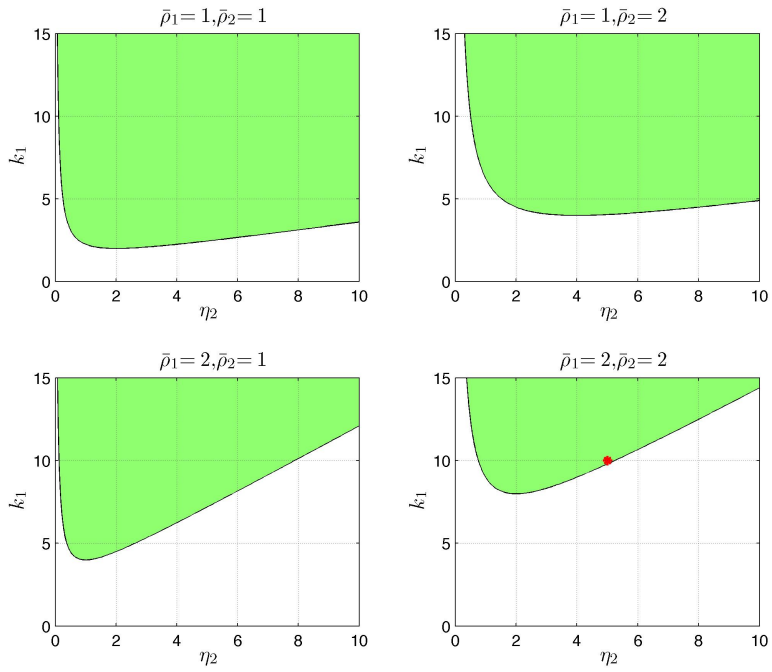

Figure 6.1: Stability region in the η_2, k_1 parameters space for the case $p_1(z_1) = 1$ (i.e. $\rho_1(x,t) = 2\varrho_1(t)|x_1|^{\frac{1}{2}}$), $p_2(z_1, z_2) = 1$, and $\varphi(t) \equiv 1$. Two different values of the perturbation bounds $\bar{\varrho}_1$ and $\bar{\varrho}_2$ are shown.

$x_{2e} = 0$ without loss of generality, then, $\forall \epsilon_2 > 0$, $\exists \delta_2 > 0$ such that if $\mid x_{20} \mid < \delta_2$ then $\forall t > t_0$, $\mid x_2 \mid < \epsilon_2$. Using lemma 6.1, $f^{-1}(\delta_2) \subset \epsilon_1$, and $\mid x_1 \mid < \epsilon_1$ whenever $\mid x_{10} \mid < f^{-1}(\delta_2)$. So the first system $s_1(X_1)$ is also stable.
The same reasoning is valid for attractivity, but now orbits are inside an ϵ-ball from a given $t = t_\epsilon$. Notice t_ϵ is the same for both systems since there is no time-scaling. □

Lemma 6.2. *The change of coordinates given by* $(z_1, z_2) \longmapsto (\mid x_1 \mid^{1/2} sign(x_1), x_2)$ *is a homeomorphism.*

Corollary 6.1. *The homomorphism transforming system (6.1) in the* (x, t)*-coordinates into (6.4) in the* (z, t)*-coordinates, given by the change of coordinates (6.3) and the identity transformation for the time parameter –i.e. with no time-scaling– is a time-invariant homeomorphism, and consequently a stability preserving map.*

Secondly, we analyze the homomorphism transforming system (6.4) in the (z, t)-coordinates into system (6.6) in the (z, τ)-coordinates, given by the identity coordinate transformation and the time-scaling (6.5). For time invariant systems, stability of equilibrium points in the sense of Lyapunov is a property of the orbits independent of their parametrization. Consequently, under the conditions for equivalence of regular curves explained below (Kühnel, 2005), any reparametrization (i.e. time-scaling) will preserve stability.

Definition 6.1. *A regular curve is an equivalence class of regular parametrized curves, where the equivalence relationship is given by regular (orientation preserving) parameter transformations* $\xi : [\alpha, \beta] \longrightarrow [a, b]$*, with* $\dot{\xi} > 0$*, and* ξ *bijective and continuously differentiable.*

In our context, we will define the required time scaling to be a regular parameter transformation ξ, i.e. $\dot{\xi} \neq 0$ must hold everywhere. Since equilibrium points are singularities, we will consider the system orbits to be represented by the curves with time interval I spanning from initial conditions to the equilibrium. To fulfill the definition above, the time scaling ξ must be one-to-one, and onto. The fact that ξ must be *onto* ensures the whole orbit (a regular curve) is covered by both parametrizations. The condition $\dot{\xi} > 0$, except perhaps in a set of measure zero, ensures both "times" go forward since it makes ξ strictly increasing. Finally, for a function ξ to be one-to-one with positive derivative every-

where, it is sufficient to prove it is strictly increasing. Then we must prove it is also onto and hence a bijection.

Proposition 6.1. *Under the conditions for equivalence of regular curves given in definition 6.1, any reparametrization (i.e. time-scaling) will preserve stability.*

Proof The proof is straightforward from the standard definition of stability in the sense of Lyapunov, and the facts that re-parameterizing the orbit will not change it and time in both parameterizations moves in the same direction. □

Now it is proved the above conditions are also sufficient for attractivity and, consequently asymptotic stability. Denote by T_{t_0} the set $\{t \in T : t \geq t_0\}$ for some initial time instant t_0.

Theorem 6.2. *Any homomorphism given by the identity transformation for the coordinates and a time-scaling defined by a strictly increasing and onto function $\xi : t \longrightarrow \tau$ preserves attractivity.*

Proof Since the coordinates transform to themselves, the homomorphism only introduces a reparametrization of the orbits (which are regular curves) by means of the time-scaling ξ. Since ξ is strictly increasing, there is ξ^{-1} with positive derivative everywhere. There are two possible cases:

1. ξ^{-1} is unbounded, mapping T_{τ_0} to T_{t_0}. Then $\forall T$, $\exists \tau_T : \forall \tau > \tau_T$, $t = \xi^{-1}(\tau) > T$. Taking $T = \xi^{-1}(\tau_\epsilon)$, and given that ξ^{-1} is strictly increasing, eventually $t > T$ and, if $\mid z(\tau) \mid < \epsilon$, then $\mid x(t) \mid < \epsilon$ too.

2. ξ^{-1} is bounded. The previous reasoning can be reproduced willy-nilly, but now we must additionally prove that ξ^{-1} is onto. Since ξ^{-1} is strictly increasing and bounded there is t_f such that $t \in [t_0, t_f]$ and $t \to t_f$ when $\tau \to \infty$. Therefore, if $z(\tau) \to z_{eq}$ then $x(t_f) = z_{eq} = x_{eq}$ by the identity of coordinates, proving finite time convergence to the equilibrium point of the original system. □

Corollary 6.2. *Any re-parameterization as defined in 6.1 preserves asymptotic stability.*

Proof From Proposition 6.1, and Theorem 6.2 any re-parameterization as defined in 6.1 preserves both stability and attractivity. Therefore, it preserves asymptotic stability. □

Proposition 6.2. *Choosing the time-scaling ξ implicitly, by giving its inverse ξ^{-1} as defined in equation (6.5) the corresponding homomorphism fulfills Corollary 6.2.*

Proof Due to the modulus function, no matter what $\mid z_1(\tau) \mid$ does, except being identically zero, the integral defines a strictly increasing function. So it is an injection and has an inverse, defining the regular parameter transformation ξ we need. □

Finally, because of transitivity, the composition of stability preserving maps is also a stability preserving map. The combination of the nonlinear change of coordinates (6.3) and the time-scale transformation (6.5) is equivalent to the composition of the homomorphisms defined above. Therefore, this combination is a stability preserving map. Consequently, the system (6.1) in the (x,t)-coordinates is asymptotically stable if and only if the system (6.6) in the (z,τ)-coordinates is.

In particular, the convergence rate can be obtained from:

$$t_f \stackrel{\triangle}{=} \lim_{\tau\to\infty} t(\tau) = \lim_{\tau\to\infty} \int_0^\tau |z_1(\xi)| d\xi \tag{6.20}$$

If the integral is divergent as $\tau \to \infty$ (e.g $z_1 = \mathcal{O}(1/\tau)$) we are in the first case in Theorem (6.2). Otherwise, if it is convergent (e.g $z_1 = \mathcal{O}(1/\tau^2)$), we are in the second case, and finite-time convergence is achieved in the original (x,t)-coordinates.

6.4 Bound on finite-time convergence

Let us consider again equation (6.14) rewritten as:

$$V' = -\frac{1}{2}\bar{z}^T\mathbf{Q}\bar{z} \leq -\frac{1}{2}\bar{z}^T\bar{z}\underline{\lambda}_{\mathbf{Q}}(\tau) = -\underline{\lambda}_{\mathbf{Q}}(\tau)V(\tau) \tag{6.21}$$

where $\underline{\lambda}_{\mathbf{Q}}(\tau)$ is the minimum eigenvalue of $\mathbf{Q}(\tau)$. Notice, for every initial condition and every τ there is either a minimum eigenvalue of Q or a lower bound since by positive definiteness the eigenvalues are always positive. Application of the comparison lemma leads to

$$|z_1| \leq \|\bar{z}\| \leq \|\bar{z}(\tau_0)\| e^{-\frac{1}{2}\int \underline{\lambda}_{\mathbf{Q}}(\tau)d\tau} \tag{6.22}$$

It then follows, using (6.20) and (6.22), that

$$t_f \leq \|\bar{z}(\tau_0)\| \int_0^\infty e^{-\frac{1}{2}\int \underline{\lambda}_{\mathbf{Q}}(\tau)d\tau} d\xi \leq \frac{2}{\underline{\lambda}_{\mathbf{Q},\min}} \|\bar{z}(\tau_0)\| \tag{6.23}$$

where $\underline{\lambda}_{\mathbf{Q},\min} \triangleq \min_{\tau} \underline{\lambda}_{\mathbf{Q}}(\tau)$. Since $\frac{1}{\underline{\lambda}_{\mathbf{Q}}} = \frac{\overline{\lambda}_{\mathbf{Q}}}{\underline{\lambda}_{\mathbf{Q}}\overline{\lambda}_{\mathbf{Q}}} = \frac{\overline{\lambda}_{\mathbf{Q}}}{\det \mathbf{Q}}$, then t_f in equation (6.23) can be bounded by

$$t_f < 2\|\bar{z}(\tau_0)\| \frac{\max\limits_{\tau,z_1} \mathrm{tr}\mathbf{Q}}{\min\limits_{\tau,z_1} \det \mathbf{Q}} \tag{6.24}$$

For instance, if $\rho_1(z,\tau) \equiv 0$, and $k_1\eta_2 > \bar{\varrho}_2^2$ one easily gets

$$t_f < 2\|\bar{z}(\tau_0)\| \frac{k_1+\eta_2}{k_1\eta_2 - \bar{\varrho}_2^2}. \tag{6.25}$$

6.5 Example

A super-twisting observer has been tuned using the proposed approach. The perturbation term $\rho_1(x,t)$ takes the form of (6.17), with $p_1(x_1) = 1 + 1.5|x_1|^{1/2}$, and $\varrho_1(t)$ being a bounded noise. The order of $p_1(x_1)$ and an upper bound on its coefficients are assumed to be known so as to build the bounding function $\bar{p}_1(x_1)$ according to (6.18). The perturbation term $\rho_2(x,t)$ has been obtained as the derivative of an unknown signal $u(t)$ with bounded time derivative $\|\rho_2(x,t)\|_\infty \leq 2$, but at $t = 1sec$, and $t = 2sec$ when a step and impulse respectively were injected as disturbances in $u(t)$. The bounds of the unknown signal derivative and the integrator input noise have been set to $\bar{\varrho}_2(x,t) = 2$ and $\bar{\varrho}_1(x,t) = 2$ respectively. Chosing $\eta_1 = 2.5$, $\eta_2 = 5$, and $\bar{p} = 1.5$ the observer parameters where obtained using (6.19).

The simulation results are shown in Fig. C.2. Three zooms around the time instants $t = 0sec$, $t = 1sec$, and $t = 2sec$ are shown. At other time instants in between, the real and estimated signals are indistinguishable. The top plot depicts the input signal to the observer $y(t)$ (in blue dashed line), and the estimated signal $\hat{y}(t)$ (in red solid line). The real integrator input $u(t)$ –with noise, in cyan, and without noise in dashed blue– and its estimated value $\hat{u}(t)$ (in red solid line) are displayed in the bottom plot. It is seen that the observer output converges in less than $0.02sec$ and perfectly tracks the evolution of $u(t)$ when the appropriate conditions hold. At $t = 1sec$ and $t = 2sec$ the derivative of $u(t)$ is larger than the assumed bound $\bar{\varrho}_2(x,t)$, and the observer output diverges and then converges rapidly, putting in evidence the occurrence of an abrupt fault, as the derivative of $u(t)$ overly differed from the expected one.

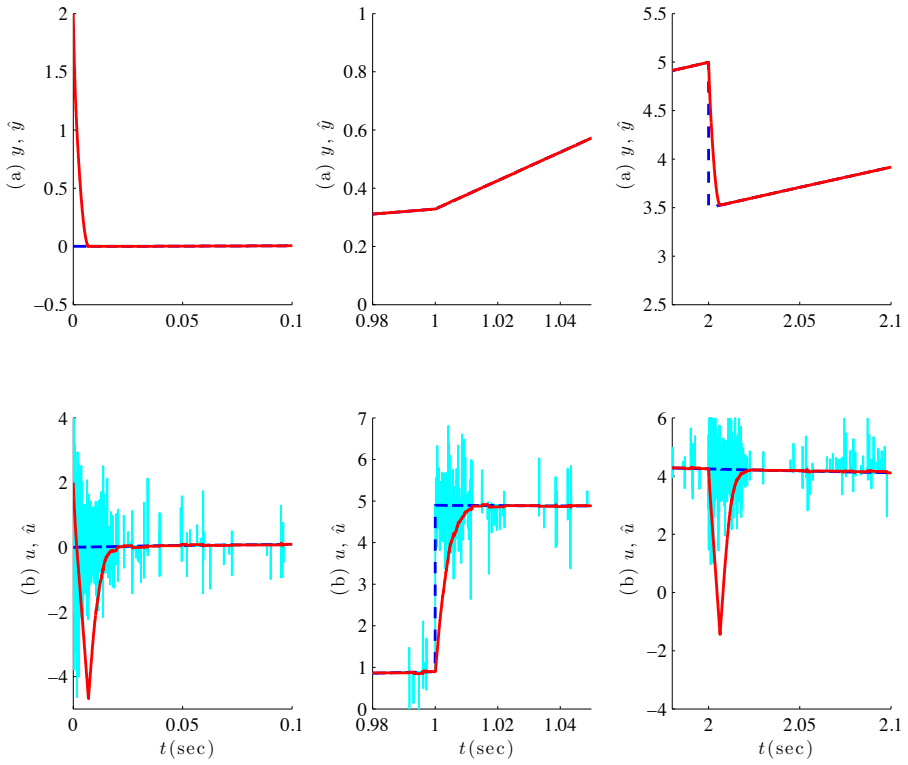

Figure 6.2: Super-twisting observer response. Zooms around the time instants $t = 0sec$, $t = 1sec$, and $t = 2sec$.

6.6 Conclusions

In this contribution the problem of designing algorithms with finite-time convergence has been adressed by decoupling the stability analysis problem from that of finite-time convergence. This allows simple design methods and stability proofs to be derived in a wide set of cases. In order to show the proposed approach, it has been applied to give an alternative proof of the super-twisting second-order sliding mode algorithm. This alternative approach allowed a simple design of a generalised SOSM coping with a broad class of perturbations. An estimate of the convergence time can be easily obtained in the transformed time-space. The approach can be extended to systems that can be robustly

controlled in the coordinates-time transformed space for any coordinates dependent time-scaling fulfilling Corollary 6.2. Finite-time convergence will be achieved under the conditions of case 2 in Theorem 6.2.

Chapter 7

Second-Order Sliding Mode Observer for Multiple Kinetic Rates Estimation in Bioprocesses

If you make listening and observation
your occupation
you will gain much more than you can
by talk.

Robert Baden-Powell

Abstract: Specific kinetic rates are key variables regarding metabolic activity in bioprocesses. They are non-linear functions of concentrations and operating conditions and therefore of difficult access for process control. In this paper, a multiple kinetic rates observer based on second-order sliding mode ideas is proposed. The main difference with other proposals is that smooth estimates are achieved in finite-time without adding additional dynamics. The resulting estimator is robust against uncertainty in the model of the estimated variables. Experimental results from continuous fermentation of *S. cerevisiae* are presented, where microbial specific growth rate and net ethanol production rate are estimated.

7.1 Introduction

Nowadays, biotechnological processes are applied in a wide range of industries for the production of enzymes, recombinant proteins, and high-value metabolic products. An important control problem of these processes is to achieve a desired metabolic condition (Jobé et al., 2003). The specific reaction rates contain information that is closely related to microbial activity. The knowledge of these signals have at least two relevant applications. First, reaction rates can be used in closed-loop control for improving process productivity. For instance, certain industrial problems have been related to the problem of regulating the specific growth rate (μ) of microorganism (Ren and Yuan, 2005; Soons et al., 2006). Second, the on-line availability of such information during the cultivation stage enhances bioprocess monitoring, which is essential for quality control, process reproducibility and early problem detection (Vojinovic et al., 2006).

Regretfully, specific reaction rates are in general not accessible since they are unmeasurable and uncertain non-linear functions of states (concentrations) and operating conditions (temperature, pH, pressure, etc). In this context, the use of observers (*software sensors*) to obtain an on-line estimation of specific rates avoids the problem of model identification while adds information for closed-loop control schemes and culture studies (Farza et al., 1998).

A survey of relevant methods applied to state estimation in bioprocesses can be found in Venkateswarlu (2004). Particularly, several model-based observers have been proposed for the reaction rate estimation problem. They include adaptive estimator for microbial growth rate in Bastin and Dochain (1986), extended Kalman filter in Shimizu et al. (1989), asymptotic observers for parameter estimation in Bastin and Dochain (1990), high gain observers of specific rates in (Farza et al., 1998; Gauthier et al., 1992; Martinez-Guerra et al., 2001), and sliding mode based observers in (Picó et al., 2009a; Rahman et al., 2010; De Battista et al., 2011). Other approach, which does not rely on process model but requires training data sets, is based on artificial neural networks (Karakuzu et al., 2006).

In the sliding mode observers (SMO), the idea is to enforce a sliding regime on the subspace for which the state estimation error is zero by means of a discontinuous action. Then, the observer output copies the

measured state despite disturbances and allows the reconstruction of the signal of interest (Edwards and Spurgeon, 1998; De Battista et al., 2012a). In the problem of kinetic rates estimation, the unknown signals appear in the time-derivative of the states. First-order sliding mode observers were developed in Picó et al. (2009a) to deal with specific growth rate and substrate estimation from on-line biomass measurement. Although the exact estimation of μ was a high-frequency discontinuous signal, it was useful for constructing the substrate observer. The resulting estimates were robust under typical model uncertainties while exhibiting first order dynamics. In Rahman et al. (2010), substrate measurements were used to estimate the substrate consumption rate. The observer error dynamics is exponentially stable whereas model uncertainties and disturbances are rejected. Thereafter, in De Battista et al. (2011) a second-order sliding mode observer of μ was presented. More precisely, the proposal is a modified version of the "super twisting" algorithm, a high-order sliding mode algorithm presented in Levant (1998). In this case, the observer provides of smooth estimation that exhibits finite-time convergence and is robust to typical process model uncertainties.

This work is intended to generalise preliminary results in De Battista et al. (2011). The multiple rates estimation problem requires to deal with an additional time-varying function. Therefore, further modifications are required in both the observer's structure as in the proposition of stability conditions. From bioprocess control viewpoint, the goal is to add information about the microorganism activity so as to increase on-line signals for closed-loop control and bioprocess monitoring. Therefore, the observer proposed here is applied to estimate p specific kinetic rates of production or consumption based on p related on-line measurements of process variables. The main difference with other continuous time proposals is that the estimates are achieved in finite-time and from then on, no additional dynamics is added. Besides, differing from first-order SM proposals the resulting estimations are smooth. Consequently, no additional smoothing elements would be required in closed-loop configurations. Further, robustness is expected since no model of each kinetic rate is assumed.

The rest of the chapter is organised as follows. In Section 7.2 the problem to be solved and a typical state-space model for a bioprocess in a stirred-tank are presented. Then, in Section 7.3, the proposed ob-

server is formulated. Section 7.4 presents results in which microbial specific growth rate and net ethanol production rate in continuous fermentation of *Saccharomyces cerevisiae* are estimated from experimental data. Finally, in Section 7.5, concluding remarks are given.

7.2 Bioprocess model and problem statement

A biotechnological process taking place in a stirred tank can be described by the following state-space model (Bastin and Dochain, 1990) A biotechnological process taking place in a stirred tank can be described by the following state-space model (Bastin and Dochain, 1990)

$$\frac{d\boldsymbol{\xi}}{dt} = \boldsymbol{K}\boldsymbol{r}(\boldsymbol{\xi},t) - D(t)\boldsymbol{\xi}(t) + \boldsymbol{F}(t) - \boldsymbol{Q}(\boldsymbol{\xi}), \tag{7.1}$$

where $\boldsymbol{\xi}(t) \in \mathbb{R}^n_+$ is the state vector, $\boldsymbol{K}$ is an $(n \times m)$ pseudo-stoichiometric coefficients matrix, $\boldsymbol{r}(\cdot) \in \mathbb{R}^m$ the reaction rates vector, $D(t) \in \mathbb{R}_+$ the dilution rate, $\boldsymbol{F}(t) \in \mathbb{R}^n_+$ the input flow rate vector and $\boldsymbol{Q}(\boldsymbol{\xi}) \in \mathbb{R}^n_+$ the gaseous outflow rate vector.

Equation (7.1) describes the dynamics of the (bio)chemical species in the culture, which evolve according to m reaction rates $\boldsymbol{r}(\boldsymbol{\xi},t)$. Since the reactions can take place only in presence of certain necessary reactants, $r_i(\cdot)$ is zero whenever the concentration of one of the required reactants is zero. Then, the reactions can be factorised as $r_i(\boldsymbol{\xi},t) = \alpha_i(\boldsymbol{\xi},t)\prod_{j\in\mathcal{J}_i}\xi_j$ where $\alpha_i(\cdot)$ is generally a nonlinear function and $\mathcal{J}_i$ denotes the set of required reactants (Bastin and Dochain, 1990). In matrix form, this results in

$$\boldsymbol{r}(\boldsymbol{\xi},t) = \boldsymbol{G}(\boldsymbol{\xi},t)\boldsymbol{\alpha}(\boldsymbol{\xi},t), \tag{7.2}$$

where $\boldsymbol{G}(\boldsymbol{\xi},t)$ is an $(m \times m)$ state-dependent diagonal matrix.

The $\alpha_i(\cdot)$ defined in (7.2) are called the *specific* reaction rates per unit of *each* reactant (other definitions such as per unit of biomass are usually used, see Perrier et al. (2000)). These nonlinear time-varying functions provide important knowledge about the bioprocess (e.g. microbial specific growth rate, oxygen specific uptake rate, specific production rate of metabolites) but its modelling and parameter identification can be extremely difficult. In order to add information about the process (possibly for on-line process control), a software sensor of specific reaction rates will be developed.

Particularly, the goal is to derive a robust observer of a subset of p specific reaction rates, namely $\boldsymbol{\alpha}_p(t) = \begin{bmatrix}\alpha_1(t), & \ldots, & \alpha_p(t)\end{bmatrix}^T$. To this end, let consider that p available measurements of $\boldsymbol{\xi}(t)$ are rearranged in a vector $\boldsymbol{z}$, i.e. $\boldsymbol{z}(t) = \begin{bmatrix}\xi_1(t), & \ldots, & \xi_p(t)\end{bmatrix}^T$. Let $\boldsymbol{K}_p$ and $\boldsymbol{G}_p(\cdot)$ be the corresponding $(p \times p)$ submatrices of $\boldsymbol{K}$ and $\boldsymbol{G}(\cdot)$, respectively whereas $\boldsymbol{F}_p$ and $\boldsymbol{Q}_p$ are the corresponding $(p \times 1)$ vectors arranged from $\boldsymbol{F}$ and $\boldsymbol{Q}$. Assume the following:

Assumption 7.1. The state variables are positive and bounded.

Assumption 7.2. $\boldsymbol{G}_p$, $\boldsymbol{F}_p$ and $\boldsymbol{Q}_p$ are available.

Assumption 7.3. A bound for each α_i time derivative $\bar{\rho}_i > 0$ is known.

Assumption 7.4. The matrix $\boldsymbol{K}_p$ is invertible.

Assumption 7.5. Diagonal matrices $\boldsymbol{G}_1$, $\boldsymbol{G}_2$ such that $\boldsymbol{0} < \boldsymbol{G}_1 \leq \boldsymbol{G}_p(\cdot) \leq \boldsymbol{G}_2$ holds are known.

Note that A.7.1 holds for the bioprocess variables (e.g. components concentrations and volume). A.7.2 is a common assumption in the literature regarding the availability of certain on-line measurements (e.g Perrier et al. (2000)). A.7.3 states that a bound of each kinetic dynamics is available, which can be determined from practice knowledge of the bioprocess. A.7.4 ensures that p reaction rates can be estimated from the p measured variables. Otherwise, the measured vector would not provide enough information about the reactions. From the discussion of eq. (7.2), the elements of $\boldsymbol{G}_p$ are products of state variables which all remain positive and bounded. In the event that one required reactant vanishes, then at least one reaction no longer takes place. In that case, the estimation of the reaction rate has no sense and consequently the estimation problem should be reconsidered. The diagonal elements of $\boldsymbol{G}_1$ and $\boldsymbol{G}_2$ in A.7.5 should be selected by the user based on his own knowledge about the particular process being monitored.

Now, from the model (7.1) and the previous discussion, the following system is considered

$$\frac{d\boldsymbol{z}}{dt} = \boldsymbol{K}_p\boldsymbol{G}_p(\cdot)\boldsymbol{\alpha}_p(\boldsymbol{\xi}, t) - D\boldsymbol{z} + \boldsymbol{F}_p - \boldsymbol{Q}_p, \tag{7.3}$$

$$\frac{d\boldsymbol{\alpha}_p}{dt} = \boldsymbol{R}\boldsymbol{\rho}(t), \tag{7.4}$$

in which $\boldsymbol{\alpha}_p(t)$ is the vector of specific kinetic rates to be estimated and $\boldsymbol{R} = diag\{\bar{\rho}_i\}$ arranges the bounds of the time derivatives. Note that $\boldsymbol{\rho}(t)$ is a vector of p unknown continuous functions where $\|\boldsymbol{\rho}(t)\|_\infty \leq 1$ holds.

7.3 A Second-order Observer of Specific Kinetic Rates

7.3.1 Definitions

In this section the following notation is used

$$\boldsymbol{G}_o = (\boldsymbol{G}_1 + \boldsymbol{G}_2)/2, \tag{7.5a}$$
$$\Delta\boldsymbol{G} = (\boldsymbol{G}_2 - \boldsymbol{G}_1)/2, \tag{7.5b}$$
$$\delta = \left\|\boldsymbol{G}_o^{-1}\Delta\boldsymbol{G}\right\|_\infty, \tag{7.5c}$$
$$\check{\boldsymbol{G}}_p(\cdot) = \boldsymbol{G}_o^{-1}\boldsymbol{G}_p(\cdot), \tag{7.5d}$$

where $\|\cdot\|_\infty$ stands here for the induced ∞-norm of the matrix.

Remark 7.1. Recalling definition and assumptions for $\boldsymbol{K}_p$, $\boldsymbol{G_o}$ and $\boldsymbol{R}$, it is straightforward to see that $\boldsymbol{K}_p\boldsymbol{G}_o\boldsymbol{R}$ is nonsingular.

Let define an auxiliary vector $\boldsymbol{\sigma}$ as

$$\boldsymbol{\sigma} = (\boldsymbol{K}_p\boldsymbol{G}_o\boldsymbol{R})^{-1}(\boldsymbol{z} - \hat{\boldsymbol{z}}), \tag{7.6}$$

where $\hat{\boldsymbol{z}}$ is an estimation of $\boldsymbol{z}$.

Finally, let $SIGN(\cdot)$: $\mathbb{R}^p \to \mathbb{R}^p$, $ABS(\cdot)$: $\mathbb{R}^p \to \mathbb{R}^{p\times p}$, defined as:

$$SIGN(\boldsymbol{\sigma}) = col(sign(\sigma_i)), \tag{7.7}$$
$$ABS(\boldsymbol{\sigma}) = diag\{|\sigma_i|\}. \tag{7.8}$$

From eq. (7.6), it follows that if there exists $T^* > 0$ such that $\boldsymbol{\sigma} \equiv \boldsymbol{0}$ holds for all $t > T^*$, i.e. if the system can be steered to evolve over the sliding surface defined by $\boldsymbol{\sigma}(\boldsymbol{z}) = \boldsymbol{0}$ in finite-time, then $\hat{\boldsymbol{z}} \equiv \boldsymbol{z}$ is achieved.

Since the previous comment is the core idea to estimate the reaction rates, the objective now is the design of a dynamic system which enforces eq. (7.6) to vanish in finite-time.

7.3.2 Main result

Proposition 7.1. *The system defined by:*

$$\frac{d\hat{\boldsymbol{z}}}{dt} = \boldsymbol{K}_p\left(\boldsymbol{G}_p(\cdot)\boldsymbol{R}\boldsymbol{u}_1 + 2k_2\boldsymbol{G}_o\boldsymbol{R}\boldsymbol{u}_2\right) - D\boldsymbol{z} + \boldsymbol{F}_p - \boldsymbol{Q}_p, \tag{7.9a}$$

$$\frac{d\boldsymbol{u}_1}{dt} = k_1 SIGN(\boldsymbol{\sigma}), \tag{7.9b}$$

$$\boldsymbol{u}_2 = (ABS(\boldsymbol{\sigma}))^{1/2}\, SIGN(\boldsymbol{\sigma}), \tag{7.9c}$$

$$\hat{\boldsymbol{\alpha}} = \boldsymbol{R}\boldsymbol{u}_1, \tag{7.9d}$$

is a second-order sliding mode observer for (7.3)-(7.4)*. There exists suitable design constants $k_1 > 1$ and $k_2 > 0$ for which finite-time convergence of specific reaction rates, i.e. $\hat{\boldsymbol{\alpha}}(t) \equiv \boldsymbol{\alpha}_p(t)\ \forall t > T^*$ for some finite $T^* > 0$, is achieved.*

In order to prove Prop. 7.1, given $\widetilde{\boldsymbol{\alpha}} = \boldsymbol{\alpha}_p - \hat{\boldsymbol{\alpha}}$, the error coordinates dynamics $(\boldsymbol{\sigma}, \widetilde{\boldsymbol{\alpha}})$ is:

$$\frac{d\boldsymbol{\sigma}}{dt} = \boldsymbol{R}^{-1}\left(\check{\boldsymbol{G}}_p(\cdot)\widetilde{\boldsymbol{\alpha}} - 2k_2\boldsymbol{R}\boldsymbol{u}_2\right), \tag{7.10}$$

$$\frac{d\widetilde{\boldsymbol{\alpha}}}{dt} = \boldsymbol{R}\left(\boldsymbol{\rho}(t) - k_1 SIGN(\boldsymbol{\sigma})\right). \tag{7.11}$$

Applying the change of coordinates $(\boldsymbol{x}_1, \boldsymbol{x}_2) = (\boldsymbol{R}\boldsymbol{u}_2, \widetilde{\boldsymbol{\alpha}})$ to system (7.9), yields

$$\frac{d\boldsymbol{x}_1}{dt} = \boldsymbol{R}(ABS(\boldsymbol{x}_1))^{-1}\left(-k_2\boldsymbol{x}_1 + \frac{\check{\boldsymbol{G}}_p(\cdot)}{2}\boldsymbol{x}_2\right), \tag{7.12}$$

$$\frac{d\boldsymbol{x}_2}{dt} = \boldsymbol{R}(ABS(\boldsymbol{x}_1))^{-1}\left(ABS(\boldsymbol{x}_1)\boldsymbol{\rho}(t) - k_1\boldsymbol{x}_1\right), \tag{7.13}$$

where the identities

$$SIGN(\boldsymbol{x}_1) = SIGN(\boldsymbol{\sigma}),$$
$$ABS(\boldsymbol{x}_1) = \boldsymbol{R}(ABS(\boldsymbol{\sigma}))^{1/2},$$

were used (see eq. (7.9c)).

Recalling definitions (7.5a)-(7.5d) it is seen that

$$\boldsymbol{G}_p(\cdot) \in \{\boldsymbol{G}_o + \Delta\boldsymbol{G}\boldsymbol{U}_p\}, \tag{7.14a}$$

$$\check{\boldsymbol{G}}_p(\cdot) \in \{\boldsymbol{I}_p + \boldsymbol{G}_o^{-1}\Delta\boldsymbol{G}\boldsymbol{U}_p\}, \tag{7.14b}$$

where $\boldsymbol{I}_p$ denotes the $(p \times p)$ identity matrix and $\boldsymbol{U}_p$ is a $(p \times p)$ diagonal matrix such that $\|\boldsymbol{U}_p\|_\infty \leq 1$.

Therefore, using (7.14) the following differential inclusion holds

$$\begin{aligned}\frac{d\boldsymbol{x}}{dt} \in &\begin{pmatrix} \boldsymbol{R}[ABS(\boldsymbol{x}_1)]^{-1} & \boldsymbol{0} \\ \boldsymbol{0} & \boldsymbol{R}[ABS(\boldsymbol{x}_1)]^{-1} \end{pmatrix} \cdot \\ &\cdot \begin{pmatrix} -k_2\boldsymbol{I}_p & \frac{1}{2}\left(\boldsymbol{I}_p + \delta\boldsymbol{U}_p\right) \\ -\left(k_1\boldsymbol{I}_p - \boldsymbol{U}_p\right) & \boldsymbol{0} \end{pmatrix} \boldsymbol{x}.\end{aligned} \tag{7.15}$$

Now, given the i_{th} kinetic rate arrange a vector $\boldsymbol{\zeta}_i$ with the i_{th} components of $\boldsymbol{x}_1$ and $\boldsymbol{x}_2$ (i.e. $\boldsymbol{\zeta}_i = \begin{bmatrix} x_{1i} & x_{2i} \end{bmatrix}^T$). The corresponding differential inclusion is

$$\frac{d\boldsymbol{\zeta}_i}{dt} = \frac{\overline{\rho}_i}{|x_{1i}|}\boldsymbol{A}(t)\boldsymbol{\zeta}_i \in \frac{\overline{\rho}_i}{|x_{1i}|}\begin{pmatrix} -k_2 & \frac{1}{2}\left(1 + \delta U_i\right) \\ -\left(k_1 - U_i\right) & 0 \end{pmatrix}\boldsymbol{\zeta}_i, \tag{7.16}$$

where U_i is the (i,i) entry of $\boldsymbol{U}_p$.

It will be shown that each of these coordinates converges in finite time to the origin independently of the others. For this purpose, the candidate Lyapunov function $V(\boldsymbol{\zeta}_i) = \sum_i \boldsymbol{\zeta}_i^T \boldsymbol{P}\boldsymbol{\zeta}_i$ (Moreno and Osorio, 2008) is considered. The time derivative of $V(t)$ results

$$\dot{V}(t) = \sum_i \frac{\overline{\rho}_i}{|x_{1i}|}\boldsymbol{\zeta}_i^T\left(\boldsymbol{A}^T(t)\boldsymbol{P} + \boldsymbol{P}\boldsymbol{A}(t)\right)\boldsymbol{\zeta}_i, \tag{7.17}$$

with $\boldsymbol{A}(t)$ given in (7.16). The goal is to determine $\boldsymbol{P} \succ 0$ such that $\dot{V}(t) < 0$ along any nonzero solution of eq. (7.16). To this end, consider the following proposition.

Proposition 7.2. *Consider the polytopic linear differential inclusion*

$$\dot{\boldsymbol{\zeta}} = \boldsymbol{A}(t)\boldsymbol{\zeta}, \quad \boldsymbol{A}(t) \in \mathcal{A} \tag{7.18}$$

with

$$\begin{aligned}\mathcal{A} &= co\bigcup_{\mathrm{i}} \boldsymbol{A}_{\mathrm{i}}, \quad \mathrm{i} = 1, \ldots, 4 \\ \boldsymbol{A}_{\mathrm{i}} &= \begin{bmatrix} -k_2 & \frac{1}{2}(1 + \delta v_{\mathrm{i}}) \\ -(k_1 - u_{\mathrm{i}}) & 0 \end{bmatrix}, \\ u &= \{-1, -1, 1, 1\}, \quad v = \{-1, 1, -1, 1\}.\end{aligned} \tag{7.19}$$

Then, for every $k_1 > 1$ and $0 < \delta < 1$ there exists suitable values of k_2 such that (7.18) *is quadratically stable for all $\boldsymbol{A}(t) \in \mathcal{A}$.*

Stability of system (7.18) was proved in De Battista et al. (2011) for the case $\delta = 0$ with the Lyapunov function $V(\boldsymbol{\zeta}) = \boldsymbol{\zeta}^T \boldsymbol{P} \boldsymbol{\zeta}$. This proposition is an extension of the proposed in De Battista et al. (2011) to deal with $\delta > 0$. The main difference consists in the requirement of a grid covering the space (k_1, δ) instead of k_1 in order to include all the possible systems described by eq. (7.18).

A polytopic linear differential inclusion is said quadratically stable if there exists $V(\boldsymbol{\zeta}) = \boldsymbol{\zeta}^T \boldsymbol{P} \boldsymbol{\zeta}$, $\boldsymbol{P} \succ 0$ that decreases along every non-zero trajectory of system (7.18).

Since $\dot{V}(\boldsymbol{\zeta}) = \boldsymbol{\zeta}^T (\boldsymbol{A}^T(t)\boldsymbol{P} + \boldsymbol{P}\boldsymbol{A}(t))\boldsymbol{\zeta}$, a necessary and sufficient condition for quadratic stability is

$$\begin{aligned} \boldsymbol{P} &\succ 0, \\ \boldsymbol{A}^T(t)\boldsymbol{P} + \boldsymbol{P}\boldsymbol{A}(t) &\prec 0 \quad \forall \boldsymbol{A}(t) \in \mathcal{A}. \end{aligned} \tag{7.20}$$

This is equivalent to determine the existence of a common Lyapunov matrix $\boldsymbol{P}$ for all the vertices of the polytope $\mathcal{A}$, i.e. that verifies the following constraints

$$\mathcal{F} = \left\{ \begin{array}{l} \boldsymbol{P} \succ 0 \\ \boldsymbol{Q}_i \stackrel{\triangle}{=} -(\boldsymbol{A}_i^T \boldsymbol{P} + \boldsymbol{P}\boldsymbol{A}_i) \succ 0 \end{array} \right\}. \tag{7.21}$$

for $i = 1 \ldots 4$.

Now rewriting A_i in a convenient way,

$$\boldsymbol{A}_i = k_2 \boldsymbol{A}_0 + \boldsymbol{A}_i^*, \tag{7.22}$$

where

$$\begin{aligned} \boldsymbol{A}_0 &= \begin{bmatrix} -1 & 0 \\ 0 & 0 \end{bmatrix}, \\ \boldsymbol{A}_1^* &= \begin{bmatrix} 0 & \frac{1}{2}(1+\delta) \\ -(k_1 - 1) & 0 \end{bmatrix}, \\ \boldsymbol{A}_2^* &= \begin{bmatrix} 0 & \frac{1}{2}(1+\delta) \\ -(k_1 + 1) & 0 \end{bmatrix}, \\ \boldsymbol{A}_3^* &= \begin{bmatrix} 0 & \frac{1}{2}(1-\delta) \\ -(k_1 - 1) & 0 \end{bmatrix}, \\ \boldsymbol{A}_4^* &= \begin{bmatrix} 0 & \frac{1}{2}(1-\delta) \\ -(k_1 + 1) & 0 \end{bmatrix}. \end{aligned} \tag{7.23}$$

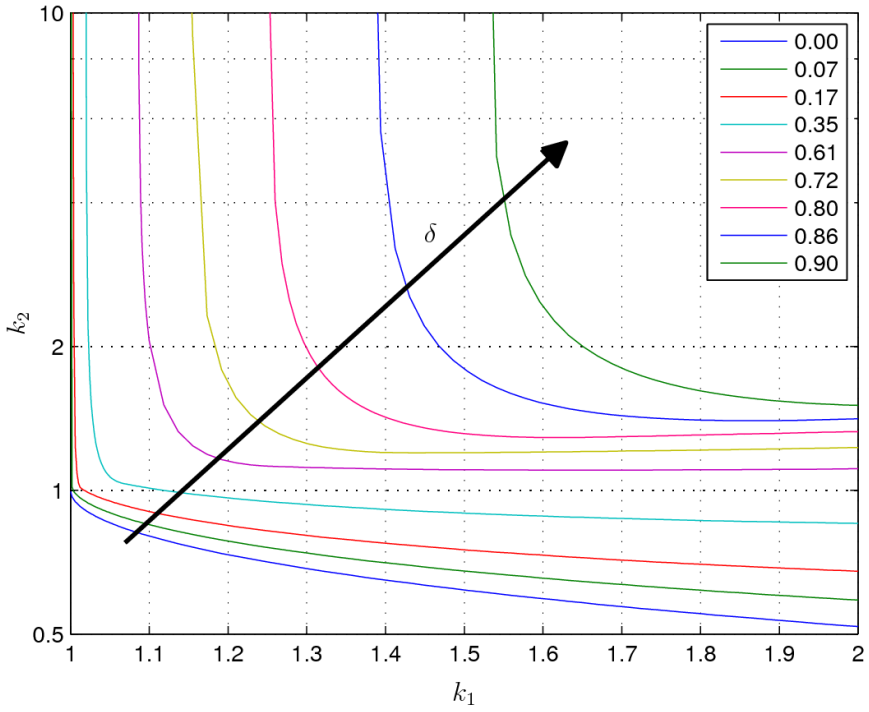

Figure 7.1: Values of k_1 and k_2 for which system (7.18) is quadratically stable

The existence of a common Lyapunov $\boldsymbol{P}$ for any $k_1 > 1$ and $0 < \delta < 1$ can be determined by checking the feasibility of the following generalised eigenvalue problem (GEVP) in $\boldsymbol{P}$ and k_2 for both fixed $k_1 > 1$ and $0 < \delta < 1$ (Boyd et al., 1994):

$$\begin{array}{ll} \min & k_2 \\ s.t. & k_2 > 0, \quad \boldsymbol{P} \succ 0, \quad \mathcal{F}^*, \end{array} \tag{7.24}$$

with

$$\mathcal{F}^* = \left\{ (\boldsymbol{A}_i^{*^T}\boldsymbol{P} + \boldsymbol{P}\boldsymbol{A}_i^*) + k_2(\boldsymbol{A}_0^T\boldsymbol{P} + \boldsymbol{P}\boldsymbol{A}_0) \prec 0; \right\}, \tag{7.25}$$

for $i = 1 \ldots 4$.

A GEVP is a quasi-convex optimisation problem. In this case, it can be solved using a bisection algorithm on k_2 and determining the feasibility of the remaining linear matrix inequality (LMI). A grid covering

the desired values of k_1 for some desired value δ was made, and the corresponding LMIs were solved with YALMIP (Löfberg, 2012). Figure 7.1 shows the set of values of k_1 and k_2 for which the LMI problem is feasible, for different values of the parameter δ. For all points within the resulting sets of parameters, Proposition 7.2 holds.

Now, values of k_1 and k_2 for Proposition 7.1 follows from the application of Proposition 7.2. That is, given $k_1 > 1$ and certain δ, the value of k_2 is selected such that eq. (7.18) is quadratically stable. Recall that δ stands for the maximum element of $\left\|\boldsymbol{G}_o^{-1}\Delta\boldsymbol{G}\right\|$ thus this value is suitable to get $\dot{V}(t) < 0$ for all the reaction rates.

Finally, for suitable k_1 and k_2 the system reaches a neighbourhood of the sliding surface and thus the sliding-mode regime is established. From then on, the so-called *invariance condition* ($\boldsymbol{\sigma} \equiv \mathbf{0}$) holds Utkin et al. (1999). Consequently, for certain T^*, $\hat{\boldsymbol{z}}(t) \equiv \boldsymbol{z}(t)\ \forall t > T^*$. By equating expressions (7.3) and (7.9a), $\hat{\boldsymbol{\alpha}}(t) = \boldsymbol{\alpha}_p(\boldsymbol{\xi}, t)$ is obtained. Note in eq. (7.9c) that when the system is restricted to the sliding surface $\boldsymbol{\sigma} = \mathbf{0}$ the matrix $ABS(\boldsymbol{\sigma})$ is the zero matrix, and thus $\boldsymbol{u}_2 = \mathbf{0}$.

7.4 Experimental results

In this section, the sliding mode observer developed in Section 7.3 is evaluated experimentally. The application consists in estimating the specific production rate of ethanol (q_e) and the specific growth rate (μ) of the strain *S. cerevisiae* (T73) in a continuous-mode fermentation. To this end, on-line measurements of biomass (x) and ethanol (e) concentrations were collected. Biomass measurements were taken with a sensor based on measurement of the optical density (Navarro et al., 2001b). Samples taken every 12 sec are filtered over a time-window of $120\ sec$. Ethanol concentration was monitored using a Raven Biotech's stand-alone methanol sensor with sample time of $120\ sec$. The volume was 3 L and the total fermentation time was 93 h. During the first 23 hours batch cultivation was carried out. After that, the dilution rate profile shown with dash-dotted line in Fig. 7.3 was applied. A set-point step in D from 0.18 to $0.22\ h^{-1}$ is produced at $t \approx 50\ h$.

The proposal is assessed for two possible scenarios. First, the SMO is tested in the conditions described above and second, the observer is evaluated for two typical sensor failures which were digitally generated. In the latter case, the results are compared with a high gain observer.

Particularly, the continuous time estimator described by

$$\frac{d}{dt}\begin{pmatrix}\hat{x}\\ \hat{e}\end{pmatrix} = \begin{pmatrix}\hat{x} & 0\\ 0 & \hat{x}\end{pmatrix}\begin{pmatrix}\hat{\mu}\\ \hat{q}_e\end{pmatrix} - \frac{F_{in}}{v}\begin{pmatrix}\hat{x}\\ \hat{e}\end{pmatrix} - 2\theta_1\begin{pmatrix}\hat{x}-x\\ \hat{e}-e\end{pmatrix}, \tag{7.26a}$$

$$\frac{d}{dt}\begin{pmatrix}\hat{\mu}\\ \hat{q}_e\end{pmatrix} = \frac{-\theta_1^2}{\hat{x}}\begin{pmatrix}\hat{x}-x\\ \hat{e}-e\end{pmatrix}, \tag{7.26b}$$

which is presented in Farza et al. (1998) was implemented.

The main difference of this class of observers with the SMO is that in the former there is an addition of dynamics. This fact is important regarding closed loop applications. For instance, if eq. (7.26) is applied for feedback, $2p$ integrators are added to closed loop dynamics. Consequently, closed loop stability must be analysed when the feedback signals are taken from the high gain observer. The same comment holds for other algorithms such as asymptotic observers. On the other hand, the SM approach provides convergence in finite-time to the target variables and from then on no additional dynamics is added. This fact simplifies the control system design.

The mass-balance eqs. for the process are:

$$\frac{dx}{dt} = \mu x - Dx, \tag{7.27a}$$

$$\frac{ds}{dt} = q_s x + D(s_r - s), \tag{7.27b}$$

$$\frac{de}{dt} = q_e x - De, \tag{7.27c}$$

where $D = F_{in}/v$ is the dilution rate, s the substrate concentration, s_r the input substrate concentration and v the (constant) working volume.

Since x and e are the measured state variables, the corresponding subsystem is of dimension $p = 2$. Note in (7.27) that μ and q_e are the specific kinetic rates per unit of biomass. The corresponding subsystem in the form of eq. (7.3) is

$$\frac{d\boldsymbol{z}}{dt} = \begin{pmatrix}1 & 0\\ 0 & 1\end{pmatrix}\begin{pmatrix}x & 0\\ 0 & x\end{pmatrix}\begin{pmatrix}\mu\\ q_e\end{pmatrix} - D\boldsymbol{z}, \tag{7.28}$$

where $\boldsymbol{z} = \begin{bmatrix}x & e\end{bmatrix}^T$, $\boldsymbol{\alpha}_p = \begin{bmatrix}\mu & q_e\end{bmatrix}^T$ and $\boldsymbol{F}_p = \boldsymbol{Q}_p = \boldsymbol{0}$. In this factorization $\boldsymbol{K}_p = \boldsymbol{I}_2$ and $\boldsymbol{G}_p = x\boldsymbol{I}_2$.

Therefore, matrices $\boldsymbol{G}_1$ and $\boldsymbol{G}_2$ (see eqs. (7.5)) are determined bounding for above ($\overline{x}$) and below ($\underline{x}$) the expected biomass excursion.

The values $\underline{x} = 2\ g\ L^{-1}$ and $\overline{x} = 18\ g\ L^{-1}$ were selected, which resulted conservative enough bounds. Accordingly, the matrices $\boldsymbol{G}_1$ and $\boldsymbol{G}_2$ are

$$\boldsymbol{G}_1 = 2\boldsymbol{I}_2,$$
$$\boldsymbol{G}_2 = 18\boldsymbol{I}_2,$$

and therefore $\boldsymbol{G}_o = 10\boldsymbol{I}_2$, $\Delta\boldsymbol{G} = 8\boldsymbol{I}_2$ and $\delta = 0.80$.

The bounds $\bar{\rho}_i$ were selected as 0.1 and 0.25, respectively and therefore $\boldsymbol{R} = diag\left\{0.1 \quad 0.25\right\}$. These bounds can in practice be adjusted according to previous experience about the bioprocess and from model simulations (Perrier et al., 2000; De Battista et al., 2012a).

The resulting values of k_2 for several values of k_1 were obtained by solving the problem (7.24)-(7.25). These results are depicted in Fig. 7.1. It is seen for any δ that the lower is k_1, the greater is the minimum k_2. In order to get a feasible minimisation problem for $\delta = 0.8$ with a small k_2, $k_1 = 1.35$ was selected. From problem (7.24)-(7.25), the minimum k_2 is 1.5715 and then $k_2 = 1.75$ was selected. Other possibility for the designing of the gains includes the adaptive-gain approach, see for instance (Shtessel et al., 2010; Evangelista et al., 2013).

7.4.1 Results

The SMO was initialised with the first samples, i.e. $\hat{\boldsymbol{z}}(t_0) = (x(t_0), e(t_0))$ and $(\hat{\mu}(t_0), \hat{q}_e(t_0)) = (0, 0)$. Figure 7.2 shows biomass and ethanol time profiles and their corresponding variables $\hat{z}_1$ and $\hat{z}_2$ almost overlapped, respectively.

Figure 7.3 shows $\hat{\mu}(t)$ and the switching coordinate σ_1. In this fermentation the feeding profile was applied in open-loop operation, i.e. μ was not regulated by feedback. Recall that if steady-state operation of continuous fermentation is reached then $\mu = D$ (see eq. (7.27a)). However, it can be seen between hours 67 and 79 that μ was greater than D due to depletion of ethanol. This illustrates monitoring capabilities of the proposal.

The on-line estimation of $q_e(t)$ gives the net production of ethanol, i.e. the balance between excreted ethanol due to fermentative growth on s and consumed ethanol due to oxidative growth on e. Figure 7.4 shows $\hat{q}_e(t)$ and the switching coordinate σ_2. The decrease observed in q_e from $t \approx 67\ h$ is in accordance with the growth observed in Fig. 7.3.

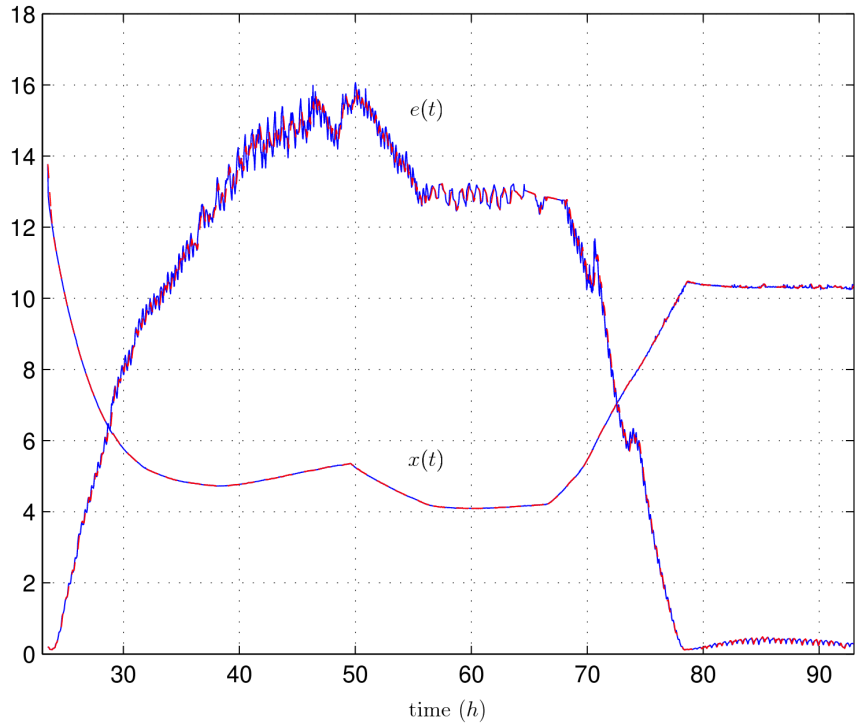

Figure 7.2: Time profile of $x(t)$ (blue-solid), $\hat{x}(t)$ (red-dash) and $e(t)$ (blue-solid), $\hat{e}(t)$ (red-dash) in the continuous fermentation (7.27)

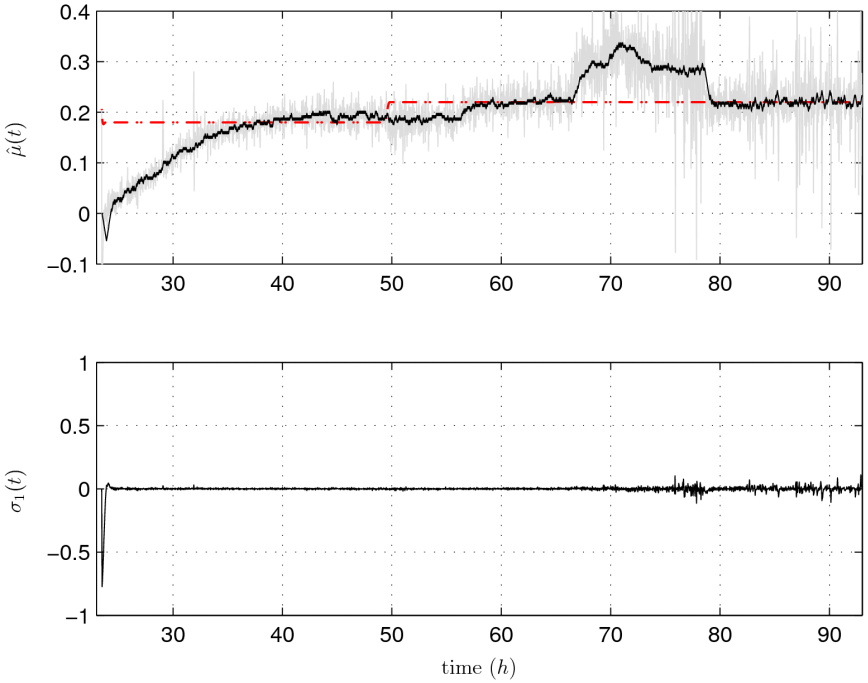

Figure 7.3: Estimated specific growth rate $\hat{\mu}(t)$ with SMO (black) and eq. (7.29) (grey), dilution rate (dash-dotted) (above); switching coordinate σ_1 (below)

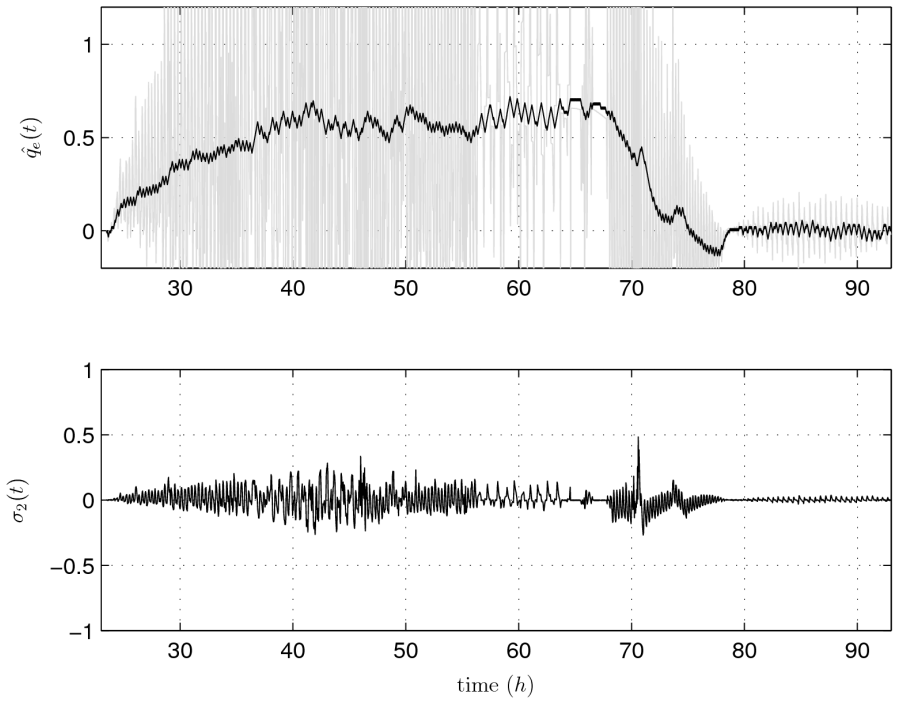

Figure 7.4: Estimated specific ethanol production rate $\hat{q}_e(t)$ with SMO (black) and eq. (7.29) (grey) (above); switching coordinate σ_2 (below)

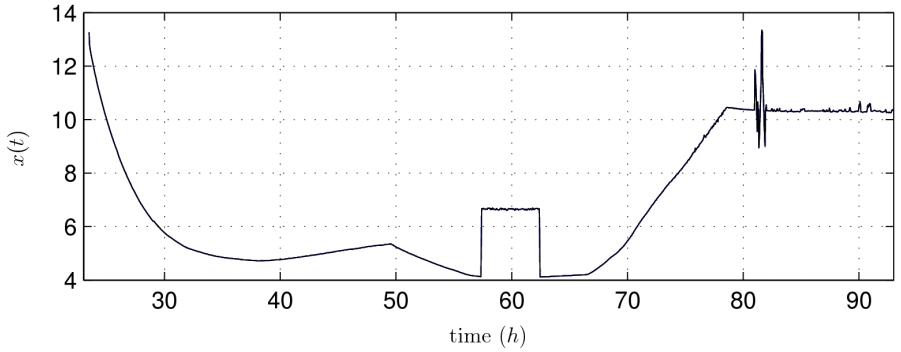

Figure 7.5: Time profile of $x(t)$ with faults in measurement

Equation (7.29) presents the crude estimation of $\alpha(t)$ obtained by model inversion from (7.3)

$$\hat{\alpha}(t) = \boldsymbol{G}_p^{-1}\boldsymbol{K}_p^{-1}\left(\frac{d\boldsymbol{z}}{dt} + D\boldsymbol{z} - \boldsymbol{F}_p + \boldsymbol{Q}_p\right). \tag{7.29}$$

Although this solution is simpler than most of the proposed algorithms, the result is strongly affected by measurement noise as shown in Fig. 7.3 and 7.4 in grey lines. A possible solution would be to add a lowpass filter, but the delay and filter dynamics could be detrimental in closed-loop configuration.

7.4.2 Comparison with high gain observers under sensor failure

Figure 7.5 shows two typical sensor failures in biomass concentration measurement: a drift in the time interval $[57, 63]$ and some spikes at $t = 81\ h$. This type of problem should be early detected to take corrective actions. Note in eqs. (7.27) that a problem in x affects estimation of both μ and q_e.

Algorithm (7.26) was initialised with the same conditions as the SMO. It was tuned with parameter $\theta_1 = 4.0$ looking for a comparable response with the SMO. Although θ_1 can be chosen high enough to ensure fast speed of convergence, this parameter tuning involves a trade-off between convergence speed and noise sensitivity. Besides, given its simplicity there is only one parameter to tune which in turn may be

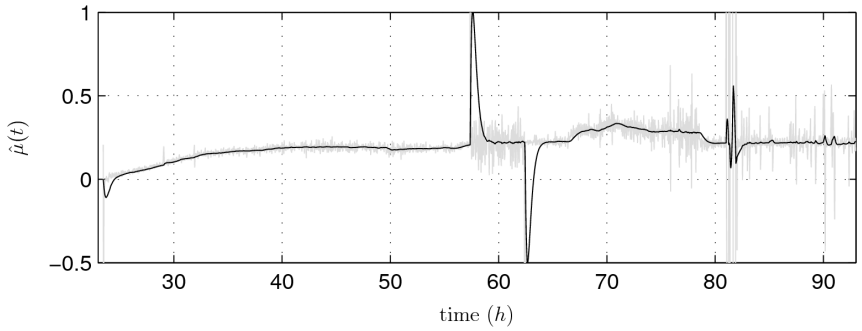

Figure 7.6: Response under sensor failure with high gain observer: eq. (7.26) vs eq. (7.29)

problematic when the measurements have different level of noise (as in the case of biomass and ethanol measurements presented in Fig. 7.2).

The result for the high gain algorithm under sensor failure is presented in Fig. 7.6. Given the drift in x, a response with large overshoot in $\hat{\mu}$ appears. Besides, the spikes in x generates additional fast changes in $\hat{\mu}$. Although this output behaviour shows a failure, it would not be acceptable in closed-loop control. On the other hand, the result of μ estimation with the SMO under the same scenario is presented in Fig. 7.7. As can be observed, the coordinate σ_1 early detects the fault exhibiting a problem detection feature of the proposal. Even more important, the effect of the drift on $\hat{\mu}$ is strongly reduced because the time derivative of each $\hat{\alpha}_i$ is bounded by the observer. In fact, the corresponding $\overline{\rho}_i$ allows to adjust that bound. Note that the spikes at $t = 81\ h$ are completely rejected in the estimator and detected by the residual σ_1.

Finally, the result for q_e estimation is presented in Fig. 7.8. For the selected gain, the high gain approach exhibits worse response than the SMO until $t = 70\ h$.

7.5 Conclusions

The on-line kinetic rates estimation problem in bioprocesses was addressed. The proposed second-order SM observer is able to estimate multiple specific kinetic rates from related measurements of process variables even though no particular model of each kinetic rate was as-

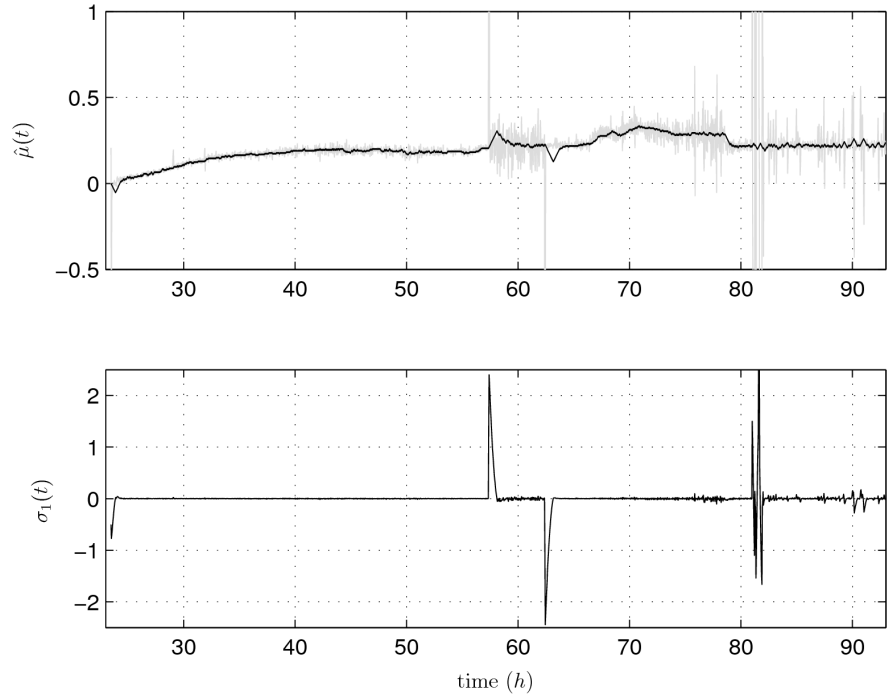

Figure 7.7: Response under sensor failure for $\mu(t)$: SMO vs eq. (7.29) (above) and switching coordinate (below)

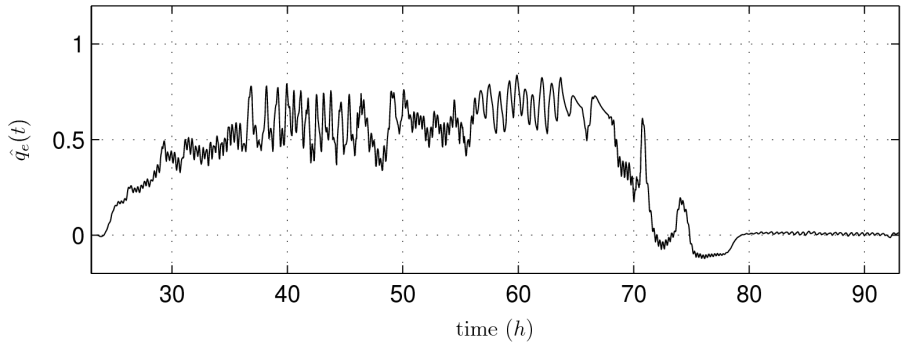

Figure 7.8: Estimated specific ethanol production rate $\hat{q}_e(t)$ with high gain observer

sumed.

Certainly, only upper bounds of the time derivatives are required. Global finite-time convergence is achieved by choosing a suitable observer structure. This property is particularly important in control applications because the observer does not add dynamics that might destabilise the closed loop.

The observer performance was assessed using experimental data from con-tinuous-mode fermentation of *S. cerevisiae*. Microbial specific growth rate and net ethanol production rate were estimated. The proposed algorithm was compared with a high gain observer under normal operation and for two typical sensor faults. Particularly, the SMO showed better noise rejection in the noisiest signal and better transient response under sensor drifts and spikes.

Chapter 8

Specific Kinetic Rates Regulation in Multi-Substrate Fermentation Processes

A person who never made a mistake
never tried anything new.

Albert Einstein

Abstract: The regulation of the biomass specific growth rate is an important goal in many biotechnological applications. To achieve this goal in fed-batch processes, several control strategies have been developed employing a closed loop version of the exponential feeding law, an estimation of the controlled variable and some error feedback term. Moreover, in some bioprocesses there is more than one feeding flow entering the bioreactor and supplying different nutrients or substrates. Hence, the problem of estimating multiple substrate consumption rates together with the specific growth rate of the microorganism becomes relevant. In this context, the dynamic behavior of fed-batch processes with multiple substrates and Haldane kinetics is further investigated. In particular, a nonlinear PI control law based on a partial state feedback with gain dependent on the output error is used. Then, with a recent developed algorithm for several kinetic rates estimation based on second-order sliding mode (SM) ideas, we extend

the mentioned control strategy to a multi-substrate fed-batch bioprocess. The observer provides smooth estimates that converge in finite time to the time-varying parameters and allows independent design of the observer and controller dynamics. The features of the proposed estimation and control strategies are assessed by simulation in different scenarios.

8.1 Introduction

The expanding biotechnological industry is demanding more efficient, reliable and safe processes to optimize production and improve quality. Control engineers have to overcome a large number of obstacles to control fed-batch fermentations. They must deal with complex dynamic behavior of microorganisms, strong modeling approximations, external disturbances, nonlinear and even inherently unstable dynamics, scarce on-line measurements of most representative variables, etc. In Smets et al. (2004) a description of the history and state of the art in the field of fermentation fed-batch process control is presented.

From a biological standpoint, the control of a biotechnological process would be to make microorganisms reach a (possibly time-varying) metabolic state at which their physiological behavior is appropriate for the desired goals: e.g. production of a given metabolite or protein. These metabolic states are usually related to growth rate (Ihssen and Egli, 2004; Gnoth et al., 2008). Also growth rate is related to substrate consumption rate. Thus, tuning the feed rate to achieve either constant substrate concentration in the broth or constant metabolite production rate are common strategies in the area (Valentinotti et al., 2003; Oliviera et al., 2004; Jenzsch et al., 2006).

Current availability of more on-line reliable biomass and volume measurement devices allow direct control of specific growth rate. This is especially true for small and medium scale bioreactors used to produce enzymes and/or high-added values specialty metabolites. This has enabled a research line dedicated to develop generic and robust controllers based on the minimal modeling concept. In Picó-Marco et al. (2005), a sliding mode controller applicable to the regulation of growth-linked fed-batch processes is presented. Just on-line measurement of

biomass concentration and volume, as well as an upper-bound on the growth rate are needed. Other authors have incorporated an estimation of the controlled variable to the control algorithms, obtained from on-line measurement of biomass concentration (Smets et al., 2004; Gnoth et al., 2008; Smets et al., 2002; Dabros et al., 2010). Pioneering work in the field of growth rate observers was performed in Bastin and Dochain (1986).

In De Battista et al. (2012b), a different approach is proposed to design non-linear PI controllers which relies on geometric properties of the process and specification structures. Ideas and concepts of invariant control and passivity are combined to achieve PI controllers that outperform previous developments where some of these ideas were exploited separately (Picó-Marco et al., 2005; De Battista et al., 2006). In Pico-Marco and Navarro (2008), an invariant and stabilizing controller is used to control dual-substrate fed-batch fermenters using only biomass measurement and growth rate estimation. Thereafter in Nuñez et al. (2013), an algorithm for several kinetic rates estimation based on second-order sliding mode ideas was presented, providing smooth estimates, which are achieved in finite-time and without adding dynamics. In this paper, we use the mentioned previous work to estimate several substrate consumption rates and extend the nonlinear PI control (De Battista et al., 2012b) for multi-substrate fed-batch fermentation in order to track desired consumption rates for each substrate.

The work is organized as follows. The next section presents the control problem. In Section 8.3 the second-order sliding mode observer together with the invariant control and the PI correction terms are presented for the case of multi-substrate fermentation with non-monotonic kinetics. Section 8.4 shows the observer and controller performance using simulation data with realistic noise and perturbations. Finally, in Section 8.5 the main conclusions of the work are given.

8.2 Problem formulation

Consider biphasic biomass growth. The commonly used model to describe dual-substrate fed-batch fermentations accepts the following description in state-space (Bastin and Dochain, 1990; Dunn et al., 2003;

Chang, 2003):

$$\mathcal{S}: \begin{cases} \dot{x} = f(\mu_1, \mu_2)x - (D_1 + D_2)x \\ \dot{s}_1 = -y_1\mu_1(s_1)x + D_1 s_{1in} - (D_1 + D_2)s_1 \\ \dot{s}_2 = -y_2\mu_2(s_2)x + D_2 s_{2in} - (D_1 + D_2)s_2 \\ \dot{v} = (D_1 + D_2)v = F_1 + F_2 \end{cases} \tag{8.1}$$

where $f(\cdot)$ is the specific growth rate, usually the sum or the product of its arguments. Additionally, the state variables are x biomass concentration, s_i concentration of substrate in the tank, and v volume. The specific consumption rates μ_i are unknown nonlinear function of substrates. In the following we will center the analysis in the case of non-monotonic Haldane kinetics, where the consumption rates have the following form:

$$\mu_i(s_i) = \mu_{mi} \frac{1 + 2\sqrt{k_{si}/k_{ii}}}{(k_{si}/s_i) + 1 + (s_i/k_{ii})}. \tag{8.2}$$

The parameters y_i are yield coefficients. The other two parameters $s_{i\text{in}}$ are the substrate concentrations in the corresponding feeding flow. Finally, the D_i dilution rates are equal to the ratios F_i/v. The substrates may play different roles (see Zinn et al. (2004)). For example in two common cases:

1. Both substrates are carbon sources and contribute both to growth and production.

2. One substrate is a carbon source mainly affecting growth and the other one a nitrogen source affecting production and product characteristics.

In either case there are mainly two goals from the process point of view:

1. It is desirable to keep a given specific growth rate $f = \mu_{ref}$, and hence consumption rates μ_1 and μ_2 corresponding to a desired physiological state at which the microorganism behaves optimally with respect to production, does not produce inhibiting products, etc.

2. It has been reported in Kellerhals et al. (1999) and Xu et al. (2005) that in many instances the ratio s_1/s_2 affects the product characteristics, e.g. in PHB production the bioplastic physical properties.

Both goals could be achieved by regulating the consumption rates for each substrate using $F_{1,2}$. This constitutes the main problem addressed in this work.

Note that controller and observer design is subject to the following constraints:

- The only on-line measurable variables are volume and biomass and one of the substrates concentration.
- The control signals are nonnegative.
- The yield coefficients $y_{1,2}$ and the influent substrate concentration s_{in} are uncertain parameters that, moreover, may vary during the process.
- The specific consumption rates μ_i are not precisely known. We only assume they are Haldane-like non-monotonous functions, some initial estimation of the maximum consumption rates (an informed guess is enough), estimated upper bounds on their time derivative, and a rough idea of the region $(\mu_i(s_i), s_i)$ where the functions $\mu_i(s_i)$ live.

Thus, in the next section we extend a non linear PI controller for growth regulation (De Battista et al., 2012b) to a multi-substrate fermentation and we combine it with the multiple rate high-order sliding mode observer developed in Nuñez et al. (2013) in order to estimate the consumption rates of each substrate. Then we introduce the estimates into the controller to adapt the invariant gains, improving the robustness with respect to model uncertainties and perturbations.

8.3 Nonlinear PI controller and second order sliding mode observer

In this section, we present the nonlinear PI controller for growth regulation developed in De Battista et al. (2012b). Then we show how to tune the multi-rate observer developed in Nuñez et al. (2013) for this particular case. Having estimates of the multiple consumption rates, allows us to extend the control to the multi-substrate case.

8.3.1 Nonlinear PI control

Consider the system (8.1). We start by applying an invariant control (Pico-Marco and Navarro, 2008), from where we obtain the invariant gains $\lambda_{r1,r2}$. The basic idea is to take a reference model of exponential growth (compatible with the control objectives) and make the generated goal manifold for our system (8.1) to be invariant. That is, if the system is driven to the manifold, it will stay on it. This is achieved with the invariant gains, which can be calculated from the reference substrates from (8.1),

$$s_{r1} = k_{s1}\frac{\mu_{r1}}{\mu_{m1}-\mu_{r1}} \tag{8.3}$$

$$s_{r2} = k_{s2}\frac{\mu_{r2}}{\mu_{m2}-\mu_{r2}} \tag{8.4}$$

as follows

$$\lambda_{r1} = \frac{s_{r1}y_2\mu_{r2} - s_{r2}y_1\mu_{r1} + s_{2in}y_1\mu_{r1}}{s_{2in}s_{1in} - s_{2in}s_{r1} - s_{1in}s_{r2}} \tag{8.5}$$

$$\lambda_{r2} = \frac{-s_{r1}y_2\mu_{r2} + s_{r2}y_1\mu_{r1} + s_{2in}y_2\mu_{r2}}{s_{2in}s_{1in} - s_{2in}s_{r1} - s_{1in}s_{r2}} \tag{8.6}$$

Then we can use these gains as initial conditions for the adaptation algorithm (nonlinear PI) from (De Battista et al., 2012b), but extended to a multi-substrate fermentation in the following way (for $i = 1, 2$):

$$\mathcal{C}: \begin{cases} F_i = \lambda_i x v \\ \lambda_i = \lambda_{ai}\left(1 - \tanh\left(\dfrac{k}{\mu_{ri}}(\hat{\mu}_i - \mu_{ri})\right)\right) \\ \dot{\lambda}_{ai} = -\phi\lambda_{ai}^2 x\dfrac{\hat{\mu}_i - \mu_{ri}}{\mu_{ri}}\,,\ \lambda_{ai}(t_0) = \lambda_{ri}, i = 1, 2. \end{cases} \tag{8.7}$$

Where k is the proportional gain of the controller and ϕ is the integral gain which determines the speed of adaptation of λ_i. Notice we need an estimation $\hat{\mu}_i$ of the consumption rates, in order achieve output error injection into the algorithm. Thus, we will use the previously mentioned observer for the substrates consumption rates estimation.

Assuming the growth rate of the microorganisms is related directly with the consumption rates of the substrates in an additive way

$$\mu = \mu_1 + \mu_2, \tag{8.8}$$

we will in fact estimate the specific growth rate and the consumption rate of the measured substrate. Then, we can simply subtract the estimated consumption rate from the growth rate in order to obtain the other consumption rate. Other relationships can be handled easily (e.g. multiplicative consumption rates).

8.3.2 Multiple rates observer

In order to estimate the specific growth rate and the consumption rate of the measured substrate we will use the observer developed in (Nuñez et al., 2013). First consider the following system which describes the measured variables z in a state-space model of a bioprocess stirred tank (Bastin and Dochain, 1990):

$$\begin{cases} \dot{z} = \boldsymbol{K}_p \boldsymbol{G}_p(\cdot)\alpha_p - Dz + F \\ \dot{\alpha}_p = \boldsymbol{R}\rho(t), \end{cases} \tag{8.9}$$

where $\boldsymbol{K}_p$ is a pseudo-stoichiometric matrix, D is the dilution rate, and F is the input flow rate. $\boldsymbol{G}_p(\cdot)\alpha_p$ represents the reaction rates which are linearly combined by the rows of $\boldsymbol{K}_p$. The specific reaction rates for each reactant are α_p and $\boldsymbol{G}_p(\cdot)$ is a diagonal matrix. Finally $\boldsymbol{R} = diag\{\bar{\rho}_i\}$ arranges the bounds of the time derivatives of the rates α_p. Note, that $\rho(t)$ is an unknown vector of continuous functions where $\|\rho(t)\|_\infty \leq 1$.

Then the second order sliding mode observer $\mathcal{O}$ converges to the specific reaction rates $\hat{\alpha} \equiv \alpha_p$ in finite-time (Nuñez et al., 2013).

$$\mathcal{O}: \begin{cases} \dot{\hat{z}} = \boldsymbol{K}_p \left(k_1 \boldsymbol{G}_p(\cdot)\boldsymbol{R}u + 2k_2 \boldsymbol{G}_o \boldsymbol{R} \mathrm{ABS}(\sigma)^{1/2} \mathrm{SIGN}(\sigma) \right) \\ \qquad - Dz + F \\ \dot{u} = k_1 \mathrm{SIGN}(\sigma) \\ \hat{\alpha} = \boldsymbol{R}u \end{cases} \tag{8.10}$$

with

$$\sigma = \left(\boldsymbol{K}_p \boldsymbol{G}_o \boldsymbol{R}\right)^{-1} (z - \hat{z}) \tag{8.11}$$

where $\boldsymbol{G}_o$ is a matrix related to the bounds on $\boldsymbol{G}_p(\cdot)$. The functions $\mathrm{ABS}(\sigma) = diag\{|\sigma_i|\}$ and $\mathrm{SIGN}(\sigma) = col(sign(\sigma_i))$ are matrix extensions of the respective scalar functions.

Comment on stability and convergence. For details on the stability analysis of the controller and convergence of the observer see respectively (De Battista et al., 2012b; Nuñez et al., 2013). In combining the two strategies, the only precaution to take is that the observer should converge before the process state leaves the domain of attraction (if it is not global). Anyway, in the practical industrial operation, there is always a batch open-loop phase previous to switching the fed-batch phase on. The observer will converge during this phase.

8.3.2.1 Observer Implementation

In order to use this observer in our particular case, we take the first and second equations from (8.1), which are the dynamics of the measured variables, hereafter $z = [x, s_1]^\top$,and we rearrange them, obtaining:

$$\dot{z} = \begin{pmatrix} 1 & 0 \\ 0 & -y_1 \end{pmatrix} \begin{pmatrix} x & 0 \\ 0 & x \end{pmatrix} \begin{pmatrix} \mu \\ \mu 1 \end{pmatrix} - (D_1 + D_2)\, z + \begin{pmatrix} 0 \\ D_1 s_{1in} \end{pmatrix} \tag{8.12}$$

where $\alpha_p = [\mu, \mu_1]^\top$. Note that in this factorization $\boldsymbol{G}_p = x\boldsymbol{I}_2$ and

$$\boldsymbol{K}_p = \begin{pmatrix} 1 & 0 \\ 0 & -y_1 \end{pmatrix}. \tag{8.13}$$

In order to tune the observer, upper ($\boldsymbol{G}_1$) and lower ($\boldsymbol{G}_2$) bounds for $\boldsymbol{G}_p$ need to be obtained to calculate $\boldsymbol{G}_o = \frac{\boldsymbol{G}_2+\boldsymbol{G}_1}{2}$, $\Delta\boldsymbol{G} = \frac{\boldsymbol{G}_2-\boldsymbol{G}_1}{2}$ and $\delta = \|\boldsymbol{G}_o^{-1}\Delta\boldsymbol{G}\|_\infty$. The presupposed excursion of the biomass x gives us conservative bounds $\boldsymbol{G}_1 = 0.2\boldsymbol{I}_2$ and $\boldsymbol{G}_2 = 15\boldsymbol{I}_2$. From where we get $\boldsymbol{G}_o = 7.6\boldsymbol{I}_2$ and $\delta = 0.9737$. With this we can calculate the suitable gains k_1 and k_2 (Table 8.1) to ensure finite-time convergence, by solving the associated GEVP problem (details omitted for brevity, see Nuñez et al. (2013)).

8.4 Simulations

In order to test the behaviour of the controller and observer described in this paper, simulations in three realistic scenarios have been performed. The model from (Chang, 2003) has been used with the following parameters and test conditions.

The controller and observer parameters used in the simulations are also listed in Table 1.

Table 8.1: Parameters and test scenarios

Process parameters and test scenarios			
$\mu_{m1}[1/h]$	0.47	$\mu_{m2}[1/h]$	0.5
$k_{s1}[g/L]$	0.5	$k_{s2}[g/L]$	0.55
$k_{i1}[g/L]$	2	$k_{i1}[g/L]$	2.1
$y_1{}^a$	2.1	y_2	2
$s_{1in}[g/L]$	15	$s_{2in}[g/L]$	15
$V(t_0)[L]$	0.2	$V_f[L]$	15
$s_1(t_0)[g/L]$	$[1, 5, 1]$	$s_2(t_0)[g/L]$	$[0.5, 4, 0.5]$
$x(t_0)[g/L]$	0.5		
Controller and observer parameters			
λ_{ri}	$[1, 1, 0.7]\lambda_i$	$\mu_r[1/h]$	0.33
$\mu_{r1}[1/h]$	0.18	$\mu_{r1}[1/h]$	0.15
k	3	ϕ	30
k_1	2.9592	k_2	2.3038
ρ_1	0.25	ρ_2	0.2

[a] Parameter y_1 in Scenario 3 grows at 3% per hour since $t = 10h$.

Note that by the assumption (8.8), the reference value for the specific growth rate is $\mu_r = 0.33$.

Scenario 1. Low initial substrate concentration. In this first scenario, the aim is to show the performance of the controller and observer from low initial concentration of substrates and under nominal conditions. The proper invariant gains λ_{ri} are known (or calculated from the model parameters). The results are presented in Figure 8.1.

Scenario 2. High initial substrate concentration. The second scenario shows the convergence property of the proposed controller from a high initial substrate concentration. The initial condition is selected beyond the maxima of the Haldane functions of both substrates. This is an inherently unstable region.

In fact, the control has the opposite effect to what is expected, thus producing a positive feed-back. To avoid wash-out, λ_1 and λ_2 are bounded, so that the substrate concentration inevitably falls below the max-

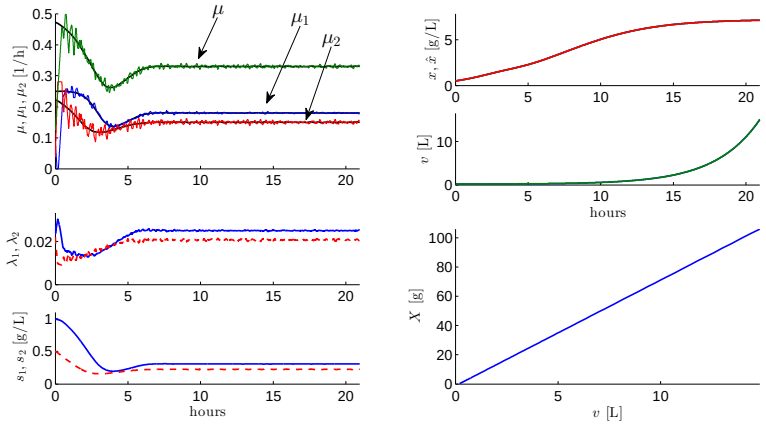

Figure 8.1: (Scenario 1) Responses from low initial substrates concentration under nominal conditions, *i.e.* invariant gains λ_{ri}, are known. The two plots at the bottom left show λ and substrate: blue-solid is λ_1,s_1 and red-dashed is λ_2,s_2

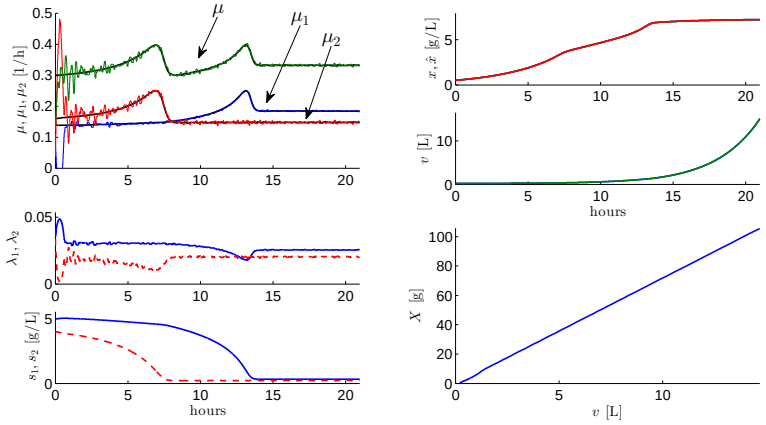

Figure 8.2: (Scenario 2) Responses from very high initial substrates concentration under nominal conditions, *i.e.* invariant gains λ_{ri}, are known. In the bottom left plots, of λ and substrate, blue-solid is λ_1,s_1 and red-dashed is λ_2,s_2

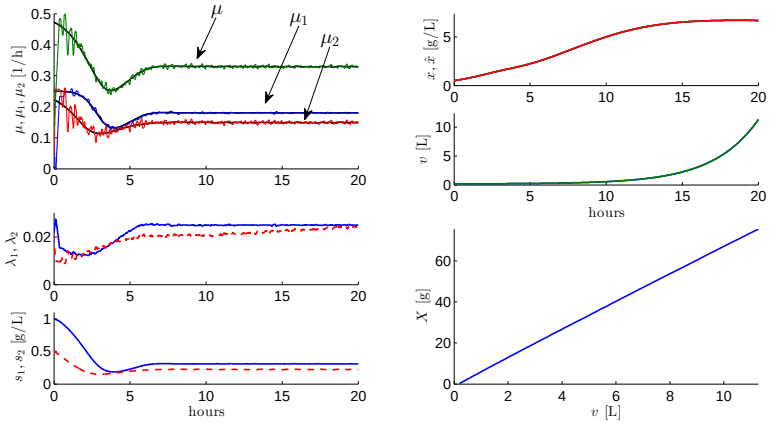

Figure 8.3: (Scenario 3) Responses from low initial substrates concentration under uncertain conditions. In the bottom left plots, of λ and substrate, blue-solid is λ_1,s_1 and red-dashed is λ_2,s_2

ima of the kinetic rate functions. Once in this region, the controller stabilizes the process around the goal trajectory. Notice that setting the bounds on λ_1 and λ_2 requires having a rough idea of the region $\mu_i(s_i), s_i$ where the functions $\mu_i(s_i)$ live, and a lower bound in the yield coefficients. But it does not require a precise model of the reaction kinetics.

Scenario 3. Robustness against parameter uncertainty. In this third scenario we evaluate the robustness of the proposed control and observer with respect to parameter uncertainty. One of the invariant gains, λ_{r1} is underestimated by a 30%. Further, after $t = 10h$, the yield coefficient y_{s1} is increased at the rate of 2% per hour. The evolution of the process variables is shown in Figure 8.3. See that, in the presence of the uncertain and time varying parameter, the control law is still tracking the desired $\mu_{r1,2}$ by adapting the parameter λ_1.

8.5 Conclusions

In this work we extended the previous proposed nonlinear proportional-integral control to multi-substrate fed-batch processes for multiple ki-

netic rates regulation. This was possible due to recent development of an algorithm for several kinetic rates estimation based on second-order sliding mode ideas, which allows us to obtain the consumption rates for each substrate together with the specific growth rate of the microorganism measuring only biomass and one of the substrates.

Robustness properties of both strategies are inherited. The controller provides robustness to model uncertainties and disturbances, which is one of its main attractive features. The observer provides noise rejection, and finite-time convergence of the consumption rates estimates. The latter allows to independently design the observer and the controller.

Performance of the system was shown by simulation of realistic scenarios, with noise, parameters uncertainty, and high initial substrate concentration, where an increase in concentration of substrates produces a decrease in growth rate, and therefore the fermentation is in an intrinsically unstable region.

Part III

Synthetic genetic circuits design

Chapter 9

Control of protein concentrations in heterogeneous cell populations

Mathematics is Biology's next microscope, only better; Biology is Mathematics' next physics, only better.

Joel E. Cohen

Abstract: In this work we propose a synthetic gene circuit for controlling the variability in protein concentration at a population level. The circuit, based on the use of an intracellular nonlinear controller coupled to a cell-to-cell communication mechanism, allows for independent control of the mean and variance of a signalling molecule across cell population. Via a piecewise affine approximation of the nonlinearity, we provide set invariance results that imply the stability of the closed loop system. We also obtain closed-form expressions for the mean and variance as a function of the tuneable parameters of the controller. The predictions offered by the theoretical analysis are in agreement with numerical

simulations performed with physiologically realistic parameters in *Escherichia coli*.

9.1 Introduction

Since the seminal works of Elowitz and Leibler (2000) and Gardner et al. (2000), a number of biomolecular devices have been developed to perform circuit-like functions in living cells, including switches, pulse generators and logic gates (Purnick and Weiss, 2009). Substantial efforts are being undertaken to scale up synthetic biology from individual modules to whole systems capable of executing complex functions (Khalil and Collins, 2010).

An area of particular relevance is the design of collective cell behavior, whereby a prescribed population response results from the interaction between individual cells. A common approach to induce collective behaviors is to use cell-to-cell communication mechanisms. These typically rely on the quorum sensing machinery from *V. fischeri* and have been used for diverse purposes such as population synchronization (McMillen et al., 2002), cell density control (Kobayashi et al., 2004), engineered pattern formation (Basu et al., 2005) and the design of synthetic ecosystems (Balagaddé et al., 2008).

Gene expression is an inherently stochastic process, and it is widely acknowledged that genetic noise plays a key role in cellular dynamics (Elowitz et al., 2002). At a population level, the effect of noise becomes apparent by the fact that genetically identical cells produce the same protein at different concentrations. The variability in protein concentrations can be quantified with high-throughput technologies such as flow cytometry, which allow to characterize the variability in terms of the population histograms for the protein abundance (Zechner et al., 2012).

In this work we combine an intracellular feedback controller with a cell-to-cell communication mechanism designed to control the mean and variance of the signalling molecule Acyl-Homoserine Lactone (AHL) across a population of cells. AHL is an autoinducer molecule that diffuses in the extracellular medium and acts as a communication signal between cells. The feedback controller regulates the production of the protein LuxI, which in turn controls the synthesis of AHL (Fig. 9.1).

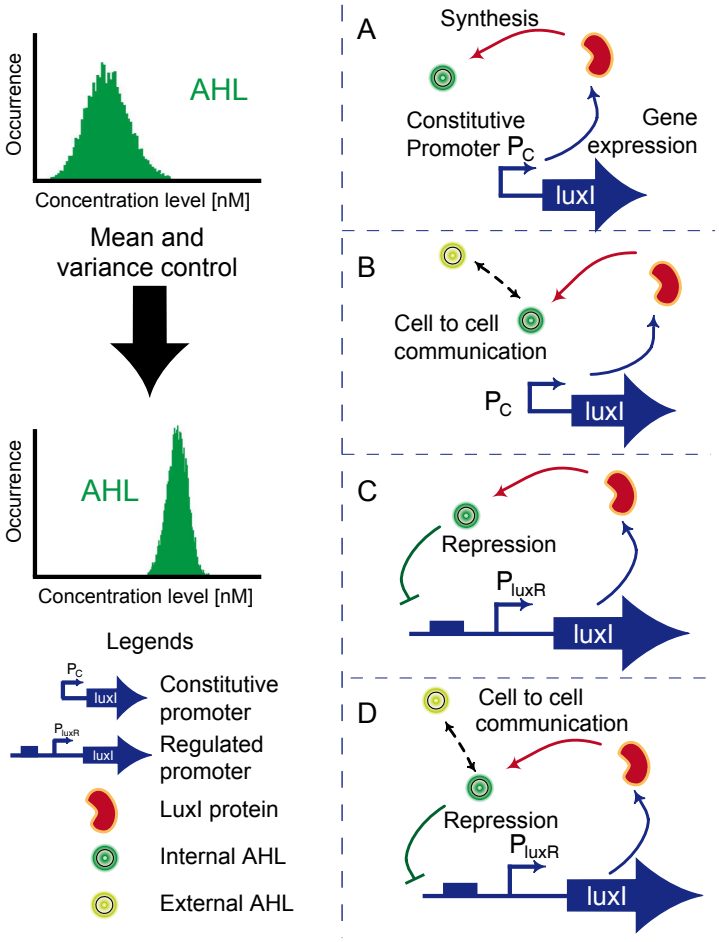

Figure 9.1: Different architectures for controlling the AHL distribution across a population. The core principle is to use the PluxR promoter as an interface to control the production of LuxI (thus modulating AHL and the cell-to-cell communication). (**A**) Open loop production of LuxI without communication. (**B**) Open loop production of LuxI with communication. (**C**) Feedback-regulated production of LuxI without communication. (**D**) Feedback-regulated production of LuxI with communication.

This mentioned heterogeneity in a population of cells is usually modelled via deterministic ODEs with parameters sampled from a given

probability distribution, which is sometimes termed as *extrinsic noise* (Swain et al., 2002). The same approach was used in this work to account for variability across the population.

We first consider an ODE model for the intracellular genetic circuit coupled with the dynamics of AHL export and uptake (Section 9.2). The saturable behavior of promoter activity translates into a sigmoidal nonlinearity in the feedback controller. By approximating the nonlinearity with a piecewise affine function (Section 9.3), we find conditions under which the system operates in a linear regime (Section 9.4). We rely on set-invariance results similar to those developed in Esfandiari and Khalil (1991) for continuous implementations of sliding mode control, and in (Vignoni et al., 2013a) for a sliding mode reference conditioning scheme for coordination of multi-agents. Our main results are closed-form expressions for the mean and variance of AHL across the population (Section 9.5). These indicate how a target mean and variance can be achieved independently by fine-tuning the controller parameters. The predictions offered by our theoretical analysis are in agreement with numerical simulations (Section 9.6) performed with physiologically realistic parameters of *Escherichia coli*.

9.2 System description

9.2.1 Cell-to-cell communication and feedback controller

The proposed circuit combines two engineered gene networks previously implemented in *E. coli*: a cell-to-cell communication system (Fuqua et al., 2001), and a synthetic repressible promoter (Egland and Greenberg, 2000), see Fig. 9.2. The cell-to-cell communication circuit uses components taken from the quorum sensing system of *V. fischeri* (Kaplan and Greenberg, 1985; Schaefer et al., 1996). The feedback circuit comprises a luxI gene under the control of the PluxR promoter. The protein LuxI is the AHL synthase. AHL in turn can bind the protein LuxR and form a complex that binds to the PluxR promoter and represses the expression of the luxI gene. The circuit therefore a negative feedback loop between the concentration of intracellular AHL and the expression of luxI gene.

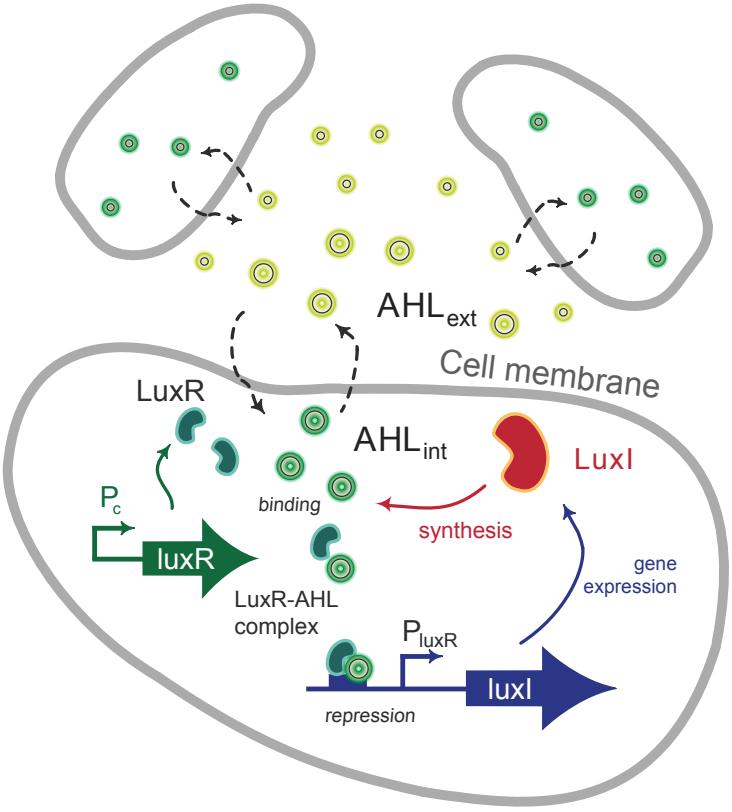

Figure 9.2: Schematic of the intracellular feedback control circuit in one cell and the cell-to-cell communication mechanism.

9.2.2 Mathematical model

In a population of N cells, the concentrations of LuxI, internal AHL and external AHL can be modelled by the following set of ODEs

$$\dot{x}_1^i = \kappa_0 + \kappa_1 \frac{\theta^n}{\theta^n + {x_2^i}^n} - \gamma_1 x_1^i, \tag{9.1}$$

$$\dot{x}_2^i = \kappa_2 x_1^i - d\left(x_2^i - x_e\right) - \gamma_2 x_2^i, \tag{9.2}$$

$$\dot{x}_\mathrm{e} = \frac{d_\mathrm{e}}{N} \sum_{i=1}^{N} \left(x_2^i - x_\mathrm{e}\right) - \gamma_\mathrm{e} x_\mathrm{e}, \tag{9.3}$$

where x_1^i is the concentrations of LuxI protein in the i^{th} cell, x_2^i is the concentration of internal AHL in the i^{th} cell, and x_e is the concentration of external AHL.

In equation (9.1) modelling the LuxI concentration, κ_0 is the tightness or basal expression of the promoter, and κ_1 is the dynamic range of the promoter. The regulatory effect of the promoter is modelled as a Hill-like function, whereby n is the Hill coefficient and θ is the half concentration constant or repression threshold.

In equation (9.2) modelling the internal AHL concentration, the kinetic constant κ_2 models first order AHL synthesis, whereas d is the internal transport constant. Both molecules, LuxI and internal AHL, are subject to first order degradation processes with kinetic constants γ_1 and γ_2, respectively. The kinetic constant d_{e} is the external transport constant and γ_{e} is the degradation rate of external AHL. Note that in (9.3) we take into account the difference between the external and internal volumes with the factor $\frac{1}{N}$, as in Mina et al. (2013).

In the model (9.1–9.3) we have made the following approximations: a) we assume the expression of mRNA is in a quasi-stationary state, neglecting the fast transient required by the mRNA concentration to reach its steady-state value, b) we consider the DNA/repressors complex also reaches very quickly its steady state value, allowing us to model the repression with a Hill function, c) we do not explicitly model the dimerization of the LuxR protein and its binding to AHL, and d) we assume that the LuxR gene is constitutively expressed and is not a limiting factor in the process.

For the purpose of obtaining analytic results, we model the variability between cells by taking the tightness of the PluxR promoter, κ^0, as a random variable with a normal distribution ($\kappa^0 \sim \mathcal{N}\left(\mu, \sigma^2\right)$). Here μ and σ^2 are the mean and variance across the population. However, to obtain more biologically-realistic results, more sources of variability should be included in the analysis. In the simulations we validated our analytical results by adding variability in all remaining parameters (we draw the parameters for each cell from a random distribution, see Fig. 9.4 and Section 9.6).

The following notation will be used hereafter: the partial states x_1 and x_2 are defined as $x_1 = \left[x_1^1, \ldots, x_1^{\text{N}}\right]^T \in \mathbb{R}^{\text{N}}$, $x_2 = \left[x_2^1, \ldots, x_2^{\text{N}}\right]^T \in \mathbb{R}^{\text{N}}$ and the full state $x = [x_1, x_2, x_{\text{e}}]^T \in \mathbb{R}^{2\text{N}+1}$. The vector of equilibrium points of the partial states x_1 and x_2 for the whole ensemble will be de-

noted $\bar{x}_1$ and $\bar{x}_2$. The equilibrium of x_e can be expressed as a function of the equilibrium points of x_2^i:

$$\bar{x}_{\mathrm{e}} = \frac{1}{N}\left(\frac{d_{\mathrm{e}}}{d_{\mathrm{e}}+\gamma_{\mathrm{e}}}\right)\sum_{i}^{N}\bar{x}_2^i = \frac{\epsilon}{N}\sum_{i}^{N}\bar{x}_2^i = \frac{\epsilon}{N}\mathbf{1}_{\mathrm{N}}^T\bar{x}_2, \tag{9.4}$$

where $\epsilon = \frac{d_{\mathrm{e}}}{d_{\mathrm{e}}+\gamma_{\mathrm{e}}}$, and $\bar{x}_{\mathrm{e}}, \bar{x}_2^i$ are the equilibrium values of x_e and x_2^i. The vector $1_{\mathrm{N}} \in \mathbb{R}^{\mathrm{N}}$ denotes the vector with all its elements equal to 1.

The variability of the promoter tightness κ^0 translates into a probability distribution for the steady state concentrations of LuxI and internal AHL across the population. In the remaining of the paper we will focus on quantifying this distribution, exploring how the intracellular feedback controller together with the cell-to-cell communication can be used to reduce variability of gene expression in the population.

9.3 Approximation of the intracellular controller

To simplify the analysis, we approximate the Hill function in (9.1) by the piecewise affine saturation function shown in Fig. 9.3. Its slope is taken to be the same as that of the Hill function at the half concentration constant θ, which is a sensible approximation for the typical values of the Hill coefficient n. Under this approximation, equation (9.1) can be rewritten as:

$$\dot{x}_1^i = u_{sat}(x_2^i) - \gamma_1 x_1^i, \tag{9.5}$$

with

$$u_{\mathrm{sat}}(x_2^i) = \begin{cases} \kappa_0^i + \kappa_1 & \text{if} \quad x_2^i < \theta - \delta \\ \kappa_0^i - \frac{\kappa_1 n}{4\theta}x_2^i + \frac{\kappa_1 n}{4} + \frac{\kappa_1}{2} & \text{if} \quad \left|x_2^i - \theta\right| < \delta \\ \kappa_0^i & \text{if} \quad x_2^i > \theta + \delta, \end{cases} \tag{9.6}$$

and δ being the midpoint of the linear section:

$$\delta = \frac{2\theta}{n}. \tag{9.7}$$

As mentioned before, the Hill function, together with its approximation u_{sat}, can be understood as a controller with fixed structure and tunable parameters. Our goal is to tune the controller parameters so as

to shape the statistical distribution of the steady state concentration of AHL. We can conveniently reparameterize the saturation function u_{sat} using only three parameters. Rewriting (9.6) using $S = \frac{\kappa_1 n}{4\theta}$, $T = \theta$, $R = \frac{\kappa_1}{2}$ and $\delta = \frac{R}{S}$ we obtain

$$u_{sat}(x_2^i) = \begin{cases} \kappa_0 + 2R & \text{if} \quad x_2^i < T - \delta \\ \kappa_0 - S\left(x_2^i - T\right) + R & \text{if} \quad \left|x_2^i - T\right| < \delta \\ \kappa_0 & \text{if} \quad x_2^i > T + \delta. \end{cases} \tag{9.8}$$

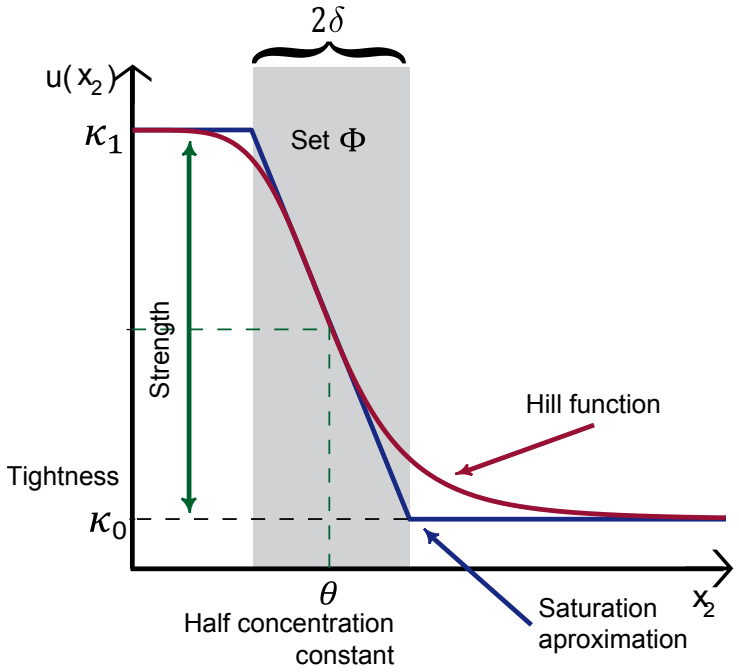

Figure 9.3: Characteristic of the promoter. Hill function and its piecewise affine approximation for $n = 5$, $\theta = 5$ resulting in $\delta = 2$.

9.4 Operation in the linear regime

In this section we obtain sufficient conditions under which the set

$$\Phi_x = \left\{x \in \mathbb{R}^{2N+1} : \left|\bar{x}_2^i - T\right| \leq \delta, \forall i = 1, \ldots, N\right\}, \tag{9.9}$$

is an attractive invariant set for all the cells in the interconnected population (see Fig. 9.3). Later in Section 9.5 we will use this result to obtain closed-form expressions for the mean and variance of the protein concentration.

We first define the mean system states as $[\tilde{x_1}, \tilde{x_2}, x_e]^T$, with

$$\tilde{x}_j = \frac{1}{\mathrm{N}} \sum_{i=1}^{\mathrm{N}} x_i^j, \; j = 1, 2. \tag{9.10}$$

The dynamics of the mean system can be expressed by

$$\dot{\tilde{x}}_1 = \rho - \gamma_1 \tilde{x}_1, \tag{9.11}$$

$$\dot{\tilde{x}}_2 = \kappa_2 \tilde{x}_1 - (d + \gamma_2)\, \tilde{x}_2 + d x_e, \tag{9.12}$$

$$\dot{x}_{\mathrm{e}} = d_{\mathrm{e}} \tilde{x}_2 - (d_{\mathrm{e}} + \gamma_{\mathrm{e}})\, x_{\mathrm{e}}. \tag{9.13}$$

Where $\rho = \frac{1}{\mathrm{N}} \sum_{i=1}^{\mathrm{N}} u_{sat}(x_2^i)$. Notice that $\frac{1}{\mathrm{N}} \sum_{i=1}^{\mathrm{N}} \kappa_0^i = \tilde{\kappa}_0$ is the sample estimator of the mean μ, and that using (9.8) we get $\frac{1}{\mathrm{N}} \sum_{i=1}^{\mathrm{N}} u_{sat}(x_2^i) \in [\mu, 2R + \mu]$.

Equation (9.11) corresponds to an exponentially stable linear system with bounded input ρ and time constant $1/\gamma_1$. Therefore, $\tilde{x}_1$ there will get arbitrarily close to its steady state $\tilde{x}_1 \in \left[\frac{\mu}{\gamma_1}, \frac{\mu+2R}{\gamma_1}\right]$ after a finite time $t^\star$. The same argument holds for the subsystem formed by (9.12)-(9.13) with bounded input $\tilde{x}_1$, and thus x_{e} will get arbitrarily close to its steady state

$$x_{\mathrm{e}} \in \frac{\epsilon \kappa_2}{d\,(1-\epsilon) + \gamma_2} \left[\frac{\mu}{\gamma_1}, \frac{\mu + 2R}{\gamma_1}\right], \tag{9.14}$$

after a finite time $t^{\star\star} > t^\star$.

Since x_{e} is a bounded signal, equations (9.2), (9.5) and (9.8) for the i^{th} cell can be rewritten using the variable change $z = x^i$:

$$\begin{cases} \dot{z}_1 = -\gamma_1 z_1 + u(z_2) \\ \dot{z}_2 = \kappa_2 z_1 - (d + \gamma_2) z_2 + z_{\mathrm{e}}, \end{cases} \tag{9.15}$$

where $z = [z_1, z_2]^T \in \mathbb{R}^2$ and $z_{\mathrm{e}} = x_{\mathrm{e}}$ is a bounded external perturbation with bounds $\underline{z}_{\mathrm{e}} < z_{\mathrm{e}} < \overline{z}_{\mathrm{e}}$ from (9.14). Note that the index i was dropped for simplicity of notation.

The idea is to obtain a bound on the control signal $u(z_2)$ that ensures convergence of the trajectories of (9.15) to the set Φ, and that makes it

invariant, with Φ defined as:

$$\Phi = \left\{ z \in \mathbb{R}^2 : \underline{z}_2 < z_2 < \overline{z}_2 \right\}. \tag{9.16}$$

To this end, it is convenient to use a structure for $u(z_2)$ which is more general than equations (9.6) and (9.8):

$$u(z_2) = \begin{cases} \kappa_1 + \kappa_0 & z_2 < \underline{z}_{2u} \\ u_{in}(z_2) & \underline{z}_{2u} < z_2 < \overline{z}_{2u} \\ \kappa_0 & z_2 > \overline{z}_{2u}. \end{cases} \tag{9.17}$$

with $\kappa_0 < u_{in}(z_2) < \kappa_1 + \kappa_0$ a bounded but not necessary continuous function of z_2 and $\underline{z}_2 < \underline{z}_{2u}$ and $\overline{z}_{2u} < \overline{z}_2$.

Note that making $T - \delta = \underline{z}_2$ and $T + \delta = \overline{z}_2$, equations (9.6) and (9.8) plus κ_0 represent (9.17), and when the set Φ is invariant, then the set Φ_x (9.9) is also invariant. Also, the set Φ can be rewritten as $\Phi = \underline{\Phi} \cap \overline{\Phi}$, the intersection of two sets $\underline{\Phi}$ and $\overline{\Phi}$ where

$$\underline{\Phi} = \left\{ z \in \mathbb{R} : \underline{\phi}(z_2) = -z_2 + \underline{z}_2 < 0 \right\} \tag{9.18}$$

and

$$\overline{\Phi} = \left\{ z \in \mathbb{R} : \overline{\phi}(z_2) = z_2 - \overline{z}_2 < 0 \right\}. \tag{9.19}$$

In Esfandiari and Khalil (1991) a boundary layer set is proven to be uniformly ultimately bounded, for systems with unitary relative degree (where the control action u appears explicitly in the first derivative of the output ϕ). The system in (9.15), however, has relative degree two when we take the control to be $u(z_2)$ and the outputs to be $\underline{\phi}(z_2)$ and $\overline{\phi}(z_2)$. To overcome this problem, we exploit the triangular structure of the system and design $u(z_2)$ using a backstepping-like approach. We can then use geometric invariance ideas to make the desired set Φ invariant. With this technique we get the following result.

Theorem 9.1. *The set Φ is an invariant and attractive set for z_2 if the following inequalities hold*

$$\kappa_0 + \kappa_1 > \gamma_1 \frac{(d + \gamma_2)\, \underline{z}_2 - \underline{z}_{\mathrm{e}}}{\kappa_2} \tag{9.20}$$

and

$$\kappa_0 < \gamma_1 \frac{(d + \gamma_2)\, \overline{z}_2 - \overline{z}_{\mathrm{e}}}{\kappa_2} \tag{9.21}$$

9.5 Control of protein mean and variance

In this section we show that the mean and variance of the AHL concentration across the cell population can be controlled independently with different parameters of the controller. This constitutes the main contribution of this paper.

Under the conditions of Theorem 9.1 we know that every individual system will eventually operate in the linear regime:

$$\dot{x}_1^i = \kappa_0^i - S\left(x_2^i - T\right) + R - \gamma_1 x_1^i, \tag{9.22}$$

The dynamics of the whole ensemble can then be written as a $(2N+1)-$dimensional linear system:

$$\dot{x} = \left[\begin{array}{cc|c} -\gamma_1 \mathbf{I}_{\mathrm{N}} & S\mathbf{I}_{\mathrm{N}} & 0_{\mathrm{N}} \\ \kappa_2 \mathbf{I}_{\mathrm{N}} & -\left(d+\gamma_2\right)\mathbf{I}_N & d1_{\mathrm{N}} \\ \hline 0_{\mathrm{N}}^T & \frac{d_{\mathrm{e}}}{N} 1_{\mathrm{N}}^T & -\left(d_{\mathrm{e}}+\gamma_{\mathrm{e}}\right) \end{array}\right] x + \left[\begin{array}{c} \kappa_0 + (ST+R)\,1_{\mathrm{N}} \\ 0_{\mathrm{N}} \\ \hline 0 \end{array}\right], \tag{9.23}$$

We define the matrix Π_{N} as

$$\Pi_{\mathrm{N}} = \mathbf{I}_{\mathrm{N}} - \frac{1}{N}\mathbf{1}_{\mathrm{N}\times\mathrm{N}}, \tag{9.24}$$

where $\mathbf{I}_{\mathrm{N}} \in \mathbb{R}^{\mathrm{N}\times\mathrm{N}}$ is the identity matrix and $\mathbf{1}_{\mathrm{N}\times\mathrm{N}} \in \mathbb{R}^{\mathrm{N}\times\mathrm{N}}$ has all its entries equal to 1.

Note that Π_{N} is idempotent (*i.e.* $\Pi_{\mathrm{N}}\Pi_{\mathrm{N}} = \Pi_{\mathrm{N}}$) and satisfies $\Pi_{\mathrm{N}} 1_{\mathrm{N}} = 0_{\mathrm{N}}$.

Setting $\dot{x} = 0$ in (9.23) and using (9.4) we get a system of $2N$ linear equations for the steady states $\bar{x}_1$ and $\bar{x}_2$:

$$\left[\begin{array}{cc} \gamma_1 \mathbf{I}_{\mathrm{N}} & S\mathbf{I}_{\mathrm{N}} \\ \kappa_2 \mathbf{I}_{\mathrm{N}} & -\left[d\left(1-\epsilon\right)+\gamma_2\right]\mathbf{I}_{\mathrm{N}} - d\epsilon\Pi_{\mathrm{N}} \end{array}\right] \left[\begin{array}{c} \bar{x}_1 \\ \bar{x}_2 \end{array}\right] = \left[\begin{array}{c} \kappa_0 + (ST+R)\,1_{\mathrm{N}} \\ 0_{\mathrm{N}} \end{array}\right] \tag{9.25}$$

Theorem 9.2. *Under the conditions for Theorem 1, the mean and variance of the distribution of x_2 for a population of N cells can be controlled independently by tuning the parameters of each cell intracellular controller as follows:*

$$\mathrm{E}\left\{\bar{x}_2^i\right\} = \frac{1}{S+\beta}\left(\mu + ST + R\right) \tag{9.26}$$

$$\mathrm{Var}\{\bar{x}_2^i\} = \left[\frac{1}{(S+\beta-\epsilon d)^2} + \frac{1}{N}\left(\frac{1}{(S+\beta)^2} - \frac{1}{(S+\beta-\epsilon d)^2}\right)\right]\sigma^2 \quad (9.27)$$

The expression in (9.27) indicates that the variance can be controlled independently from the mean with the parameter S, and its sensitivity is

$$\frac{\partial \mathrm{Var}\{\bar{x}_2^i\}}{\partial S} = -\frac{2}{N}\left[\frac{1}{(S+\beta)^3} + \frac{N-1}{N\,(S+\beta-\epsilon d)^3}\right]\sigma^2, \quad (9.28)$$

which indicates that a steep feedback (i.e. with a high value of S) tends to reduce the population level variability.

9.6 Simulations

To demonstrate the potential of the proposed control strategy, we ran numerical simulations of the different control architectures shown in Fig. 9.1. The parameters values used are shown in Table 9.1. These are physiologically realistic values for *E. coli*, and similar to those typically found in the literature (Kaplan and Greenberg, 1985; Egland and Greenberg, 2000; Kæ rn et al., 2005; Smith et al., 2008; Weber et al., 2013; Mina et al., 2013).

In order to compare the different architectures, we observe the variances and adjust the means to be similar in all cases.

Note that nowadays, the Ribosome Binding Site (RBS) strength is one of the more suitable biological tuning knobs, which can be selected with high predictability (Egbert and Klavins, 2012). Thus, consider rewriting (9.1) taking into account the RBS strength in the following way:

$$\dot{x}_1^i = \mathrm{RBS}_s\left(\hat{\kappa}_0^i + \hat{\kappa}_1^i \frac{\theta^n}{\theta^n + {x_2^i}^n}\right) - \gamma_1 x_1^i. \quad (9.29)$$

The new parameters $\hat{\kappa}_0$ and $\hat{\kappa}_1$ are fixed among all the examples to a 10% of leakiness and 10-fold dynamic range (Kæ rn et al., 2005; Mina et al., 2013; Weber et al., 2013). Hence, the RBS strength RBS_s will be used as the only tuning knob in order to have the same mean of AHL in architectures B, C and D than in architecture A.

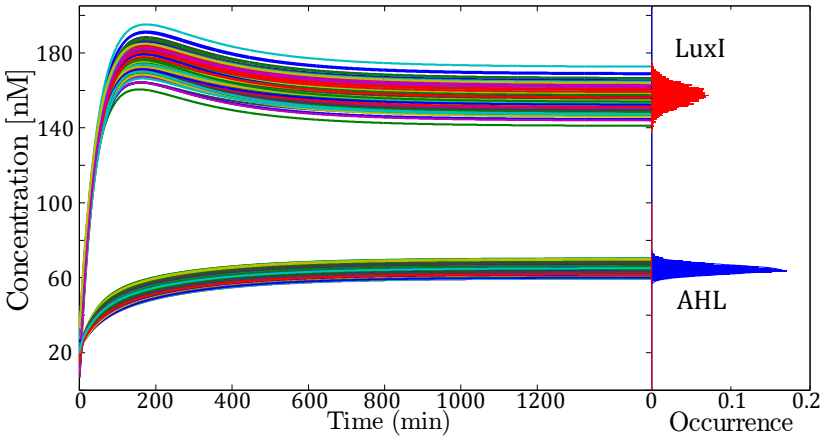

Figure 9.4: Time course and steady state histogram of 10.000 cells for architecture D with closed loop with cell to cell communication (with $n = 1.5$)

Fig. 9.4 shows the simulation of 10000 ODEs (equations 9.1-9.2) one for each cell i. The values for the parameters were drawn from a normal distribution with mean equal to the nominal value of the parameter in Table 9.1 and a variance of 5% of that value. The steady state distributions for all the architectures (see Fig. 9.5) were obtained from the same kind of simulations with corresponding parameters (Table 9.1).

In Fig. 9.5 we can see how the different architectures impact on the steady state distribution of AHL. The mean, the variance, and the coefficient of variation (CV) of AHL resulting from the simulations are shown also in Table 9.1.

From the results in Table 9.1 and from the distributions of AHL in Fig. 9.5, it appears that both the feedback-regulated production of LuxI, and the cell-to-cell communication through AHL are required for best performance. Case D (bottom plot from Fig. 9.5) have smaller variances than cases A, B and C (top plot from Fig. 9.5).

Also comparing the two distributions in the bottom plot from Fig. 9.5 it appears that a steep feedback $n = 3$ tends to reduce the population level variability as predicted by (9.28) with respect to a less steeper one $n = 1.5$.

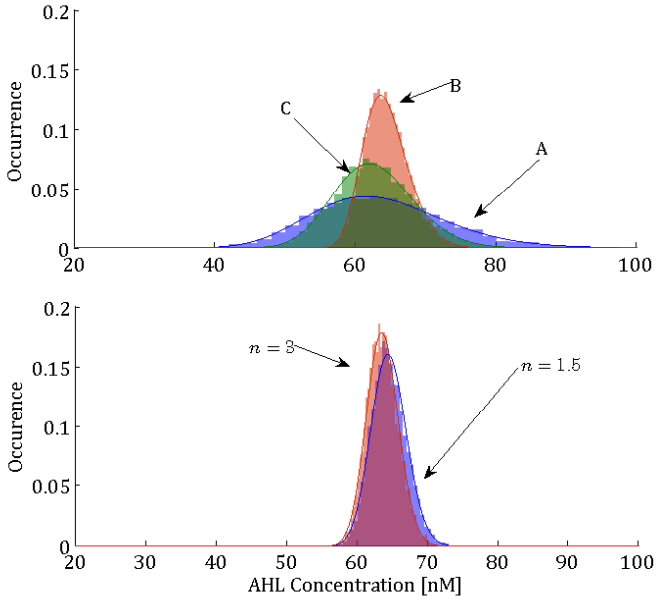

Figure 9.5: Steady state distributions for 10.000 cells of AHL concentration in the different architectures of Fig. 9.1. In the top figure architectures A, B and C are shown. The bottom figure shows, architecture D with $n = 1.5$ and also with a steeper controller $n = 3$.

Table 9.1: Nominal values for the parameters used in the simulations. Mean, variance and CV for each architecture.

	Architecture						
Parameter	A	B	C	D		Units	Reference
γ_1	0.0173					min^{-1}	[20,21]
RBS_s	0.76	15	0.125	4.6	4.6	nM.min^{-1}	[19,21]
θ	-	-	63.24			nM	[15,21]
n	-	-	1.5	1.5	3	-	[15]
κ_2	0.04					min^{-1}	[21]
d	-	0.3	-	0.3		min^{-1}	[16]
d_e	-	0.006	-	0.006		min^{-1}	[16]
γ_2	2.82e-3					min^{-1}	[18,20]
$\mathrm{E}\{x_2^i\}$	63.55	64.36	62.65	63.25	63.25	nM	
$\mathrm{Var}\{x_2^i\}$	89.43	10.10	32.13	6.23	4.12	nM	
$\mathrm{CV}\{x_2^i\}$	0.1488	0.0494	0.0905	0.0395	0.0321		

9.7 Conclusions

In this paper, we investigated the design of a synthetic gene controller aimed at reducing gene expression variability at the population level. As a proposed synthetic biology implementation, we considered a cell-to-cell communication system coupled with an intracellular genetic controller characterized by a sigmoidal nonlinearity. To simplify the mathematical analysis, the nonlinearity was approximated by a piecewise linear function. Based on this approximation, we established: (i) conditions under which the non saturated region of the controller is an attractive invariant set, and (ii) closed-form expressions for the first two moments of the distribution of AHL across a population. We also demonstrated how the parameters of the controller can be fine-tuned to independently control the mean and the variance of the distribution.

With the progress of current experimental techniques, adjusting genetic parameters has become feasible and has paved the way for the use of rigorous control-theoretic approaches for the design of genetic circuits. In this line we think that having a model-based guideline to design genetic networks has tremendous potential in Synthetic Biology.

For example, changing cooperativity with protein sequestration techniques (Buchler and Cross, 2009) can allow us to tune S (the slope of the nonlinearity), whereas sequence repeats in the spacer region of the RBS (Egbert and Klavins, 2012) can be used to adjust R by changing the RBS strength. The threshold T can also be tuned with similar techniques (Buchler and Cross, 2009), for example by shifting the position where the complex LuxR-AHL binds (called Lux-box) (Egland and Greenberg, 2000) or by making single point mutations in the Lux-box.

As a proof of concept, in this work we proposed the basis for protein distribution control along a population by controlling the distribution of the signalling molecules AHL. Using this signal to drive the production of a protein of interest could be used to control its distribution. We are working in that direction and investigating different ways in which this could be done. We are also considering the implementation of the proposed genetic circuit *in vivo* using synthetic biological parts (for example Biobricks), and the analysis of mixed population scenarios in which feedback-regulated cells coexist with unregulated ones, so as to design distributed approaches to biocomputing.

General discussion

The work behind this Thesis employed ideas of set invariance and sliding modes to successfully deal with different relevant control problems in nonlinear systems.

Motivated by the appearance of sigmoidal functions when modeling biological systems, a continuous approximation of sliding mode control was explored as an analytical framework for new understanding of biological systems. Using also invariance techniques, the invariance of a set (the boundary layer set) was proven for a system with a sigmoidal nonlinearity and a relative degree of two between the controlled output and the sigmoidal function. This framework was applied to the design and control of genetic circuits in synthetic biology approaches and as a result the reduction of the variance of a molecule in the genetic circuit was achieved, this is an important result setting the bases for new research and for possible new implementations in synthetic biology using a model based approach. The Control of complex systems group where this Thesis was developed is planning to build a *living lab* in order to test the validity of all this ideas performing synthetic biology experiment.

In order to better control bioproduction processes is necessary to access to different kinetic rates of the microorganisms from noisy measurements of other variables, with this motivation second order sliding modes were used in order to design robust estimators for those variables. First using a change of coordinates and linear matrix inequalities (LMIs) the stability and design criteria for specific growth rate estimators was performed, and then the same was done for multiple kinetic rates estimators. Additionally, with a change of time coordinates a more constructive approach was investigated to design the same second order sliding mode algorithm with more analytical results. The appropriateness of this estimators was successfully studied in a simulation proof of

concept incorporating them into growth rate controllers. The estimators designed here are in the process to be implemented in laboratory scale bioreactors in the biotechnology company Biopolis SL, which collaborates the the Control of Complex Systems group where this Thesis was developed.

Inspired in biological aspect of animal societies, like flocking, schooling or consensus, sliding modes reference conditioning was used to design coordination control of interconnected systems. Sliding modes reference conditioning methodology allowed to incorporate constraints into the design, such as physical constraints of the systems together with *virtual* constraints taking into account the coordination desires. The method has two possible architectures, a local and a global one. Both preserve the robustness properties of the sliding modes, so as the coordination can be configured independently of the individual systems regulation. This method is leading now to the development of a research topic devoted to flight formation control and is being implemented using UAVs at the Universitat Politécnica de Valéncia.

Conclusions of the Thesis

This Thesis presented ideas and methodologies based on invariance principles and sliding mode control used to deal with different problems. Coordination of interconnected constrained systems, estimation of unknown input signals and design and control of synthetic biology systems. What is very interesting is that the nature of the systems is of very small relevance and the methodologies proposed can be applied to either a collection of flying robots or to the estimation of complex bioprocesses or to the genetic circuit of living cells.

The main contributions of this work where summarized on the introduction, and a particular conclusion section closes each chapter. Those are both repeated here for convenience. A general discussion of the results was done above. Here, general conclusions and future-work lines are discussed.

The main contributions of the Thesis are:

- The development of a method to coordinate dynamical systems with different dynamic properties by means of a sliding mode auxiliary loop shaping the references given to the systems as function of the local and global goals, the achievable performance of each system and the available information of each system.

- Design methods for second order sliding mode algorithms. The methods decouple the problem of stability analysis from that of finite-time convergence of the super-twisting sliding mode algorithm. A nonlinear change of coordinates and a time-scaling are used to provide simple, yet flexible design methods and stability proofs. Application of the method to the design of finite-time convergence estimators of bioprocess kinetic rates and specific biomass growth rate, from biomass measurements. Also the estimators are

validated with experimental data.

- The proposal of a strategy to reduce the variability of a cell-to-cell communication signal in synthetic genetic circuits. The method uses set invariance and sliding mode ideas applied to gene expression networks to obtain a reduction in the variance of the communication signal. Experimental approaches available to modify the characteristics of the gene regulation function are described.

The particular conclusions of each article included in this Thesis are:

- **SMRCoord: Systems coordination**, presented on Part I, is a novel strategy using ideas of set invariance and sliding mode reference conditioning is developed to deal with the coordination of multi-agents and formation control problem. The proposed methodology has an interesting potential to be expanded in order to overcome more general coordination problems. This is inherent to its definition, *i.e.* the coordination goals are reflected in the design of the sliding manifolds.

  The fact that the individual systems dynamics are *hidden* to the coordination system, and only the necessary information about the subsystems constraints is communicated to it, makes the proposed methodology transparent and allows dealing with a broad kind of systems to be coordinated, as soon as they can be *reference conditioned*.

  Additionally, the features of the SMRC and the SM itself are inherited by the proposal, such as robustness properties of SM control, but not the usual problems of SM like chattering, because the technique is implemented as a part of a numeric algorithm in a digital environment.

  Practical applications of the proposed algorithm, for example in AR-Drone® Quadrotors flying in a controlled formation, can be implemented as auxiliary supervisory loops to the trajectory planing algorithm for the virtual leader and stabilizing controllers of the individual agents. The research group is working towards this implementation.

  In the theoretical side, an interesting future research line we are working is on the extensions of the proposed methodology to deal

with multiple constraint per system, in which case the problem is how to decide the direction of the control action. Also we are working in the case of constrained systems, and how to incorporate these constraint into the coordination, in order to have a formation control which also takes care of the individual systems constraint, resulting in a robust formation control against disturbances coming from individual limitations in the multi-agent systems.

- **Stability preserving maps for finite-time convergence** In this contribution we have addressed the problem of designing algorithms with finite-time convergence. Departing from previous approaches, the problem of stability analysis and that of finite-time convergence have been decoupled. This allows simple, yet flexible, design methods and stability proofs. The problem of designing a super-twisting second-order sliding mode algorithm, coping with a broad class of perturbations, has been used to show the proposed approach. A nonlinear change of coordinates and a time-scaling are used. In the new coordinates and time space, the transformed system is stabilized using any appropriate standard design method. Conditions under which the combination of the nonlinear coordinates transformation and the time-scaling is a stability preserving map have been provided. Under these conditions, stability of the system in the transformed space implies stability of the original system. Moreover, if convergence in the transformed space is faster than $\mathcal{O}(1/\tau)$ –where τ is the transformed time– then convergence in the original coordinates and time-scale takes place in finite-time.

  Decoupling the problem of stability analysis from that of finite-time convergence allows the approach to be readily extended to other cases. Possibilities are diverse. For instance, extension to higher-order sliding modes with order higher than two. Tackling with additional constraints –e.g. constraints on the injected error terms that may appear in controllers design– can be done at the transformed time-coordinates space, where standard approaches –e.g. a nested saturations-based design– can be used, the finite-time convergence in the original dynamics achieved provided the coordinates and time-scale transformations fulfill the conditions stated in Section 6.3. Nested finite-time designs may also be a

possibility, allowing for super-fast convergence rates.

- **Second-Order Sliding Mode Observer for Multiple Kinetic Rates Estimation in Bioprocesses** The on-line kinetic rates estimation problem in bioprocesses was addressed. The proposed second-order SM observer is able to estimate multiple specific kinetic rates from related measurements of process variables even though no particular model of each kinetic rate was assumed.

  Certainly, only upper bounds of the time derivatives are required. Global finite-time convergence is achieved by choosing a suitable observer structure. This property is particularly important in control applications because the observer does not add dynamics that might destabilise the closed loop.

  The observer performance was assessed using experimental data from continuous-mode fermentation of *S. cerevisiae*. Microbial specific growth rate and net ethanol production rate were estimated. The proposed algorithm was compared with a high gain observer under normal operation and for two typical sensor faults. Particularly, the SMO showed better noise rejection in the noisiest signal and better transient response under sensor drifts and spikes.

- **Specific Kinetic Rates Regulation in Multi-Substrate Fermentation Processes** In this work we extended the previous proposed nonlinear proportional-integral control to multi-substrate fed-batch processes for multiple kinetic rates regulation. This was possible due to recent development of an algorithm for several kinetic rates estimation based on second-order sliding mode ideas, which allows us to obtain the consumption rates for each substrate together with the specific growth rate of the microorganism measuring only biomass and one of the substrates.

  Robustness properties of both strategies are inherited. The controller provides robustness to model uncertainties and disturbances, which is one of its main attractive features. The observer provides noise rejection, and finite-time convergence of the consumption rates estimates. The latter allows to independently design the observer and the controller.

  Performance of the system was shown by simulation of realistic scenarios, with noise, parameters uncertainty, and high initial sub-

strate concentration, where an increase in concentration of substrates produces a decrease in growth rate, and therefore the fermentation is in an intrinsically unstable region.

- **Control of protein concentrations in heterogeneous cell populations** In this contribution, we investigated the design of a synthetic gene controller aimed at reducing gene expression variability at the population level. As a proposed synthetic biology implementation, we considered a cell-to-cell communication system coupled with an intracellular genetic controller characterized by a sigmoidal nonlinearity. To simplify the mathematical analysis, the nonlinearity was approximated by a piecewise linear function. Based on this approximation, we established: (i) conditions under which the non saturated region of the controller is an attractive invariant set, and (ii) closed-form expressions for the first two moments of the distribution of AHL across a population. We also demonstrated how the parameters of the controller can be fine-tuned to independently control the mean and the variance of the distribution.

  With the progress of current experimental techniques, adjusting genetic parameters has become feasible and has paved the way for the use of rigorous control-theoretic approaches for the design of genetic circuits. In this line we think that having a model-based guideline to design genetic networks has tremendous potential in Synthetic Biology.

  As a proof of concept, in this work we proposed the basis for protein distribution control along a population by controlling the distribution of the signalling molecules AHL. Using this signal to drive the production of a protein of interest could be used to control its distribution. We are working in that direction and investigating different ways in which this could be done. We are also considering the implementation of the proposed genetic circuit *in vivo* using synthetic biological parts (for example Biobricks), and the analysis of mixed population scenarios in which feedback-regulated cells coexist with unregulated ones, so as to design distributed approaches to biocomputing.

Future work The above review of the obtained results presents some open issues which need a further study and can lead to new research lines.

- **Coordination of dynamical systems:** In this topic, the GCSC research group is already working in the practical implementation of the proposed methodology in unmanned aerial vehicles (UAVs), namely Parrot® ARDrone Quadrotors. Three Career Final Projects (PFC) supervised by this Thesis' author and works in collaboration with the CPOH group at UPV, are leading to new publications in the area of practical implementation of flight formation control algorithms. Several issues arises when going from theory and simulation to a practical and real life implementation, for instance sampling time, discretization, geo-localization, absolute and relative reference frameworks, sensor fusion and state estimation, battery-life optimization are some of the open problems in this line of research.

- **Second order sliding modes algorithms:** The author is actually supervising a Master Thesis in the line of using the results obtained in this Thesis to fine-tune practical implementations of the kinetic rate estimators in Lactic fermentation processes in the biotech company Biopolis S.L. in a collaboration project between the company and the authors research group. The main problem to be addressed is to incorporate performance measures of the estimators in the design process. The results given in this Thesis are a parameter region guaranteeing stability and finite time convergence of the error dynamic. The issue is to find now the best set of parameters inside this region taking into account the performance of the observer. One of the approaches that are taking place is to find a relationship between the dynamical properties of the transformed LPDI to the nonlinear observer, in order to tune the last one with information of classical performance conditions in the former one.

- **Synthetic genetic circuits design:** This research line is the more active one. Several sub-lines are being explored. The research group, and lead by the author of this Thesis, is working in model reduction from complete reaction models to small and manageable models. The reduced models are being used to make stochastic

models in order to consider the intrinsic variability of the genetic circuits. Additionally, the linear noise approximation (LNA) is being used in the same model used in the las part of this Thesis to complete that work and unify the extrinsic noise contribution with the intrinsic one. LNA in a population level will help to understand how the cell-to-cell communication comes to the rescue in order to decrease the variability across the population.

Bibliography

Que otros se jacten de las páginas que
han escrito; a mí me enorgullecen las
que he leído.

Jorge Luis Borges

ABORHEY, S. and WILLAMSON, D. State amd parameter estimation of microbial growth process. *Automatica*, vol. 14, pages 493–498, 1978.

ALON, U. How to choose a good scientific problem. *Molecular Cell*, vol. 35(6), pages 726–728, 2009.

AMANN, H. *Ordinary differential equations: an introduction to nonlinear analysis*. Walter de Gruyter, 1990.

ANTONELLI, G. Interconnected Dynamic Systems: An Overview on Distributed Control. *Control Systems Magazine, IEEE*, vol. 33(1), pages 76–88, 2013.

ASTOLFI, A. and ORTEGA, R. Immersion and invariance: a new tool for stabilization and adaptive control of nonlinear systems. *Automatic Control, IEEE Transactions on*, vol. 48(4), pages 590–606, 2003. ISSN 0018-9286.

BACCIOTTI, A. and ROSIER, L. *Liapunov functions and stability in control theory*. Springer Verlag, 2005. ISBN 3540213325.

BALAGADDÉ, F. K., SONG, H., OZAKI, J., COLLINS, C. H., BARNET, M., ARNOLD, F. H., QUAKE, S. R. and YOU, L. A synthetic Escherichia coli predator-prey ecosystem. *Molecular systems biology*, vol. 4, page 187, 2008. ISSN 1744-4292.

BARBOT, J., PERRUQUETTI, W. and DEKKER, M. *Sliding mode control in engineering*. M. Dekker, 2002.

BARTOLINI, G., FERRARA, A. and USANI, E. Chattering avoidance by second-order sliding mode control. *Automatic Control, IEEE Transactions on*, vol. 43(2), pages 241–246, 1998. ISSN 0018-9286.

BARTOLINI, G., PISANO, A., PUNTA, E. and USAI, E. A survey of applications of second-order sliding mode control to mechanical systems. *International Journal of Control*, vol. 76, pages 875–892, 2003.

BASTIN, G. and DOCHAIN, D. On-line Estimation of microbial specific growth rates. *Automatica*, vol. 22, pages 705–709, 1986.

BASTIN, G. and DOCHAIN, D. *On-line Estimation and Adaptive Control of Bioreactors*. Elsevier, Amsterdam, The Nederlands, 1990.

BASU, S., GERCHMAN, Y., COLLINS, C. H., ARNOLD, F. H. and WEISS, R. A synthetic multicellular system for programmed pattern formation. *Nature*, vol. 434(7037), pages 1130–1134, 2005.

BLANCHINI, F. Set invariance in control. *Automatica*, vol. 35(11), pages 1747 – 1767, 1999. ISSN 0005-1098.

BLANCHINI, F. and MIANI, S. *Set-theoretic methods in control*. Springer, 2008.

BLASCO, X., GARCÍA-NIETO, S. and REYNOSO-MEZA, G. Control autónomo del seguimiento de trayectorias de un vehículo cuatrirrotor. Simulación y evaluación de propuestas. *Revista Iberoamericana de Automática e Informática Industrial RIAI*, vol. 9(2), pages 194–199, 2012.

BONDAREV, A. G., BONDAREV, S. A., KOSTYLEVA, N. E. and UTKIN, V. I. Sliding modes in systems with asymptotic state observers. *Automation and Remote Control*, vol. 46(6), pages 49–64, 1985.

BOYD, S., EL GHAOUI, L., FERON, E. and BALAKRISHNAN, V. *Linear Matrix Inequalities in System and Control Theory*, vol. 15 of *Studies in Applied Mathematics*. Society for Industrial and Applied Mathematics {(SIAM)}, 1994. ISBN 0-89871-334-X.

BUCHLER, N. E. and CROSS, F. R. Protein sequestration generates a flexible ultrasensitive response in a genetic network. *Molecular Systems Biology*, vol. 5, 2009. ISSN 1744-4292.

CAO, Y., REN, W. and MENG, Z. Decentralized finite-time sliding mode estimators and their applications in decentralized finite-time formation tracking. *Systems and Control Letters*, vol. 59(9), pages 522–529, 2010. ISSN 0167-6911.

CAO, Y., YU, W., REN, W. and CHEN, G. An Overview of Recent Progress in the Study of Distributed Multi-agent Coordination. *Industrial Informatics, IEEE Transactions on*, vol. 9(1), pages 427–438, 2013.

CHANG, D.-M. The Snowball Effect in Fed-Batch Bioreactions. *Biotechnology Progress*, vol. 19(3), pages 1064–1070, 2003. ISSN 1520-6033.

CHEN, C. and PENG, S. Design of a sliding mode control system for chemical processes. *Journal of Process Control*, vol. 15, pages 515–530, 2005.

CHIU, C.-S. Derivative and integral terminal sliding mode control for a class of mimo nonlinear systems. *Automatica*, vol. 48(2), pages 316–326, 2012.

CLARKE, F. *Optimization and nonsmooth analysis*. Society for Industrial Mathematics, 1990. ISBN 0898712564.

CORTEŚ, J. Finite-time convergent gradient flows with applications to network consensus. *Automatica*, vol. 42(11), pages 1993–2000, 2006.

CORTES, J. Discontinuous dynamical systems. *Control Systems Magazine, IEEE*, vol. 28(3), pages 36–73, 2008. ISSN 0272-1708.

CRUZ-ZABALA, E., MORENO, J. and FRIDMAN, L. Uniform robust exact differentiator. *IEEE Transactions on Automatic Control*, vol. 56(11), pages 2727–2733, 2011.

DABROS, M., SCHULER, M. M. and MARISON, I. W. Simple control of specific growth rate in biotechnological fed-batch processes based on enhanced online measurements of biomass. *Bioprocess and biosystems engineering*, vol. 33(9), pages 1109–1118, 2010.

DÁVILA, J., FRIDMAN, L. and LEVANT, A. Second-order sliding-mode observer for mechanical systems. *IEEE Transactions on Automatic Control*, vol. 50(11), pages 1785–1789, 2005.

DE BATTISTA, H., PICÓ, J., GARELLI, F. and NAVARRO, J. L. Reaction rate reconstruction from biomass concentration measurement in bioreactors using modified second-order sliding mode algorithms. *Bioprocess and Biosystems Engineering*, vol. 35(9), pages 1615–1625, 2012a. ISSN 1615-7591.

DE BATTISTA, H., PICÓ, J., GARELLI, F. and VIGNONI, A. Specific growth rate estimation in bioreactors using second-order sliding observers. In *11th International Symposium on Computer Applications in Biotechnology*, vol. 11, pages 251–256. 2010.

DE BATTISTA, H., PICÓ, J., GARELLI, F. and VIGNONI, A. Specific growth rate estimation in (fed-)batch bioreactors using second-order sliding observers. *Journal of Process Control*, vol. 21(7), pages 1049–1055, 2011. ISSN 09591524.

DE BATTISTA, H., PICÓ, J. and PICÓ-MARCO, E. Globally stabilizing control of fed-batch processes with haldane kinetics using growth rate estimation feedback. *Journal of Process Control*, vol. 16, pages 865–875, 2006.

DE BATTISTA, H., PICÓ, J. and PICO-MARCO, E. Nonlinear PI control of fed-batch processes for growth rate regulation. *Journal of Process Control*, vol. 22(4), pages 789–797, 2012b. ISSN 0959-1524.

DOCHAIN, D. State and parameter estimation in chemical and biochemical processes: a tutorial. *Journal of Process Control*, vol. 13(8), pages 801–818, 2003.

DUNN, I., HEINZLE, E., INGHAM, J. and P\VRENOSIL, J. *Biological Reaction Engineering. Dynamic Modelling Fundamentals with Simulation Examples*. Wiley-VCH Verlag, 2003.

EDWARDS, C., FOSSAS, E. and FRIDMAN, L., editors. *Advances in Variable Structure and Sliding Mode Control*. Lecture Notes in Control and Information Sciences. Springer Berlin Heidelberg New York, 2006.

EDWARDS, C. and SPURGEON, S. K. *Sliding Mode Control: Theory and Applications*. Taylor & Francis, UK, 1st edition, 1998.

EFIMOV, D. and FRIDMAN, L. Global sliding-mode observer with adjusted gains for locally Lipschitz systems. *Automatica*, vol. 47(3), pages 565–570, 2011.

EGBERT, R. G. and KLAVINS, E. Fine-tuning gene networks using simple sequence repeats. *Proceedings of the National Academy of Sciences of the United States of America*, 2012. ISSN 1091-6490.

EGLAND, K. A. and GREENBERG, E. P. Conversion of the Vibrio fischeri Transcriptional Activator, {LuxR}, to a Repressor. *Journal of Bacteriology*, vol. 182(3), pages 805–811, 2000. ISSN 0021-9193.

ELOWITZ, M. B. and LEIBLER, S. A synthetic oscillatory network of transcriptional regulators. *Nature*, vol. 403(6767), pages 335–338, 2000. ISSN 0028-0836.

ELOWITZ, M. B., LEVINE, A. J., SIGGIA, E. D. and SWAIN, P. S. Stochastic Gene Expression in a Single Cell. *Science*, vol. 297(5584), pages 1183–1186, 2002.

ESFANDIARI, F. and KHALIL, H. K. Stability analysis of a continuous implementation of variable structure control. *Automatic Control, {IEEE} Transactions on*, vol. 36(5), pages 616–620, 1991.

EVANGELISTA, C., PULESTON, P., VALENCIAGA, F. and FRIDMAN, L. M. Lyapunov-designed super-twisting sliding mode control for wind energy conversion optimization. *Industrial Electronics, IEEE Transactions on*, vol. 60(2), pages 538–545, 2013. ISSN 0278-0046.

FARZA, M., BUSAWON, K. and HAMMOURI, H. Simple Nonlinear Observers for On-line Estimation of Kinetic Rates in Bioreactors. *Automatica*, vol. 34(3), pages 301–318, 1998.

FILIPPOV, A. and ARSCOTT, F. *Differential equations with discontinuous righthand sides*. Springer, 1988. ISBN 902772699X.

FRIDMAN, L. and LEVANT, A. *Sliding Mode control in Engineering*. Control Engineering Series. Marcel Dekker, 2002.

FUQUA, C., PARSEK, M. R. and GREENBERG, E. P. Regulation of gene expression by cell-to-cell communication: acyl-homoserine lactone quorum sensing. *Annual review of genetics*, vol. 35(1), pages 439–468, 2001.

GALZI, D. and SHTESSEL, Y. UAV formations control using high order sliding modes. In *American Control Conference*. IEEE, 2006.

GARCÍA-NIETO, S., BLASCO, X., SANCHÍS, J., HERRERO, J. M., REYNOSO-MEZA, G. and MARTÍNEZ-IRANZO, M. Trackdrone lite. 2012.

GARCÍA-NIETO, S., BLASCO, X., SANCHÍS, J., HERRERO, J. M., REYNOSO-MEZA, G. and MARTÍNEZ-IRANZO, M. TRACKDRONE LITE. 2012.

GARDNER, T. S., CANTOR, C. R. and COLLINS, J. J. Construction of a genetic toggle switch in Escherichia coli. *Nature*, vol. 403(6767), pages 339–342, 2000. ISSN 0028-0836.

GARELLI, F., MANTZ, R. and DE BATTISTA, H. Limiting interactions in decentralized control of {MIMO} systems. *Journal of Process Control*, vol. 16(5), pages 473–483, 2006a.

GARELLI, F., MANTZ, R. and DE BATTISTA, H. Partial decoupling of non-minimum phase processes with bounds on the remaining coupling. *Chemical Engineering Science*, vol. 61, pages 7706–7716, 2006b.

GARELLI, F., MANTZ, R. and DE BATTISTA, H. Sliding mode reference conditioning to preserve decoupling of stable systems. *Chemical Engineering Science*, vol. 62(17), pages 4705–4716, 2007.

GARELLI, F., MANTZ, R. J. and DE BATTISTA, H. *Advanced Control for Constrained Processes and Systems*. The Institution of Engineering and Technology, 2011.

GAUTHIER, J. P., HAMMOURI, H. and OTHMAN, S. A Simple Observer for Nonlinear Systems: Applications to Bioreactors. *IEEE Transactions on Automatic Control*, vol. 37(6), pages 875–880, 1992.

GNOTH, S., JENZSCH, M., SIMUTIS, R. and LÜBBERT, A. Control of cultivation processes for recombinant protein production: a review. *Bioprocess and biosystems engineering*, vol. 31(1), pages 21–39, 2008.

GONZÁLEZ, J., FERNÁNDEZ, G., AGUILAR, R., BARRON, M. and ÁLVAREZ RAM\'IREZ, J. Sliding mode observer-based control for a class of bioreactors. *Chemical Engineering Journal*, vol. 83, pages 25–32, 2001.

GRACIA, L., GARELLI, F. and SALA, A. Integrated sliding-mode algorithms in robot tracking applications. *Robotics and Computer-Integrated Manufacturing*, vol. 29(1), pages 53–62, 2013.

GRACIA, L., SALA, A. and GARELLI, F. A supervisory loop approach to fulfill workspace constraints in redundant robots. *Robotics and Autonomous Systems*, vol. 60(1), pages 1–15, 2012.

GUAY, M. Observer linearization by output-dependent time-scale transformations. *IEEE Trans on Automatic Control*, vol. 47(10), pages 1730–1735, 2002.

GUO, P., ZHANG, J., LYU, M. and BO, Y. Sliding Mode Control for Multi-agent System with Time-Delay and Uncertainties: An LMI Approach. *Mathematical Problems in Engineering*, vol. 2013(Article ID 805492), page 12 pages, 2013.

HANUS, R., KINNAERT, M. and HENROTTE, J. Conditioning technique, a general anti-windup and bumpless transfer method. *Automatica*, vol. 23(6), pages 729–739, 1987.

HE, W. and CAO, J. Consensus control for high-order multi-agent systems. *IET Control Theory and Applications*, vol. 5(1), pages 231–238, 2011.

HERRMANN, G., SPURGEON, S. and EDWARDS, C. A model-based sliding mode control methodology applied to the {HDA}-plant. *Journal of Process Control*, vol. 13(2), pages 129–138, 2003.

HUNG, J., GAO, W. and HUNG, J. C. Variable structure control: a survey. *IEEE Transactions on Industrial Electronics*, vol. 40(1), pages 2–22, 1993.

HUNG, L.-C., LIN, H.-P. and CHUNG, H.-Y. Design of self-tuning fuzzy sliding mode control for {TORA} system. *Expert Systems with Applications*, vol. 32(4), pages 1164–1182, 2007.

IHSSEN, J. and EGLI, T. Specific growth rate and not cell density controls the general stress response in Escherichia coli. *Microbiology*, vol. 150(6), pages 1637–1648, 2004.

JAFARIAN, M. and DE PERSIS, C. Exact formation control with very coarse information. In *American Control Conference (ACC), 2013*, pages 3026–3031. IEEE, 2013.

JENSEN, H. J. *Self-organized criticality: emergent complex behavior in physical and biological systems*, vol. 10. Cambridge university press, 1998.

JENZSCH, M., GNOTH, S., BECK, M., KLEINSCHMIDT, M., SIMUTIS, R. and A. LUBBERT. Open-loop control of the biomass concentration within the growth phase of recombinant protein production processes. *Journal of Biotechnology*, vol. 127(1), pages 84–94, 2006.

JOBÉ, A. M., HERWIG, C., SURZYN, M., WALKER, B., MARISON I. AND-VON STOCKAR, U., MARISON, I. and VON STOCKAR, U. Generally applicable fed-batch culture concept based on the detection ofmetabolic state by on-line balancing. *Biotechnology and Bioengineering*, vol. 82(6), pages 627–639, 2003. ISSN 1097-0290.

KÆ RN, M., ELSTON, T. C., BLAKE, W. J. and COLLINS, J. J. Stochasticity in gene expression: from theories to phenotypes. *Nature Reviews Genetics*, vol. 6(6), pages 451–464, 2005.

KAPLAN, H. B. and GREENBERG, E. P. Diffusion of autoinducer is involved in regulation of the Vibrio fischeri luminescence system. *Journal of Bacteriology*, vol. 163(3), pages 1210–1214, 1985.

KARAKUZU, C., TÜRKER, M. and ÖZTÜRK, S. Modelling, on-line state estimation and fuzzy control of production scale fed-batch baker's yeast fermentation. *Control Engineering Practice*, vol. 14(8), pages 959–974, 2006. ISSN 0967-0661.

KELLERHALS, M. B., KESSLER, B. and WITHOLT, B. Closed-loop control of bacterial high-cell-density fed-batch cultures: Production of mcl-PHAs by Pseudomonas putida KT2442 under single-substrate and cofeeding conditions. *Biotechnology and bioengineering*, vol. 65(3), pages 306–315, 1999.

KHALIL, A. S. and COLLINS, J. J. Synthetic biology: applications come of age. *Nature reviews. Genetics*, vol. 11(5), pages 367–379, 2010. ISSN 1471-0064.

KIVIHARJU, K., SALONEN, K., MOILANEN, U. and EERIKAINEN, T. Biomass measurement online: the performance of in situ measurements and software sensors. *Journal of Industrial Microbiology and Biotechnology*, vol. 35(7), pages 657–665, 2008.

KOBAYASHI, H., KAERN, M., ARAKI, M., CHUNG, K., GARDNER, T. S., CANTOR, C. R. and COLLINS, J. J. Programmable cells: interfacing natural and engineered gene networks. *Proceedings of the National Academy of Sciences of the United States of America*, vol. 101(22), page 8414, 2004.

KÜHNEL, W. *Differential geometry. Curves - surfaces - manifolds*, vol. 16 of *Student mathematical library*. AMS, 2005.

LAI, N. O., EDWARDS, C. and SPURGEON, S. K. An implementation of an output tracking dynamic discrete-time sliding mode controller on an aircraft simulator. In *Proceedings of the 2006 International Workshop on Variable Structure Systems, VSS'06*, pages 35–40. IEEE-CSS, 2006.

LEMESLE, V. and GOUZÉ, J. L. Hybrid bounded error observers for uncertain bioreactor models. *Bioprocess and Biosystem Engineering*, vol. 27, pages 311–318, 2005.

LENCASTRE FERNANDES, R., NIERYCHLO, M., LUNDIN, L., PEDERSEN, A. E., PUENTES TELLEZ, P., DUTTA, A., CARLQUIST, M., BOLIC, A., SCHÄPPER, D., BRUNETTI, A. C. ET AL. Experimental methods and modeling techniques for description of cell population heterogeneity. *Biotechnology advances*, vol. 29(6), pages 575–599, 2011.

LEVANT, A. Sliding order and sliding accuracy in sliding mode control. *International Journal of Control*, vol. 58(6), pages 1247–1263, 1993.

LEVANT, A. Robust exact differentiation via sliding mode technique. *Automatica*, vol. 34(3), pages 379–384, 1998.

LEVANT, A. Universal {SISO} sliding-mode controllers with finite time convergence. *IEEE Transactions on Automatic Control*, vol. 46, pages 1447–1451, 2001.

LEVANT, A. Higher-order sliding modes, differentiation and output-feedback control. *International Journal of Control*, vol. 76(9/10), pages 924–941, 2003.

LEVANT, A. Homogeneity approach to high-order sliding mode design. *Automatica*, vol. 41(5), pages 823–830, 2005.

LIU, L. Robust cooperative output regulation problem for non-linear multi-agent systems. *Control Theory & Applications, IET*, vol. 6(13), pages 2142–2148, 2012.

LÖFBERG, J. YALMIP : A Toolbox for Modeling and Optimization in {MATLAB}. In *Proceedings of the CACSD Conference*. Taipei, Taiwan, 2004.

LÖFBERG, J. Automatic robust convex programming. *Optimization methods and software*, vol. 27(1), pages 115–129, 2012.

MANTZ, R. and DE BATTISTA, H. Sliding mode compensation for windup and direction of control problems in two-input - two-output {PI} controllers. *Industrial Engineering and Chemistry research*, vol. 41, pages 3179–3185, 2002.

MANTZ, R., DE BATTISTA, H. and BIANCHI, F. Sliding mode conditioning for constrained processes. *Industrial Engineering and Chemistry Research*, vol. 43, pages 8251–8256, 2004.

MARECZEK, J., BUSS, M. and SPONG, M. Invariance control for a class of cascade nonlinear systems. *Automatic Control, IEEE Transactions on*, vol. 47(4), pages 636–640, 2002. ISSN 0018-9286.

MARTINEZ-GUERRA, R., GARRIDO, R. and OSORIO-MIRON, A. Parametric and State Estimation by means of high-gain Nonlinear Observers: Application to a Bioreactor. In *Proceedings of the American Control Conference*, vol. 5, pages 3807–3808. 2001.

MCMILLEN, D., KOPELL, N., HASTY, J. and COLLINS, J. J. Synchronizing genetic relaxation oscillators by intercell signaling. *Proceedings of the National Academy of Sciences*, vol. 99(2), page 679, 2002.

MICHEL, A. N. and WANG, K. *Qualitative theory of dynamical systems. The role of stability preserving mappings*, vol. 186 of *Monographs and Textbooks in Pure and Applied Mathematics*. Marcel Dekker, 1995.

MINA, P., DI BERNARDO, M., SAVERY, N. J. and TSANEVA-ATANASOVA, K. Modelling emergence of oscillations in communicating bacteria: a structured approach from one to many cells. *Journal of The Royal Society Interface*, vol. 10(78), 2013.

MORENO, J. and OSORIO, M. A Lyapunov approach to second-order sliding mode controllers and observers. In *Proceedings of the 47th IEEE Conference on Decision and Control*. 2008.

MORENO, J. A. Lyapunov analysis of non homogeneous Super-Twisting algorithms. In *2010 11th International Workshop on Variable Structure Systems VSS*, pages 534–539. IEEE, 2010.

MOYA, P., ORTEGA, R., NETTO, M., PRALY, L. and PICÓ, J. Application of nonlinear time-scaling for robust controller design of reactionsystems. *International Journal of Robust and Nonlinear Control*, vol. 12, pages 57–69, 2002.

NAGUMO, M. Über die lage der integralkurven gewöhnlicher differentialgleichungen. *Proc. Phys.-Math. Soc. Japan (3)*, vol. 24, pages 551–559, 1942.

NAVARRO, J., PICÓ, J., BRUNO, J., PICÓ-MARCO, E. and VALLÉS, S. Online method and equipment for detecting, determining the evolution and quantifying a microbial biomass and other substances that absorb light along the spectrum during the development of biotechnological processes (Patents EP20020751179, and US Patent 6975403). Technical report, 2001a.

NAVARRO, J., PICO, J., BRUNO, J., PICO-MARCO, E. and VALLES, S. Online method and equipment for detecting, determining the evolution and quantifying a microbial biomass and other substances that absorb light along the spectrum during the development of biotechnological processes. {P}atent {ES}20010001757, {EP}20020751179. 2001b.

NUÑEZ, S., DE BATTISTA, H., GARELLI, F., VIGNONI, A. and PICÓ, J. Second-order sliding mode observer for multiple kinetic rates estimation in bioprocesses. *Control Engineering Practice*, vol. 21(9), pages 1259–1265, 2013.

OLFATI-SABER, R., FAX, J. A. and MURRAY, R. M. Consensus and Cooperation in Networked {Multi-Agent} Systems. *Proceedings of the {IEEE}*, vol. 95(1), pages 215–233, 2007.

OLIVIERA, R., SIMUTIS, R. and DE AZEVEDO, S. Design of a stable adaptive controller for driving aerobic fermentationprocesses near maximum oxygen transfer capacity. *Journal of Process Control*, vol. 14, pages 617–626, 2004.

PERRIER, M., DE AZEVEDO, S., FERREIRA, E. and DOCHAIN, D. Tuning of observer-based estimators: theory and application to the on-line estimation of kinetic parameters. *Control Engineering Practice*, vol. 8, pages 377–388, 2000.

PICÓ, J., DE BATTISTA, H. and GARELLI, F. Smooth sliding-mode observers for specific growth rate and substrate from biomass measurement. *Journal of Process Control*, vol. 19(8), pages 1314–1323, 2009a.

PICÓ, J., GARELLI, F., DE BATTISTA, H. and MANTZ, R. Geometric invariance and reference conditioning ideas for control of overflow metabolism. *Journal of Process Control*, vol. 19, pages 1617–1626, 2009b.

PICÓ, J., PICÓ-MARCO, E., VIGNONI, A. and DE BATTISTA, H. Stability preserving maps for finite-time convergence: Super-twisting sliding-mode algorithm. *Automatica*, vol. 49(2), pages 534–539, 2013. ISSN 00051098.

PICO-MARCO, E. and NAVARRO, J. L. A Closed-Loop Exponential Feeding Law for Multi-Substrate Fermentation Processes. In *Proceedings of the 17th World Congress The International Federation of Automatic Control Seoul, Korea, July*, pages 9685–9689. 2008.

PICÓ-MARCO, E., PICÓ, J. and DE BATTISTA, H. Sliding mode scheme for adaptive specific growth rate control in biotechnologicalfed-batch processes. *International Journal of Control*, vol. 78(2), pages 128–141, 2005.

PISANO, A., ORLOV, Y. and USAI, E. Tracking Control of the Uncertain Heat and Wave Equation via Power-Fractional and Sliding-Mode Techniques. *SIAM Journal on Control and Optimization*, vol. 49, page 363, 2011.

PITARCH, J. L., SALA, A. and ARINO, C. V. Closed-Form Estimates of the Domain of Attraction for Nonlinear Systems via Fuzzy-Polynomial Models. *Systems, Man and Cybernetics: Part B, IEEE Transactions on*, 2013.

POLYAKOV, A. and POZNYAK, A. Lyapunov function design for finite-time convergence analysis. *Automatica*, vol. 45(2), pages 444–448, 2009.

PURNICK, P. E. M. and WEISS, R. The second wave of synthetic biology: from modules to systems. *Nature reviews. Molecular cell biology*, vol. 10(6), pages 410–422, 2009. ISSN 1471-0080.

RAHMAN, A. F. N. A., SPURGEON, S. K. and YAN, X.-G. A Sliding Mode Observer for Estimating Substrate Consumption Rate in a Fermentation Process. In *11th International Workshop on Variable Structure Systems*. 2010.

RAO, S. and GHOSE, D. Achieving consensus amongst self-propelling agents by enforcing sliding modes. In *Proceedings of 11th International Workshop on Variable Structure Systems*, pages 404–409. 2010.

RAO, S. and GHOSE, D. Sliding mode control-based algorithms for consensus in connected swarms. *International Journal of Control*, vol. 84(9), pages 1477–1490, 2011.

REN, H. and YUAN, J. Model-based specific growth rate control for Pichia pastoris to improve recombinant protein production. *J Chem Technol Biotechnol*, vol. 80, pages 1268–1272, 2005.

REN, W., BEARD, R. W. and ATKINS, E. M. Information consensus in multivehicle cooperative control. *Control Systems Magazine, {IEEE}*, vol. 27(2), pages 71–82, 2007.

RESPONDEK, W., POGROMSKY, A. and NIJMEIJER, H. Time scaling for observer design with linearizable error dynamics. *Automatica*, vol. 40(2), pages 277–285, 2004.

REVERT, A., GARELLI, F., PICO, J., DE BATTISTA, H., ROSSETTI, P., VEHI, J. and BONDIA, J. Safety Auxiliary Feedback Element for the Artificial Pancreas in Type 1 Diabetes. *Biomedical Engineering, IEEE Transactions on*, vol. 60(8), pages 2113–2122, 2013. ISSN 0018-9294.

SANTIESTEBAN, R., FRIDMAN, L. and MORENO, J. A. Finite-time convergence analysis for Twisting controller via a strict Lyapunov function. In *Variable Structure Systems (VSS), 2010 11th International Workshop on*, pages 1–6. IEEE, 2010.

SCHAEFER, A. L., VAL, D. L., HANZELKA, B. L., CRONAN, J. E. and GREENBERG, E. P. Generation of cell-to-cell signals in quorum sensing: acyl homoserine lactone synthase activity of a purified Vibrio fischeri LuxI protein. *Proceedings of the National Academy of Sciences*, vol. 93(18), pages 9505–9509, 1996.

SHIMIZU, H., TAKAMATSU, T., SHIOYA, S. and SUGA, K.-I. An algorithmic approach to constructing the on-line estimation system for the specific growth rate. *Biotechnology and Bioengineering*, vol. 33(3), pages 354–364, 1989. ISSN 1097-0290.

SHTESSEL, Y. B., MORENO, J. A., PLESTAN, F., FRIDMAN, L. M. and POZNYAK, A. S. Super-twisting adaptive sliding mode control: A {L}yapunov design. In *Decision and Control (CDC), 2010 49th IEEE Conference on*, pages 5109–5113. 2010. ISSN 0743-1546.

SIRA-RAMÍREZ, H. Differential geometric methods in variable structure systems. *International Journal of Control*, vol. 48(4), pages 1359–1390, 1988.

SIRA-RAMÍREZ, H. Sliding regimes in general non-linear systems: a relative degree approach. *International Journal of Control*, vol. 50, pages 1487–1506, 1989.

SLOTINE, J. J. and LI, W. *Applied Nonlinear Control*. Prentice-Hall, New Jersey, 1st edition, 1991.

SMETS, I., BASTIN, G. and VAN IMPE, J. Feedback stabilization of fed-batch bioreactors: non-monotonic growth kinetics. *Biotechnology Progress*, vol. 18, pages 1116–1125, 2002.

SMETS, I., CLAES, J., NOVEMBER, E., BASTIN, G. and VAN IMPE, J. Optimal adaptive control of (bio)chemical reactors: past, present and future. *Journal of Process Control*, vol. 14, pages 795–805, 2004.

SMITH, C., SONG, H. and YOU, L. Signal discrimination by differential regulation of protein stability in quorum sensing. *Journal of molecular biology*, vol. 382(5), page 1290, 2008.

SONTAG, E. D. Some new directions in control theory inspired by systems biology. *Systems biology*, vol. 1(1), pages 9–18, 2004.

SOONS, Z., VOOGT, J. A., VAN STRATEN, G. and VAN BOXTEL, A. J. B. Constant specific growth rate in fed-batch cultivation of bordetella pertussis using adaptive control. *Journal of Biotechnology*, vol. 125(2), pages 252–268, 2006. ISSN 0168-1656.

SWAIN, P. S., ELOWITZ, M. B. and SIGGIA, E. D. Intrinsic and extrinsic contributions to stochasticity in gene expression. *Proceedings of the National Academy of Sciences of the United States of America*, vol. 99(20), pages 12795–12800, 2002. ISSN 0027-8424.

TANNER, H. G., JADBABAIE, A. and PAPPAS, G. J. Flocking in fixed and switching networks. *IEEE Transactions on Automatic Control*, vol. 52(5), pages 863–868, 2007. ISSN 0018-9286.

UTKIN, V. and LEE, H. Chattering problem in sliding mode control systems. In *Proceedings of the 2006 International Workshop on Variable Structure Systems, VSS'06*, pages 346–350. IEEE-CSS, 2006.

UTKIN, V. Y. Variable structure systems with sliding modes. *IEEE Transactions on Automatic Control*, vol. 22(2), pages 212–222, 1977.

UTKIN, V. Y. About second order sliding mode control, relative degree, finite-time convergence and disturbance rejection. In *Variable Structure Systems (VSS), 2010 11th International Workshop on*, pages 528–533. IEEE, 2010.

UTKIN, V. Y., GULDNER, J. and SHI, J. *Sliding Mode Control in Electromechanical Systems*. Taylor & Francis, London, 1st edition, 1999.

VALENTINOTTI, S., SRINIVASAN, B., HOLMBERG, U., BONVIN, D., CANNIZZARO, C., RHIEL, M. and VON STOCKAR, U. Optimal operation of fedbatch fermentations via adaptive control of overflow metabolite. *Control Engineering Practice*, vol. 11, pages 665–674, 2003.

VENKATESWARLU, C. Advances in monitoring and state estimation of bioreactors. *Journal of Scientific & Industrial Research*, vol. 63, pages 491–498, 2004.

VIGNONI, A. *Coordination in dynamical systems: a sliding mode reference conditioning approach.*. Master thesis, Universitat Politècnica de València, http://personales.upv.es/alvig2/MT/vignoni-mthesis.pdf, 2011.

VIGNONI, A., GARELLI, F., GARCÍA-NIETO, S. and PICÓ, J. UAV reference conditioning for formation control via set invariance and sliding modes. In *3rd IFAC Workshop on Distributed Estimation and Control in Networked Systems*, pages 317–322. Santa Barbara, CA, USA, 2012a.

VIGNONI, A., GARELLI, F. and PICÓ, J. Coordinación de sistemas con diferentes dinámicas utilizando conceptos de invarianza geométrica y modos deslizantes. *Revista Iberoamericana de Automática e Informática Industral (RIAI)*, vol. 10(4), pages 390–401, 2013a.

VIGNONI, A., GARELLI, F. and PICÓ, J. Sliding Mode Reference Coordination of constrained feedback systems. *Mathematical Problems in Engineering*, vol. 2013(Article ID 764348), page 12 pages, 2013b.

VIGNONI, A., NUÑEZ, S., DE BATTISTA, H., PICÓ, J., PICÓ-MARCO, E. and GARELLI, F. Specific Kinetic Rates Regulation in Multi-Substrate Fermentation Processes. In *12th International Symposium on Computer Applications in Biotechnology*, in press. 2013c.

VIGNONI, A., OYARZÚN, D. A., PICÓ, J. and STAN, G.-B. Control of protein concentrations in heterogeneous cell populations. In *2013 European Control Conference (ECC)*, pages 3633–3639. 2013d.

VIGNONI, A., OYARZÚN, D. A., PICÓ, J. and STAN, G.-B. Control of protein concentrations in heterogeneous cell populations. (in revision), 2014.

VIGNONI, A., PICÓ, J., GARELLI, F. and DE BATTISTA, H. Sliding mode reference conditioning for coordination in swarms of non-identical multi-agent systems. In *Variable Structure Systems, 12th IEEE International Workshop on*, pages 231–236. Mumbai, India, 2012b. ISBN 9781457720673.

VIGNONI, A., PICÓ, J., GARELLI, F. and DE BATTISTA, H. Dynamical systems coordination via sliding mode reference conditioning. In *Proceedings of the 18th IFAC . . .* , vol. 18 of *1*, pages 11086–11091. 2011.

VOJINOVIC, V., CABRAL, J. M. S. and FONSECA, L. P. Real-time bioprocess monitoring: Part {I}: In situ sensors. *Sensors and Actuators B: Chemical*, vol. 114(2), pages 1083–1091, 2006. ISSN 0925-4005.

ŠABANOVIC, A. Variable Structure Systems With Sliding Modes in Motion Control - A Survey. *Industrial Informatics, IEEE Transactions on*, vol. 7(2), pages 212–223, 2011. ISSN 1551-3203.

WALGAMA, K., RÖNNBÄCK, S. and STERNBY, J. Generalization of conditioning technique for anti-windup compensators. *IEE Proceedings on Control Theory and Applications*, vol. 139(2), pages 109–118, 1992.

WEBER, M., BUCETA, J. and OTHERS. Dynamics of the quorum sensing switch: stochastic and non-stationary effects. *BMC systems biology*, vol. 7(1), page 6, 2013.

WU, L., SU, X. and SHI, P. Sliding mode control with bounded L2 gain performance of Markovian jump singular time-delay systems. *Automatica*, vol. 48(8), pages 1929–1933, 2012.

XU, J., GUO, B., ZHANG, Z., WU, Q., ZHOU, Q., CHEN, J., CHEN, G. and LI, G. A mathematical model for regulating monomer composition of the microbially synthesized polyhydroxyalkanoate copolymers. *Biotechnology and bioengineering*, vol. 90(7), pages 821–829, 2005.

YOUNG, K. D., UTKIN, V. Y. and OZGÜNER, U. A control engineer's guide to sliding mode control. *IEEE Transactions on Control Systems Technology*, vol. 7(3), pages 328–342, 1999.

ZAMBONI, N., FENDT, S. M., RUHL, M. and SAUER, U. 13C-based metabolic flux analysis. *Nature Protocols*, vol. 4, pages 878–892, 2009.

ZECHNER, C., RUESS, J., KRENN, P., PELET, S., PETER, M., LYGEROS, J. and KOEPPL, H. Moment-Based Inference Predicts Bimodality in Transient Gene Expression. *PNAS*, vol. 109(21), pages 8340–8345, 2012.

ZINN, M., WITHOLT, B. and EGLI, T. Dual nutrient limited growth: models, experimental observations, and applications. *Journal of biotechnology*, vol. 113(1), pages 263–279, 2004.

Appendices

Appendix A

Proofs

A.1 Global topology analysis

Consider the case of having $N = 2$, two individual systems, for the sake of clarity. The state space representation of the closed loop system (when the reference conditioning loop is active) is:

$$\dot{\mathbf{x}} = f(x) + g(x)w_g + h(x) + \mathbf{p} \tag{A.1}$$

with

$$x = \begin{bmatrix} r_{f1} \\ r_{f2} \\ r \end{bmatrix}, \qquad f(x) = \begin{bmatrix} -\alpha_1(r_{f1} - r) \\ -\alpha_2(r_{f2} - r) \\ -\lambda r \end{bmatrix} \tag{A.2}$$

and

$$g(x) = \begin{bmatrix} 0 \\ 0 \\ -\lambda \end{bmatrix}, \; h(x) = \begin{bmatrix} -\alpha_1 w_1 \\ -\alpha_2 w_2 \\ 0 \end{bmatrix}, \; \mathbf{p} = \begin{bmatrix} 0 \\ 0 \\ \lambda c_g \end{bmatrix} \tag{A.3}$$

where f is the drift vector field, g is the control vector field, $\mathbf{p}$ acts as a perturbation and h comprises the discontinuous actions of the internal conditioning loops, which are not considered as perturbations because these two signals are responsible for the difference between r and r_{fi}. Calculating the gradient of the constraint ϕ_χ we get:

$$\frac{\partial \phi_\chi}{\partial x} = \begin{bmatrix} -\dfrac{\partial \chi}{\partial r_{f1}} & -\dfrac{\partial \chi}{\partial r_{f2}} & 1 \end{bmatrix}. \tag{A.4}$$

Note the difference between ϕ_χ^+ and ϕ_χ^- in not reflected in their gradients, thus $\frac{\partial \phi_\chi}{\partial x}$ will be used to refer either ϕ_χ^+'s gradient or ϕ_χ^-'s gradient.

The Lie derivatine of ϕ_χ in the direction of f is

$$L_f\phi_\chi = \frac{\partial\chi}{\partial r_{f1}}\alpha_1\left(r_{f1}-r\right) + \frac{\partial\chi}{\partial r_{f2}}\alpha_2\left(r_{f2}-r\right) - \lambda r \tag{A.5}$$

and in the direction of g is

$$L_g\phi_\chi = -\lambda \tag{A.6}$$

Then to ensure the invariance of the set Φ_χ, the explicit invariance condition (A.28) must hold. Being the filter F_g stable, then $\lambda > 0$ and

$$L_g\phi_\chi = -\lambda < 0. \tag{A.7}$$

Which to ensure (A.28),

$$w_g^{\phi_\chi} = \frac{\alpha_1}{\lambda}\frac{\partial\chi}{\partial r_{f1}}r_{f1} + \frac{\alpha_2}{\lambda}\frac{\partial\chi}{\partial r_{f2}}r_{f2} - \left(\frac{\alpha_1}{\lambda}\frac{\partial\chi}{\partial r_{f1}} + \frac{\alpha_2}{\lambda}\frac{\partial\chi}{\partial r_{f2}} + 1\right)r \tag{A.8}$$

Consider a fixed constant $\left|w_g^+\right|, \left|w_g^-\right| < \infty$, and $w_g^\star > 0$.If F_g is a filter BIBO stable with bounded input $|w_g| \leq \max\left\{\left|w_g^+\right|, \left|w_g^-\right|\right\} = w_g^\star$ and c_g (assuming a bounded global target), note that $|r| < K_r$. Since the filters F_i also have bounded inputs (r and w_i), then $|r_{fi}| < K_{r_{fi}}$.

Also the bound on $\left\|\frac{\partial\chi}{\partial r_{fi}}\right\| < K_{\chi_i}$ is necessary, but only depends in the selection of function χ.

Then, $\exists\ w_g^{\sigma_\chi}$ such as

$$\left|w_g^{\phi_\chi}\right| \leq \frac{1}{\lambda}\left[\sum_{i=1}^{N}\left(K_{r_i}K_{\chi_i}\right) + K_r\right] \leq K \leq w_g^\star \tag{A.9}$$

and is possible to choose $w_g^- \leq -w_g^\star$ and $w_g^+ \geq w_g^\star$ from the previous inequality to ensure the invariance of the set Φ_χ.

A.2 Local topology analysis

The extended dynamics of the system will be analyzed in order to design the SMRC parameters of the local topology. Assuming the systems start from inside the invariant set, *i.e.* all constraints are met, their trajectories evolve up so they reach the boundary, then the corresponding

constraint activates forcing the system to slide on the boundary surface until the system by itself comes back inside the invariant set. This analysis is done with the i-th systems, considering information coming from the j-th one.

For the analysis, let us first rewrite the i-th system controller and filter dynamics as follows. From equations (3.13) and (3.14), and using $e_i = d_{ci}^{-1}\left(v_i - c_{ci}x_{ci}\right)$, it follows:

$$\dot{x}_{ci} = \left(A_{ci} - b_{ci}d_{ci}^{-1}c_{ci}\right)x_{ci} + b_{ci}d_{ci}^{-1}v_i \tag{A.10}$$

$$\begin{aligned}\dot{v}_i = {} & c_{ci}\left(A_{ci} - b_{ci}d_{ci}^{-1}c_{ci} - \alpha_i\right)x_{ci} + \left(c_{ci}b_{ci}d_{ci}^{-1} - \alpha_i\right)v_i \\ & - d_{ci}\alpha_i\tilde{w}_i + d_{ci}\alpha_i(r + y_i) - d_{ci}\dot{y}_i\end{aligned} \tag{A.11}$$

Therefore, consider the extended state

$$x_{ie} \stackrel{\triangle}{=} [x_i, x_{ci}, v_i]^T \in \mathbb{R}^{n+n_c+1}.$$

The joint dynamics are given in equation (A.12).

$$\dot{x}_{ie} = \begin{bmatrix} f_i(x_i) + g_i(x_i)v_i \\ \left(c_{ci}\bar{b}_{ci} + \alpha_i\right)v_i + c_{ci}\left(\bar{A}_{ci} - \alpha_i\right)x_{ci} \\ \bar{b}_{ci}v_i + \bar{A}_{ci}x_{ci} + b_i\rho_i \end{bmatrix} + \begin{bmatrix} 0 \\ 0 \\ b_i \end{bmatrix}\tilde{w}_i \tag{A.12}$$

with

$$\begin{aligned}\bar{A}_{ci} &= \left(A_{ci} - b_{ci}d_{ci}^{-1}c_{ci}\right) \\ \bar{b}_{ci} &= b_{ci}d_{ci}^{-1} \\ b_i &= -d_{ci}\alpha \\ \rho_i &= b_i^{-1}\left[d_{ci}\alpha_i(r - y_i) - d_{ci}\dot{y}_i\right]\end{aligned} \tag{A.13}$$

To make the invariance condition (A.28) hold for constraint ϕ_i^+ we have from (3.18)

$$\frac{\partial\phi_i^{\pm}}{\partial x_{ie}} = [0 \quad 0 \quad 1] \tag{A.14}$$

and

$$w_i^{\phi_i} = -\frac{\bar{b}_{ci}v_{ip}^{\pm} + \bar{A}_{ci}x_{ci}}{b_i} - \rho_i. \tag{A.15}$$

Now for the virtual constraints, let us first incorporate the j-th systems and rewrite in a more convenient way the previous joint dynamics, using

$$v_i = c_{ci}x_{ci} + d_{ci}e_i = c_{ci}x_{ci} + d_{ci}r_{fi} - d_{ci}y_i,$$

and considering the extended state

$$x_{ije} \triangleq [x_i, x_{ci}, r_{fi}, x_j, x_{cj}, r_{fj}]^T \in \mathbb{R}^{n_i+n_{ci}+1+n_j+n_{cj}+1}.$$

$$\dot{x}_{ije} = \begin{bmatrix} f_i(x_i) + g_i(x_i)\left(c_{ci}x_{ci} + d_{ci}r_{fi}\right) - g_i(x_i)d_{ci}y_i \\ A_{ci}x_{ci} + b_{ci}r_{fi} - b_{ci}y_i \\ -\alpha_i r_{fi} + \alpha_i r \\ f_j(x_j) + g_j(x_j)\left(c_{cj}x_{cj} + d_{cj}r_{fj}\right) - g_j(x_j)d_{cj}y_j \\ A_{cj}x_{cj} + b_{cj}r_{fj} - b_{cj}y_j \\ -\alpha_j r_{fj} + \alpha_j r \end{bmatrix} + \begin{bmatrix} 0 \\ 0 \\ -\alpha_i \\ 0 \\ 0 \\ \alpha_j \end{bmatrix} w_{ij} \tag{A.16}$$

Remark A.1. In this case, in order to express the extended joint dynamics with respect to only one discontinuous action, the fact that $w_{ij} = -w_{ji}$ has been used.

And to make the invariance condition (A.28) hold for constraint ϕ_{ij} we have from (3.19)

$$\frac{\partial \phi_{ij}}{\partial x_{ije}} = [0 \quad 0 \quad \text{sign}(r_{fi} - r_{fj}) \quad 0 \quad 0 \quad - \text{ sign}(r_{fi} - r_{fj})], \tag{A.17}$$

and

$$w_i^{\phi_{ij}} = -\frac{\alpha_i r_{fi} - \alpha_j r_{fj}}{\alpha_i + \alpha_j} - \frac{\alpha_i - \alpha_j}{\alpha_i + \alpha_j} r \tag{A.18}$$

Then the discontinuous signals amplitudes M_i and M_{ij} are designed using the previous analysis.

In first place, the reason why w_{ij} is selected as in (3.17) is because $L_g\phi_{ij} = \text{ sign}(r_{fi} - r_{fj})(\alpha_i + \alpha_j)$ changes its sign depending on $r_{fi} - r_{fj}$. Then to meet (A.28), w_{ij} has also to change its sign in the same way. Then, M_{ij} can be selected to make (A.28) hold

$$M_{ij} > w_i^{\phi_{ij}} \tag{A.19}$$

In second place, M_i has to be selected according with the usual procedure Garelli et al. (2011) according with (A.28), but large enough to dominate the rest of the discontinuous terms M_{ij}, as the systems constraints are required to hold everywhere, because they are more important than the virtual coordination ones. The previous statement allows us to give the systems a feasible reference that can be followed without violating their constraints.

In the worst case, $(r_{fi} - r_{fj})$ has the same sign $\forall\ i \neq j$, and at the same time opposite sign than w_i, then

$$M_i > \sum_{i \neq j} M_{ij} + w_i^{\phi} \tag{A.20}$$

with w_i^{ϕ} from (A.15).

A.3 Minimum χ function generalized gradient

Now lets consider the minimum of the conditioned references as χ function,

$$\chi(r_{fi}) = r_{f\min} = \min\{r_{fi}\ : i \in \{1, \ldots, N\}\}. \tag{A.21}$$

Remember the r_{fi} is the solution of equation (3.8). This equation is a linear differential equation with discontinuous right hand side (w_i) and cannot be analyzed in terms of continuity and differentiability using the traditional tools. Instead, equation (3.8) can be reformulated in terms of a differential inclusion in the form

$$\begin{aligned} \dot{r}_{fi} &= f\,(x, w_i) \\ \dot{r}_{fi} &\in G[f](x) \end{aligned} \tag{A.22}$$

using the state vector

$$x = \begin{bmatrix} r_{fi} \\ r \end{bmatrix} \tag{A.23}$$

where $f : \mathbb{R}^2 \times \mathcal{W} \longrightarrow \mathbb{R}$, $\mathcal{W} = \left\{w_i^-, w_i^+\right\} \subseteq \mathbb{R}$ is the set of allowable control values and with $G[f](x)$ being the following set-valued map

$$G[f](x) \stackrel{\triangle}{=} \{f(x, w_i)\ : w_i \in \mathcal{W}\} \tag{A.24}$$

which captures all directions in $\mathbb{R}$ that can be generated at x with control belonging to $\mathcal{W}$.

We know that a set-valued map $G[f](x)$ is locally Lipschitz if $f(x, w_i)$ is locally Lipschitz (Filippov and Arscott, 1988, see), and the differential inclusion (A.22) will have solution in the sense of Filippov and its solution will be also locally Lipschitz (Bacciotti and Rosier, 2005, see Theorem 1.5).

Then from Rademacher's theorem (Clarke, 1990) every locally Lipschitz function f is differentiable almost everywhere in the sense of

Lebesge measure. Moreover, the function will have a *generalized gradient* ∂f in the set of points where f is not differentiable, with similar properties of critical points and descent direction than the *normal* gradient.

Then from Cortes (2008, Proposition 7.), being the r_{fi} functions locally Lipschitz, the following statements hold for $r_{f\min}$.

- i) $r_{f\min}$ is locally Lipschitz,
- ii) Let I_{min} denote the set of indices i for which $r_{fi} = r_{f\min}$. Then

$$\partial r_{f\min} \subseteq \text{co} \bigcup \{\partial r_{fi} \ : i \in I_{min}\}. \tag{A.25}$$

And as the convex hull of bounded functions is bounded, the gradient of χ is bounded, which ensures the invariant set $\mathcal{S}_{inv}$ existence, according to (A.9). As far as the necessary bounds on any selected χ function holds, is possible to generate coordination with that policy.

A.4 Proof of Theorem 9.1

Proof. The proof will be sketched in four steps, two for the set $\underline{\Phi}$ (9.18) and another two for the set $\overline{\Phi}$ (9.19). First we will use $z_1 = u^\star$ as a virtual control action in the second equation of system (9.15). This will allow us to find the set $\underline{\mathcal{S}}$ of all z_1 that make $\underline{\Phi}$ an invariant set for z_2. In the second design step, we will find the set of all $u(z_2)$ that make $\underline{\mathcal{S}}$ invariant for z_1.For the remaining two steps we proceed in a similar way to make $\overline{\mathcal{S}}$ and $\overline{\Phi}$ invariant sets for z_1 and z_2 respectively.

First consider

$$\begin{cases} \dot{z}_2 = \kappa_2 u^\star - (d+\gamma_2) z_2 + z_{\text{e}} \\ \underline{\phi}(z_2) = -z_2 + \underline{z}_2 \end{cases} \tag{A.26}$$

And now the goal is to find $u^\star$ in order to make set $\underline{\Phi}$ invariant.

$$\underline{\Phi} = \left\{ z_2 \in \mathbb{R}^+ : \underline{\phi}(z_2) < 0 \right\} \tag{A.27}$$

This is equivalent to find bounds on $u^\star$ to make the vector field point inside $\underline{\Phi}$, when z_2 reaches the boundary of the set $\underline{\Phi}$.

Consider the z_2-system (A.26). Using $f(z_2, z_{\text{e}}) = -(d+\gamma_2) z_2 + z_{\text{e}}$ and $g(z_2) = \kappa_2$ it is possible to rewrite $\dot{z}_2 = f(z_2, z_{\text{e}}) + g(z_2) u^\star$. In order

to find the lower bound $u^\star$, we need to find the direction of the vector field with respect to the boundary of the set $\underline{\Phi}$. To obtain the control signal that makes $\underline{\Phi}$ invariant, we apply the explicit invariance condition **?**:

$$u \begin{cases} \leq u^\phi & : z \in \partial\Phi \wedge L_g\phi > 0 \\ \geq u^\phi & : z \in \partial\Phi \wedge L_g\phi < 0 \\ \text{not defined} & : z \in \partial\Phi \wedge L_g\phi = 0 \\ \text{free} & : z \in \Phi \setminus \partial\Phi \end{cases} \tag{A.28}$$

Here $L_f\phi$ accounts for the Lie derivative of ϕ along the direction of the vector field f, and $u^\phi = -\frac{L_f\phi}{L_g\phi}$.

In our case, we get

$$u^{\star\underline{\phi}} = -\frac{(d+\gamma_2)\, z_2 - z_{\mathrm{e}}}{-\kappa_2} \tag{A.29}$$

and hence $\underline{z}_2$ is an upper bound of z_2. For the perturbation term z_e, we will use its lower bound $\underline{z}_{\mathrm{e}}$, as it is an anti-cooperative term with respect to z_2. We obtain the following lower bound for $u^\star$, that we will call $u^\star_{min}$:

$$u^\star_{min} = \frac{d + \gamma_2 \underline{z}_2 - \underline{z}_{\mathrm{e}}}{\kappa_2} \tag{A.30}$$

Then, if the following holds

$$u^\star > u^\star_{min}, \quad \forall z_2 \notin \underline{\Phi}. \tag{A.31}$$

the trajectory of z_2 is forced to remain inside $\underline{\Phi}$.

Secondly, we proceed with the first equation of system (9.15). Remembering that $u^\star = z_1$, we have

$$\begin{cases} \dot{z}_1 = -\gamma_1 z_1 + u(z_2) \\ \underline{\sigma}(z_1) = -z_1 + u^\star_{min} \end{cases} \tag{A.32}$$

Define the set $\underline{\mathcal{S}}$ as:

$$\underline{\mathcal{S}} = \left\{ z_1 \in \mathbb{R}^+ : \underline{\sigma}(z_1) < 0 \right\} \tag{A.33}$$

when $z_2 \notin \underline{\Phi}$. The goal now is to find a bound on $u(z_2)$ so as to make the set $\underline{\mathcal{S}}$ invariant.

Using the same methodology and the explicit invariant condition, we get

$$u^{\underline{\sigma}} = \gamma_1 z_1. \tag{A.34}$$

To bound z_1 we use the fact that the application of the control signal (A.34) is only required when $\underline{\sigma} > 0$. Hence $u^{\star}_{min}$ is an upper bound of z_1. This allows us to obtain the bound u_{min} for u:

$$u_{min} = \gamma_1 u^{\star}_{min} = \gamma_1 \frac{(d+\gamma_2)\,\underline{z}_2 - \underline{z}_{\mathrm{e}}}{\kappa_2} \tag{A.35}$$

Then the set $\underline{\Phi}$ is an invariant and attractive set for z_2 if

$$u(z_2) > \gamma_1 \frac{(d+\gamma_2)\,\underline{z}_2 - \underline{z}_{\mathrm{e}}}{\kappa_2} \quad \forall z_2 \notin \underline{\Phi} \tag{A.36}$$

Equivalent steps can be applied with the set $\overline{\Phi}$ to obtain:

$$u(z_2) < \gamma_1 \frac{(d+\gamma_2)\,\overline{z}_2 - \overline{z}_{\mathrm{e}}}{\kappa_2} \quad \forall z_2 \notin \overline{\Phi}. \tag{A.37}$$

Now, using $u(z_2) = \kappa_0$ when $z_2 \notin \overline{\Phi}$, and $u(z_2) = \kappa_0 + \kappa_1$ when $z_2 \notin \underline{\Phi}$, we get that the following inequalities

$$\kappa_0 + \kappa_1 > \gamma_1 \frac{(d+\gamma_2)\,\underline{z}_2 - \underline{z}_{\mathrm{e}}}{\kappa_2} \tag{A.38}$$

and

$$\kappa_0 < \gamma_1 \frac{(d+\gamma_2)\,\overline{z}_2 - \overline{z}_{\mathrm{e}}}{\kappa_2} \tag{A.39}$$

must hold to make Φ an invariant set. □

A.5 Proof of Theorem 9.2

Proof. Consider the system in (9.2), (9.3) and (9.5) with the approximation in (9.8) under the conditions of Theorem 9.1, then all cells in the population operate in the linear region Φ. From (9.25) we have

$$\gamma_1 \bar{x}_1 + S\bar{x}_2 = \kappa_0 + (ST + R)\,1_N \tag{A.40}$$

and

$$\bar{x}_1 = \left[\left(d\,(1-\epsilon) - \gamma_2\right)\mathbf{I_N} + d\epsilon\Pi_N\right]\frac{\bar{x}_2}{\kappa_2}. \tag{A.41}$$

Replacing (A.41) in (A.40), we obtain

$$\left[\left(S+\frac{\left[d\left(1-\epsilon\right)+\gamma_2\right]\gamma_1}{\kappa_2}\right)\mathbf{I_N}+d\epsilon\Pi_N\right]\bar{x}_2=\kappa_0+\left(ST+R\right)1_N. \quad \text{(A.42)}$$

Exploiting the structure of the matrix in (A.42) we obtain a closed-form expression for $\bar{x}_2$ (details omitted for brevity):

$$\bar{x}_2=\left[\frac{1}{\alpha}\mathbf{I_N}+\left(\frac{1}{\alpha-\epsilon d}-\frac{1}{\alpha}\right)\Pi_N\right]\left(\kappa_0+\left(ST+R\right)1_N\right), \quad \text{(A.43)}$$

where $\beta=\frac{[d(1-\epsilon)+\gamma_2]\gamma_1}{\kappa_2}$ and $\alpha=S+\beta$.

If $\kappa^0\sim\mathcal{N}\left(\mu,\sigma^2\right)$, the expected value of $\bar{x}_2$ along the population can be computed using properties of the Π_{N} matrix:

$$\mathrm{E}\left\{\bar{x}_2\right\}=\frac{1}{S+\beta}\left(\mu+ST+R\right)1_N \quad \text{(A.44)}$$

A closed-form expression for the variance of x_2 can be obtained similarly

$$\mathrm{Var}\{\bar{x}_2\}=\left[\frac{1}{\alpha^2}\mathbf{I}_{\mathrm{N}}+\left(\frac{1}{\left(\alpha-\epsilon d\right)^2}-\frac{1}{\alpha^2}\right)\Pi_{\mathrm{N}}\right]\sigma^2\mathbf{I}_{\mathrm{N}}. \quad \text{(A.45)}$$

The expressions in (9.26)–(9.27) can be finally obtained directly from (A.44)–(A.45). □

Appendix B

Generalized Super-Twisting Algorithm background and motivation

B.1 Motivation for alternative stability proof for GSTA

B.1.1 Super-twisting algorithm

Consider the first order system (B.1):

$$\dot{y}_1 = u(t) + \rho_1(y,t) \tag{B.1}$$

where $u(t)$ is the unknown input signal, and $\rho_1(y,t)$ is an input perturbation term –e.g. representing some unmodelled dynamics. In particular, if $\rho_1(y,t) \equiv 0$ we have a pure integrator. The super-twisting exact differentiation algorithm proposed in Levant (1998) allows to build a second order sliding mode observer for the unknown input signal $u(t)$ using measurements of the system output y_1.

Redefine $y_2 \stackrel{\triangle}{=} u$, and define the error signals $x_i = y_i - \hat{y}_i$, $i = 1, 2$, where $\hat{y}_i$ is the estimation of y_i. The super-twisting-based observer is given by (B.2).

$$\begin{aligned} \dot{\hat{y}}_1 &= \hat{y}_2 + k_1 \left|x_1\right|^{\frac{1}{2}} \operatorname{sign}(x_1) \\ \dot{\hat{y}}_2 &= k_3 \operatorname{sign}(x_1) \end{aligned} \tag{B.2}$$

Notice that two high gain terms are injected. The one acting on the second state is discontinuous, while the one acting on the first state is continuous. This term can be interpreted as a continuous approximation of the discontinuous sign function in a neighborhood of the origin.

From equations (B.1) and (B.2) the following error dynamics are obtained:

$$\begin{aligned} \dot{x}_1 &= x_2 - k_1 \left|x_1\right|^{\frac{1}{2}} \ \mathrm{sign}(x_1) + \rho_1(x,t) \\ \dot{x}_2 &= -k_3 \ \mathrm{sign}(x_1) + \rho_2(x,t) \end{aligned} \tag{B.3}$$

where $\rho_2(x,t) \stackrel{\triangle}{=} \dot{u}(t)$. Equation (B.3) actually defines the super-twisting algorithm. Notice that, being x_1 the output, the discontinuity appears in its second derivative.

B.1.2 Preliminary analysis of the super-twisting algorithm.

Consider the change of coordinates:

$$(z_1, z_2) \longrightarrow \left(\left|x_1\right|^{\frac{1}{2}} \ \mathrm{sign}(x_1), x_2 \right) \tag{B.4}$$

Notice that $\frac{\partial z_1}{\partial x_1} = \frac{1}{2}|x_1|^{-\frac{1}{2}}$ is discontinuous at the origin. Therefore, the transformation (B.4) is a homeomorphism buy not a diffeomorphism. In the new coordinates, equation (B.3) becomes:

$$\dot{z} = \frac{1}{|z_1|} \begin{bmatrix} -\frac{k_1}{2} & \frac{1}{2} \\ -k_3 & 0 \end{bmatrix} z + \begin{bmatrix} \frac{1}{|z_1|} \frac{1}{2} \rho_1(z,t) \\ \rho_2(z,t) \end{bmatrix} \tag{B.5}$$

Now, define the time-scale transformation:

$$t = \int |z_1| d\tau \tag{B.6}$$

and $z' \stackrel{\triangle}{=} \frac{dz}{d\tau} = |z_1| \dot{z}$. Then equation (B.5) can be expressed in the new time-scale as:

$$z' = \begin{bmatrix} -\frac{k_1}{2} & \frac{1}{2} \\ -k_3 & 0 \end{bmatrix} z + \begin{bmatrix} \frac{1}{2} \rho_1(z,\tau) \\ \rho_2(z,\tau)|z_1| \end{bmatrix} \tag{B.7}$$

If the perturbation signals have structure $\rho_1(z,\tau) = \rho_1(\tau)|z_1|$, and $\rho_2(z,\tau) = \rho_2(\tau)$, equation (B.7) can be expressed as the linear time-

varying system:

$$\begin{aligned} z' &= \begin{bmatrix} -\frac{k_1}{2} & \frac{1}{2} \\ -k_3 & 0 \end{bmatrix} z + \begin{bmatrix} \frac{1}{2}\rho_1(\tau)|z_1| \\ \rho_2(\tau)|z_1| \end{bmatrix} \\ &= \begin{bmatrix} -\frac{k_1-\tilde{\rho}_1(\tau)}{2} & \frac{1}{2} \\ -\left(k_3-\tilde{\rho}_2(\tau)\right) & 0 \end{bmatrix} z \end{aligned} \tag{B.8}$$

with $\tilde{\rho}_i = \rho_i \operatorname{sign}(z_1)$.

It is interesting to notice that in order to compensate for a perturbation ρ_1 on the x_1 dynamics, one will require the algorithm to have some term to dominate the unknown perturbation. This term can be understood as an upper bounding function for the perturbation. Therefore, the structure of the least upper bound function on the perturbation will define the order of the sliding mode. For instance, if $\rho_1(x,t) = \rho_1(t)$ with $\|\rho_1(t)\|_\infty = \bar{\rho}_1$, then it is clear that a discontinuous term showing up in the first derivative will be needed. If we require for second order sliding behaviour, the perturbation ρ_1 must be smooth with respect to x_1. In particular, as seen before, the super-twisting algorithm can cope with perturbations $\rho_1(z,\tau) = |z_1|\frac{\rho_1(\tau)}{2}$, that is, $\rho_1(x,t) = \rho_1(t)|x_1|^{\frac{1}{2}}$ in the original coordinates.

A Linear Matrix Inequality based Lyapunov stability analysis of the linear time-varying system (B.8) has been used previously in De Battista et al. (2011) to derive a robust observer providing a finite-time smooth estimate of the time-varying specific growth rate in a class of bioreactions.

In the next sections we refine this methodology. To this end, we will first use a nonlinear coordinates transformation, and a time-scale one, so as to transform the original system into a new one amenable for constructively finding a smooth control Lyapunov function. Stability is determined for the system in the transformed coordinates and time-scaled space. The time-scale is chosen so that convergence faster than asymptotic in the transformed space corresponds to finite-time converge in the original one. To prove the original system is also stable, the technique of stability preserving maps will be used (Michel and Wang, 1995). This will allow us, for instance, to modify the super-twisting error injection terms so as to cope with a broader class of perturbations $\rho_1(x,t)$ and $\rho_2(x,t)$.

B.2 Constructive design of the super-twisting algorithm.

Consider again, as starting point, the problem of estimating the input signal to an integrator from measurements of its output (i.e. the problem of taking derivative of the output signal). Now –see equation (B.9)– the correction terms $u_1(x_1)$ and $u_2(x_1)$ are to be designed.

$$\begin{aligned} \dot{x}_1 &= x_2 + u_1(x_1) + \rho_1(x,t) \\ \dot{x}_2 &= u_2(x_1) + \rho_2(x,t) \end{aligned} \tag{B.9}$$

Consider, on the other hand, the coordinates transformation:

$$(z_1, z_2) \longrightarrow (|x_1|^{\alpha}\ \mathrm{sign}(x_1), x_2) \tag{B.10}$$

being its inverse:

$$(x_1, x_2) \longrightarrow \left(z_1\,|z_1|^{\frac{1-\alpha}{\alpha}}, z_2\right) \tag{B.11}$$

with $0 < \alpha \leq 1$ for the transformation to be a homeomorphism as seen in Section **??**. Using (B.11) and $\dot{z}_1 = \alpha\,|z_1|^{\frac{\alpha-1}{\alpha}}\,\dot{x}_1$, we get:

$$\begin{aligned} \dot{z}_1 &= \alpha\,|z_1|^{\frac{\alpha-1}{\alpha}}\,z_2 + \alpha\,|z_1|^{\frac{\alpha-1}{\alpha}}\,u_1(z_1) + \alpha\,|z_1|^{\frac{\alpha-1}{\alpha}}\,\rho_1(z,t) \\ \dot{z}_2 &= u_2(z_1) + \rho_2(z,t) \end{aligned} \tag{B.12}$$

Now apply the time-scaling

$$t = \int |z_1|^{\frac{1-\alpha}{\alpha}}\,d\tau \tag{B.13}$$

and assume the perturbation term $\rho_1(z,\tau)$ has structure given by:

$$\rho_1(z,\tau) = \rho_1(\tau)|z_1|r(z_1) \tag{B.14}$$

with $r(z_1) = \mathcal{O}(1)$ as $z_1 \to 0$, i.e. a bounded function at $z_1 = 0$. Then:

$$\begin{aligned} z_1' &= \alpha z_2 + \alpha u_1(z_1) + \alpha\rho_1(\tau)|z_1|r(z_1) \\ z_2' &= |z_1|^{\frac{1-\alpha}{\alpha}}\,u_2(z_1) + |z_1|^{\frac{1-\alpha}{\alpha}}\,\rho_2(z,\tau) \end{aligned} \tag{B.15}$$

Remark: Notice that if $\alpha = 1/2$, $u_1(z_1(\tau)) = -\alpha k_1 z_1$, and $u_2(z_1(\tau))) = -\frac{k_3}{|z_1|}z_1$, one retrieves the original super-twisting algorithm.

Let us now apply, for instance, the Lyapunov redesign methodology to stabilize system (B.15). To this end, consider the control signal $u_1(\tau)$ is decomposed as:

$$u_1(z_1) = u_{1b}(z_1) - \eta_1 g(|z_1|) z_1 \tag{B.16}$$

with $\eta_1 \geq \bar{\rho}_1 = \|\rho_1(\tau)\|_\infty$ and $|r(z_1)| \leq g(|z_1|) < \infty$ so that

$$\eta_1 g(|z_1|) > \tilde{\rho}_1(\tau) r(z_1) \quad \forall z_1 \tag{B.17}$$

Now, let us consider the Lyapunov function $V = \frac{1}{2} z_1^2$. Taking τ-time derivative, and assuming the control signals u_1 and u_2 will be designed later so that $z_2 = \xi(z_1)$ achieves $V_1' \leq 0$:

$$\begin{aligned} V_1' &= \alpha \xi(z_1) z_1 + \alpha u_{1b}(z_1) z_1 - \\ &\quad - \alpha z_1^2 \left[\eta_1 g(|z_1|) - \tilde{\rho}_1(\tau) r(z_1)(z_1) \right] \\ &\leq \alpha \xi(z_1) z_1 + \alpha u_{1b}(z_1) z_1 \leq 0 \end{aligned} \tag{B.18}$$

Now, let us define the error signal:

$$\bar{z}_2 = z_2 - \xi(z_1) \tag{B.19}$$

Its dynamics being:

$$\begin{aligned} \bar{z}_2' = |z_1|^{\frac{1-\alpha}{\alpha}} u_2(z_1) + |z_1|^{\frac{1-\alpha}{\alpha}} \rho_2(z,\tau) - \\ - \frac{\partial \xi(z_1)}{\partial z_1} \left[\alpha \bar{z}_2 + \alpha \xi(z_1) + \alpha u_{1b}(z_1) - \right. \\ \left. - \alpha z_1 (\eta_1 g(|z_1|) - \alpha \tilde{\rho}_1(\tau) r(z_1)) \right] \end{aligned} \tag{B.20}$$

Consider now the re-designed Lyapunov function:

$$V_2 = \frac{1}{2} z_1^2 + \frac{1}{2} \bar{z}_2^2 \tag{B.21}$$

Taking τ-time derivative:

$$\begin{aligned}
V_2' &= \alpha\bar{z}_2 z_1 + \alpha\xi(z_1)z_1 + \alpha u_{1b}(z_1)z_1 + \bar{z}_2|z_1|^{\frac{1-\alpha}{\alpha}}u_2(z_1) + \\
&- \alpha z_1^2\left[\eta_1 g(|z_1|) - \tilde{\rho}_1(\tau)r(z_1)\right] + \\
&+ \bar{z}_2|z_1|^{\frac{1-\alpha}{\alpha}}\rho_2(z,\tau) - \bar{z}_2\frac{\partial\xi(z_1)}{\partial z_1}\left[\alpha\bar{z}_2 + \alpha\xi(z_1) + \right. \\
&+ \left.\alpha u_{1b}(z_1) - \alpha z_1\left[\eta_1 g(|z_1|) - \tilde{\rho}_1(\tau)r(z_1)\right]\right] \\
&\leq \alpha\xi(z_1)z_1 + \alpha u_{1b}(z_1)z_1 - \alpha\frac{\partial\xi(z_1)}{\partial z_1}\bar{z}_2^2 + \\
&+ \bar{z}_2 z_1\alpha\frac{\partial\xi(z_1)}{\partial z_1}\left[\eta_1 g(|z_1|) - \tilde{\rho}_1(\tau)r(z_1)\right] + \\
&+ \bar{z}_2\left[\alpha z_1 + |z_1|^{\frac{1-\alpha}{\alpha}}u_2(z_1) + |z_1|^{\frac{1-\alpha}{\alpha}}\rho_2(z,\tau) - \right. \\
&\left. -\alpha\frac{\partial\xi(z_1)}{\partial z_1}\xi(z_1) - \alpha\frac{\partial\xi(z_1)}{\partial z_1}u_{1b}(z_1)\right]
\end{aligned} \tag{B.22}$$

Now, choose $\xi(z_1) = \eta_2 z_1$, so that $\frac{\partial\xi(z_1)}{\partial z_1} = \eta_2$, and

$$\begin{aligned}
u_{1b}(z_1) &= -(\eta_2 + k_1(z_1))z_1 \\
u_2(z_1) &= -\alpha(\eta_3 + \eta_2 k_1(z_1))z_1|z_1|^{\frac{\alpha-1}{\alpha}}
\end{aligned} \tag{B.23}$$

with $k_1(z_1) > 0$. Then

$$\begin{aligned}
V_2' \leq &-k_1(z_1)\alpha z_1^2 - \eta_2\alpha\bar{z}_2^2 + \\
&+ \bar{z}_2 z_1\alpha\eta_2\left[\eta_1 g(|z_1|) - \tilde{\rho}_1(\tau)r(z_1)\right] + \\
&+ \bar{z}_2 z_1\left[\frac{|z_1|^{\frac{1-\alpha}{\alpha}}}{z_1}\rho_2(z,\tau) + \alpha(1-\eta_3)\right]
\end{aligned} \tag{B.24}$$

Define:

$$\begin{aligned}
\Psi_1(z_1,\tau) &\stackrel{\triangle}{=} \eta_1 g(|z_1|) - \tilde{\rho}_1(\tau)r(z_1) \geq 0 \\
\Psi_2(z,\tau) &\stackrel{\triangle}{=} |z_1|^{\frac{1-2\alpha}{\alpha}}\tilde{\rho}_2(z,\tau) + \alpha(1-\eta_3)
\end{aligned} \tag{B.25}$$

Notice $\Psi_1(z_1,\tau)$ is non negative. Also notice $\Psi_2(z_1,\tau)$ will be bounded as $z_1 \to 0$ provided $\alpha \leq 1/2$.

Using the previous definitions, equation (B.24) can be expressed as:

$$\begin{aligned}
V_2' &\leq -k_1(z_1)\alpha z_1^2 - \eta_2\alpha\bar{z}_2^2 + \bar{z}_2 z_1\left[\alpha\eta_2\Psi_1(z_1,\tau) + \Psi_2(z,\tau)\right] \\
&= -\alpha\begin{bmatrix} z_1 & \bar{z}_2 \end{bmatrix}\begin{bmatrix} k_1(z_1) & -\frac{\alpha\eta_2\Psi_1+\Psi_2}{2\alpha} \\ -\frac{\alpha\eta_2\Psi_1+\Psi_2}{2\alpha} & \eta_2 \end{bmatrix}\begin{bmatrix} z_1 \\ \bar{z}_2 \end{bmatrix}
\end{aligned} \tag{B.26}$$

At this point, it is interesting to summarize and observe the structure of the injected correction terms:

$$\begin{aligned} u_1(z_1,\tau) &= -\left[\eta_2 + k_1(z_1)\right] z_1 - \eta_1 g(|z_1|) z_1 \\ u_2(z_1,\tau) &= -\alpha \left[\eta_3 + \eta_2 k_1(z_1)\right] z_1 |z_1|^{\frac{\alpha-1}{\alpha}} \end{aligned} \tag{B.27}$$

In the original x-dynamics:

$$\begin{aligned} u_1(x_1,t) &= -\left[\eta_2 + k_1(x_1) + \eta_1 g(|x_1|^\alpha)\right] |x_1|^\alpha \operatorname{sign}(x_1) \\ u_2(x_1,t) &= -\alpha \left[\eta_3 + \eta_2 k_1(x_1)\right] |x_1|^{(2\alpha-1)} \operatorname{sign}(x_1) \end{aligned} \tag{B.28}$$

Notice for $u_2(x_1,t)$ to be bounded as $x_1 \to 0$ the condition $\alpha \geq 1/2$ must be imposed. This, along with the requirement $\alpha \leq 1/2$ for $\Psi_2(z_1,\tau) = \mathcal{O}(1)$ as $z_1 \to 0$ imposes the restriction $\alpha = \frac{1}{2}$ that will be used hereafter.

On the other hand, for $u_1(z_1,\tau)$ to be continuous the terms $k_1(z_1)$, and $g(|z_1|)$ will be required to be continuous. Since the coordinates transformation is homeomorphic, $u_1(x_1,t)$ will be continuous.

Let us now consider different scenarios regarding the perturbation term $\rho_1(z,\tau)$.

B.2.1 Case $r(z_1) \equiv 0$

In this case, $\rho_1(z,\tau) = 0$ and, from equation (B.25) it is clear that $\Psi_1(z_1,\tau) = \eta_1 g(|z_1|)$. Therefore, in this case $\eta_1 = 0$ can be chosen. By also choosing $k_1(z_1(x_1)) = k_1$, and $\eta_3 = 1$ we have:

$$\begin{aligned} V_2' &\leq -k_1(z_1)\alpha z_1^2 - \eta_2 \alpha \bar{z}_2^2 + \bar{z}_2 z_1 \Psi_2(z,\tau) \\ &= -\frac{1}{2} \begin{bmatrix} z_1 & \bar{z}_2 \end{bmatrix} \begin{bmatrix} k_1 & -\tilde{\rho}_2(z,\tau) \\ -\tilde{\rho}_2(z,\tau) & \eta_2 \end{bmatrix} \begin{bmatrix} z_1 \\ \bar{z}_2 \end{bmatrix} \\ &\triangleq -\frac{1}{2} \begin{bmatrix} z_1 & \bar{z}_2 \end{bmatrix} \mathbf{Q} \begin{bmatrix} z_1 \\ \bar{z}_2 \end{bmatrix} \end{aligned} \tag{B.29}$$

This can be easily solved provided $\bar{\rho}_2 = \|\tilde{\rho}_2(z,\tau)\|_\infty < \infty$, as $k_1\eta_2 > \bar{\rho}_2^2$ must be satisfied for $\mathbf{Q}$ to be positive definite.

In the original x-dynamics:

$$\begin{aligned} u_1(x_1,t) &= -\nu_1 |x_1|^{\frac{1}{2}} \operatorname{sign}(x_1) \\ u_2(x_1,t) &= -\nu_2 \operatorname{sign}(x_1) \end{aligned} \tag{B.30}$$

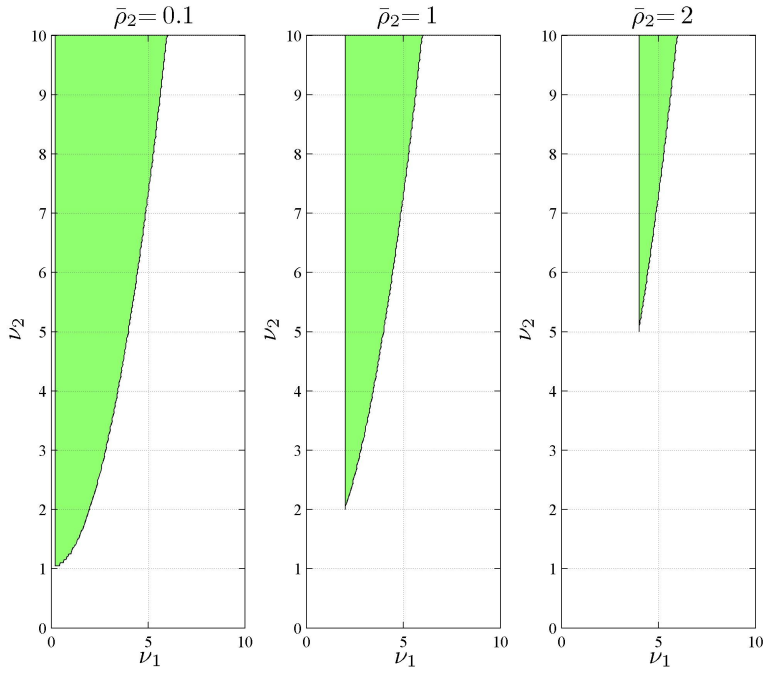

Figure B.1: Stability region for the gains ν_1, ν_2 in the case $\rho_1(z,\tau) = 0$, for different values of the perturbation bound $\bar{\rho}_2$.

with

$$\begin{aligned} \nu_1 &= \eta_2 + k_1 \\ \nu_2 &= 1 + \eta_2 k_1 \end{aligned} \tag{B.31}$$

that clearly takes the form of the super-twisting algorithm, but with a special relationship between the gains of the injected terms u_1 and u_2. The stability region for the gains ν_1, ν_2 can be easily plotted (see figure B.1).

The stability region in the space (ν_1, ν_2) can be expressed in terms of the perturbation bound $\bar{\rho}_2$. Thus, for ν_2, taking into account equation (B.31) and the condition $k_1\eta_2 > \bar{\rho}_2^2$ for positive definiteness of $\mathbf{Q}$, one simply has $\nu_2 > 1 + \bar{\rho}_2^2$. For ν_1 the limit of the stability region can be obtained by minimizing $\nu_1 = k_1 + \eta_2$ subject to $k_1\eta_2 = \nu_2 - 1$. This gives $\nu_1 > 2\bar{\rho}_2$. These limits correspond to the frontier of the region in figure

B.1.

B.2.2 Case $r(z_1) \not\equiv 0$

Now, the class of perturbations we are considering is:

$$\rho_1(z,\tau) = \rho_1(\tau)|z_1|r(z_1) \tag{B.32}$$

Two interesting subcases arise now.

Function $r(z_1)$ is constant. In this case –without losing generality $r(z_1) = 1$ can be assumed– the perturbation term $\rho_1(x,t)$ in the original dynamics is:

$$\rho_1(x,t) = 2\rho_1(t)|x_1|^{\frac{1}{2}} \tag{B.33}$$

Indeed, in this case, by choosing $g(|z_1|) = 1$, and $\eta_3 = 1 + \eta_1\eta_2$ equation (B.26) gives:

$$\mathbf{Q} = \begin{bmatrix} k_1 & -q_{12}(z,\tau) \\ -q_{12}(z,\tau) & \eta_2 \end{bmatrix} \tag{B.34}$$

with $q_{12}(z,\tau) \stackrel{\triangle}{=} \tilde{\rho}_2(z,\tau) - \frac{\eta_2}{2}\tilde{\rho}_1(\tau)$. Recall $\|\tilde{\rho}_1(z,\tau)\|_\infty \leq \eta_1$. The perturbed term $q_{12}(z,\tau)$ takes values in the interval:

$$q_{12}(z,\tau) \in \left[-\bar{\rho}_2 - \frac{\eta_2}{2}\bar{\rho}_1, \bar{\rho}_2 + \frac{\eta_2}{2}\bar{\rho}_1\right]. \tag{B.35}$$

Therefore, the condition for positive definiteness of $\mathbf{Q}$ in equation (B.34) becomes $k_1 > 0$ and:

$$\eta_2 k_1 > \left[\bar{\rho}_2 + \frac{\eta_2}{2}\bar{\rho}_1\right]^2 \tag{B.36}$$

The injected correction terms in the original x-dynamics are:

$$\begin{aligned} u_1(x_1,t) &= -\left[\eta_2 + \eta_1 + k_1\right]|x_1|^{\frac{1}{2}}\ \mathrm{sign}(x_1) \\ u_2(x_1,t) &= -\left[1 + \eta_2(\eta_1 + k_1)\right]\ \mathrm{sign}(x_1) \end{aligned} \tag{B.37}$$

Figure B.2 shows the stability region in the η_2, k_1 parameters space for several values of $\bar{\rho}_1$, and $\bar{\rho}_2$. Notice how the gains in equation (B.37) must be increased as the values of $\bar{\rho}_1$, and $\bar{\rho}_2$ do.

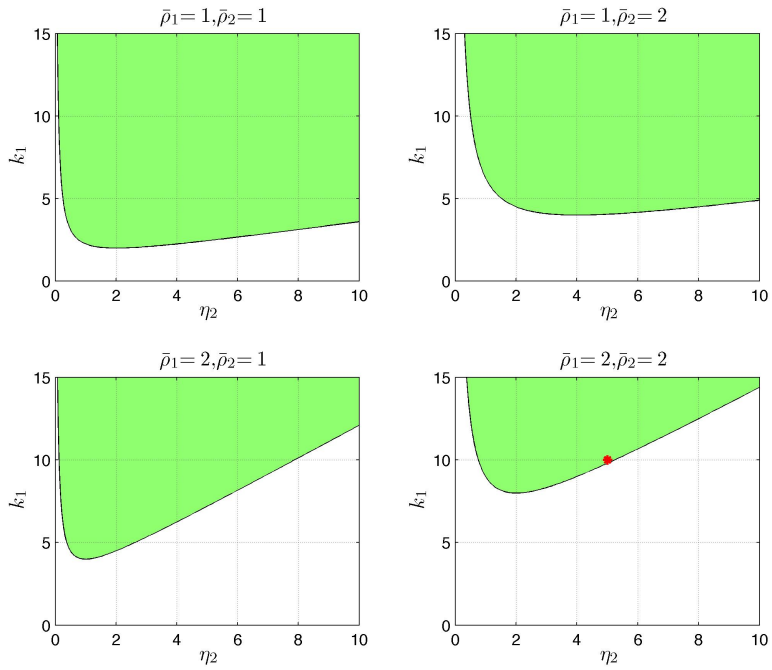

Figure B.2: Stability region in the η_2, k_1-parameters space for the case $\rho_1(z,\tau) = \rho_1(\tau)|z_1|$. Two different values of the perturbation bounds $\bar{\rho}_1$ and $\bar{\rho}_2$ are shown.

Function $r(z_1)$ is not constant. In this case:

$$\mathbf{Q} = \begin{bmatrix} k_1(z_1) & -q_{12}(z,\tau) \\ -q_{12}(z,\tau) & \eta_2 \end{bmatrix} \tag{B.38}$$

where if $\eta_3 = 1+\eta_1\eta_2 g(|z_1|)$ is chosen the off the diagonal term becomes $q_{12}(z,\tau) \stackrel{\triangle}{=} \tilde{\rho}_2(z,\tau) - \frac{\eta_2}{2}\tilde{\rho}_1(\tau)r(z_1)$.

Notice that for $\mathbf{Q}$ to be positive definite, the polynomial $k_1(z_1)$ will have to dominate the square of the terms in the secondary diagonal. Therefore, for $k_1(z_1)$ to be bounded –recall this polynomial will form part of the injected correction terms u_1, and u_2– we must have $r(z_1)$ bounded for bounded z_1.

Thus, for instance, assume $r(z_1) = r_0 + r_1 z_1 + \ldots + r_\beta z_1^\beta$, with $\beta \geq 0$, so that

$$\rho_1(z,\tau) = \rho_1(\tau)|z_1|\left[r_0 + r_1 z_1 + \ldots + r_\beta z_1^\beta\right] \tag{B.39}$$

Define $\bar{r} \stackrel{\triangle}{=} \max(r_0,\ldots,r_\beta)$, $\bar{\beta}$ the number of coefficients of the polynomial (B.39), and:

$$\begin{aligned} g(|z_1|) &\stackrel{\triangle}{=} \bar{\beta}\bar{r}|z_1|^\gamma \\ \gamma &= \begin{cases} \beta\ , & |z_1| > 1 \\ 0\ , & |z_1| \leq 1 \end{cases} \end{aligned} \tag{B.40}$$

Condition (B.17) is satisfied and, using an argument analogous to that of the previous subsection, a suficient condition for positive definiteness of $\mathbf{Q}$ in equation (B.38) is:

$$\eta_2 k_1(z_1) > \left[\bar{\rho}_2 + \frac{\eta_2\eta_1}{2}\bar{\beta}\bar{r}|z_1|^\gamma\right]^2 \tag{B.41}$$

where $\bar{\rho}_2 = \|\tilde{\rho}_2(z,\tau)\|_\infty$. If $k_1(z_1)$ is chosen as a polynomial in $|z_1|$:

$$k_1(z_1) = [k_{1a} + k_{1b}|z_1|^\gamma]^2 \tag{B.42}$$

then, a positive definiteness sufficient condition for $\mathbf{Q}$ in equation (B.38) is:

$$\begin{aligned} k_{1a} &> \frac{\bar{\rho}_2}{\sqrt{\eta_2}} \\ k_{1b} &> \frac{\sqrt{\eta_2}\eta_1}{2}\bar{\beta}\bar{r} \end{aligned} \tag{B.43}$$

In the original x-dynamics:

$$\begin{aligned} u_1(x_1,t) &= -\left[\eta_2 + k_1(x_1) + \bar{\eta}_1|x_1|^{\frac{\gamma}{2}}\right]|x_1|^{\frac{1}{2}}\ \mathrm{sign}(x_1) \\ u_2(x_1,t) &= -\left[1 + \eta_2\left(k_1(x_1) + \bar{\eta}_1|x_1|^{\frac{\gamma}{2}}\right)\right]\ \mathrm{sign}(x_1) \end{aligned} \tag{B.44}$$

with $k_1(x_1) = \left[k_{1a} + k_{1b}|x_1|^{\frac{\gamma}{2}}\right]^2$, and $\bar{\eta}_1 \triangleq \eta_1\bar{\beta}\bar{r}$.

Appendix C

Algorithms and examples.

C.1 Individual systems dynamics

The individual systems dynamics used are different, and with different controllers and constraints. The controllers are proportional-integral with the following expression:

$$PI : Kp\left(1 + \frac{1}{sT_i}\right) \tag{C.1}$$

The values for the parameters used in all the simulations are shown in the table C.1.

Table C.1: Systems dynamics.

System	States	Outputs	$u_p^{\pm}$	K_p	T_i
1	$\dot{x} = -10x + 4u$	$y(x) = 5x$	± 10	18	0.33
2	$\dot{x} = \begin{bmatrix} -22 & 0 \\ 1 & 0 \end{bmatrix} x + \begin{bmatrix} 4 \\ 0 \end{bmatrix} u$	$y(x) = \begin{bmatrix} 0 & 6.25 \end{bmatrix} x$	± 12	20	0.25
3	$\dot{x} = \begin{bmatrix} -18 & -4.25 \\ 4 & 0 \end{bmatrix} x + \begin{bmatrix} 2 \\ 0 \end{bmatrix} u$	$y(x) = \begin{bmatrix} 0 & 3.25 \end{bmatrix} x$	± 10	10	0.16
4	$\dot{x} = -15x + 4u$	$y(x) = 5x$	± 8	22	0.16
5	$\dot{x} = \begin{bmatrix} -20 & 0 \\ 1 & 0 \end{bmatrix} x + \begin{bmatrix} 4 \\ 0 \end{bmatrix} u$	$y(x) = \begin{bmatrix} 0 & 5 \end{bmatrix} x$	± 12	25	0.25

C.2 Extended example Chapter 6

This section presents a numerical example that illustrates the previous analysis and theoretical results from Chapter 6. Let consider a first order integrator with unknown input signal $u(t)$ and noise $\rho_1(x,t)$ as in (**??**).

A super-twisting observer will be tuned using the proposed approach. The structure of the perturbation term $\rho_1(x,t)$ in this example will take the form of (**??**), with $\rho_1(t)$ being gaussian noise $\mathcal{N}(0,1)$. The values of the parameters k_1, η_1, and η_2, have been selected taking a point in the stable region according with the supposed bounds of the unknown signal derivative $\bar{\rho}_2(x,t)$ and the integrator input noise $\bar{\rho}_1(x,t)$. In this particular case, the values have been chosen so that:

$$\begin{aligned} \bar{\rho}_1(x,t) &= 2 \\ \bar{\rho}_2(x,t) &= 2 \end{aligned} \tag{C.2}$$

The resulting selected values for the observer gains are (see red dot in Fig. **??**):

$$\begin{aligned} \eta_1 &= 2.5 \\ \eta_2 &= 5 \\ k_1 &= 10 \end{aligned} \tag{C.3}$$

The unknown input signal has been chosen as:

$$u(t) = \begin{cases} \sin(t) & 0 < t < 0.5 \\ \sin(t) + (t - 0.5) & 0.5 < t < 1 \\ \sin(t) + (t - 0.5) - 4(t - 1) & t > 1 \end{cases} \tag{C.4}$$

A step at $t = 1sec$, and an impulse at $t = 2sec$ were injected as disturbances in $u(t)$.

The simulation results are shown in Fig. C.1. The top plot depicts the input signal to the observer $y(t)$ (in blue dashed line), and the estimated signal $\hat{y}(t)$ (in red solid line). The real integrator input $u(t)$ –with noise, in cyan, and without noise in dashed blue– and its estimated value $\hat{u}(t)$ (in red solid line) are displayed in the bottom plot. A more detailed plot is shown in Fig. C.2.

It is seen that the observer output converges in less than $0.25sec$ and perfectly tracks the evolution of $u(t)$ when the appropriate conditions hold. At $t = 1sec$ and $t = 2sec$ the derivative of $u(t)$ is larger than

the assumed bound $\bar{\rho}_2(x,t)$, and the observer output diverges and then converges rapidly, putting in evidence the occurrence of an abrupt fault, as the derivative of $u(t)$ overly differed from the expected one. This fact can be seen also in Fig. C.3, where the evolution of the system around the second order sliding surface $(x_1, \dot{x}_1)$ is displayed.

Remark C.1. In a real case the signal $u(t)$ is unknown. Therefore, it is not possible to calculate $\dot{x}_1$. In this simulated example it has been obtained for the sake of showing the convergence of the algorithm.

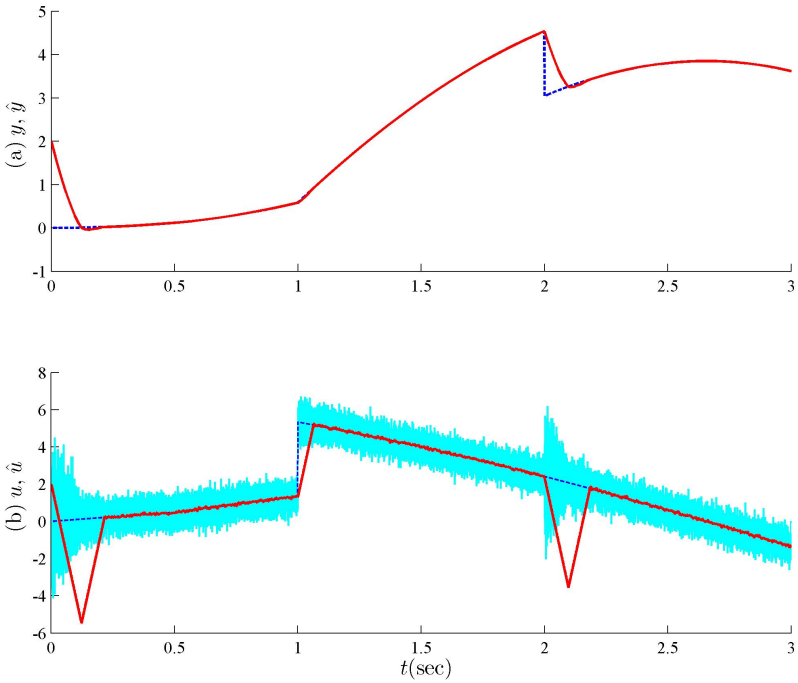

Figure C.1: Examples response.

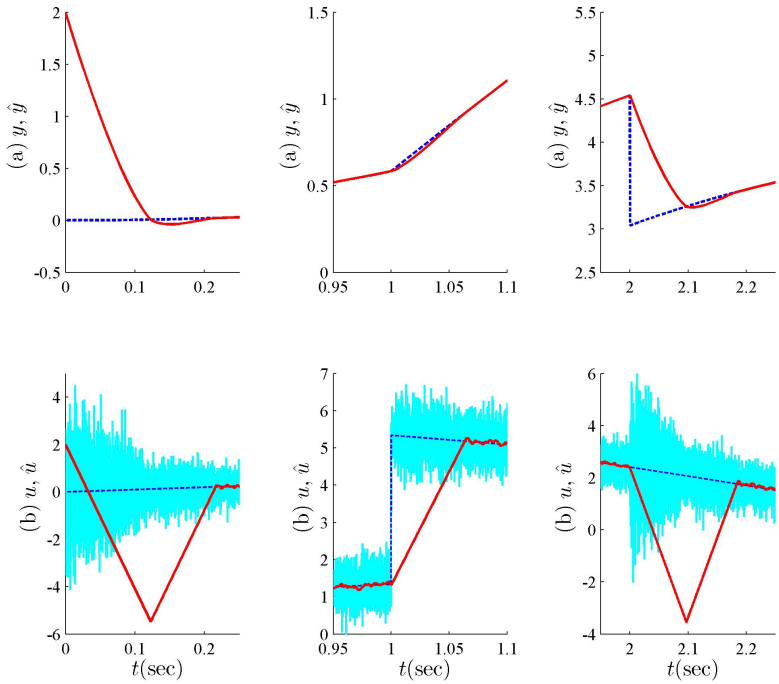

Figure C.2: Examples response zoom.

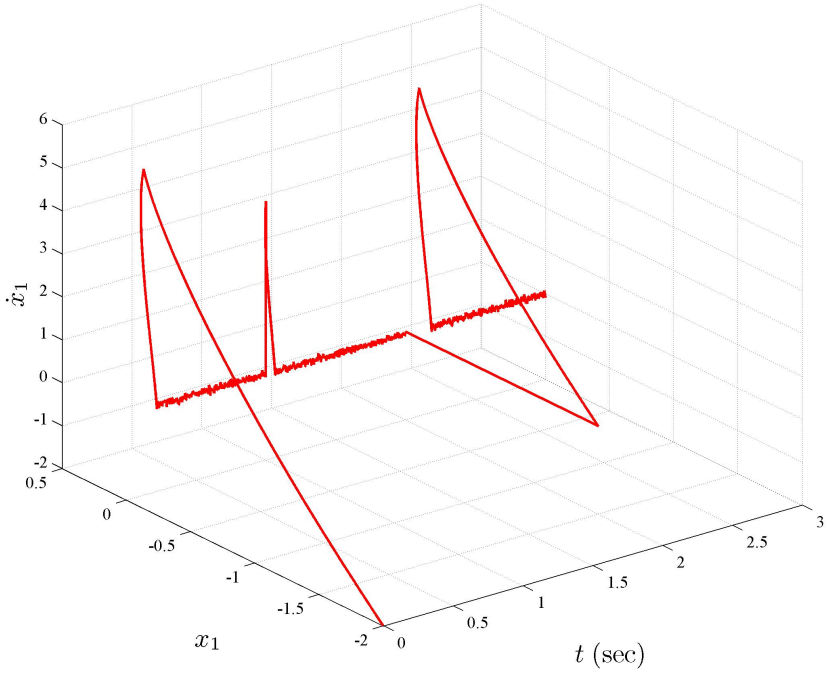

Figure C.3: Sliding surface coordinates.